Identification and Characterization of PDE8 Inhibitors Using a Fission Yeast Based High-throughput Screening Platform

Author: Didem Demirbas Cakici

Boston College

The Graduate School of Arts and Sciences

Biology Department

IDENTIFICATION AND CHARACTERIZATION OF PDE8 INHIBITORS USING A FISSION YEAST BASED HIGH-THROUGHPUT SCREENING PLATFORM

a dissertation

by

DIDEM DEMIRBAS CAKICI

submitted in partial fulfillment of the requirements

for the degree of

Doctor of Philosophy

March 2011

ABSTRACT

IDENTIFICATION AND CHARACTERIZATION OF PDE8 INHIBITORS USING A FISSION YEAST BASED HIGH-THROUGHPUT SCREENING PLATFORM

By Didem Demirbas Cakici

Advisor: Charles S. Hoffman, PhD

In this thesis, I describe the development of a screening platform for detecting PDE8A inhibitors using the cAMP-dependent glucose sensing pathway of the fission yeast *Schizosaccharomyces pombe*, which led us to discover several PDE8A selective inhibitors. In this system, the only PDE of the fission yeast is replaced with mammalian PDE8A1 in strains that have been engineered such that PDE inhibition is required to allow cell growth. Using this system, I screened 56 compounds obtained from PDE4 and PDE7 high throughput screens (HTSs) and identified a PDE4-PDE8 dual specificity inhibitor. Using this as a positive control, I developed a robust high-throughput screen (HTS) for PDE8A inhibitors and screened 240,267 compounds at the Harvard Medical School ICCB Screening Facility. Approximately 0.2 % of the screened compounds were potential PDE8A inhibitors with 0.03% displaying significant potency. Secondary assays of 367 of the most effective compounds against strains expressing PDE8A (both full length and catalytic domain), PDE4A and PDE7A or PDE7B led to the selection of structurally diverse compounds for further testing. To profile the selectivity of twenty-eight of these compounds, dose response assays were conducted using 16 yeast strains that express different PDE isoforms (representing all PDE families with the exception of

the PDE6 family). These assays identified compounds with different patterns of inhibition, including structurally-distinct PDE8A-specific inhibitors. By evaluating the effects of these compounds for steroid production in mouse Leydig cells, biologically active compounds that can elevate steroid production were identified.

DEDICATION

To my beloved parents Melahat and Mustafa Demirbas

Science is the only true guide in life.

Mustafa Kemal Ataturk

ACKNOWLEDGEMENT

First, I would like to thank my advisor Professor Charles Hoffman. I cannot explain enough how grateful I am to him for his patience, support, and guidance throughout my PhD. From the moment he explained my rotation project, I knew I was at the right place. Charlie is a brilliant scientist and an excellent mentor from whom I have learned tremendous amount of knowledge and gained true inspiration. His dedication and passion in science has been very inspiring and influential for my scientific development. I am also thankful to him for believing in this project even when nothing seemed to work. His knowledge, continuous mentoring, approachability and excellent guidance have been invaluable for my training as a graduate student. I feel very lucky and privileged to be his student.

I am also grateful to members of my thesis committee for being very generous in giving time from their busy schedules and being very supportive throughout the whole process. I would like to thank Professor Anthony T. Annunziato for his valuable contributions and especially for teaching me the beautiful world of chromatin along with how to think critically in every aspect of science. I would like to thank Professor Junona Moroianu for her valuable contributions, for always creating a positive environment, for her continuous encouragement and support. I also would like to thank Professor Marc-Jan Gubbels for his valuable contributions both on my comprehensive exam and thesis committees; his attention to detail has always motivated me to do better. I would like to thank Professor Hugh Cam for joining to my thesis committee and for his valuable inputs.

I am thankful to former and present members of the Hoffman Lab. In the Hoffman Lab, I had opportunity to work with excellent scientists. I wish to thank Dr. Douglas Ivey, Dr. Lili Wang and Richard Kao for patiently answering my questions, for the support and training they provided and for their friendship when I first joined the lab. I would like to thank former Hoffman lab colleague Manal Alaamery for her support and help not only in research and science but also in other aspects of life and for her true friendship; she made many routine days memorable. I am thankful to Dr. Arlene Wyman for her continuous support, help and kindness. Her passion in science has been deeply inspirational for me. I wish to thank Ozge Ceyhan for her wonderful friendship since she came to BC, for her continuous support in every little thing related to lab and also related to life. I feel very privileged to have her as a part of my life. I also wish to thank Christina, Maia, Roxanne, Fan, James, Matt, Dani, Brian, Alex, Catherine, Dayna, Ana, and Kristina for the positive atmosphere and joyful times in the lab that they all contributed.

I would like to thank the Chemical Biology Platform of the Broad Institute of Harvard and MIT as being the first place where I learned the essence of high throughput screening. I am extremely thankful to ICCB Screening Facility at Harvard Medical School, especially to Drs. Caroline Shamu, Dave Wrobel and Jen Nale and Andrew Daab.

I wish to thank Dr. Joe Beavo who generously accepted me to visit his lab to test some of my compounds. I am extremely grateful for his generosity and hospitality and for

enormous amount of knowledge and inspiration that I learned from him during my two-week visit. I would like to thank Lisa Tsai and Dr. Masami Shimizu for making this short visit very productive. I am thankful especially to Masami for her encouragement and technical expertise and assistance in testing my compounds on cells from PDE8 knock-out mouse. I also would like to thank Prof. Thomas Chiles for generously providing space to perform some of the mammalian cell assays and to Chenjia Xu and Fay Dufort for their support and help. Finally, I would like to thank to excellent scientists of Boston College Biology Department, especially to Prof. Jeffrey Chuang for teaching me bioinformatics during my rotation in his lab and to Drs. Mike Piatelli and Daniel Kirschner for being my teaching mentors and helping me to excel as a teacher.

I feel very lucky to be surrounded by wonderful friends at Boston College and beyond. Thank you Arleide, Steven, Katie, Mikey, Marisa, Stephane, Nevine, Robin, Tomasz, Yun, Jerome, Julian, Howard, Brooke, Deniz, Zeynep A., Zeynep O., Kevin, Cheryl, Pascal, Maria, Karie, Kieth, Lea, Lulu, Derek, Kristin, Guliz, Kivanc, Begum, Feyza, Anas, Purna, Melanie, Seda, Efsun and Pedro for being there for me at joyful times as well as hard times. They all made Boston a second home for me.

I am indebted to my husband Ozgur Cakici who made me feel his support, trust and love even from the other side of the world. I am aware of the many sacrifices he made for me, I am thankful for his endless support and most importantly for his friendship. I would like to thank Ozgur also for his scientific expertise in structural biology and technical help.

It is so hard to explain my gratitude for my parents Melahat and Mustafa Demirbas. I am thankful for their enduring love and support in everything I do in life and for teaching me the importance of education, honesty, kindness and hardwork. And of course, I am thankful to my dear brother Onur Demirbas for being my best friend. I simply cannot imagine a life without him. I also wish to thank all my friends and family in Turkey for their support and understanding for all of the special moments that I missed including weddings, celebrations, remembrances, get-togethers and arrivals of new babies.

Finally I would like to thank the Boston College community and the Biology Department. I am thankful to Peter Marino, Colette, Donna and Bill for their help and assistance. I also wish to thank Boston College Board of Trustees and NIH grant R21 GM079662.

TABLE OF CONTENTS

LIST OF FIGURES

LIST OF TABLES

CHAPTER ONE

1 INTRODUCTION

Cells have evolved extensive and precise ways of elucidating specific cellular responses to external stimuli via the mechanisms referred to as signal transduction pathways. In these systems, the first messengers or extracellular cues are detected by the cell and the signal is amplified by production of intracellular second messengers to regulate downstream biological processes. The first second messenger cyclic adenosine monophosphate (cAMP) was discovered by Sutherland and colleagues during their investigations on the hormonal control of glycogen breakdown (Rall and Sutherland. 1958). Since the discovery of cAMP in 1950s, the signaling pathways via cyclic nucleotides (cAMP and cGMP) have been extensively studied.

1.1 CYCLIC AMP SIGNALING

Cyclic AMP signaling mediates a diverse range of cellular responses including metabolic events, neurotransmitter release, muscle contraction, hormone secretion, ion channel conductance, learning and memory, apoptosis, inflammation, cell growth and differentiation (Beavo and Brunton. 2002).

Upon binding of ligands –hormones, neurotransmitters, growth factors- to their specific receptors that are located on the plasma membrane of the target cell, receptor coupled

GTP binding proteins (G-proteins) are activated. The stimulatory G protein (Gs) triggers the activation of the enzyme adenylyl cyclase, which converts ATP to cAMP (Daniel *et al*. 1998). The targets of cAMP include cAMP-dependent protein kinase A (PKA), cyclic nucleotide gated ion channels, and the guanine nucleotide exchange factors Epac1 and Epac2 (Figure 1.1). The spatial and temporal control of cAMP signaling is controlled not only by the presence of various forms of adenylyl cyclase and target proteins but also by its degradation with various isoforms of phosphodiesterases (Houslay and Milligan. 1997). This control is further orchestrated by organization of members of the cAMP signaling pathway by A-kinase anchoring proteins (AKAPs). These proteins compartmentalize cellular responses to cAMP by assembling PKA, phosphoprotein phosphatases, phosphodiesterases and other signaling effectors into localized complexes (Logue and Scott. 2010).

1.1.1 Cyclic AMP Production

Cyclic AMP is produced by adenylyl cylase from ATP (Figure 1.2). Adenylyl cyclase (AC) is an enzyme that can be activated or inhibited by various subunits of heterotrimeric guanine nucleotide binding proteins (G proteins). There are 10 different forms of AC in mammalian systems, 9 of which are transmembrane proteins.

Figure 1.1 Targets of cyclic AMP

Known targets of cyclic AMP include cAMP-dependent protein kinase A (PKA), cyclic nucleotide gated ion channels, and the guanine exchange factors Epac1 and Epac2.

Figure 1.1 Targets of cyclic AMP

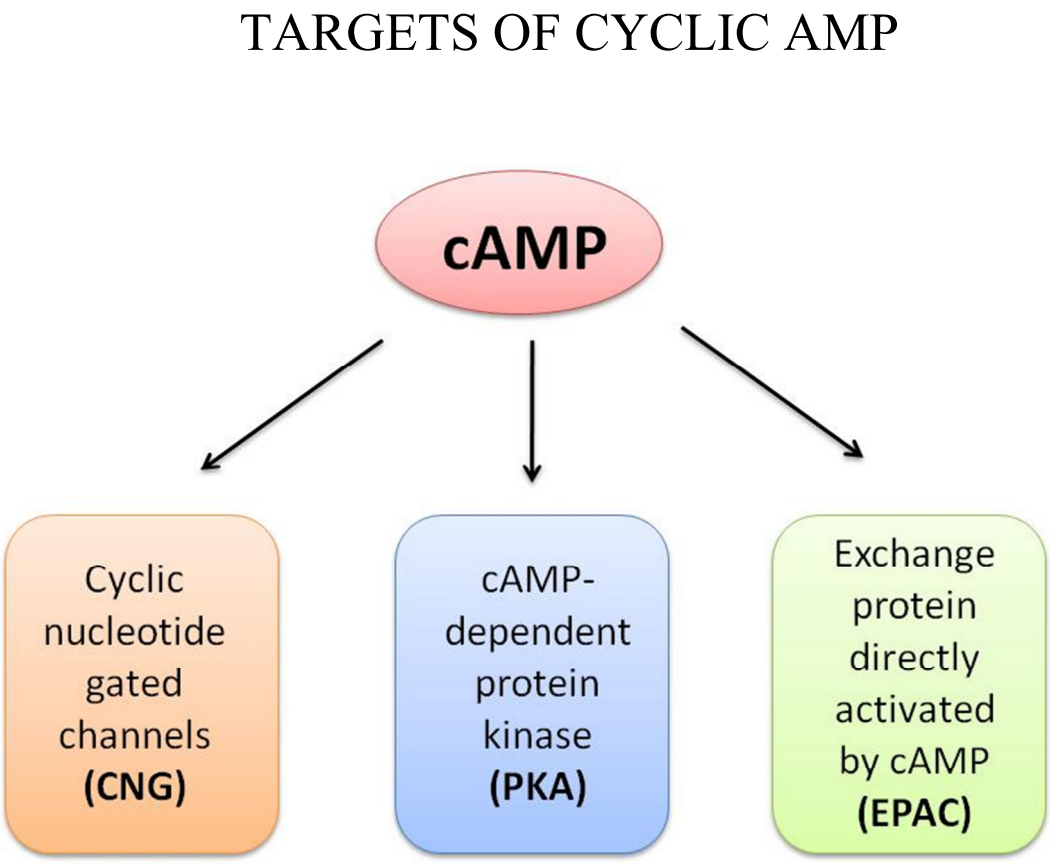

Figure 1.2 Synthesis and hydrolysis of cAMP

Cyclic AMP is synthesized from ATP by the action of adenylyl cyclase and hydrolyzed by phosphodiesterase enzyme.

Figure 1.2 Synthesis and hydrolysis of cAMP

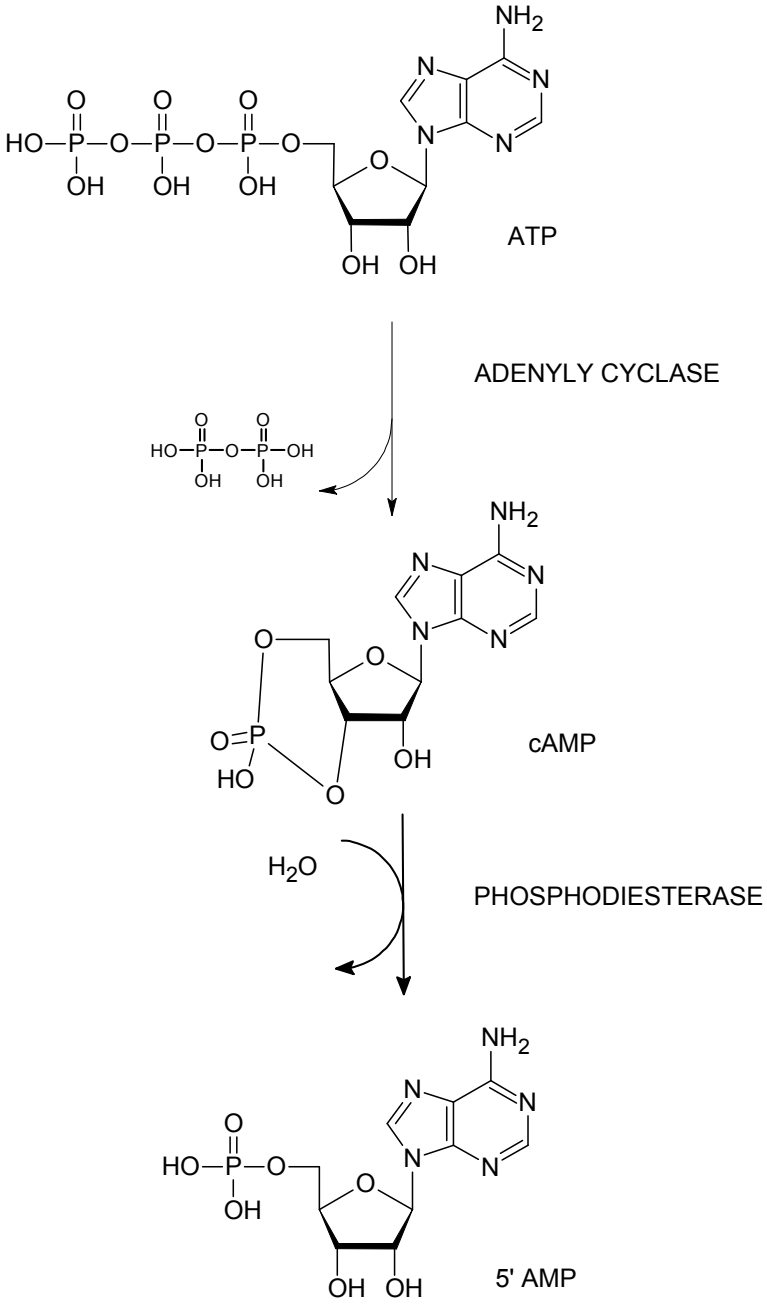

1.1.2 Targets of Cyclic AMP

1.1.2.1 PKA

The first identified effector of cAMP is cAMP-dependent protein kinase A (PKA). It is composed of two regulatory (R) and two catalytic subunits (C). When bound to regulatory subunits, catalytic subunits are inactive. The binding of cAMP to regulatory subunits induces a conformational change that disrupts the interaction between catalytic and regulatory subunits to activate PKA. As a kinase, PKA phosphorylates other proteins to alter their activity, cellular location or stability. Besides phosphorylating enzymes involved in nutrient metabolism, PKA can also activate cAMP-responsive transcription factors (CREB -cAMP response element-binding) by phosphorylation and in this way regulates expression of target genes (Daniel *et al*. 1998). Transcription factors CREM (cAMP response element modulator) and ATF-1 (activating transcription factor-1) are also controlled by PKA.

1.1.2.2 Cyclic Nucleotide-Gated Channels

Cyclic nucleotide-gated (CNG) channels are non-selective cation channels which are activated by cGMP or cAMP binding. They were first identified in retinal photoreceptors and olfactory sensory neurons and play an important role in signal transduction pathways of vision and olfaction. CNG channels form heterotetrameric complexes consisting of two or three different types of subunits. CNG channel activity is modulated by Ca^{2+}/calmodulin and by phosphorylation. In olfactory sensory neurons, the prototypical cAMP signaling cascade starts with binding of an odorant molecule to its receptor, which

activates a G protein (G_{olf}). This is followed by activation of adenylyl cyclase (ACIII) and cAMP production. cAMP opens calcium permeable CNG channels and causes the depolarization of the membrane (Kaupp and Seifert. 2002).

1.1.2.3 Exchange Protein Directly Activated by cAMP

In addition to PKA and CNG channels, cAMP also affects another target called exchange protein directly activated by cAMP (Epac, also known as cAMP-GEF). Epac proteins function as guanine nucleotide exchange factors (GEFs) for Ras-like small GTPases Rap1 and Rap2. They are directly activated upon cAMP binding. In the inactive state, the Epac regulatory domain blocks its catalytic domain to sterically prevent binding of Rap. Upon cAMP binding, the regulatory region undergoes a conformational change to activate Epac. Utilization of Epac selective cAMP analogs showed that cardiac contraction, insulin secretion and vascular permeability are some of the cAMP regulated processes that are mediated by the action of Epac. For most of these processes, Epac functions in cooperation with PKA. The coordination of both cAMP effectors for obtaining a specific response is structured by AKAPs. (Gloerich and Bos. 2010; Grandoch *et al*. 2010).

1.2 MAMMALIAN PHOSPHODIESTERASES: PDE SUPERFAMILY

The specific control of the cyclic nucleotide signal is tailored in part by the presence of different phosphodiesterases in mammalian tissues. There are three different classes of phosphodiesterase enzymes. Class I enzymes are specifically involved in breaking the

phosphodiester bond in the cyclic nucleotides to produce 5'AMP or 5'GMP (Figure 1.2). The phosphodiesterase superfamily consists of 11 families, which are classified according to their structure, regulation, biochemical and pharmacological characteristics. Among these, PDE4, PDE7 and PDE8 are cAMP-specific PDEs; PDE5, PDE6 and PDE9 are cGMP-specific PDEs and PDE1, PDE2, PDE3, PDE10, PDE11 can act on both cAMP and cGMP (Figure 1.3) (Bender and Beavo. 2006; Conti and Beavo. 2007).

1.2.1 PDE1

There are three genes in the PDE1 family; PDE1A, PDE1B and PDE1C. The members of this family are uniquely sensitive to calcium and calcium calmodulin (CaM). They have relatively high affinity for cGMP and show different affinities toward cAMP (Kakkar *et al*. 1999)(Bender and Beavo. 2006; Lugnier. 2006). PDE1A is highly expressed in the brain, PDE1B found in the brain, heart and skeletal muscle (Yu *et al*. 1997; Loughney *et al*. 1996), while PDE1C is mostly found in the olfactory epithelium and present in the testis (Yan *et al*. 1995; Yan *et al*. 1996).

Figure 1.3 PDE superfamily

There are 11 families in the PDE superfamily. PDE4, PDE7 and PDE8 are cAMP-specific PDEs; PDE5, PDE6 and PDE9 are cGMP-specific PDEs and others can hydrolyze both cAMP and cGMP.

Figure 1.3 PDE superfamily

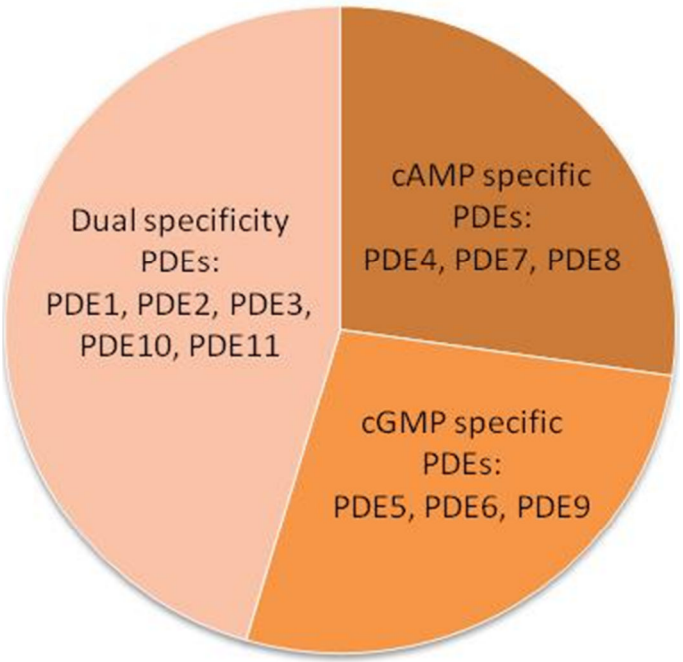

1.2.2 PDE2

PDE2 hydrolyzes both cAMP and cGMP and is allosterically regulated by both cyclic nucleotides with positive cooperative kinetics, with cGMP being the major regulator (Martins *et al*. 1982). The only gene in this family, PDE2A, has two GAF domains, which are important in dimerization and cGMP binding (Martinez *et al*. 2002). Upon cGMP binding, the K_m for cAMP binding decreases and the rate of hydrolysis increases dramatically. Thus, this enzyme is also referred to as the cGMP-stimulated PDE and considered to be important for stimuli that elevate cGMP to reduce cAMP signaling (Lerner and Epstein. 2006). PDE2A is present in the adrenal medulla, heart, rat ventricle, brown adipose tissue, liver and brain (Coudray *et al*. 1999; Yanaka *et al*. 2003).

1.2.3 PDE3

The PDE3 family consists of two genes: PDE3A and PDE3B. PDE3 can hydrolyze both cAMP and cGMP with a higher rate of hydrolysis for cAMP but higher affinity for cGMP that behaves as a competitive inhibitor of cAMP; thus PDE3 enzymes are considered as cGMP inhibited cAMP phosphodiesterases (Lugnier. 2006). PDE3A is present in the heart, platelets, vascular smooth muscle and oocytes and PDE3B is mainly found in pancreatic beta cells, adipocytes, hepatocytes and spermatocytes. Functionally, it was shown that PDE3A knock-out mice are infertile as the oocytes do not complete meiosis (Masciarelli *et al*. 2004). On the other hand, PDE3B overexpression was found to cause impaired insulin secretion and glucose intolerance (Harndahl *et al*. 2004).

1.2.4 PDE4

The PDE4 family is the largest PDE family with four genes; PDE4A, PDE4B, PDE4C and PDE4D that produce various isoforms due to differences in transcriptional start sites and splicing. These enzymes are cAMP-specific; hydrolyzing cAMP with K_m values ranging between 1 to 4 μM (Houslay and Adams. 2003). The PDE4 family is specifically inhibited by rolipram (K_i =0.8 μM). The long forms of PDE4 isoforms contain two upstream conserved regions (UCR), UCR1 and UCR2 in the N termini of the enzymes. There are shorter isoforms that lack one or both of the UCRs. PDE4 activity is increased by PKA mediated phosphorylation in the UCR1 region and demonstrated to be important as a short-term feedback mechanism. ERK phosphorylation within the C terminus of the catalytic domain has also been shown to regulate PDE4 activity. PDE4 enzymes are mainly present in the brain, inflammatory cells, cardiovascular tissues and smooth muscles. Differential expression and various intracellular compartmentalization of the isoforms make the PDE4 family a critical component of cAMP signaling. Functionally, PDE4D knock-out mice showed delayed growth, female infertility and an antidepressant-like profile (Jin *et al*. 1999; Zhang *et al*. 2002). PDE4B deficiency causes the inability to induce TNF alpha secretion upon lipopolysaccahride stimulation in mice (Jin and Conti. 2002).

1.2.5 PDE5

The PDE5 family is a cGMP-specific PDE family consisting of a single gene: PDE5A. The enzyme has two GAF domains that allow cGMP levels to control PDE5 activity

(Lugnier. 2006). PDE5 enzyme was first purified and characterized from human, bovine and rat vascular smooth muscle. PDE5 is mainly expressed in lung, heart and cerebellum in mouse (Giordano *et al*. 2001), in pulmonary arteri in rat (Pauvert *et al*. 2002), and in isolated cardiomyctes in dogs (Senzaki *et al*. 2001). PDE5 was first demonstrated to be involved in vasorelaxation and mediate the nitric oxide/cGMP relaxing effect (Schoeffter *et al*. 1987). The PDE5 inhibitor sildenafil was found to be very effective in treating erectile dysfunction during clinical trials and led to the emergence of other FDA approved PDE5 inhibitors (vardenafil and tadalafil). Recent studies suggest that these compounds are effective in the treatment of other conditions beyond erectile dysfunction such as pulmonary hypertension (Wilkins *et al*. 2008) and Duchenne muscular dystrophy (Adamo *et al*. 2010).

1.2.6 PDE6

PDE6 is the main PDE in retinal photoreceptors and critical for rhodopsin signal transduction. It is composed of two large catalytic subunits (alpha, beta or alpha-alpha), two inhibitory small subunits (gamma) and a delta subunit; all of which are expressed from separate genes and have different compositions in rods and cons. There are two GAF domains in PDE6. Phototransduction starts with activation of rhodopsin by absorption of a photon, which in turn activates G protein transducin. GTP bound transducin Tα subunit activates catalytic PDE6αβ subunits by changing the conformation of the γ subunit to expose the active site and hence allow cGMP hydrolysis. The decrease

in cGMP concentrations upon light stimulus is transmitted by retinal neurons to optic nerve and brain (Lugnier. 2006).

1.2.7 PDE7

The PDE7 family contains two genes PDE7A and PDE7B, which encode for cAMP-specific enzymes devoid of GAF domains and other regulatory domains. They have high affinity for cAMP (K_m = 0.2 μM) and low V_{max} values (Michaeli *et al*. 1993; Bloom and Beavo. 1996). PDE7A is widely distributed in human proinflammatory cells, immune cells and epithelial cells (Smith *et al*. 2003; Miro *et al*. 2000). The development of PDE7 specific inhibitors BRL50481 and BC30 and demonstration of their effect in decreasing TNFα secretion from U937 cells have shown the importance of PDE7 family in inflammation (Alaamery *et al*. 2010).

1.2.8 PDE8

The PDE8 family is composed of two genes; PDE8A and PDE8B. They encode for enzymes with high affinity and specificity for cAMP. They are unusually insensitive to the general PDE inhibitor 3-isobutyl-1-methylxanthine (IBMX) (Vasta. 2006). There are PAS and REC domains in the N termini of the PDE8 proteins that are unique to this family (Soderling *et al*. 1998b; Wang *et al*. 2001a). PDE8A mRNA is expressed in the testis, eye, liver, skeletal muscle, heart, kidney, ovary and brain (Soderling *et al*. 1998b). PDE8B protein is mainly found in the thyroid gland and brain (Hayashi *et al*. 1998b). Studies of knock-out mice show that PDE8A is important in steroid production in testis,

and that PDE8B is important in steroidogenesis in the adrenal gland (Tsai *et al*. 2010; Vasta *et al*. 2006).

1.2.9 PDE9

The PDE9 family contains the single gene PDE9A, which encodes for a high affinity cGMP-specific PDE. Like the PDE8 enzymes, PDE9A is insensitive to IBMX. PDE9 is mainly found in the spleen, small intestine and brain in humans (Soderling *et al*. 1998c;Fisher *et al*. 1998b). More than 20 splice variants of PDE9A have been observed (Rentero *et al*. 2003).

1.2.10 PDE10

The single member of this family, PDE10A is a dual substrate PDE with a lower K_m for cAMP and a higher V_{max} value for cGMP. Thus, it is suggested to be a cAMP-inhibited cGMP PDE. PDE10A contains two GAF domains. It is mainly found in brain, heart, placenta, thyroid and testis (Lugnier. 2006). Recent studies using a transgenic Huntington's disease mice model suggest that PDE10A might be associated with neuropathology of this disease (Hebb *et al*. 2004).

1.2.11 PDE11

This family contains a dual substrate PDE11A, which can hydrolyze both cAMP and cGMP with similar V_{max} values and with K_m values of 0.5 and 1 μM, respectively (Fawcett *et al*. 2000). It is found in skeletal muscle, prostate, kidney, liver, pituitary and salivary glands and testis. Similar to PDE2, 5, 6 and 10 families, PDE11A contains two

GAF domains, one of which is absent in certain splice variants (Yuasa *et al*. 2000). Knock-out mice studies suggest that PDE11 is important in spermatogenesis (Wayman *et al*. 2005).

1.2.12 Phosphodiesterases as Drug Targets

Attributable to the functional diversity of cAMP signaling pathways in various cellular responses, impairment of cAMP signaling contributes to the development and pathophysiology of many neurological, endocrine, cardiovascular and inflammatory disorders. By virtue of the presence of more than 100 isoforms of PDEs with different profiles in tissue specific distribution, regulation, and compartmentalization in the cell, specific PDE isoforms are also linked to certain physiological conditions and disease states. As a result, the development of isoform selective inhibitors can target specific functions or pathological conditions without causing many side effects.

As explained by Bender and Beavo previously (2006), in controlling the concentration of a ligand or second messenger, more rapid changes can be attained by regulation of its degradation rather than the rate of its synthesis. This basic pharmacological principle holds also true for the regulation of cAMP levels since the V_{max} values of phosphodiesterase enzymes for cyclic nucleotide hydrolysis are much higher than that of cyclases for cAMP or cGMP production. Apart from this, although certain compartments have higher cyclic nucleotide concentrations, the endogenous levels of cyclic nucleotides are not unmanageably high for a competitive inhibitor to be effective. This had been a problem for development of kinase inhibitors since ATP levels are intrinsically high in

the cell. Thus, pharmacological intervention of PDEs can result in rapid changes in cAMP levels and make them attractive drug targets.

The goal of this thesis project is to develop a fission yeast based platform for detection of inhibitors of PDE8 enzymes and use it to identify such compounds from chemical libraries. Therefore, a more in-depth introduction to the PDE8 family is presented in the following section.

1.3 PDE8 FAMILY

PDE8A is the first PDE to be discovered by means of bioinformatics due to the consensus sequence in its catalytic domain. The initial discovery of the PDE8 family was described by two separate groups who described human and mouse PDE8A, respectively (Fisher *et al*. 1998a; Soderling *et al*. 1998a). The presence of unique domains in the N terminus suggested that PDE8A is part of a new PDE family (Soderling *et al*. 1998a). The PDE8 family has a very high affinity toward cAMP and contains two genes: PDE8A and PDE8B. Orthologs of PDE8 are found in fruit flies, nematodes, sea squirts, zebrafish and pufferfish (Vasta. 2006).

1.3.1 Features of PDE8A and PDE8B

PDE8 is unique among PDE families in containing a PAS (Per, ARNT, Sim) domain in its N terminus (Soderling and Beavo. 2000; Wang *et al*. 2001b; Hayashi *et al*. 2002). The PAS domain is abbreviated from PER, ARNT, SIM proteins which are the first proteins identified to contain this domain. Proteins with PAS domains are signaling proteins and

function as a sensory module for oxygen tension, redox potential or light intensity, mediating protein-protein interactions (Vasta. 2006) (Figure 1.4).

The Beavo lab (Soderling *et al*. 1998a) showed that human and mouse PDE8A sequences share only 85% sequence identity within the catalytic domain (while other PDEs have more than 93% identity in this region). Wang *et al*. (2001) cloned cDNAs representing five full length human PDE8A splice variants from testis and T cells. They showed that human PDE8A1 encodes a hydrophilic protein of 829 amino acids and has 79% similarity to mouse counterpart at the amino acid level. Besides the PAS domain existing in mouse PDE8A1, the human PDE8A1 contains a unique REC domain which acts as a signal receiver or response regulator domain in other proteins.

Soderling *et al*. (1998) has also reported a consensus sequence for nuclear localization of the type typified by simian virus 40 large T antigen in the mouse PDE8A sequence. Unlike the mouse enzyme, human PDE8A1 does not contain a nuclear localization consensus sequence, but there are myristoylation sites in the protein. Recently, it was shown to be localized to mitochondria. It was also reported that in the human PDE8A1 promoter, there is a binding site for c-Ets-1, a transcription factor involved in expression of several immunologically important genes such as T cell receptor, CD4 etc. in T cells (Soderling and Beavo. 2000).

Figure 1.4 Domains of PDE8A and predicted structure of the PAS domain

(A) PDE8 enzymes are unique in the PDE superfamily with regard to the presence of a PAS domain. Human PDE8A also contains a REC domain. The locations of the indicated domains are drawn based on the data obtained from Conserved Domain Database of NCBI website. **(B)** The PAS domain structure is drawn according to the crystal structure of the oxygen detecting domain of FixL protein from *Bradyrizobium japonicum*. The crystal structure was retrieved from PDB website (PDB ID: 1DRM) and illustrated using Pymol.

Figure 1.4 Domains of PDE8A and predicted structure of the PAS domain

A

B

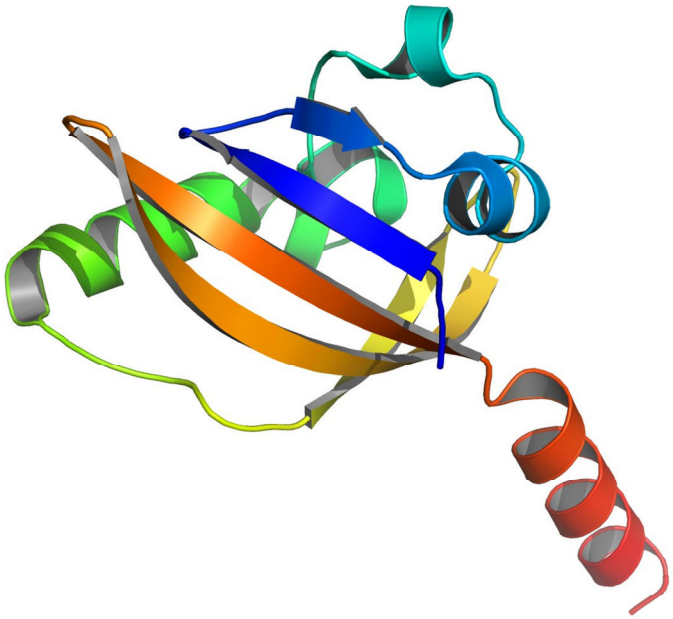

Splice variants

cDNAs representing five full-length human phosphodiesterase (PDE) 8A splice variants (PDE8As 1-5) were cloned from testis and T cells. PDE8A1 encodes a hydrophilic protein of 829 amino acids, containing an N-terminal REC domain, a PAS domain, and a C-terminal catalytic domain. Compared to PDE8A1, PDE8As 2-5 appear to be expressed in much lower abundance. Among various tissues and organs, PDE8A1 and PDE8A2 are expressed at various levels (Wang *et al*. 2001b).

1.3.2 Enzymatic characteristics

PDE8 enzymes have high affinities for cAMP with reported K_m values in the range of 40-150 nM (Fisher *et al*. 1998a; Gamanuma *et al*. 2003; Soderling *et al*. 1998a). Neither of the PDE8A and PDE8B enzymes hydrolyze cGMP, nor is their cAMP hydrolytic activity affected by cGMP (unlike PDE2 or PDE3 families for which cAMP hydrolytic activity is modulated by cGMP). The activity of PDE8A was reported to be dependent on divalent cations Mg^{2+} and Mn^{2+} (Fisher *et al*. 1998a).

The initial kinetic analysis on PDE8A were performed by Fisher *et al*. (1998) using baculovirus expressed human enzyme (truncated form of PDE8A1), which has very high affinity toward cAMP with a K_m of 55 nM for cAMP and 124 microM for cGMP. In the same study, the V_{max} (150 pmol/min/microgram recombinant enzyme) was reported to be about 10 times slower than that of PDE4. Full length PDE8A human enzyme showed a slightly lower K_m value (40 nM) when expressed from Cos-7 cells; while mouse PDE8A

enzyme displayed a K_m value of 150 nM for cAMP when expressed in Sf9 cells (Soderling *et al*. 1998a). Similar to PDE8A, human PDE8B1 is also a high-affinity cAMP-PDE with K_m value of 101 nM for cAMP, which is greater than that of PDE8A1 (40 nM) (Gamanuma *et al*. 2003).

Yan *et al.* (2009) reported a detailed protocol for refolding and purification of a large quantity of the PDE8A1 catalytic domain. They observed that the K_m of their PDE8A1 catalytic domain is significantly higher (1-1.8 μM) than those for the full length PDE8, which is uncommon when compared to the full length and catalytic domain versions of other PDE families. This may reflect the allosteric behavior of PDE8 and the regulation of the catalytic activity by its PAS domain.

PAS Domain/ IkappaB

The overexpression of recombinant human PDE8A1 was shown to physically associate with endogenous IkappaB in a PAS domain dependent manner and competes with NF-kB for IkappaB binding (Wu and Wang. 2004). In the same study, IkappaB association stimulates PDE8A enzymatic activity 6-fold.

1.3.3 Structure

Refolding of the PDE8A1 catalytic domain and its kinetic characterization by H. Ke's group (Wang *et al*. 2008) provided an important starting point for them to determine the crystal structure of PDE8A1 in the unliganded and IBMX-bound forms (Figure 1.5). The

structures indicate Tyr748 as an important residue for inhibitor binding and its mutation to phenylalanine alleviated the insensitivity of PDE8A to non-selective PDE inhibitors.

1.3.4 Tissue Distribution and Function

Tissue distribution

PDE8A expression was initially assessed by Northern blot analysis. In humans, the 4.5 kb mRNA transcript is expressed widely in many tissues with highest levels in testis, ovary, small intestine, and colon (Fisher *et al*. 1998a). Tissue distribution analysis of PDE8A mRNA in mouse indicated highest expression in testis, followed by eye, liver, skeletal muscle, heart, 7-day embryo, kidney, ovary, and brain in decreasing order (Soderling *et al*. 1998a). *In situ* hybridizations in testis, the tissue of highest expression, shows that PDE8 is expressed in the seminiferous epithelium in a stage-specific manner. Rat PDE8A transcripts are high in the liver and testis (Kobayashi *et al*. 2003).

In contrast to the wide expression of PDE8A mRNA in various tissues, Northern blot analysis indicated that the mRNA encoding human PDE8B is expressed specifically and abundantly in thyroid gland as an approximately 4.2 kb mRNA (Hayashi *et al*. 1998a). It is also expressed in lower levels in human brain, kidney, pancreas, spinal cord, placenta,

Figure 1.5 Structure of PDE8A with IBMX

Crystal structure of PDE8A catalytic domain in complex with IBMX shows the cyclic AMP binding pocket (where IBMX is located). IBMX (shown in purple in Part b) cannot inhibit PDE8A but its binding in the crystal structure identifies Tyrosine 748 as an important residue in inhibitor sensitivity (indicated by red arrow). The figures are based on the structures retrieved from PDB website (PDB ID is 3ECM) and illustrated as solvent excluded surface model (A) and ribbon representation (B) using UCSF CHIMERA.

Figure 1.5 Structure of PDE8A with IBMX

A

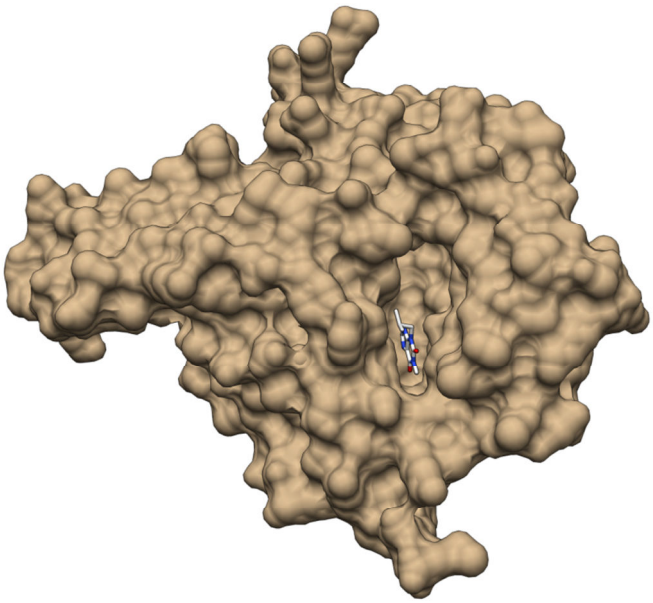

B

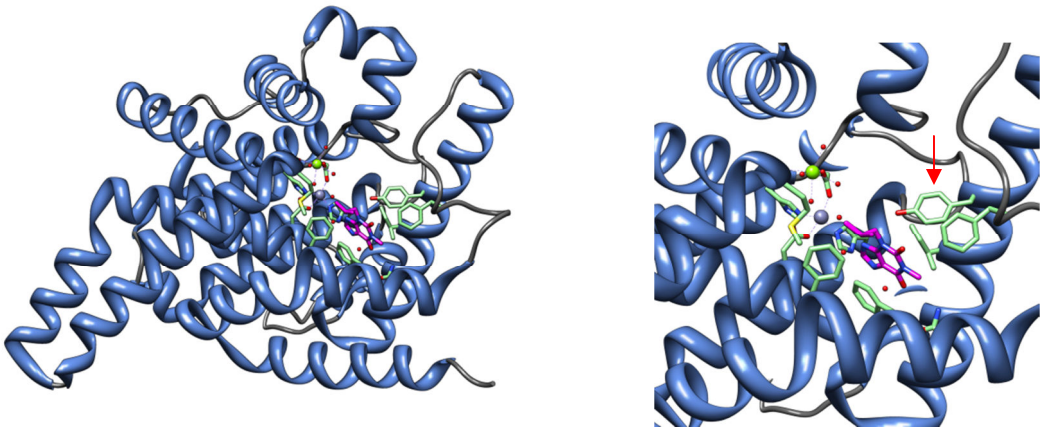

prostate and uterus. Rat PDE8B is particularly abundant in the brain and is not expressed in the thyroid gland (Kobayashi *et al*. 2003).

In a different study, the expression pattern of PDE7 and PDE8 in the brain was examined using *in situ* hybridization (Perez-Torres *et al*. 2003). Hybridization levels of PDE8A were low, whereas high levels of PDE7B and PDE8B expression was observed in hippocampal formation. When compared to control brains, PDE8B was found to be the only enzyme that shows a significant increase in cortical areas and parts of the hippocampal formation in Alzheimer's disease brains while its dependence on the disease rather than age should be addressed.

Finally, the expression profiles of ESTs listed under the human PDE8A Unigene Hs.9333 and PDE8B Unigene Hs.78106 demonstrate that these PDEs are present in most human tissues (Vasta. 2006).

Function

Studies for deciphering functions of PDE8 enzymes have been mostly limited by the unavailability of PDE8 selective inhibitors and knock-out animal models. One of the related studies suggested that PDE8A might play a role in activated lymphocytes or in T cell activation (Glavas *et al*. 2001). The Beavo lab previously had shown that PDE7A1 is up-regulated in human $CD4^+$ T cells and in a follow-up study they showed induction of PDE8A1 and PDE7A3 in human T lymphocytes when stiumulated with antibodies against CD3 and CD28. It has also been shown that PDE8A1 is constitutively expressed

in the human T-cell line Hut78 (Lerner and Epstein. 2006). In addition, PDE8 was identified as a new target for inhibition of chemotaxis of activated murine lymphocytes (Dong *et al*. 2006). The non-selective weak PDE8 inhibitor dipyridamole strongly inhibited migration of both concanavalin A stimulated and unstimulated splenocytes and PDE8A1 was upregulated following ConA stimulation.

The importance of PDE8 enzymes in steroid production was discovered upon the examination of PDE8 knock-out animals. Vasta *et al.* (2006) showed that Leydig cell function is altered by the loss of PDE8A. Leydig cells produce testosterone in the testis in response to lutenizing hormone (LH). They reported that PDE8A is expressed in Leydig cells and showed a 4 fold increase in the sensitivity of LH for testosterone production in the PDE8A knock-out mice. In another study, they observed that under fasting conditions triglyceride levels are increased in the liver of wild type mice while no increase is observed with PDE knock-out mice (Shimizu-Albergine *et al*. 2008).

In a recent study, analysis of ventricular myocytes from PDE8A knock-out mice suggests that PDE8A is a key modulator of cAMP signaling in this tissue since absence of this enzyme increases L-type Ca^{2+} channel currents and calcium transients (Patrucco *et al*. 2010).

PDE8B expression, as described above, is abundant and almost exclusively expressed in the thyroid with some additional expression in the brain (Hayashi *et al*. 1998a). Relevant to that, increased cAMP degradation has also been detected in autonomous thyroid

adenomas and PDE8B upregulation was noted in pituitary adenomas. Also, PDE8B gene variants are associated with alterations in serum TSH levels. PDE8B may thus provide a candidate target for the treatment of thyroid dysfunction (Arnaud-Lopez *et al*. 2008). Recently, some of the genetic abnormalities that predispose individuals to various adrenocortical tumors were found to be in the PDE family (Horvath *et al*. 2008b; Horvath *et al*. 2008a; Horvath and Stratakis. 2008). Mutations in PDE11A and PDE8B were detected in patients with isolated adrenal hyperplasia and Cushing syndrome (Stratakis. 2009). In another study related to insulin response, depletion of PDE8B levels in rat islets by siPDE8B increased insulin response to glucose by 70% and the potentiation is of similar magnitude during the first and second phase of insulin release (Dov *et al*. 2008). Most recently, an analysis of a PDE8B knock-out mouse model has demonstrated that PDE8B is a major regulator of steroidogenesis in the adrenal gland. The effect was also confirmed with cell lines treated with a newly published PDE8 inhibitor or an anti PDE8B shRNA construct (Tsai *et al*. 2010).

1.4 PDE INHIBITORS

As described in the previous section, PDEs are considered as good drug targets. Some compounds with PDE inhibitory activity have been therapeutically used for years. For instance, since the 19th century, caffeine has been known to be effective in asthma. We now know that caffeine also affects targets other than phosphodiesterases but being a weak inhibitor of PDEs it might exert some of its effects through cyclic AMP signaling. Likewise, natural compounds theophylline and papaverine have been used in the

treatment of several diseases. The success of these non-selective weak PDE inhibitors encouraged the development of more potent and selective PDE inhibitors.

1.4.1 Non-selective PDE Inhibitors

The early work by Earl Sutherland studying glucagon and epinephrine hormone action on phosphorylase activity in liver homogenates led to the discovery of a heat-stable nucleotide, cAMP as a second messenger (Rall and Sutherland. 1958). During these studies, it was discovered that caffeine, at high concentrations, increased the activity of phosphorylase enzyme and elevated the sensitivity to glucagon or epinephrine. This observation pointed out the presence of an enzyme that degrades cAMP and elevation of hormone sensitivity by caffeine could be explained by its inhibitory effect on this enzyme (Berthet *et al*. 1957). In 1962, Butcher and Sutherland clearly showed that methylxanthines such as caffeine, theobromine and theophylline inhibit cAMP hydrolysis (Butcher and Sutherland. 1962). These are the first identified non-selective PDE inhibitors, with IC_{50} values ranging from 100 to 1000 μM (Francis *et al*. 2011).

These methylxanthines provided an important starting point for the development of other alkylxanthines as PDE inhibitors such as 3-isobutyl-1-methylxanthine (IBMX). IBMX is considered as a general PDE inhibitor with IC_{50} values varying between 2-50 μM (Bender and Beavo. 2006) for multiple PDEs. Although it does not inhibit PDE8 and PDE9 families, it serves as an important pharmacological tool to implicate cyclic nucleotide signaling as playing a role in various biological processes.

Among the non-selective PDE inhibitors, papaverine and theophylline have been used therapeutically for years (Boswell-Smith *et al*. 2006). Like other non-selective inhibitors, they do not discriminate between different families and mostly have additional non-PDE targets. For instance, theophylline, caffeine and IBMX are also non-selective antagonists of adenosine receptors (Beavo and Reifsnyder. 1990).

Early studies of PDE-regulated processes used whole tissue homogenates and extracts, which were not suitable for finding isozyme specific inhibitors. The increased understanding and characterization of PDE isoforms along with knowledge acquired by their crystal structures has facilitated studies to search for isoform specific PDE inhibitors.

1.4.2 Selective PDE Inhibitors

Selective PDE inhibitors were initially identified by testing structurally related compounds of known non-selective inhibitors. For instance, 8-methoxymethyl IBMX can inhibit PDE1 enzymes with a 30-50 fold higher selectivity than other PDE isoforms (Wells and Miller. 1988). Similarly, erythro-9-(2-hydroxyl-3-nonyl)-adenine (EHNA) was found to be selective for the PDE2 family, although it also inhibits adenosine deaminase (Podzuweit *et al*. 1995).

Efforts to find isozyme selective inhibitors has also led to the discovery of the PDE3 inhibitors milrinone and cilostazol, which are used as drugs for acute treatment for cardiac failure and claudication respectively (Bender and Beavo. 2006; Lugnier. 2006).

On the other hand, the PDE4 specific inhibitor rolipram was first discovered as a compound with CNS activity and shown to be a potent cAMP-PDE inhibitor in the brain (Schneider *et al*. 1986; Torphy *et al*. 1992). Specific inhibition by rolipram was a point of reference in categorization of cAMP specific PDE isoforms as PDE4 family. Rolipram analogs such as piclamilast, cilomilast and roflumilast as well as benzyladenine derivatives have been developed as selective PDE4 inhibitors (George and Jeffrey. 2006). Most of the compounds developed as PDE4 inhibitors are associated with severe emetic response (Robichaud *et al*. 2002; Mori *et al*. 2010). In 2010, roflumilast was approved by European Commission for maintenance treatment of severe chronic obstructive pulmonary disease (Calverley *et al*. 2009; Fabbri *et al*. 2010), but failed to receive FDA approval.

Zaprinast, another alkylxanthine, also shows selectivity toward the PDE1, PDE5 and PDE6 families. It was initially designed for treatment of allergic diseases and showed vasorelaxant effects. This increased the focus on development of PDE5 inhibitors for various diseases relevant to vascular smooth muscle relaxation. Pfizer developed a more selective compound for PDE5 inhibition, sildenafil, for treatment of angina pectoris, whose side effect in clinical trials showed that it could be used in erectile dysfunction and led to the development of PDE5 specific compounds (vardenafil, tadalafil, udenafil) with less inhibitory effect on PDE6 as compared to sildenafil. Besides their effect on treatment of erectile dysfunction, PDE5 inhibitors are being tested for treatment of pulmonary

hypertension and Duchenne muscular dystrophy (Boswell-Smith *et al*. 2006; Lugnier. 2006).

For the PDE7 family, the only commercially-available selective inhibitor was BRL50481 until the discovery of the novel PDE7 inhibitor BC30 from Hoffman lab (Alaamery *et al*. 2010). Selective inhibitors for PDE9 and PDE10 families have been described by Pfizer (Verhoest *et al*. 2009a; Verhoest *et al*. 2009b). Recently, a PDE8 selective inhibitor –also developed by Pfizer- has been reported (Tsai *et al*. 2010; Vang *et al*. 2010).

1.4.3 Pharmacological Characteristics of PDE8

The PDE8 family is pharmacologically different from most other PDE families in that its enzymes are insensitive to IBMX (3-isobutyl-1-methyl-xanthine). IBMX is a broad spectrum inhibitor that affects the activity of all PDEs -except PDE8 and PDE9- with IC_{50} values of 2-50 μM. The non-selective PDE inhibitor papaverine weakly inhibits PDE8A at very high concentrations (174 μM), while the PDE5 inhibitor vardenafil inhibits PDE8A at 57 μM and the PDE3 inhibitor trequinsin inhibits PDE8B with IC_{50} of 2 μM. Dipyridamole, a weak selective inhibitor of PDE5 and PDE6, also inhibits PDE8A and 8B with 10 fold higher IC_{50} values (Fisher et al, 1998; Hayashi et al 1998). The PDE4 inhibitor cilomilast and L-826141 have been reported to have an inhibitory activity on PDE8s with an IC_{50} of 7 μM (Vasta, 2006).

Due to the absence of PDE8 inhibitors, dipyridamole has been used to assess PDE8 activity in various studies. However, besides being a better inhibitor of other PDEs

(PDE5 and 6), dipyridamole also inhibits adenosine deaminase and thus the results should be viewed skeptically. In late 2010, two reports used a novel PDE8 inhibitor developed by Pfizer. This compound, PF-4957325, has a low K_i value for PDE8A (0.7 nM) while it starts to inhibit other PDEs at higher concentrations (Tsai *et al*. 2010; Vang *et al*. 2010) (Figure 1.6).

Pharmacological Potential

The demonstrated role of PDE8A in the regulation of steroidogenesis in Leydig cells suggests that PDE8A inhibitors may be used to increase local production of testosterone in conditions associated with a deficit in testosterone production including andropause, idiopathic male infertility and metabolic syndrome. Also, in theory, a PDE8A activator would decrease Leydig cell sensitivity to LH and local production of testosterone, which can be used as male contraceptives or in treatment of prostate cancer (Vasta *et al*. 2006).

The pharmacological potential of modulators of PDE8 enzymes was previously explained by Vasta (Vasta. 2006) who suggested that PDE8A inhibitors could be utilized for the treatment of metabolic bone disease based on the detection of PDE8A in human osteosarcoma cell line MG-63 and in mouse osteoblastid cell line MC3T3-E1 as an increase in cAMP levels can promote osteoblastic differentiation. Similarly, a common pathophysiological mechanism of hyperthyroidism, thyroid and pituitary adenomas is the constitutive activation of the cAMP dependent mitogenic pathway. It has been proposed that an inhibitor might be beneficial to treat hypothyroidism; while activators of PDE8B

might help in pituitary adenomas and have therapeutic value in endocrine disorders. Also, expression of PDE8B in endometrial stromal cells, for which an increase in cAMP favors the uterine decidualization process and therefore supports egg implantation, might suggest it as a target as a therapy for endometrial development and implantation in subfertile women.

1.4.4 Approaches in PDE inhibitor discovery

As described earlier, the traditional starting point for development of selective inhibitors is either previously known PDE inhibitors or compounds that resemble cyclic nucleotides. These studies rely on classic medicinal chemistry approaches and use rational drug design based on the structure activity relationship to produce selective inhibitors (Manallack *et al*. 2005). The success of this approach is well documented by the development of sildenafil, where the structural analogy between cGMP and zaprinast was used to increase the selectivity for the PDE5 enzyme (Manallack *et al*. 2005; Terrett *et al*. 1996). Besides screening for the analogs of known PDE inhibitors, novel approaches such as fragment based or scaffold based lead generation are also being employed. Fragment based hits can be detected by protein crystallography and NMR (Carr *et al*. 2005), while a scaffold based approach utilizes high-throughput scintillation proximity assay followed by co-crystallography (Card *et al*. 2005). Recently, Naganuma *et al.* (2009) increased the selectivity of their lead compound to the catalytic domain of PDE4B over PDE4D using structure-activity relationship and Pfizer reported novel PDE10A- and PDE9A-specific inhibitors using structure based drug design (Verhoest *et*

al. 2009a; Verhoest *et al*. 2009b). All of these PDE inhibitor discovery methodologies can only identify the compounds that bind the active site since catalytic domain preparations and sequences are used in experimentation and design processes.

In this thesis, I developed a fission yeast based screening approach using the full length PDE8A that will detect compounds without any dependence on conserved PDE catalytic domain structure or known non-selective PDE inhibitors. By its nature, the compounds obtained from this chemical screen will be permeable to yeast cells and will show low toxicity since stimulation of growth is assessed. Compounds that promote growth are unlikely to promiscuously bind to other proteins, a lack of toxicity serves as a proxy for high specificity. In addition, since the measured phenotype is growth over the course of two days, the compounds from this screen should be chemically stable. In short, we believe a yeast growth based screen will result in better lead compounds for drug development than those selected by traditional approaches.

1.5 UTILIZATION OF YEAST AS A TOOL FOR STUDYING MAMMALIAN PDES

1.5.1 Use of Yeast to Study Mammalian Proteins

Besides serving as important model organisms for the study of biological processes in eukaryotes, the budding yeast *Saccharomyces cerevisiae* and the fission yeast *Schizosaccharomyces pombe* have been used as hosts for cloning of human genes by their ability to functionally complement a defective gene in the host yeast strain. For instance,

the human Cdc2 cyclin-dependent kinase gene was first cloned by its ability to suppress the temperature-sensitive growth of an *S. pombe cdc2*$^{-}$ mutant strain (Lee and Nurse. 1987). Yeast strains expressing human proteins are also used to study the function of the human protein and to identify mutations that alter function, as shown in a study of the p53 protein expressed in *S. pombe* (Bischoff *et al*. 1992). Use of yeast cells are also extended to cell growth based high-throughput screens which were successfully employed to find inhibitors of sirtuin NAD-dependent deacetylase (Grozinger *et al*. 2001), mammalian K^+ channel (Zaks-Makhina *et al*. 2004) and mammalian p38α kinase (Friedmann *et al*. 2006).

Previous studies with *S. cerevisiae* demonstrated the feasibility of working with mammalian PDE genes in a yeast system. *S. cerevisiae* expresses two PDE proteins, the Pde1 low-affinity enzyme and the Pde2 high-affinity enzyme (Nikawa *et al*. 1987a; Sass *et al*. 1986). Deletion of these two enzymes causes high cAMP levels, which interferes with the normal response to nutrient starvation and result in a heat shock sensitive phenotype in stationary phase cells. Complementation of PDE activity to restore heat shock resistance served as a basis for library screens to clone novel mammalian PDEs and led to the identification of the rat PDE4B and human PDE7A genes (Colicelli *et al*. 1989; Colicelli *et al*. 1991; Michaeli *et al*. 1993). In addition, the effect of PDE inhibitors could be assessed in the yeast by using heat shock sensitivity phenotype as shown by sensitivity of normally heat shock resistant PDE4B expressing strain to the PDE4 inhibitor rolipram (McHale *et al*. 1991; Pillai *et al*. 1993; Pillai *et al*. 1994; Torphy *et al*.

1992). This differential phenotype in heat shock sensitivity in the presence and absence of a PDE inhibitor was used by Colicelli lab to identify rolipram resistant PDE4B derivatives (Pillai *et al*. 1993). Thus, the use of yeast cells to study PDE enzymes is feasible since the enzymes are functional, show similar pharmacological properties as in mammalian cells and it is suitable to isolate compound insensitive PDE mutants. However, the utility of this system for large scale studies is limited due to the necessity of using significantly high concentrations of compounds to see the heat sensitivity phenotype and requirement of working with stationary phase cells.

In this study, we are using a cAMP-dependent growth phenotype in fission yeast *S. pombe* to study mammalian PDEs. As described in the next section, this growth phenotype, which successfully identified genes in the cAMP-dependent glucose sensing pathway via genetic screens, is more sensitive for the identification of chemical inhibitors of mammalian PDEs and hence it is suitable for high-throughput assays.

1.5.2 Cyclic AMP Signaling and *fbp1* Transcriptional Regulation in the Fission Yeast *S. pombe*

Both the budding yeast *S. cerevisiae* and the fission yeast *S. pombe* utilize G proteins and produce cAMP signals in response to glucose detection (D'Souza and Heitman. 2001; D'Souza *et al*. 2001; Hoffman. 2005a; Hoffman. 2005b; Lengeler *et al*. 2000; Thevelein and de Winde. 1999; Thevelein *et al*. 2000). In both yeasts, activation of adenylyl cyclase causes an elevation in cAMP levels, which is partially limited by the PDE enzyme

activity as a means of feedback regulation (Ma *et al*. 1999; Nikawa *et al*. 1987b; Wang *et al*. 2005).

Many components of the cAMP dependent glucose sensing pathway of the fission yeast have been discovered by studying mutants with defects in glucose repression of the *fbp1* gene, which encodes the gluconeogenetic enzyme fructose-1,6-bisphosphatase (Hoffman and Winston. 1990; Hoffman and Winston. 1991). The genetic identification of these mutants relied on the use of a reporter construct that expresses the *ura4* gene from the *fbp1* promoter. The *ura4* gene codes for the orotidine-5'-phosphate (OMP) decarboxylase enzyme that is required for uracil biosynthesis. However Ura4 and the Ura5 orotate phosphoribosyltransferase convert the pyrimidine analog 5FOA into a toxic form. Thus, in the presence of glucose wild type cells repress the reporter and in turn they cannot grow in medium lacking uracil. On the other hand, glucose insensitive transcript (*git*) mutants, which have defects in cAMP signaling, cannot repress the *fbp1* promoter even in the presence of glucose. Their constitutive expression of the *fbp1-ura4* reporter renders them able to grow in the absence of uracil while they become sensitive to 5FOA. Constitutive mutants include strains with defects in the Git3 G protein coupled receptor (GPCR) (Welton and Hoffman. 2000), any of the three subunits of a heterotrimeric G protein composed of the Gpa2 Gα (Nocero *et al*. 1994), the Git5 Gβ (Landry *et al*. 2000), and the Git11 Gγ (Landry *et al*. 2000; Landry and Hoffman. 2001), the Git2/Cyr1 adenylate cyclase (Hoffman and Winston. 1991), the Git1 adenylate cyclase binding protein (Kao *et al*. 2006), Hsp90 (Alaamery and Hoffman. 2008), the Git7 HSP90 co-

chaperone (Schadick *et al*. 2002), and the Pka1 PKA catalytic subunit (Jin *et al*. 1995). This reporter construct was also successfully used to identify negative regulators of PKA such as *cgs1*$^{+}$ that encodes the regulatory subunit of PKA and *cgs2*$^{+}$ that encodes the only PDE in *S. pombe*. Using the *fbp1* driven reporters, *cgs1*$^{-}$ mutations were identified in a genetic selection for suppressors of an adenylyl cyclase deletion allele (Stiefel *et al*. 2004), while *cgs2*$^{+}$ PDE gene mutations were identified in a genetic selection for suppressors of an activation defective form of adenylyl cyclase (Wang *et al*. 2005). In both selections, the *cgs1*$^{-}$ and *cgs2*$^{-}$ mutations restored 5FOA-resistant (5FOA^{R}) growth by increasing the PKA activity. Therefore, the use of *fbp1* driven reporters is beneficial in identifying mutations that either reduce PKA activity to stimulate growth in medium lacking uracil or increase PKA activity to stimulate growth in medium containing 5FOA. Since the selection is based on an increase in growth for both decreased and increased cAMP conditions, as opposed to 'no growth' phenotype, the screens were robust with low background. Recently, the successful use of this reporter in genetic screens has been extended to expedite high-throughput compound screens for chemical inhibitors of heterologously expressed PDEs.

1.5.3 The Use of *fbp1-ura4* Promoter for Screening for PDE Inhibitors

The cell growth based screen to detect PDE inhibitors was developed using the previously described glucose sensing pathway of the fission yeast. In this pathway, glucose is sensed by GPCR (Git3); which activates the Gpa2 Gα subunit of the heterotrimeric G protein Gαβγ (Gpa2-Git5-Git11). Upon activation of adenylyl cyclase

by Gpa2 (Gα), the glucose detection signal is conveyed inside the cell as elevated cAMP levels to activate cAMP dependent protein kinase A, which then represses *fbp1* transcription. One component of this pathway is Cgs2, the only PDE of the fission yeast. We replaced the *S. pombe* PDE (Cgs2) with mammalian orthologs by heterologous recombination into the *cgs2* locus. The two reporters expressed from the *fbp1* promoter (*fbp1-lacZ* and *fbp1-ura4*) allow us to study this pathway as well as the heterologously expressed mammalian PDEs (Figure 1.7).

The key to develop a strain suitable for high-throughput screen of PDE inhibitors lies in having a 5FOA sensitive strain as a starting point and in optimizing the growth conditions to achieve a differential growth phenotype in the absence and presence of potential inhibitors. An engineered 5FOA sensitive strain has sufficiently low levels of cAMP to allow expression from *fbp1-ura4* reporter. In the presence of a compound that inhibits PDE, there will be an increase in cAMP levels, which will cause repression of *fbp1*-driven transcription. Hence, in the presence of a PDE inhibitor, *ura4* is not expressed and the cells will be able to grow in 5FOA medium.

The Hoffman lab showed that introduction of minimal signaling defects can be sufficient to obtain 5FOA sensitivity for PDE4 and PDE7 enzymes, as the nature of the defect to yield 5FOA sensitivity rely on the level of cAMP hydrolytic activity of the mammalian PDE in the *S. pombe* system.

Figure 1.6 Structures of some PDE inhibitors

Structures of some PDE inhibitors are shown. (IBMX: 3-isobutyl-1-methylxanthine; EHNA: erythro-9-(2-hydroxy-3-nonly)adenine)).

Figure 1.6 Structures of some PDE inhibitors

PDE inhibitors with varying degrees of inhibition on PDE8

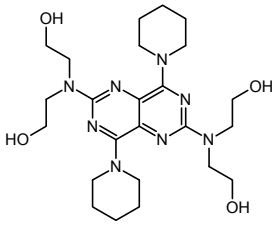

Dipyridamole

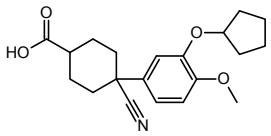

Cilomilast

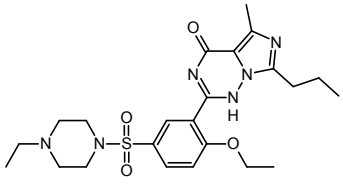

Vardenafil

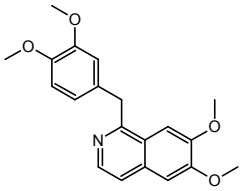

Papaverine

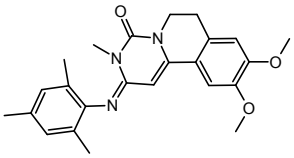

Trequinsin

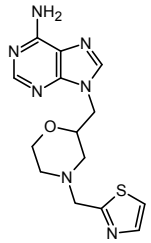

PF-4957325

PDE inhibitors that are ineffective against PDE8

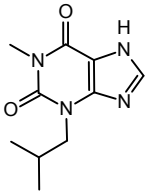

IBMX

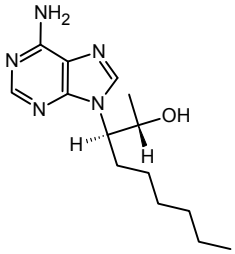

EHNA

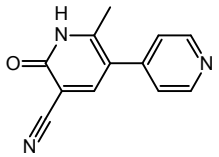

Milrinone

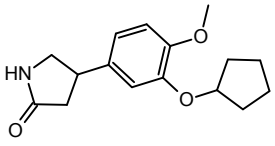

Rolipram

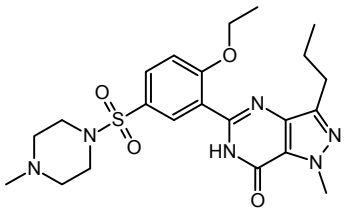

Sildenafil

Figure 1.7 Glucose sensing pathway of fission yeast

Glucose is detected through a GPCR and activates PKA as described in the text. Figure is drawn using ProteinLounge Pathway Builder Tool.

Figure 1.7 Glucose sensing pathway of fission yeast

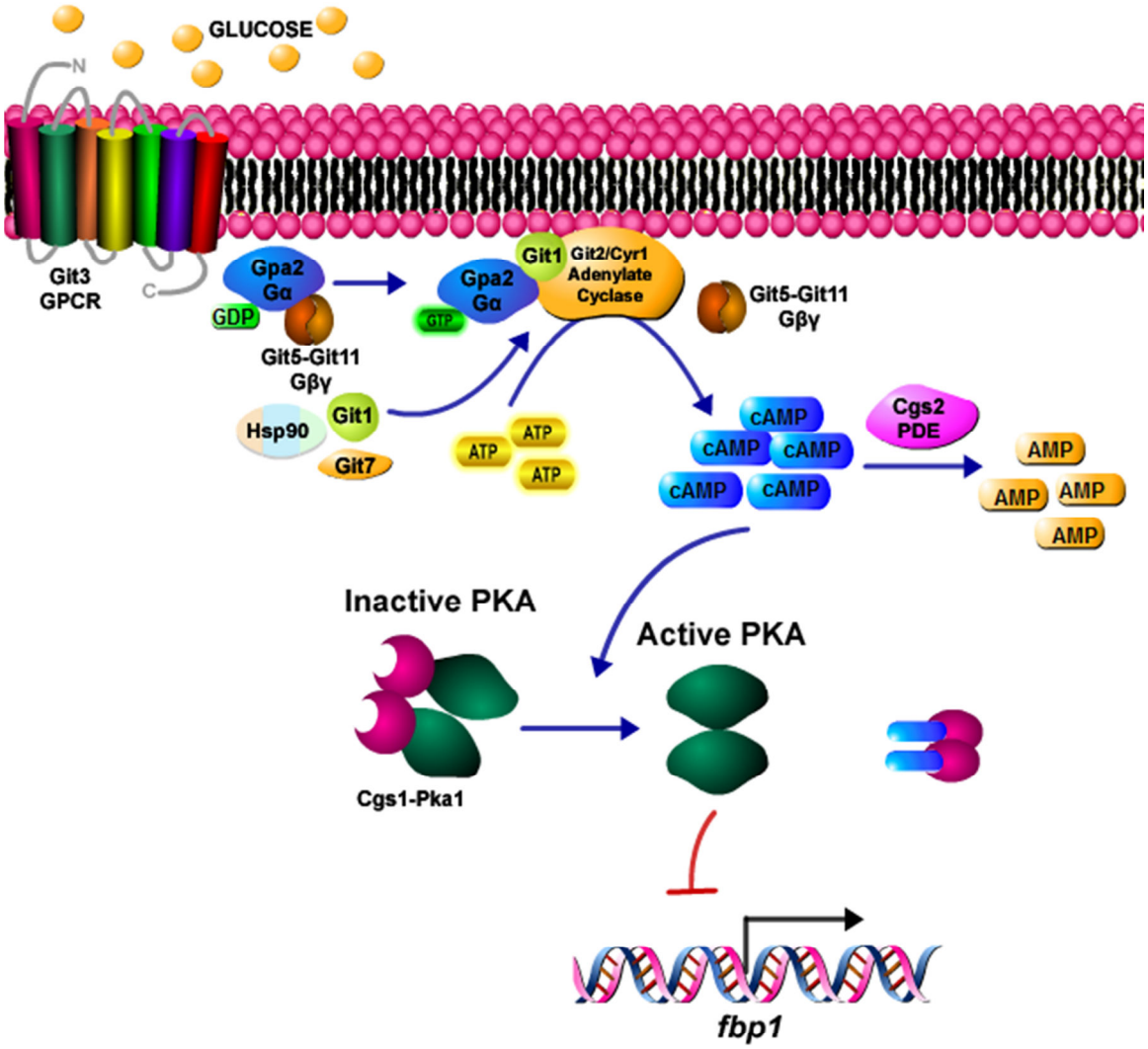

For example, a milder defect of deletion of *git11* (encodes for Gγ) is sufficient for a PDE4D3-expressing strain while a *gpa2* (Gα) deletion is required for PDE4A, PDE4B and PDE7A strains to confer 5FOA sensitivity. High-throughput screens with mouse PDE4A1, rat PDE4A5, mouse PDE4B3, human PDE7A1, and *S. pombe* PDE Cgs2 against 87,000 compounds were previously carried out at the Broad Institute. In these screens, the compounds that allowed 5FOA resistant growth with Z scores above 8.53 (the cutoff used by the Broad Institute's Chemical Biology Program) were considered as hits. Among these, previously known PDE inhibitors which included rolipram and zardaverine as PDE4 specific inhibitors were detected. Besides the known inhibitors; novel isoform selective PDE inhibitors, such as imperatorin being a PDE4B selective inhibitor and BC30 as a PDE7A inhibitor, were also discovered (Alaamery *et al*. 2010; Ivey *et al*. 2008).

On the other hand, for yeast strains expressing PDE8A, introduction of the aforementioned defects in the glucose sensing pathway are not enough to get a clean 5FOA sensitive phenotype. In this thesis, I will describe the development of a platform to screen inhibitors of PDE8A strain where a more drastic change in the glucose sensing pathway was successfully employed. This system worked well for detection of PDE8 inhibitors from a known collection of PDE inhibitors and optimized to give excellent screening conditions in high-throughput format, and eventually led to identification of novel PDE8 inhibitors. As with the PDE4 and PDE7 screen, compounds identified in this

screen show biological activity in mammalian cell culture assays even prior to further development via medicinal chemistry.

CHAPTER TWO

2 MATERIALS AND METHODS

2.1 MATERIALS

2.1.1 Yeast Strains and Growth Media

Yeast strains used in this study are listed in Table 2.1. The majority of the strains possess *fbp1::ura4*$^{+}$ and *ura4::fbp1-lacZ* reporters, which are translational fusions integrated at the *fbp1*$^{+}$ and *ura4*$^{+}$ loci, respectively (Hoffman and Winston. 1990) (Figure 2.1). Yeast was grown and maintained using yeast extract agar (YEA) and yeast extract liquid (YEL) (Gutz *et al*. 1974) supplemented with 100 mg/L adenine. Defined medium EMM (MP Biochemicals) was supplemented with required nutrients at 75 mg/L, except for L-leucine, which was at 150 mg/L. Sensitivity to 5-fluoro-orotic acid (5FOA) was determined on SC solid medium containing 0.4 g/liter 5FOA and 8% glucose as previously described (Hoffman and Winston. 1990). Liquid medium for 5FOA growth assays is the same as the solid medium, but without agar. Strain matings were performed on malt extract agar (MEA). Cells were grown at 30°C.

2.1.2 Bacterial Strains and Growth Media

ElectroTen-Blue® electroporation-competent cells (Agilent Technologies - Stratagene Products) were used as *Escherichia coli* host strain for plasmid amplification.

Table 2.1 Strain list

Strain	*Genotype*
CHP14	*h^+ fbp1::ura4$^+$ ura4::fbp1-lacZ leu1-32 ade6-M210 his7-366 cgs2-2 git3-14*
CHP861	*h^+ fbp1::ura4$^+$ ura4::fbp1-lacZ ade6-M210 his3-D1 leu1-32 gpa2::his3$^+$*
CHP870	*h^+ fbp1::ura4$^+$ ura4::fbp1-lacZ leu1-32 ade6-M210 his7-366 git3::GFP-kan*
CHP1113	*h^- fbp1::ura4$^+$ ura4::fbp1-lacZ leu1-32 his3D-1 pap1Δ::ura4 cgs2::PDE4B3 gpa2::his3$^+$*
CHP1148	*h^+ fbp1::ura4$^+$ ura4::fbp1-lacZ leu1-32 pap1Δ cgs2::PDE8A1 gpa2Δ::his3$^+$*
CHP1186	*h^+ fbp1-ura4$^+$ ura4::fbp1-lacZ leu1-32 git11Δ pap1Δ cgs2::PDE4D3*
CHP1189	*h^+ fbp1-ura4$^+$ ura4::fbp1-lacZ leu1-32 gpa2Δ pap1Δ cgs2::PDE7A1*
CHP1194	*h^+ fbp1::ura4$^+$ ura4::fbp1-lacZ leu1-32 pap1Δ git2Δ::his7$^+$ cgs2::PDE3B[LEU2$^+$]*
CHP1200	*h^- fbp1::ura4$^+$ ura4::fbp1-lacZ leu1-32 his7-366 git2Δ::his7$^+$ cgs2-2*
CHP1202	*h^+ fbp1::ura4$^+$ ura4::fbp1-lacZ leu1-32 his7-366 git2Δ::his7$^+$ cgs2::PDE8A1[LEU2$^+$]*
CHP1204	*h^- fbp1::ura4$^+$ ura4::fbp1-lacZ leu1-32 his7-366 pap1Δ git2Δ::his7$^+$ cgs2::PDE8A1[LEU2$^+$]*
CHP1205	*h^{90} fbp1::ura4$^+$ ura4::fbp1-lacZ leu1-32 his7-366 pap1Δ git2Δ::his7$^+$ cgs2::PDE8A1*
CHP1207	*h^- fbp1::ura4$^+$ ura4::fbp1-lacZ leu1-32 his7-366 pap1Δ git2Δ::his7$^+$ cgs2-2*
CHP1209	*h^- fbp1-ura4$^+$ ura4::fbp1-lacZ leu1-32 pap1Δ git3Δ cgs2::PDE7B1*
CHP1218	*h^+ fbp1::ura4$^+$ ura4::fbp1-lacZ leu1-32 pap1Δ git2Δ::his7$^+$ cgs2::PDE9A5*
CHP1220	*h^- fbp1::ura4$^+$ ura4::fbp1-lacZ leu1-32 his7-366 pap1Δ git2Δ::his7$^+$ cgs2::PDE1C4*
CHP1222	*h^- fbp1::ura4$^+$ ura4::fbp1-lacZ leu1-32 pap1D git2Δ::his7$^+$ cgs2::PDE1B1*
CHP1223	*h^- fbp1::ura4$^+$ ura4::fbp1-lacZ leu1-32 his7-366 pap1Δ git2Δ::his7$^+$ cgs2::PDE5A1*
CHP1224	*h^+ fbp1::ura4$^+$ ura4::fbp1-lacZ leu1-32 his7-366 pap1Δ git2Δ::his7$^+$ cgs2Δ::PDE11A4*
CHP1249	*h^- fbp1-ura4$^+$ ura4::fbp1-lacZ leu1-32 git3Δ pap1Δ cgs2::PDE3A*
CHP1262	*h^- fbp1-ura4$^+$ ura4::fbp1-lacZ leu1-32 gpa2Δ pap1Δ cgs2::PDE4A1*
CHP1265	*h^- fbp1::ura4$^+$ ura4::fbp1-lacZ leu1-32 his3-D1 pap1Δ gpa2Δ cgs2-2 gpa2Δ::his3$^+$*
CHP1268	*h^- fbp1-ura4$^+$ ura4::fbp1-lacZ leu1-32 git3Δ pap1Δ cgs2::PDE4B2*
CHP1346	*h^+ fbp1::ura4$^+$ ura4::fbp1-lacZ leu1-32 pap1Δ cgs2-2*
CHP1403	*h^- fbp1::ura4$^+$ ura4::fbp1-lacZ leu1-32 pap1Δ git2Δ::his7$^+$ gpa2Δ cgs2D::PDE2A2*
DDP13	*h^+ fbp1::ura4$^+$ ura4::fbp1-lacZ leu1-32 ade6-M210 cgs2::PDE8A[LEU2$^+$] gpa2::his3$^+$*
DDP26	*h^- fbp1::ura4$^+$ ura4::fbp1-lacZ leu1-32 cgs2::PDE4A1 gpa2::his3$^+$*
DDP38	*h^- fbp1::ura4$^+$ ura4::fbp1-lacZ leu1-32 his3-D1 pap1Δ gpa2Δ cgs2-2 gpa2Δ::his3$^+$ ars1(EcoRI)::pNMT1-PDE8Acatalytic*
DDP40	*h^+ fbp1::ura4$^+$ ura4::fbp1-lacZ leu1-32 pap1Δ cgs2-2 ars1(EcoRI)::pNMT1-PDE8Acatalytic*
DDP42	*h^- fbp1::ura4$^+$ ura4::fbp1-lacZ leu1-32 his3-D1 pap1Δ gpa2Δ cgs2-2 gpa2Δ::his3$^+$ ars1(EcoRI)::pNMT41-PDE8Acatalytic*
DDP44	*h^+ fbp1::ura4$^+$ ura4::fbp1-lacZ leu1-32 pap1Δ cgs2-2 ars1(EcoRI)::pNMT41-PDE8Acatalytic*
DIP72	*h^{90} fbp1::ura4$^+$ ura4::fbp1-lacZ leu1-32 ade6-M210 cgs2::PDE4B3 gpa2::his3$^+$*
JZ666	*h^{90} leu1$^-$ ade6-M216 cgs2::ura4$^+$ ura4-D18*
LWP98	*h^+ fbp1::ura4$^+$ ura4::fbp1-lacZ leu1-32 ade6-M216 his3-D1 cgs2-2 gpa2::his3$^+$*

Figure 2.1 Translational fusions for monitoring cAMP dependent growth

(A) Translational fusions *fbp1::ura4*$^{+}$ and *ura4::fbp1-lacZ* were used to monitor cAMP dependent glucose sensing pathway. **(B)** The phenotypes associated with wild type, *git* mutants and *cgs2* mutants under 8% glucose (repressed) conditions are indicated.

Figure 2.1 Translational fusions for monitoring cAMP dependent growth

A

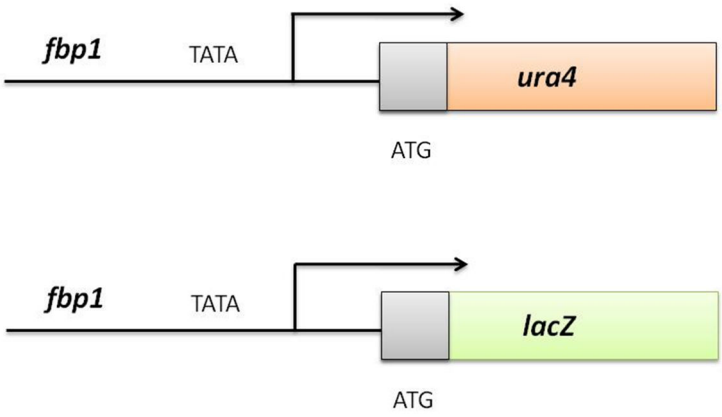

B

	Phenotype under repressed conditions		
Genotype	5FOA	Ura	β-galactosidase
Wild type	$5FOA^R$	Ura^-	Low β-gal
git mutant	$5FOA^S$	Ura^+	High β-gal
cgs2 mutant	$5FOA^R$	Ura^-	Low β-gal

Cells were grown in Luria Bertani (LB) broth (1% tryptone, 0.5% yeast extract, 1% NaCl) and transformants were selected on 100 mg/L ampicillin containing LB media. Cells were grown at 37°C.

2.1.3 Enzymes

All restriction endonuclease digestion enzymes and buffers were obtained from New England Biolabs. AccuPrime™ (Invitrogen), Herculase II Fusion DNA Polymerases (Agilent Technologies) and FailSafe™ PCR System (Epicentre Biotechnologies) enzymes were used in PCR amplification reactions.

In vitro phosphodiesterase assays were performed using full length, recombinant human PDE8A1 (USBiologicals or BPS Bioscience), partially purified full length human recombinant PDE8B (Scottish Biomedical), catalytic domain of human PDE7A (Biomol International) and catalytic domain of PDE4A10 (generously provided by Drs. H. Wang and H. Ke).

2.1.4 Compound Libraries

High throughput screening was performed against chemicals from the Harvard Medical School ICCB-Longwood compound collection. As known bioactives collections; NINDS Custom Collection 2, Biomol 3- ICCB Known Bioactives and Prestwick 1 Collection were screened. Commercial Libraries from Asinex 1, Biomol-TimTec1, Bionet 1, Bionet 2, CEREP, ChemBridge 3, ChemDiv 1, ChemDiv 2, ChemDiv 3, ChemDiv 4, ChemDiv 6, Enamine 1, Enamine 2, I.F. Lab 2, Life Chemicals 1, MayBridge 1, MayBridge 2,

MayBridge 3, Maybridge 4, Maybridge 5, MixCommercial Plate 1, MixCommercial Plate 2, MixCommercial Plate 3, Mix Commercial Plate 5, Peakdale 1 collections were screened as well as natural product extracts from the following collections; ICBG 4 Fungal Extracts, ICBG 5 Fungal extracts, ICBG-12 Fungal Extracts, MMV 1, MMV 2, MMV 3, NCDDDG 1, NCDDG 3, NCDDG 5, NCDDG2, STARR Foundation2-Extracts, Organic Fractions-NCI Plant and Fungal Extracts (Table 2.2).

2.1.5 Small Molecules

Small molecules were purchased from A.G. Scientific, Sigma, Tocris Bioscience, Specs, Maybridge, ChemDiv, ChemBridge, Enamine, Asinex, Aldrich Chemistry.

2.1.6 Assay Kits

Cyclic AMP levels were determined using an enzyme immunoassay kit from Assay Designs. Progesterone levels were quantified by Neogen or Oxford Biomedical Research immunoassay kits. Testosterone and pregnenolone detection was performed using Neogen and Diagnostics Biochem Canada Inc ELISA kits, respectively. Lastly, IL-2 assays were performed using an ELISA kit from R&D Systems.

2.2 METHODS

2.2.1 Strain Construction

Murine PDE8A1 was integrated into the chromosome under the *cgs2* promoter in two steps. First, it was amplified by PCR using oligonucleotides containing approximately 60

Table 2.2 Screened compound libraries

Commercial	Known Bioactives
ActiMolTimTec1	BIOMOL ICCB Known Bioactives 2
Asinex 1	NINDS Custom Collection 2
Bionet1	Prestwick1 Collection
Bionet (Ryan Scientific) 2	
CEREP	**Natural Products**
ChemBridge3	ICBG Fungal Extracts 12
ChemDiv1 (Combilab and International)	ICBG Fungal Extracts 4
Chemical Diversity 2	ICBG Fungal Extracts 5
ChemDiv3	Medicines for Malaria Venture
ChemDiv4	Medicines for Malaria Venture 2
ChemDiv6	Medicines for Malaria Venture 3
Enamine 1	NCDDG1
Enamine 2	NCDDG2
IFLab2	NCDDG3
Life Chemicals 1	NCDDG5
Maybridge1	Organic NCI Plant and Fungal Extracts
Maybridge2	Starr Foundation Extracts 2
Maybridge3	
Maybridge4	
Maybridge5	
Mixed Commercial Plate 1	
Mixed Commercial Plate 2	
Mixed Commercial Plate 3	
Mixed Commercial Plate 5	
Peakdale1	

nucleotides of sequence flanking the *S. pombe cgs2* gene and incorporated into the pKG3-ura4 plasmid by gap repair transformation. A restriction fragment from this plasmid that possesses about 500 bp of *cgs2* sequences flanking PDE8A was used to insert PDE8A into *cgs2* locus by homologous recombination. The homologous integration was confirmed by PCR. Standard genetic crosses and tetrad dissection were used to introduce *fbp1-lacZ* and *fbp1-ura4* reporter genes, *pap1Δ* allele and mutant alleles of components of cAMP signaling pathway such as *git3Δ*, *gpa2Δ*, *git2-2*.

2.2.1.1 Gap Repair Transformation

An overnight culture of cells were grown to log phase in YEL, refreshed by the addition of an equal volume of YEL and and grown 3-4 more hours before harvesting. Pelleted cells were washed twice with sterile distilled water and once with 1X LiAC/TE buffer. The cells were resuspended in LiAC/TE buffer to a density of ~10^8 cells/mL. 2 µL of denatured salmon sperm DNA, 3 µL of *StuI* linearized pKG3-ura4 plasmid, 7-10 µL of cleaned and concentrated PCR product were added in 100 µL of cell suspension and were incubated at room temperature for 10 minutes. After addition of 260 µL of 40 % PEG / LiAC-TE buffer, the cell suspension was further incubated for 1 h at 30°C. The cells were then treated with 43 µL DMSO and heat shocked at 42°C for 5 minutes. Gently pelleted cells were resuspended in 300-1000 µL distilled water and plated out on EMM-Leu selective medium.

Cloning of full length PDE8A into pKG3-ura4 plasmid was performed using host strain JZ666 that lacks PDE activity. Plasmid pKG3-ura4, which carries *cgs2* sequence

disrupted with *ura4* gene, was linearized within the *ura4* sequence and co-transformed with the PCR product to facilitate insertion of PDE8A into the *cgs2* locus. Transformants were selected on EMM-Leu medium. The phenotypic screening for functional PDE activity was performed where applicable.

The strain that expresses the catalytic domain of PDE8A was constructed by amplifying and cloning a 1325 bp region of the PDE8A gene into *EcoR*I-linearized pNMT1 and pNMT41 vectors via gap repair transformation. The recipient strain was also JZ666 and iodine staining of colonies grown on EMM-Leu plate was used as an assessment of PDE activity, which increases mating and thus iodine staining.

2.2.1.2 Plasmid Rescue from Yeast (Smash and Grab)

Cells were grown on EMM-Leu medium and collected by resuspending cells in sterile distilled water. Cells were collected by microcentrifugation and resuspended in 200 µL Smash and Grab buffer, 200 µL phenol-chloroform and 0.3 g glass beads and vortexed for 3 minutes as previously described by (Hoffman and Winston. 1987). Upon centrifugation for 5 minutes, the supernatant was collected. Prior to electroporation into *E. coli* cells, the plasmid mixture was cleaned by treating with equal volume of chloroform followed by isopropanol precipitation.

2.2.1.3 Transformation into *E. coli* and plasmid amplification

Ten microliters of ElectroTen-Blue® electroporation-competent cells were mixed with 1-2 µL of transforming DNA and volume was completed to 100 µL. Cells were

electroporated in 1mm gap electroporation cuvettes (Fisher) under 2250 Volts, 22.5 kV/cm, 200 ohm, 25 μF. Electroprated cells were immediately mixed with 900 μL of LB broth and incubated at 37°C for 90 minutes before being plated out in LB-Ampicillin selective media.

Single *E. coli* colonies were inoculated into LB medium and cultured overnight for plasmid amplification. Plasmids were isolated from *E. coli* cells using QIAprep Spin Miniprep Kit (Qiagen) according to manufacturer's instructions.

2.2.1.4 Knock-in Transformation by Integrating into the Chromosome

The yeast transformation was performed as described for gap repair transformation. As the transforming DNA, 10-15 μL of target DNA that has flanking sequences to the intended locus of integration was used.

For full length PDE8A integration, gap repaired plasmid that possess PDE8A was digested with restriction enzymes *Xho*I and *Pac*I and used as the transforming DNA. As the recipient strain, JZ666, which carries a *ura4*$^+$-marked disruption of *cgs2*$^+$, was used. After transformation, cells were grown overnight in YEL before being plated onto 5FOA medium. As a parallel experiment, an enrichment step was incorporated by growing cells in PM complete medium with 0.1% glucose and 3% glycerol for 2 days before plating onto 5FOA medium in order to render growth advantage to cells expressing functional phosphodiesterase. Transformants were then transferred to EMM-his plates by replica

plating and screened for sporulation, which is a phenotype associated with regained PDE activity, i.e. low cAMP levels, in the recipient host strain lacking Cgs2.

The catalytic domain of PDE8A was cloned into the *S. pombe* genome using strains CHP1265 and CHP1346 as hosts. The *Blp*I-linearized plasmid that possesses PDE8A catalytic domain under *nmt1* and *nmt41* promoters was integrated into the *ars1* region. Stable integrants were selected by picking Leu^+ colonies after subsequent replica plating of transformants onto YEA plates to allow for loss of autonomous plasmids.

2.2.1.5 Strain Mating and Tetrad Dissection

Matings were performed by mixing and plating freshly grown parent strains onto MEA plates. Followed by 1-2 days of incubation at 30°C, the cells were transferred onto a YEA plate and zygotic asci were individually selected and separated from other cells by the aid of a needle dissector. The cells were incubated at 37°C for 2-3 hours for ascus wall break down. Each spore from a single zygotic ascus was placed apart from each other in an orderly fashion and grown for a few days until they formed visible colonies. The tetrads were scored for the chosen phenotypes by replica plating onto selective media. Where no growth phenotype is available, colony PCR was performed. The presence of *fbp1-lacZ* fusion protein was detected by X-gal filter lift assay.

2.2.1.6 X-gal Filter Lift

Colonies freshly grown on YEA plates were replica plated onto nitrocellulose membrane. The membrane was submerged in liquid nitrogen for one minute and allowed to thaw. 2.5

mL of Z buffer was mixed with 150 µL X-gal substrate (5-bromo-4-chloro-3-indolyl-beta-D-galactopyranoside, 20 mg/ mL) in a Petri dish and a filter paper was placed inside. The thawed membrane was put on the filter paper with cell side up and incubated at 30°C for 10-30 minutes until the color development was observed. LacZ expressing colonies turn to blue.

2.2.1.7 Colony PCR

Colony PCR reactions were carried out using the Failsafe enzyme and buffer system according to the manufacturer's instructions. PCR reaction mixture was prepared without the template and enzyme. As template, a pin head size of freshly grown cells were transferred into each reaction tube by the aid of a pipette tip and incubated at 98°C for 10 minutes. The enzyme was added after this incubation step and regular PCR reaction was carried out.

2.2.2 β-Galactosidase Assays of *fbp1-LacZ* Expression

Beta galactosidase assays were performed on mid-log phase cultures that were pregrown in cAMP containing EMM media prior to compound treatment. After pregrowth, cells were washed in EMM and subcultured in EMM with compounds for 24 hours at 30°C aiming for mid log phase cultures. Cells were collected and the pellet was washed with water before being resuspended in breaking buffer. The cell extracts were prepared by vortexing with glass beads as previously described (Nocero *et al*. 1994). The activity of the extracts was determined by the rate of the yellow color development from ONPG

(*ortho*-Nitrophenyl-β-galactoside) substrate at 28°C. The reactions were stopped by addition of 1 M sodium carbonate and optical density was measured at 420 nm. The beta galactosidase specific activity of the extracts was quantified with respect to the total soluble protein concentration, which was determined using BCA protein assay kit (Pierce).

2.2.3 5FOA Growth Assay

Cyclic nucleotide dependent 5FOA growth response of cells was monitored in 50 µL 5FOA medium in 384-well microtiter plates (untreated, flat clear bottom). Cells were inoculated at an initial cell density of 0.5-2 x 10^5 cells/ mL. Pregrowth conditions of each strain were optimized in order to repress the *fbp1-ura4*$^+$ reporter prior to inoculation into 5FOA medium. This is most often achieved by subculturing exponential phase cells in EMM complete medium containing cAMP. The plates were then incubated at 30ºC for 48 hours in airtight containers that have moist paper towels. At the end of incubation, plates were vortexed in a microtiter dish vortexer and optical densities were measured at 600 nm using a plate reader (SpectraMax Plus).

2.2.4 Low-Throughput Screening of Compounds

Fifty-six compounds identified as inhibitors of PDEs from high-throughput screens against PDE4 and PDE7 enzymes were tested against a PDE8A-expressing strain (CHP1204). The experiments were performed with 0.5 mM cAMP in pregrowth medium and 40 µM cAMP in 5FOA. The compounds were tested at three different concentrations

of compounds (100, 50 and 25 μM) using eight different wells per condition (Figure 2.2). As a positive control, a PDE4B3-expressing strain (CHP1113) was used. Medium containing 1% DMSO was used as a negative control, while medium containing 1% DMSO and 5 mM cAMP was used as a positive control. As an internal positive control for the growth of a PDE4B3-expressing strain, 20 or 40 μM of rolipram was added to the medium. For each strain two independent cultures were used.

2.2.5 Z Factor Test

The suitability and quality of the assay conditions for high throughput format was evaluated by Z factor test as previously described by Zhang et al (1999). The Z factor coefficient ($z = 1 - \frac{3(\sigma_p+\sigma_n)}{|\mu_p-\mu_n|}$; where σ_p and σ_n are standard deviations of positive and negative controls, μ_p and μ_n are means of positive and negative controls, respectively) was calculated as a function of mean values and standard deviations of both negative and positive control values in order to reflect both the assay signal dynamic range and the data variation associated with the signal measurements. For PDE8A strains, DMSO (0.2%) was used as negative control while 5 mM cAMP or 10 or 20 μM of BC69 was used as positive control. 96 or 192 wells were used for both negative and positive control conditions for each assay.

Figure 2.2 Plate layout for high-throughput screening assays

Plate layouts for control plate and an experimental plate were indicated using actual data plates. The half of the master control plate contains DMSO while second half has 5 mM and 10 mM BC69. An experimental plate contains four wells filled with 5FOA with 0.2 % DMSO and four wells filled with 20 μM BC69, which were added after or before pinning process. The location of the in-plate controls varies in some plates depending on the empty wells in the chemical library plate.

Figure 2.2 Plate layout for high-throughput screening assays

A Master control plate for pinning

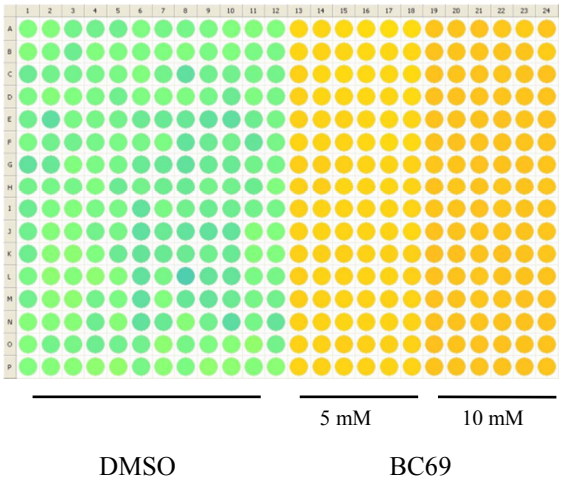

B Experimental plate with in-plate controls

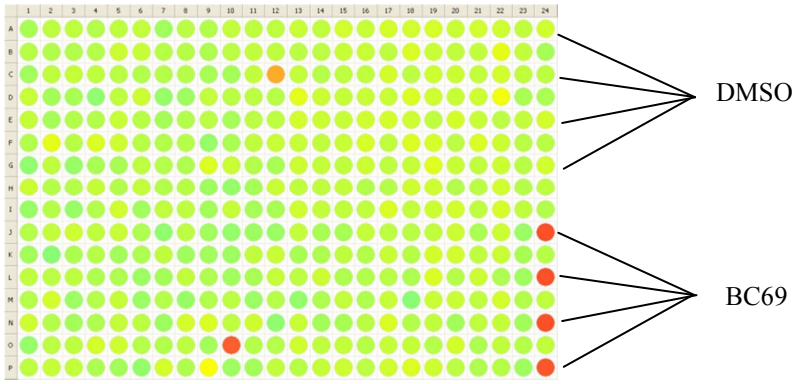

2.2.6 High-Throughput Screening

The cultures were pregrown in EMM complete medium containing 0.5 or 1 mM cAMP for CHP1204 (full length PDE8A) and DDP40 (catalytic domain of PDE8A), respectively. After delivery of 25 µL of SC-based growth medium containing 0.4 g/L 5FOA into each well of 384-well microtiter dishes (untreated, with flat clear bottoms), 100 nL compounds were pinned. Cells were then transferred into the microtiter plates at a final density of $0.5x10^5$ cells/mL or $1x10^5$ cells/mL for CHP1204 and DDP40, respectively. The 5FOA medium used for CHP1204 strain also contains 40 µM final concentration of cAMP since the strain is deleted for adenylyl cyclase. As control, a master plate containing DMSO and 5 mM and 10 mM BC69 (a compound identified as a positive control in the low-throughput screen) was prepared and used for pinning as appropriate. Other positive control dishes contained 5mM cAMP in the 5FOA medium. In addition, each plate contained four wells containing 0.2 % DMSO in the medium and four wells containing 20 µM BC69 in the medium as in-plate negative and positive controls (Table 2.3). Cultures were grown for 48 hours at 30ºC, sealed in an airtight container with moist paper towels to prevent evaporation. Optical density (OD_{600}) of each well was measured using Wallac Envision plate reader (Figure 2.3).

2.2.7 Dose Response Profiling of Compounds

Dose response profiling of compounds was performed in 5FOA medium with compound concentrations in a range of 4 orders of magnitude starting from 100 µM and performing 2/3 dilutions in 18 consecutive columns until obtaining 0.101 µM. Cells were added in 25

µL volume on top of 25 µL of 2X compound containing medium to achieve 50 µL final volume in each well. Plate incubations and OD measurements were performed according to standard 5FOA assay procedure as described.

In order to profile different phosphodiesterases (PDE) against a given compound, 16 different strains expressing different PDEs were used. The pregrowth condition and initial cell density for each strain was previously optimized by Hoffman lab members as indicated in Table 2.3.

2.2.8 *In vitro* PDE Assay

In vitro PDE assays were performed as previously described by Wang (Wang *et al*. 2005). This technique depends on measurement of the rate of substrate depletion by counting the amount of unreacted ^{3}H-cAMP after the reaction product (5'-AMP) is differentially precipitated with barium hydroxide. For Michaelis-Menten kinetics experiments, the reactions were performed in 50 mm Tris·HCl (pH 8.5), 10 mM $MgCl_2$ or 4 mM $MnCl_2$, 5 mm dithiothreitol, and 10 nM ^{3}H-cAMP with varying concentrations of cold cAMP in the presence of inhibitors or DMSO for 30 minutes. The reactions were stopped with 200 µL 0.2 M $ZnSO_4$ and 5'-AMP was precipitated with 200 µL 0.25 N $Ba(OH)_2$ by centrifugation for 15 minutes at 14000 rpm. The remaining radioactivity in the supernatant was quantified in 4 mL of scintillation fluid with Perkin Elmer liquid scintillation analyzer (Tri-Carb 2900 TR). The half maximal inhibitory concentration (IC_{50}) of inhibitors was determined using 5-11 different concentrations of compounds at a fixed cAMP concentration.

Table 2.3 Optimized growth conditions for 5FOA assays

PDE	Pregrowth supplement	Cyclic nucleotide in 5FOA medium	Cell density ($x10^5$ cells/mL)
PDE1B	2.5 mM cAMP	15 μM cAMP	0.5
PDE1C	2.5 mM cAMP	15 μM cAMP	0.5
PDE2A	0.25 mM cAMP	15 μM cAMP	2.0
PDE3A	5.0 mM cAMP	NA	1.0
PDE3B	0.25 mM cAMP	33 μM cGMP	2.0
PDE4A	5.0 mM cAMP	NA	2.0
PDE4B	5.0 mM cAMP	NA	2.0
PDE4D	200 μM rolipram	NA	1.5
PDE5A	0.25 mM cAMP	200 μM cAMP	2.0
PDE7A	2.5 mM cAMP	NA	1.0
PDE7B	2.5 mM cAMP	NA	1.0
PDE8A	0.5 mM cAMP	40 μM cAMP	0.5
PDE8A catalytic	20 μM BC69	NA	1.0
PDE9A	0.25 mM cAMP	600 μM cGMP	2.0
PDE10A	0.25 mM cAMP	15 μM cAMP	2.0
PDE11A	0.25 mM cAMP	50 μM cGMP	0.75

Figure 2.3 High-throughput screening process

High-throughput screening process starts with filling the plates with 25 µL 5FOA medium. After the delivery of 100 nL of tested compounds, cells were delivered at the optimized density. Optical density was read after 2 days of growth at 30ºC.

Figure 2.3 High-throughput screening process

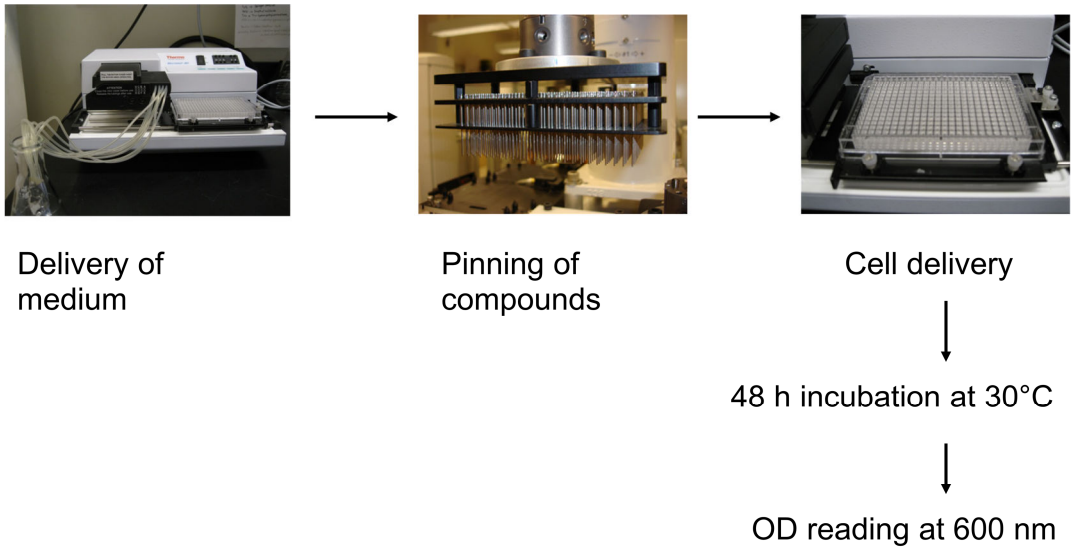

2.2.9 Measurement of Steroid Release from Mouse Leydig Tumor Cells

The mouse Leydig tumor cell line MA-10 was used to test the effect of PDE8A inhibitors on steroidogenesis. Since these cells express very low or undetectable amounts of P450c17, the enzyme with 17 alpha-hydroxylase and 17,20 lyase activities in the synthesis of steroid hormones, the major steroid output of the cells is progesterone. MA-10 cells were seeded in 24 or 48 well plates to achieve 60-80% confluency after 2-3 days in RPMI medium. Cells were washed and incubated with serum free medium for 2 hours before compound treatment. The basal progesterone levels were determined by collecting the media after 3h of inhibitor treatment in a 5% CO_2 incubator at 37°C. In order to determine the effect of the compounds in the presence of LH hormone, cells were treated with 3 ng/mL recombinant LH for 2 hours following a 2h pre-incubation with compounds. The media was collected and progesterone levels were quantified with ELISA kit for progesterone detection.

2.2.10 Measurement of Testosterone Production From Primary Leydig Cells

Leydig cells were isolated from testes of wild type and PDE8A/B knock out adult mice as previously described (Vasta et al., 2006). Immediately upon isolation, Leydig cells were resuspended in DMEM/F-12 medium supplemented with 1% BSA and 150 µL aliquots were dispensed in 48-well plates. After a few hours of incubation at 37°C to allow cell attachment, 30 µL of media with test compounds were added in duplicate wells to obtain 10 and 40 µM final concentration. The media were collected after 3 hours of incubation.

The amount of testosterone released into the media was measured by an ELISA kit from Neogen.

CHAPTER THREE

3 DEVELOPMENT OF A FISSION YEAST BASED SCREENING PLATFORM FOR IDENTIFICATION OF PDE8 INHIBITORS

In recent years, several studies began to uncover the functional roles of PDE8A and PDE8B enzymes especially in steroid formation in the Leydig cells or adrenal glands. However, the absence of commercially available PDE8-specific chemical inhibitors limits the ability of scientists to study these enzymes that may eventually serve as therapeutic targets. In this study, we aim to develop a fission yeast screening platform in order to identify PDE8 inhibitors.

3.1 CONSTRUCTION OF PDE8A EXPRESSING STRAINS

Full length mouse PDE8A gene was incorporated into the yeast genome in two steps. Firstly, the mouse PDE8A gene was PCR-amplified with PDE8A specific primers that contain *cgs2* (yeast PDE) complementary flanking regions and inserted into plasmid pKG-ura4 by gap repair transformation. Then, a restriction fragment from the gap repaired plasmid containing PDE8A with 500 bp *cgs2* flanking sequence was used for direct homologous recombination into the strain JZ666 (*cgs2*::*ura4*$^{+}$) (Figure 3.1.). In order to enrich for the desired transformants, transformation was followed by allowing cells to grow to stationary growth before cells were plated into the 5FOA medium. The cells that contain a functional PDE should be able to sense the starvation cues (i.e. have

lower cAMP levels as compared to PDE-lacking cells that have high basal cAMP levels) and would have a growth advantage compared to the host strain. This approach helped to identify colonies that express PDE8A. Although PDE8 expression did not yield a very strong mating competent phenotype, transformants were screened for their ability to sporulate in starvation medium and the candidates were confirmed to carry PDE8A by PCR. The strain expressing PDE8A from the *cgs2* locus was crossed with other strains to introduce the *fbp1::ura4*, *ura4::fbp1-lacZ* reporter genes and a *pap1* deletion to enhance drug sensitivity. Strains with different mutations in the glucose sensing pathway (i.e. glucose insensitive transcript mutants, *git*) were constructed in order to vary cAMP synthesis and generate different degrees of 5FOA sensitivity. When the strain expressing PDE8A in JZ666 background was crossed with CHP14 (*fbp1::ura4*, *ura4::fbp1-lacZ*, *git3-14*) and CHP870 (*fbp1::ura4*, *ura4::fbp1-lacZ*, *git3::GFP-Kan*), the PDE8A containing progeny turned out to be 5FOA resistant. This shows that in the fission yeast system, PDE8A is less active than Cgs2 so that there is a relatively higher level of cAMP to repress *fbp1-ura4* expression, which confers 5FOA resistance. On the other hand, when *gpa2* deletion was introduced to the PDE8A strain, partial sensitivity to 5FOA was observed in solid medium.

The strain expressing the catalytic domain of PDE8A was constructed as follows. First, a 1325 bp region of the PDE8A gene (including codons 443 to 824) was amplified and cloned into *Eco*RI-linearized pNMT1 and pNMT41 vectors via gap repair transformation. The PDE activity was assessed by iodine staining on EMM-Leu selective media.

Figure 3.1 Construction of a PDE8A-expressing strain

PDE8A was cloned into the yeast genome in two steps. **(A)** Mouse PDE8A PCR product with complementary *cgs2* sequences was cloned into linearized pKG3-ura4 plasmid by gap repair transformation. This step resulted in a plasmid that carries the PDE8A gene with *cgs2* flanking sequences. **(B)** Restriction digest of PDE8A from the gap-repaired plasmid resulted in a DNA fragment containing longer *cgs2* complementary sequences, which was used for homologous recombination of the PDE8A gene into the *cgs2* locus.

Figure 3.1 Construction of a PDE8A expressing strain

A) **Gap repair transformation**

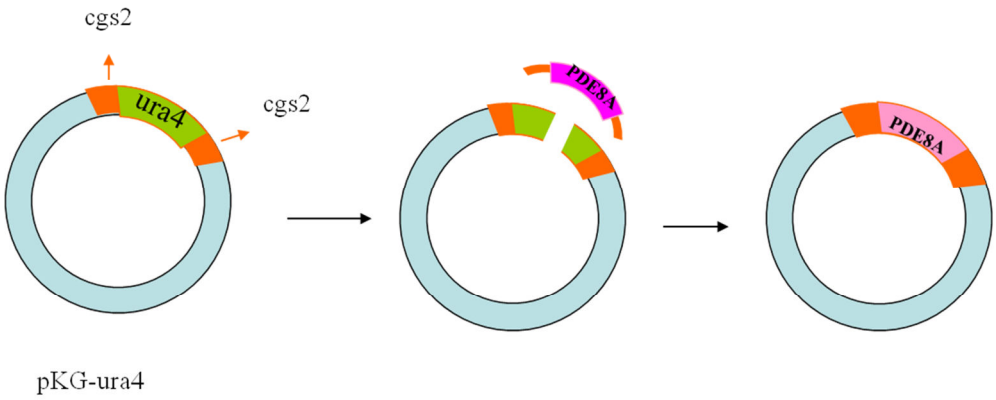

B) **Integration into the chromosome**

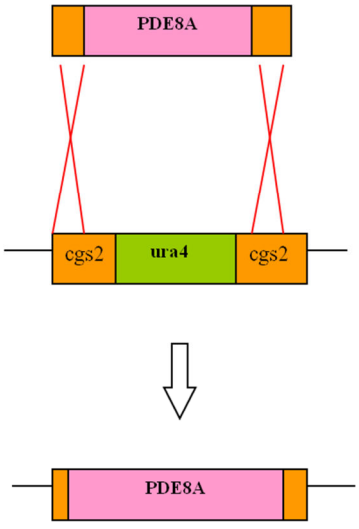

Figure 3.2 Cells that express catalytic domain of PDE8A were detected by their ability to sporulate in starvation medium

The host strain that lacks PDE cannot sporulate under starvation conditions. On the other hand, a functional PDE (in this case catalytic domain of PDE8A) restores sporulation.

Figure 3.2 Cells that express catalytic domain of PDE8A were detected by their ability to sporulate in starvation medium

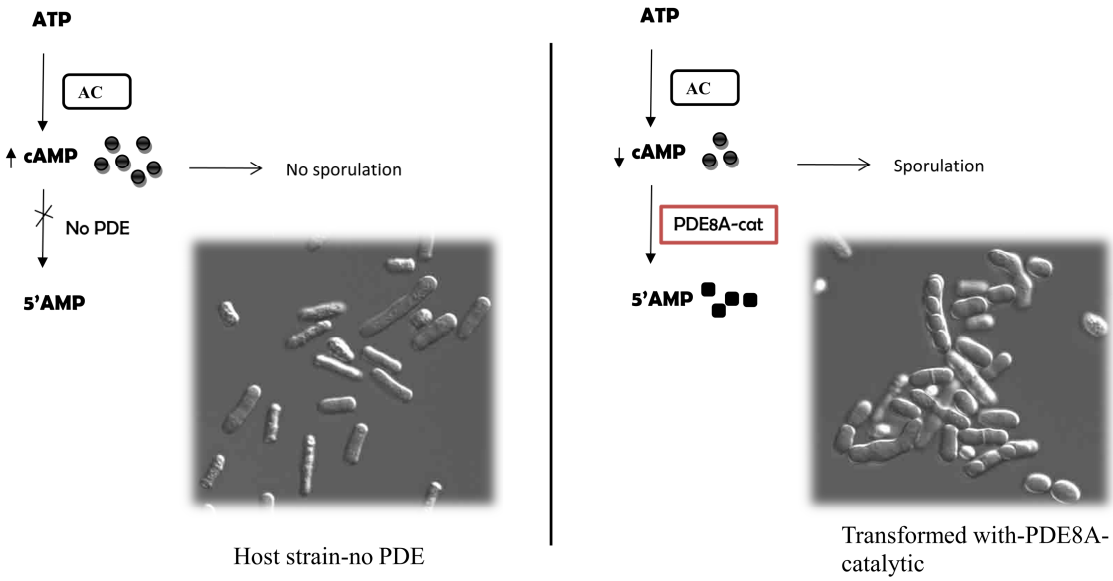

Many colonies stained dark brown, which is an indication of presence of zygotes and asci as opposed to only vegetative cells. The presence of asci was confirmed by microscopy (Figure 3.2). The presence of more visible asci at this stage compared to the strain expressing the full-length PDE8A does not indicate that the PDE8A catalytic domain is more active than the full-length enzyme as the two forms of the enzyme were expressed from promoters of different strengths. The *nmt* promoters are strong and constitutive and thus it is expected to yield more activity compared to the *cgs2* promoter.

After cloning the catalytic domain PDE8A fragment into the plasmid, linearized plasmids were integrated into the *ars1* region of strains CHP1265 and CHP1346.

3.2 ASSESSMENT OF INHIBITOR ACTIVITY *IN VIVO* BY MONITORING β-GALACTOSIDASE

The presence of a *lacZ* reporter gene under the *fbp1* promoter provides a tool for the assessment of phosphodiesterase activity and the inhibitory effect of candidate compounds on the phosphodiesterase enzyme in the cell. Inhibition of phosphodiesterase leads to elevated internal cyclic AMP levels that repress the reporter and decrease β-galactosidase activity (Figure 3.3).

In order to monitor *in vivo* PDE8 activity in the absence or presence of PDE inhibitors, I tested the β-gal levels of PDE8-expressing strain with dipyridamole, trequinsin, IBMX, and rolipram. Dipyridamole is a PDE5 and PDE6 inhibitor with weak inhibitory activity on PDE8. The PDE3 inhibitor trequinsin has been reported to inhibit PDE8B with an IC_{50}

of 2 μM and there is no data on its effect on PDE8A. 24 h treatment of these compounds at up to 200 μM did not change β-gal levels compared to control (data not shown). The inability of these compounds to affect β-gal levels could be due to poor solubility in the yeast medium or a failure to enter the yeast cells. I also tested the effect of IBMX (general PDE inhibitor that does not inhibit PDE8) and rolipram (PDE4 specific inhibitor) on a PDE8A expressing strain. As expected, they did not show an effect on β-gal levels. The experiment with rolipram was done in comparison to PDE4 expressing strains and provided some insights about the relative activities of these mammalian enzymes in the yeast (Figure 3.3.). Accordingly, PDE4A and PDE4B seem to be more active than PDE8A and their activity is lower than *S. pombe* PDE Cgs2. Although no compound was effective in changing PDE8A's activity in β-galactosidase experiments, more than 10 fold decrease in β-gal levels were observed on PDE4A and PDE4B expressing strains when treated with 50 μM rolipram. This shows the utility of this system to assess compound activity on mammalian phosphodiesterases.

3.3 BASIS OF SCREENING FOR PHOSPHODIESTERASE INHIBITORS

In *Schizosaccharomyces pombe*, cAMP signalling is controlled by the regulation of both adenylyl cyclase and phosphodiesterase (Cgs2). It is possible to control cAMP levels by modulating the phosphodiesterase activity. A screen for an inhibitor of a mammalian phosphodiesterase utilizes the 5FOA growth of a strain in which fission yeast phosphodiesterase is replaced with the mammalian ortholog.

Figure 3.3 Beta-galactosidase assays are used to assess inhibitor activity

(A) Beta-galactosidase and 5FOA growth phenotypes of an ideal candidate strain to be used for assessment of an inhibitor activity. **(B)** Beta-galactosidase activity of Cgs2 (CHP861), Cgs2-2 (LWP98), PDE4A (DDP26), PDE4B (DIP72), and PDE8A-expressing (DDP13) yeast strains after 24 h incubation with 50 and 100 μM rolipram. *cgs2-2* gene has a frameshift mutation that leads to a non-functional gene product.

Figure 3.3 Beta-galactosidase assays are used to assess inhibitor activity

A

PDE inhibitor	Relative cAMP levels	Expression from *fbp1* promoter	5FOA	β-galactosidase
-	Reduced	Higher (De-repressed)	$5FOA^S$	High β-gal
+	Increased	Lower (Repressed)	$5FOA^R$	Low β-gal

B

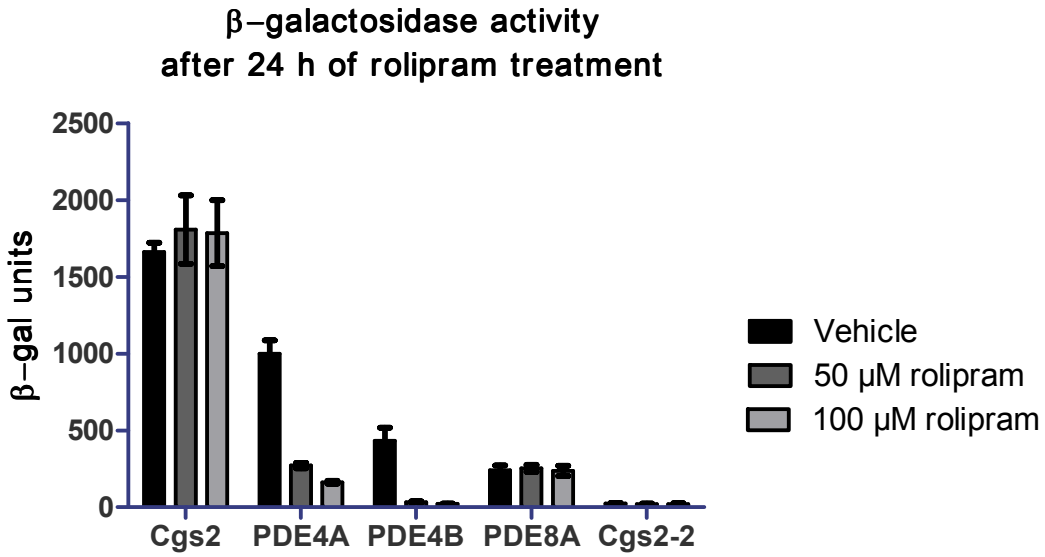

Figure 3.4 Basis of an inhibitor screen

For detection of inhibitors, the starting strain should confer 5FOA sensitivity in the absence of compounds. An effective inhibitor can elevate cAMP levels and result in 5FOA resistance.

Figure 3.4 Basis of an inhibitor screen

A) Without a PDE inhibitor

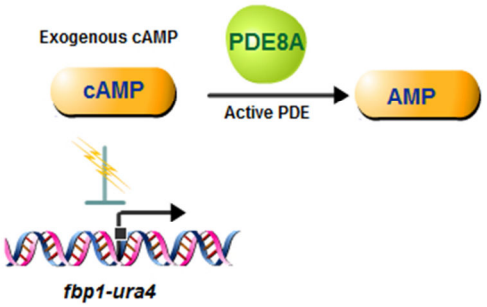

With a limited amount of cAMP in the cell, the *fbp1* promoter is derepressed and *ura4* is expressed.

NO GROWTH IN 5FOA MEDIUM

B) With a PDE inhibitor

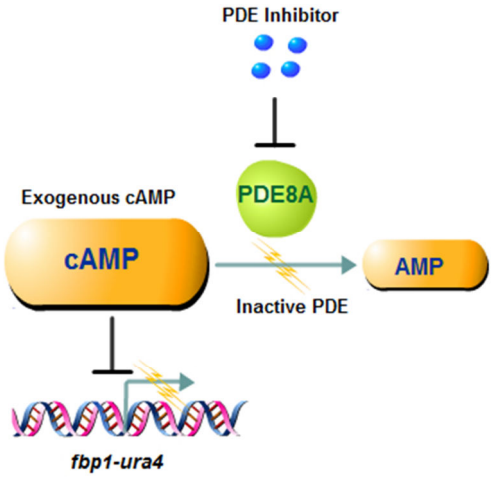

In the presence of a PDE8A inhibitor, cAMP levels increase, the *fbp1* promoter is repressed, and *ura4* is not expressed.

GROWTH IN 5FOA MEDIUM

This starting strain should have low enough cyclic AMP levels to allow the expression from the *fbp1* promoter. In this case, the *ura4* gene under the *fbp1* promoter is expressed and the starting strain cannot grow in 5FOA (5-Fluoroorotic acid) which is converted to a toxic product in the presence of *ura4* gene product OMP decarboxylase. In this system, the presence of a PDE inhibitor would increase the intracellular cAMP levels, which causes repression of the *fbp1* promoter and cells would become 5FOA resistant (Figure 3.4). Hence, the first step in creating a tool for screening for PDE inhibitors is to make a 5FOA sensitive strain with the PDE of interest. This can be achieved by introducing mutations in genes required for adenylyl cyclase activation to lower cyclic AMP synthesis.

3.4 DEVELOPMENT OF AN ASSAY TO SCREEN FOR PDE8 INHIBITORS

3.4.1 Efforts to Optimize PDE8A for Inhibitor Screening

The requirement for an effective screen to have a clean background becomes of paramount importance for high-throughput formats. This is achieved by starting with a 5FOA sensitive strain. It is also important to obtain dramatic differential growth between the positive control (2.5-5 mM cAMP and DMSO in 5FOA) and negative control (only DMSO in 5FOA) conditions.

The following efforts were made to obtain suitable conditions for screening for PDE8A inhibitors:

i) The introduction of *git3-14* (GPCR) mutation or deleting *git3* were not enough to confer 5FOA sensitive growth in a strain bearing PDE8A (this suggests that PDE8A has much less activity than Cgs2).

ii) CHP1148 strain (*pap1::ura4 cgs2::PDE8A gpa2::his3*$^{+}$) was tested for suitability for screening. The 5FOA sensitive starting strain should be pre-incubated with cyclic AMP prior to the screening in order to repress transcription at the *fbp1-ura4* reporter, creating a 5FOA resistant starting point, which will be maintained if cAMP levels could be kept high by means of inhibiting PDE. As a starting point, different cAMP concentrations in the pre-growth medium and different initial cell densities were tested separately (Figure 3.5). There was no difference between the negative and positive control conditions with different pre-growth media. Although a difference was observed between the positive and negative control conditions with $2x10^4$ cells/mL initial cell density; the difference was not robust. The required condition of drastic differential growth between positive control and negative control groups could not be achieved with this strain.

Figure 3.5 Strain CHP1148 is not suitable for inhibitor screening

PDE8A expressing strain with *gpa2* deletion (CHP1148; *pap1::ura4 cgs2::PDE8A gpa2::his3*$^{+}$) did not show any differential growth between positive and negative control conditions under different cAMP concentrations in the pre-growth medium **(A)** or with different initial cell densities **(B)**.

Figure 3.5 Strain CHP1148 is not suitable for inhibitor screening

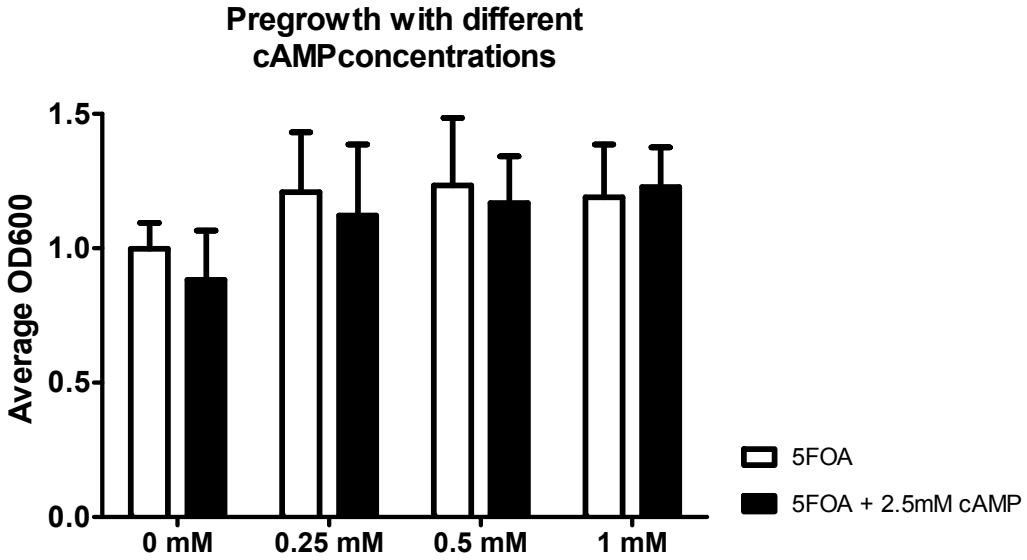

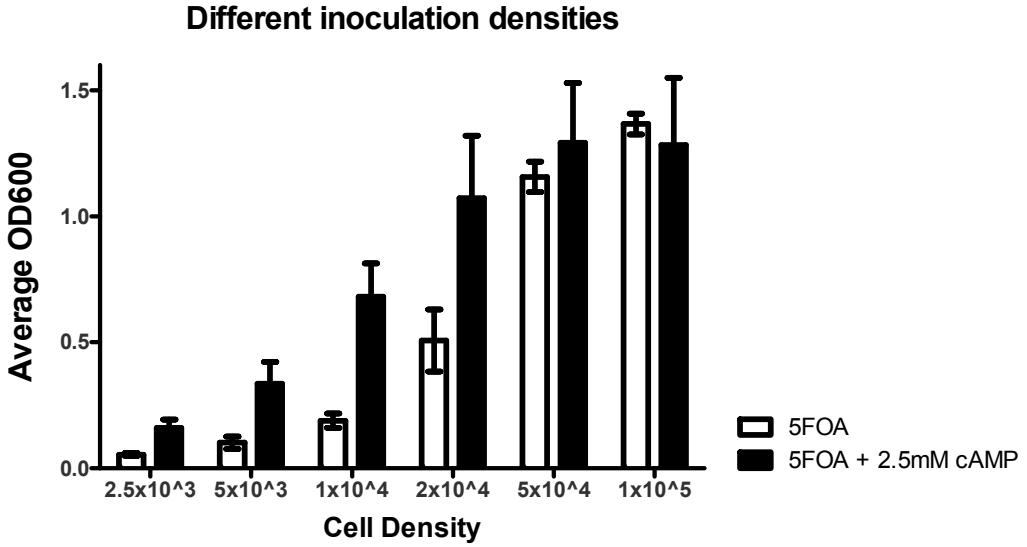

iii) More stringent 5FOA medium was tested. 0.6 and 0.8 g/L 5FOA in the medium (as opposed to 0.4) prevented the growth even in the positive control conditions (the highest optical density was 0.085 and 0.065, respectively). 0.5g/L 5FOA media seemed more promising since it allowed growth of cells with $0.25x10^5$ cells/mL initial density up to 0.33 optical density. Increased cell densities were tested with 0.45 g/L 5FOA medium. Only encouraging data was obtained with $0.5x10^5$ cells/mL initial cell density and 0.25 mM cAMP in the pre-growth medium, which yielded optical density values of 0.17 for negative control and 0.83 for positive control conditions. However, it was not reproducible under DMSO pinning conditions.

iv) A PDE8A strain with *git3* and *gpa2* double deletion was constructed but did not give a promising Z factor (data not shown).

In summary, while the *gpa2Δ* strains displayed 5FOA sensitivity on solid medium, it was insufficient sensitivity in liquid medium to allow for screening of candidate inhibitors.

3.4.2 Optimization of PDE8A Strain with Adenylyl Cyclase Deletion

Since deletion of either *git3* (GPCR) or *gpa2* (Gα) failed to confer 5FOA sensitive growth in liquid medium, a deletion of *git2* (adenylyl cyclase) was introduced into a PDE8A-expressing strain. A strain that lacks adenylyl cyclase requires external addition of cAMP to repress *fbp1* transcription. In this system, PDE activity could be detected as

judged by an increase of the level of exogenous cAMP needed to confer 5FOA-resistant growth. A *cgs2-2* strain that has no functional phosphodiesterase was used as a control to mimic a fully inhibited phosphodiesterase.

In order to select for the best strain for this experiment, various strains were subjected to 5FOA growth under cyclic AMP titration. Two of the strains are PDE8A-expressing strains that have the *LEU2* marker linked to PDE8A with or without a *pap1* deletion. Another PDE8A strain without the *LEU2* marker was also tested. For the positive control, *cgs2-2* mutation and *git2* deletion strains with and without *pap1* deletion were used. The cAMP dose response curve depicted in Figure 3.6 explains many aspects of the adenylyl cyclase deletion strategy. It shows that *pap1*$^{+}$ strains grow better than *pap1* deletion strains in 5FOA. This gene encodes for a zinc finger transcription factor that is required for expression of ABC transporters and when deleted it enhances drug sensitivity by allowing the drug to stay inside the cell longer. The increased 5FOA sensitivity of *pap1* deletion strains can be explained by higher retention of 5FOA inside the cells. Also, the PDE8A strain reaches higher optical densities earlier than the PDE8A(LEU2) strain, indicating that it has higher cAMP levels (i.e. lower phosphodiesterase activity). The increased sensitivity associated with PDE8A-LEU strain compared to PDE8A strain suggests the presence of more than one copy of PDE8A in the former strain. As a follow-up, lower cAMP concentrations in the pre-growth medium were also tested (Figure 3.7).

Figure 3.6 PDE8A strain with adenylyl cyclase deletion requires more exogenous cAMP to grow in 5FOA medium than Cgs2-2 strain

(A) Figure shows the 48 h growth behavior of adenylyl cyclase deletion strains in a cAMP titration experiment. Cells were grown in a pre-growth medium that contains 1 mM cAMP. Cells were inoculated at $0.5x10^5$ cells/mL initial cell density. **(B)** Strain pair that gives the most differential growth is shown at low cAMP concentrations. (CHP1200: *cgs2-2*, *pap1*$^+$; CHP1207: *cgs2-2*, *pap1Δ*; CHP1202: *PDE8A(LEU2)*, *pap1*$^+$; CHP1205: *PDE8A*, *pap1Δ*)

Figure 3.6 PDE8A strain with adenylyl cyclase deletion requires more exogenous cAMP to grow in 5FOA medium than Cgs2-2 strain

A

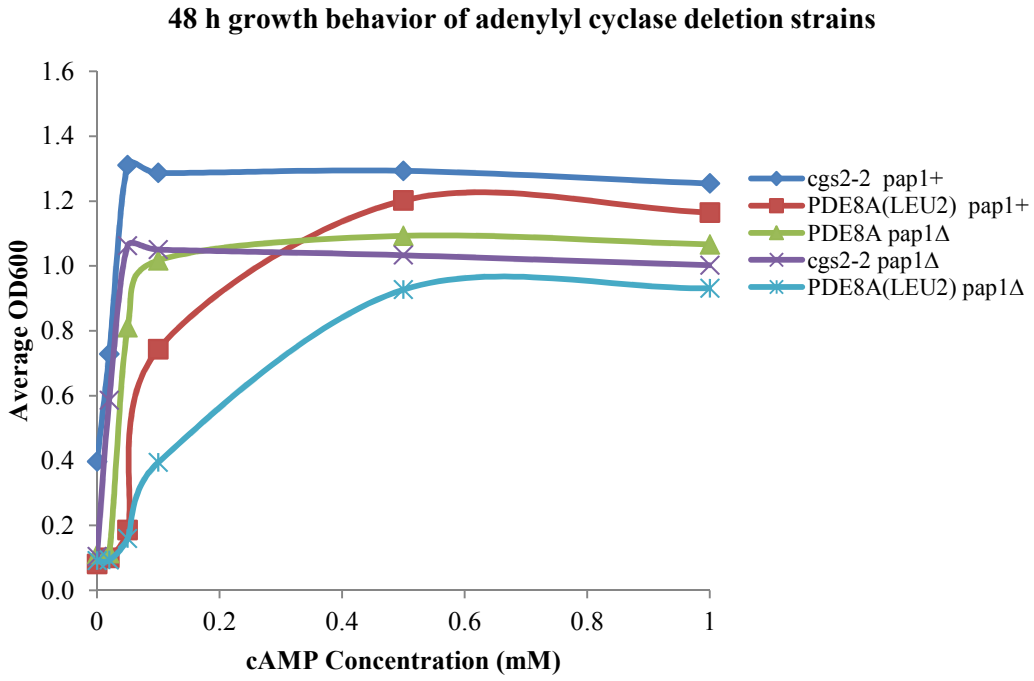

B

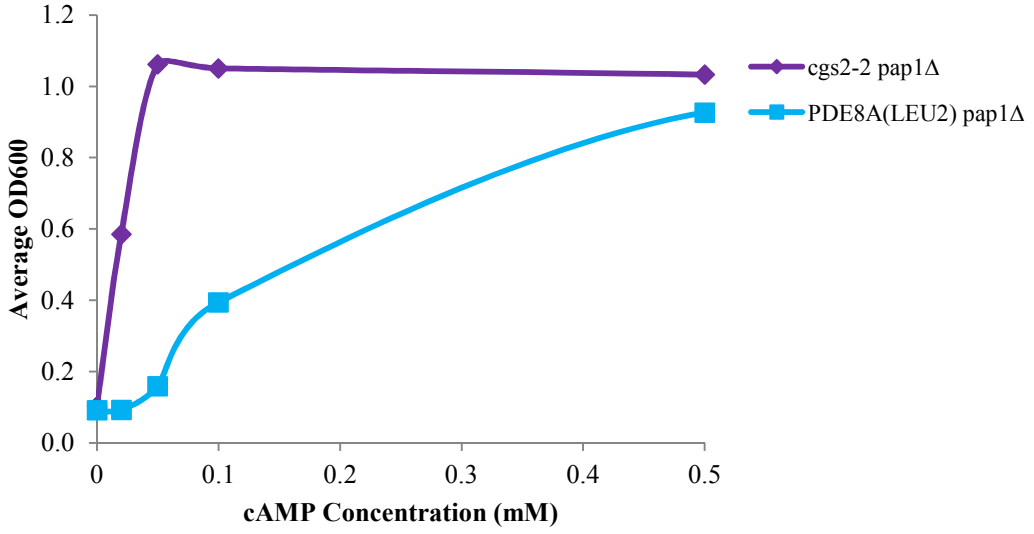

Figure 3.7 Effect of different cAMP concentrations in the pre-growth medium

The cAMP titration curve of cultures grown in different concentrations of cAMP shows that 0.5 or 1 mM cAMP in the pre-growth medium did not cause any change in the growth profile of PDE8A-expressing strain.

Figure 3.7 Effect of different cAMP concentrations in the pre-growth medium

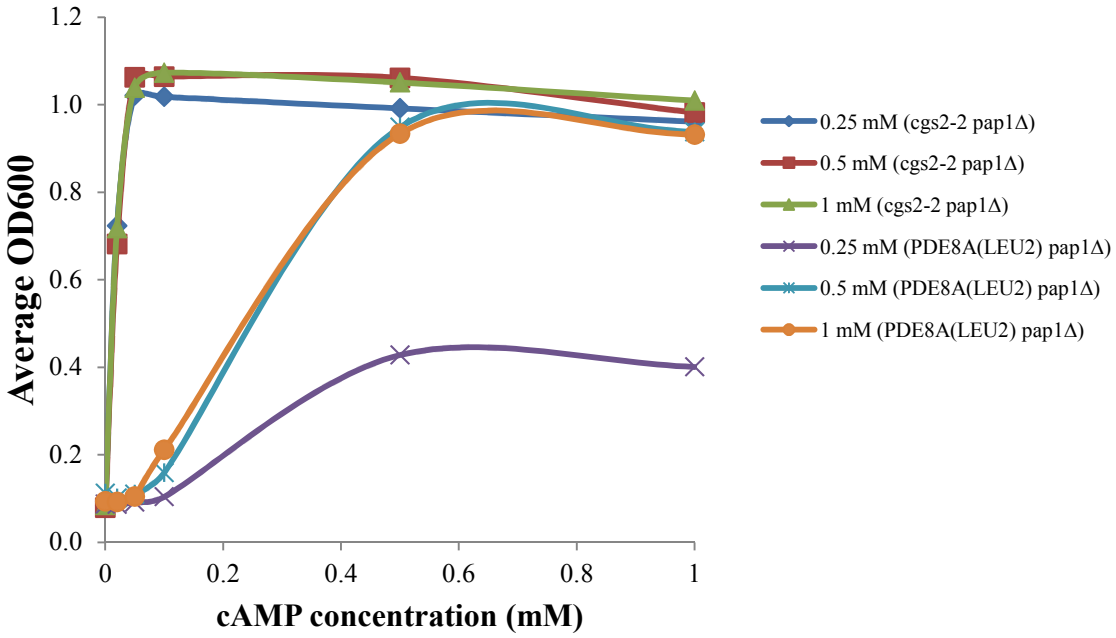

It was shown that optical density values of cultures pre-grown in media containing 1 mM, 0.5 mM, or 0.25 mM cAMP are very close to each other at 50 μM cAMP concentration in the 5FOA medium. This concentration of cAMP in 5FOA medium confers 5FOA-resistance to a strain lacking both adenylyl cyclase and PDE activity (*cgs2-2, git2*) but it is still low enough for keeping PDE8A expressing strain in 5FOA sensitive state. This suggests that when the activity of PDE8A is totally inhibited, this amount of exogenous cAMP would be enough to allow growth in 5FOA. Thus, addition of 40 μM cAMP in 5FOA growth medium was found to be the optimal condition for the screening assay.

3.5 LOW-THROUGHPUT SCREENING OF PDE8A INHIBITORS

Optimization of the PDE8A-expressing adenylyl cyclase deletion strain (CHP1204) for detection of PDE inhibitors allowed me to test fifty-six compounds that were identified from high-throughput screens against PDE4 and PDE7 enzymes. I tested each compound using three different concentrations (100, 50 and 25 μM) against two independent cultures. As a control, each compound was also tested against a PDE4B3-expressing strain (CHP1113). Positive control condition was 5 mM cAMP (and 1% DMSO) in the 5FOA medium, while 1% DMSO containing 5FOA medium served as a negative control.

The 5FOA growth response of the PDE4B3 strain in the presence of the test compounds was consistent with the known compound inhibition profile. Also, the strain responded to the PDE4 inhibitor rolipram in each experiment. Among the test collection, several compounds promoted the 5FOA growth of the PDE8A-expressing strain. An exemplary profile is shown from an experiment, where six compounds were tested (Figure 3.8). In

this assay, compound BC69 promotes the growth of strain CHP1204 (PDE8A) at each concentration. For both strains, one percent DMSO did not have an adverse effect on growth. Among the screened compounds, several compounds were found to be effective in promoting 5FOA-resistant growth. Figure 3.9 and 3.10 show the scatter plots of average absorbance values obtained at 50 μM compound concentration from culture A against culture B for PDE8A and PDE4B strains, respectively. It shows that the 5FOA growth profile of PDE8A strain is very reproducible (Figure 3.9A) while that of PDE4B strain showed discrepancy between culture A and culture B in some instances (Figure 3.10A). Figures 3.9B and 3.10B show the scatter plots of absorbance values at 100 μM against 25 μM compound concentration. This might show trends where the effect of the compound differs significantly at different concentrations. For instance, BC21 and BC24 showed better response for PDE8A strain at 100 μM and 25 μM, respectively. On the other hand, for PDE4B strain a collection of compounds responded better at the lower concentration. Finally, we can also examine the data by a scatter plot of average absorbance value for PDE8A against PDE4B strains (Figure 3.11). Accordingly, each compound that promoted growth of PDE8A strain also promoted growth of PDE4B strain. In addition, compound BC69 gave the best response among the test compounds for increasing growth of the PDE8A-expressing strain.

Figure 3.8 Compound BC69 promotes the growth of a PDE8A-expressing strain

Average optical density values of strain CHP1204 (PDE8A) **(A)** and CHP1113 (PDE4B) **(B)** in the presence of compounds BC67, BC69, BC47, BC58-6 and BC58-9 shows that BC69 promotes the 5FOA growth of both strains.

Figure 3.8 Compound BC69 promotes the growth of a PDE8A-expressing strain

A

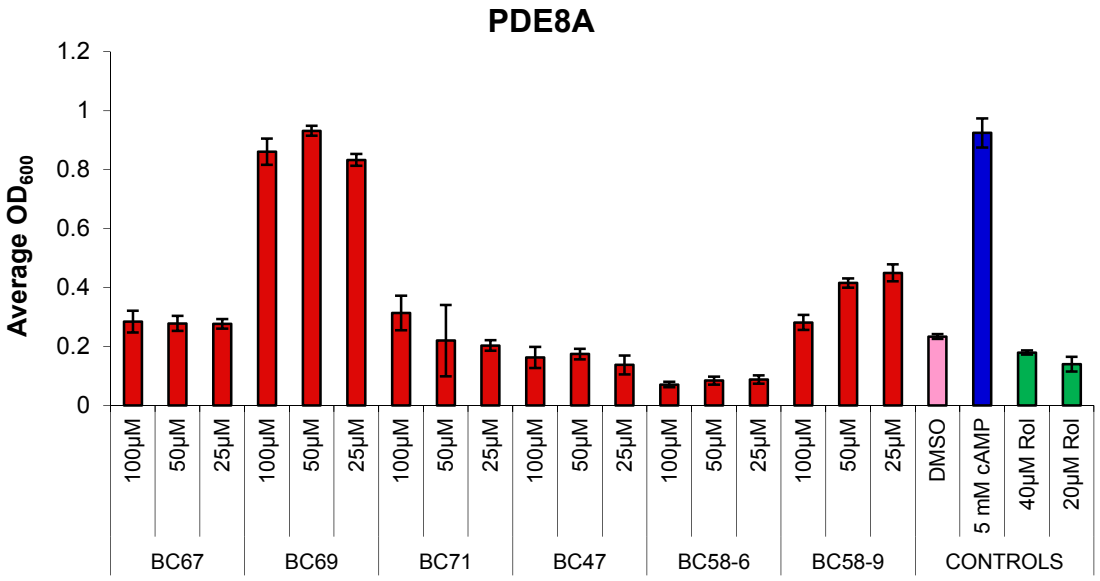

B

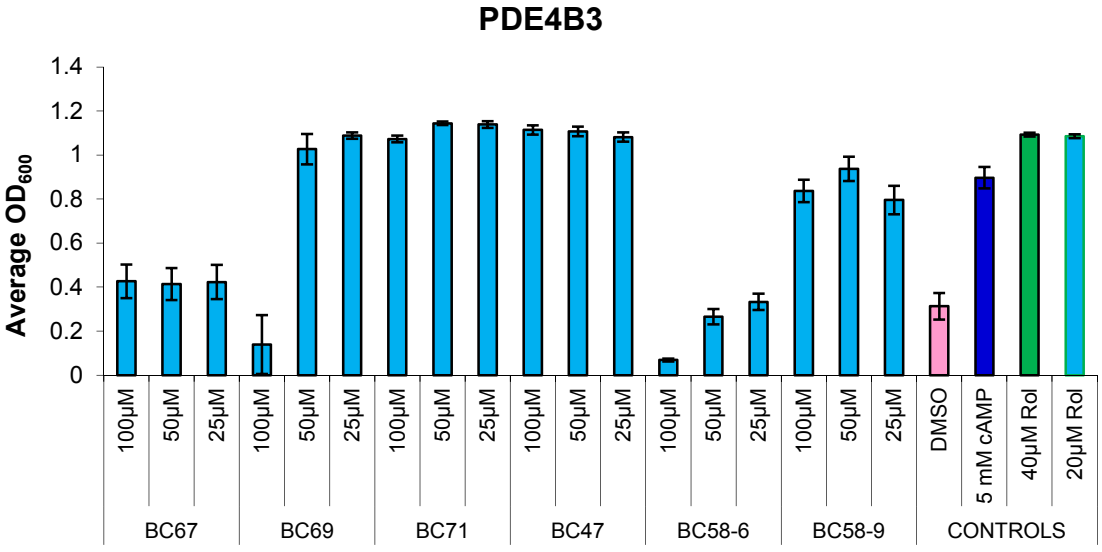

Figure 3.9 Compounds that promote 5FOA growth of a PDE8A-expressing strain are identified

(A) Scatter plots of average optical density values of culture A against culture B for CHP1204 at 50 μM compound concentration is shown. Experimental wells are shown in red, negative control DMSO is shown in blue and 5 mM cAMP control is shown in yellow. The collection of test compounds includes fifty-six PDE4 and/or PDE7 inhibitors along with other candidate PDE inhibitors from the Hoffman lab. **(B)** Scatter plot of average optical density values of 100 μM compound concentration against 25 μM compound concentration is shown. Compounds resulted in optical densities above 0.4 were labeled. Rolipram control is shown in gray.

Figure 3.9 Compounds that promote 5FOA growth of a PDE8A-expressing strain are identified

A

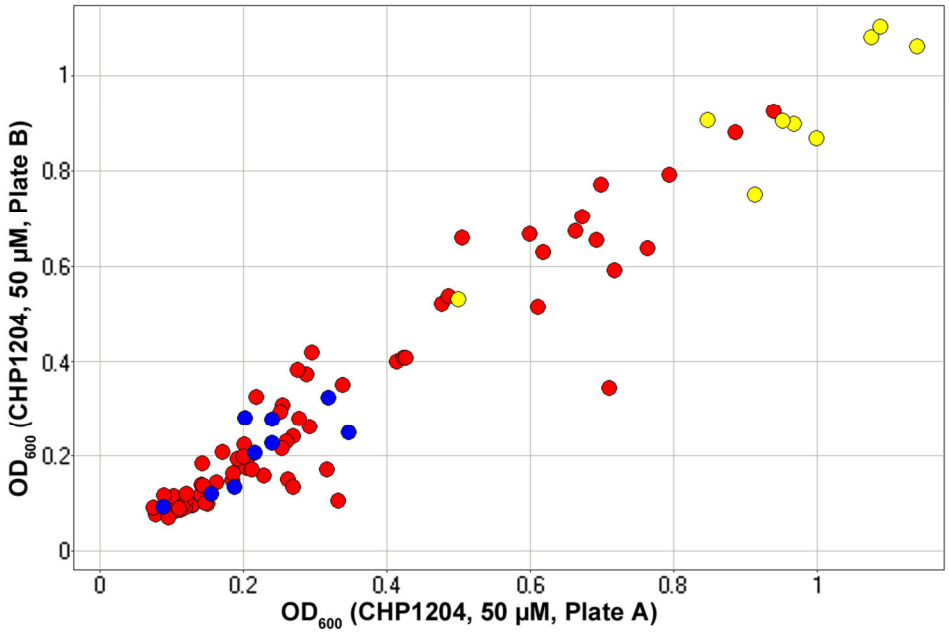

B

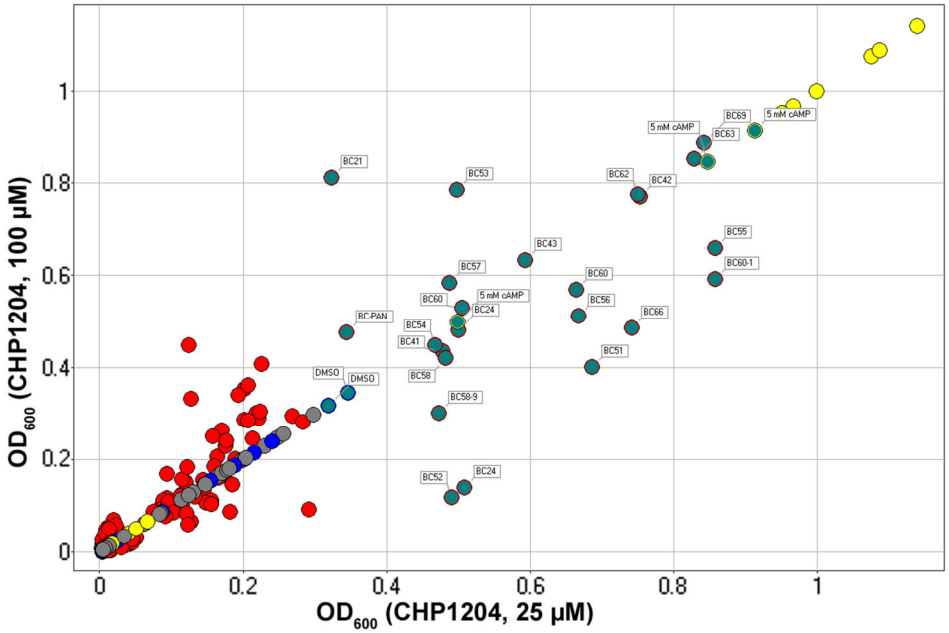

Figure 3.10 Compounds that promote 5FOA growth of PDE4B-expressing strain CHP1113 are re-confirmed

(A) Scatter plots of average optical density values of culture A against culture B for CHP1113 at 50 μM compound concentration is shown. Experimental wells are shown in light blue, negative control DMSO is shown in dark blue, rolipram control is shown in gray, and 5 mM cAMP control is shown in yellow. The collection of test compounds includes fifty-six PDE4 and/or PDE7 inhibitors along with other candidate PDE inhibitors from the Hoffman Lab. **(B)** Scatter plot of average optical density values of 100 μM compound concentration against 25 μM compound concentration is shown. Compounds resulted in optical density values above 0.6 were labeled.

Figure 3.10 Compounds that promote 5FOA growth of PDE4B-expressing strain CHP1113 are re-confirmed

A

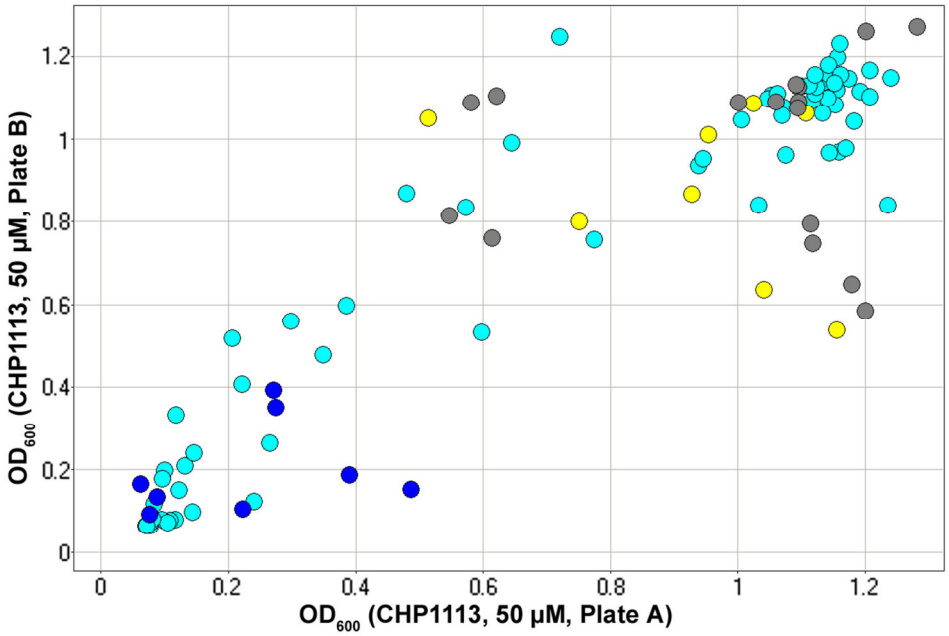

B

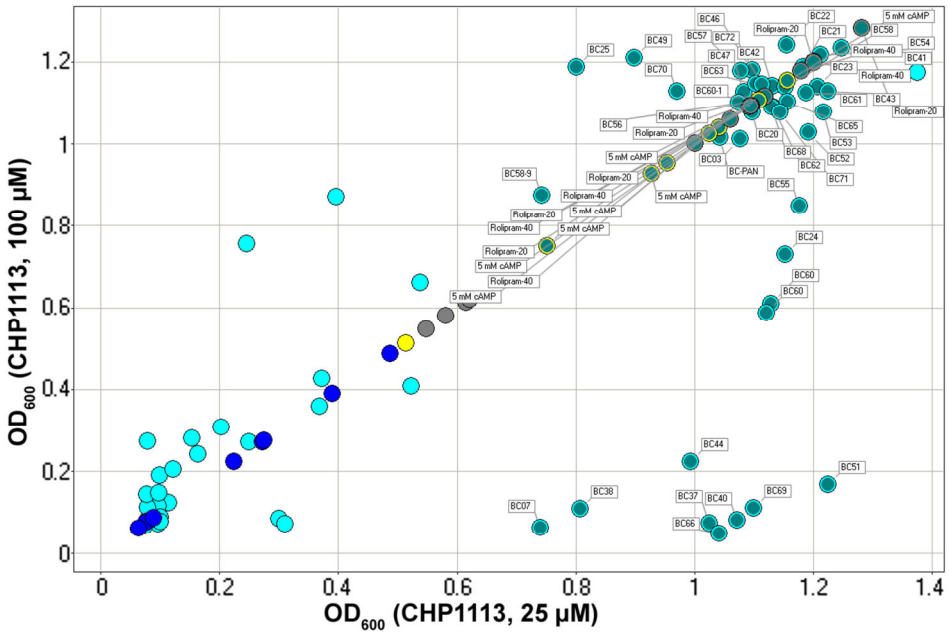

Figure 3.11 BC69 shows the strongest effect on PDE8A

(A) Scatter plot of average optical density values of PDE8A strain against PDE4B strain at 50 μM compound concentration is shown. Experimental wells are shown in purple, negative control DMSO is shown in blue, rolipram is shown in gray, and 5 mM cAMP control is shown in yellow. The collection of test compounds includes fifty-six PDE4 and/or PDE7 inhibitors along with other candidate PDE inhibitors from the Hoffman lab. **(B)** Compounds that resulted in optical density values above 0.4 for PDE8A strain are labeled. Compounds with inhibitory potential on PDE8A are from PDE4 collection since they also promote growth of PDE4B strain. BC69, which indicated with a red circle, gives the strongest growth phenotype for PDE8A.

Figure 3.11 BC69 shows the strongest effect on PDE8A

A

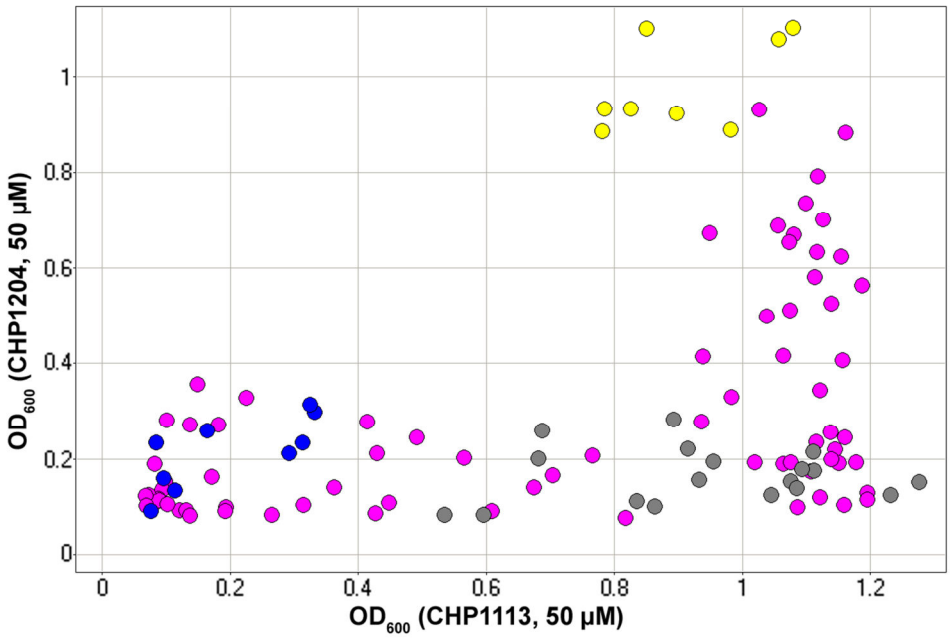

B

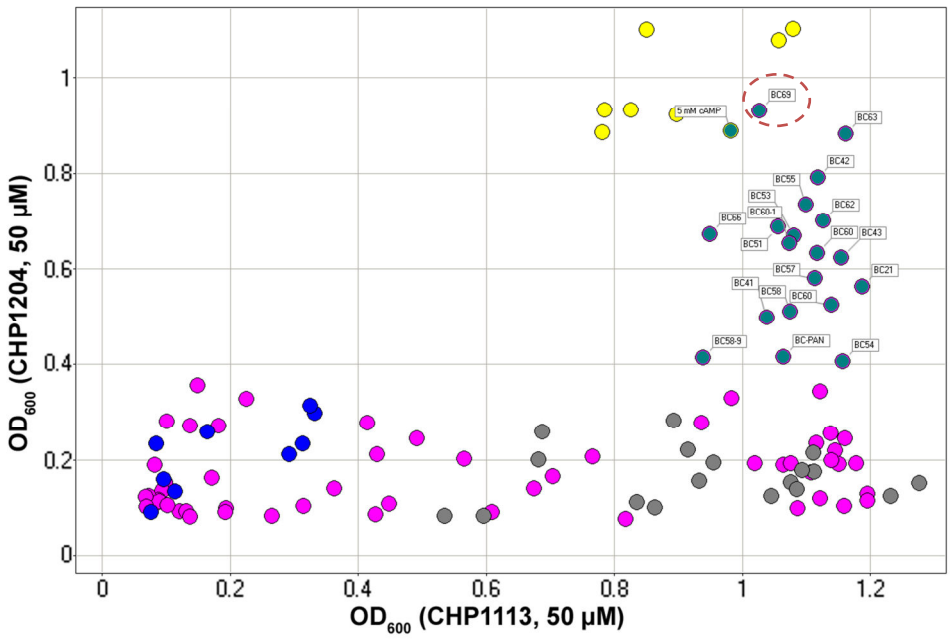

3.6 EVALUATION OF IDENTIFIED COMPOUNDS

3.6.1 Dose Response Profiling

The compounds that showed some increase in the 5FOA growth of strain CHP1204 were retested with increasing compound concentrations ranging from 0.3-80 μM. These dose response curves indicated that compounds BC21, BC24, BC39, BC42, BC51, BC55, BC60, BC62, BC63, BC66, BC69 and BC76 all increase growth of the PDE8A-expressing strain to OD>0.5 in the 5FOA medium (Figure 3.12). For BC24, the effect is a bell-shaped curve, while a wider plateau is seen with other compounds. Among these compounds, compound BC69 produced the highest growth response.

3.6.2 Cyclic AMP Titration Curves

The effect of some promising compounds (BC24, BC42, BC51, BC55, and BC69) on the growth of PDE8A (CHP1204) and Cgs2-2 (CHP1207) strains was tested in a cAMP titration experiment in order to evaluate the possibility that some compounds affect the growth response via a non-PDE target. In this experiment, a fixed concentration of the compounds was added in the 5FOA medium along with different concentrations of cAMP. If the compound is acting through PDE, then it should shift the cAMP titration curve of the strain that expresses PDE8A to the left while curve of the strain without a functional phosphodiesterase (Cgs2-2) remains unchanged. A leftward shift in the Cgs2-2 growth curve would suggest that the compound is acting on other components of the glucose sensing pathway or uracil biosynthesis pathway.

Figure 3.12 Dose response curves of identified compounds

Dose response curves of selected compounds (BC21, BC24, BC42, BC51, and BC55 on panel **A**; BC60, BC63, BC66, BC69, BC76, and dipyridamole on panel **B**) after 48 hours of growth in 5FOA medium shows that BC69 is the most effective compound in elevating growth of the PDE8A-expressing strain (CHP1204). Dipyridamole does not affect the cAMP-dependent yeast growth phenotype.

Figure 3.12 Dose response curves of identified compounds

A

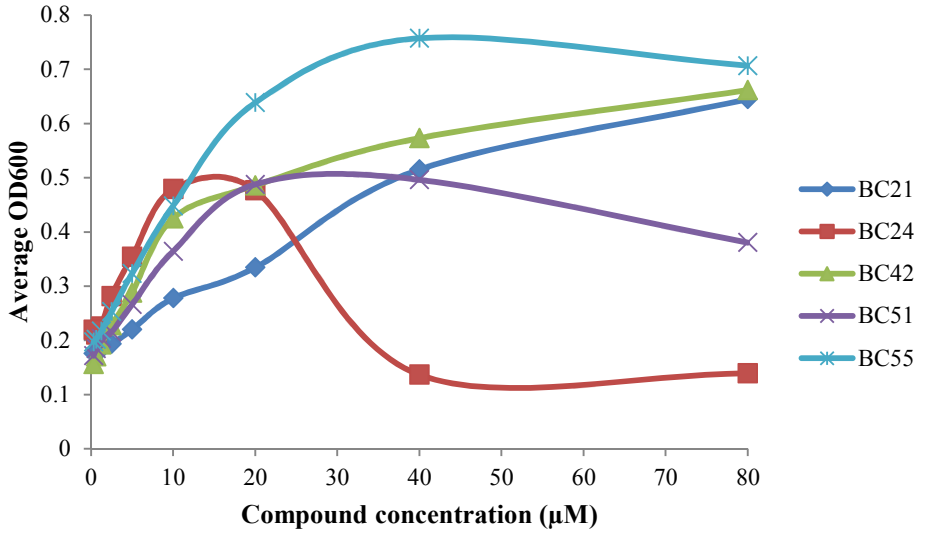

B

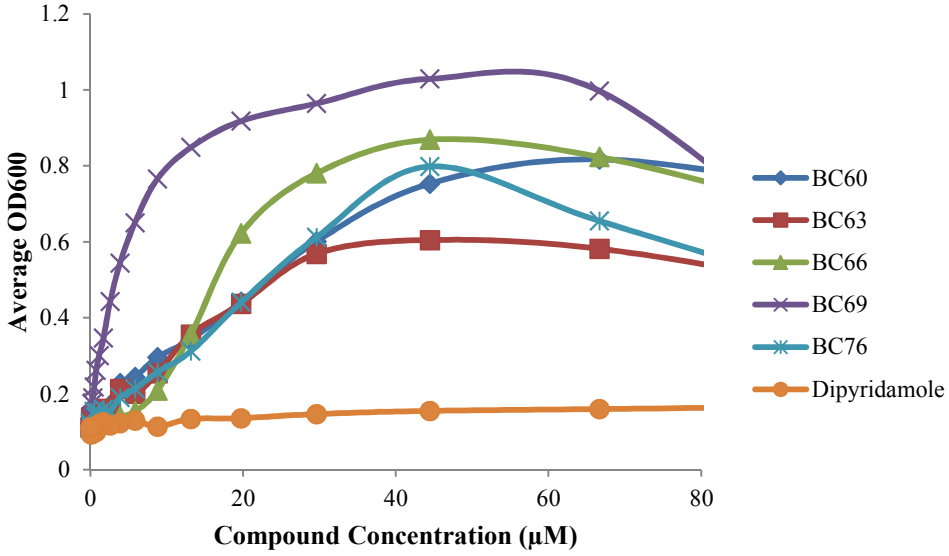

Figure 3.13 shows that compound BC24 shifts the curve of PDE8A-expressing strain furthest to the left but not as much as to reach to Cgs2-2 growth curve. The effect of BC42 seems less than BC24 while the effect of BC51 and BC55 are the least and equal to each other. Upon closer examination, BC24 barely shifts the curve of the Cgs2-2 strain while the other compounds shift the curve more to the left. This indicates that the effect of compounds BC42, BC51 and BC55 on the PDE8A strain might result from their effect on a non-PDE target (Figure 3.13B). The cAMP titration curve in the presence of BC69 shifted the curve of PDE8A, while it did not affect the curve of Cgs2-2 expressing strain that lacks functional phosphodiesterase activity (Figure 3.14).

3.7 *IN VITRO* EVALUATION OF PDE ACTIVITY

The hydrolysis of cyclic AMP by human PDE8A was monitored using radiolabeled cAMP substrate ([^{3}H]cAMP) as the tracer. The enzyme activity of recombinant full length human PDE8A1 was measured at 50 nM substrate concentration with or without inhibitors. The inhibitory effect of some promising compounds on PDE8A was verified by this *in vitro* assay (Figure 3.15). As described in the previous cAMP titration experiments with the compounds BC24, BC42, BC51, and BC55, only compound BC24 did not affect Cgs2-2 strain's growth in 5FOA, suggesting its ability to act on the PDE enzyme itself. This is further confirmed with the *in vitro* assays where unlike compounds BC21, BC42, BC51 and BC55, only BC24 seemed to inhibit PDE8A weakly. The inhibitory effect also seems greater at 10 μM compared to 20 μM; this is also consistent with the bell-shaped growth curve that is obtained by BC24.

Figure 3.13 cAMP titration curves against Cgs2-2 strain points out non-PDE targets for compounds BC42, BC51 and BC55

(A) cAMP titration curves of Cgs2-2 and PDE8A-expressing strains are generated in the presence of a fixed concentration (20 μM) of the compounds and compared to no-compound conditions. The effect of the compounds was shown by their ability to produce a leftward shift on PDE8A-expressing strain. **(B)** The 5FOA growth curve at low cAMP concentrations and the fold difference of Cgs2-2 growth in the presence and absence of compounds (OD_{600} with compound/OD_{600} no compound) are shown. The unchanged growth behavior of the Cgs2-2 strain in the presence of BC24 suggests that BC24 acts through PDE inhibition.

Figure 3.13 cAMP titration curves against Cgs2-2 strain points out non-PDE targets for compounds BC42, BC51 and BC55

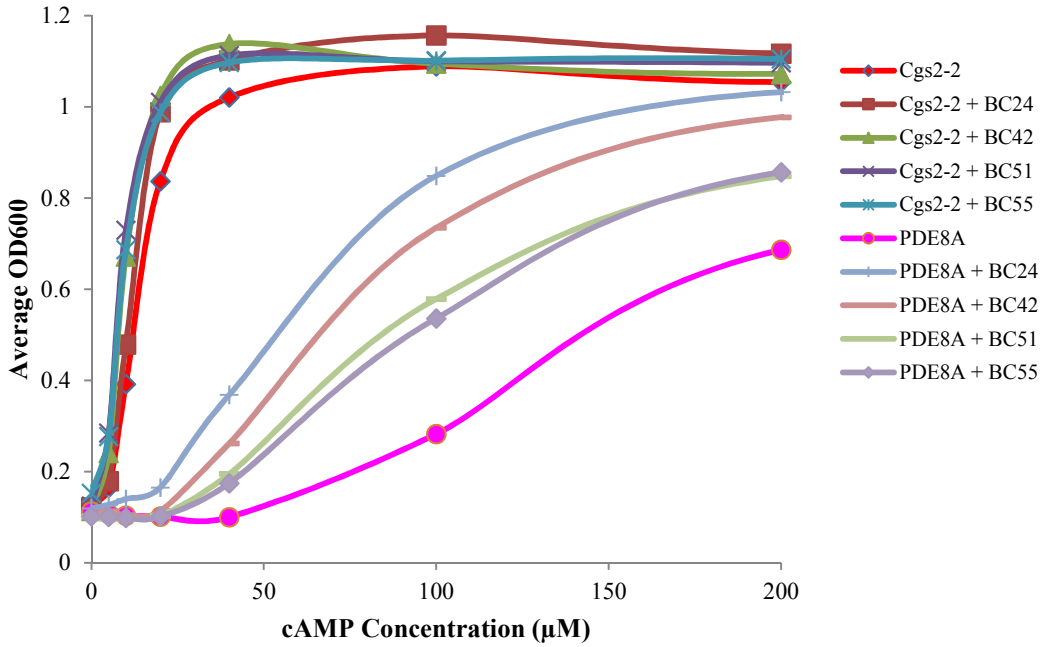

B

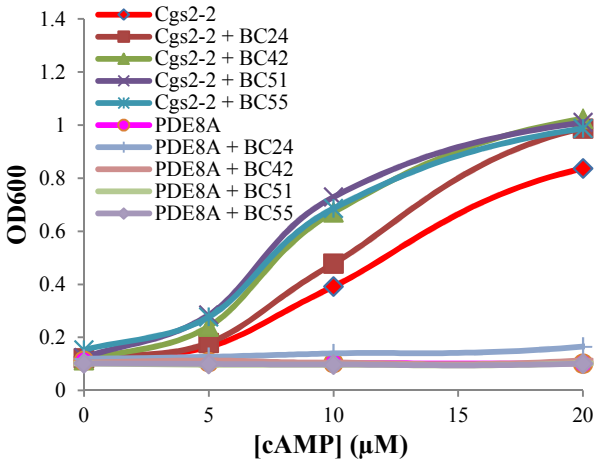

Fold increase in OD_{600} of Cgs2-2 strain in the presence of compounds

	No cAMP	5 µM	10 µM
BC24	1.0	1.1	1.2
BC42	0.9	1.5	1.7
BC51	1.0	1.7	1.9
BC55	1.2	1.7	1.8

Figure 3.14 BC69 causes a leftward shift of the PDE8A cAMP titration curve

(A) Compound BC69 shifts the cAMP titration curve of the PDE8A-expressing strain to the left, while it does not have an effect on the curve of Cgs2-2 (no PDE) strain. **(B)** The structure of compound BC69 is shown.

Figure 3.14 BC69 causes a leftward shift of the PDE8A cAMP titration curve

A

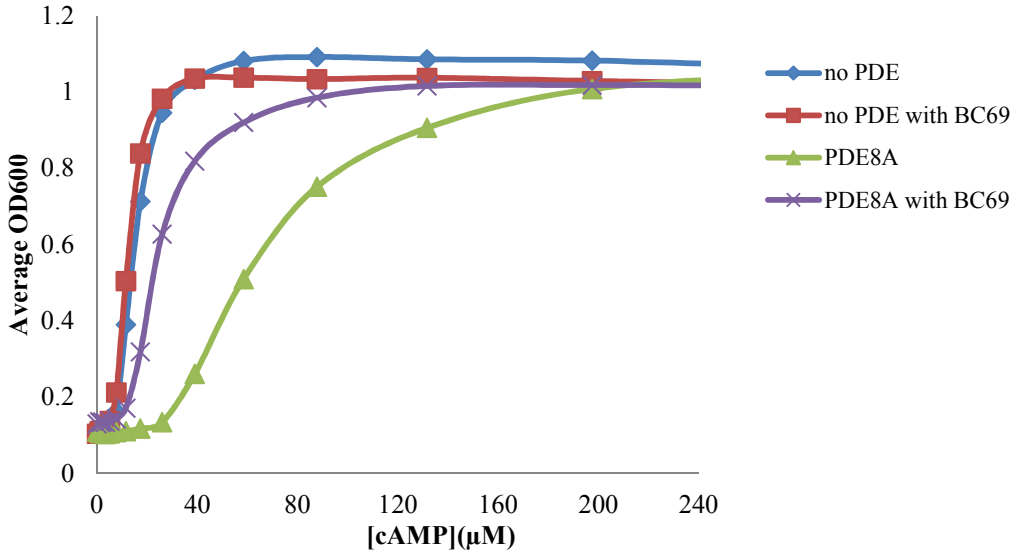

B **Structure of compound BC69**

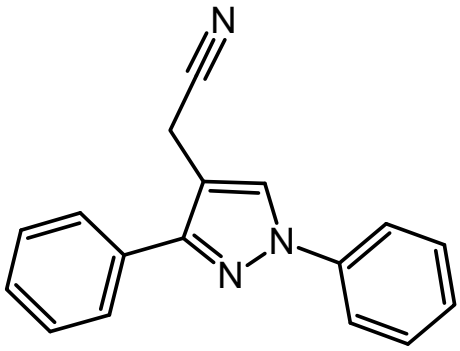

Figure 3.15 *In vitro* assays confirm PDE8 inhibition by BC69

In vitro enzyme assays with human PDE8A were performed at 10 μM and 20 μM compound concentrations in the presence of 50 nM cAMP for 20 minutes. Percent inhibition data for cAMP hydrolysis show that BC60, BC62, BC63 and BC69 inhibit human PDE8A and BC69 displays the highest inhibition.

Figure 3.15 *In vitro* assays confirm PDE8 inhibition by BC69

Percent inhibition of cAMP hydrolysis		
Compound	**10 μM**	**20 μM**
BC21	12	11
BC24	22	14
BC41	-2	-13
BC42	7	17
BC51	5	-5
BC55	5	3
BC60	38	53
BC62	N/A	66
BC63	42	49
BC66	N/A	35
BC69	N/A	72
BC76	18	31

On the other hand, compounds BC60, BC62, BC63 and BC69 inhibit human PDE8A1 in the *in vitro* enzyme assays better than other compounds with an estimated IC_{50} of 20 μM or lower. The greatest inhibition was observed with BC69.

3.8 OPTIMIZATION OF A PDE8A CATALYTIC DOMAIN STRAIN FOR INHIBITOR SCREENING

The PDE8A catalytic domain was cloned into two different plasmids under *nmt1* and *nmt41* promoters (Tommasino and Maundrell. 1991). Two different backgrounds were used for stable integration (intact cAMP signaling pathway, git^+ or *gpa2* deleted). The candidate strains were grown in different pre-growth conditions with different cell densities to attain optimum 5FOA conditions to be used in small molecule screening.

When the cells were grown at $1x10^5$ cells/ mL initial concentration with 0.5 mM cAMP in the pre-growth medium, DDP44 (pNMT41, git^+) was found to have very high OD values for both positive and negative control conditions, indicating that the expression is very low such that the strain becomes 5FOA resistant. On the other hand, DDP40 (pNMT1, git^+) and DDP42 (pNMT41, *gpa2Δ*) had very low values for 5FOA and did not grow in cAMP, a condition that can be considered as 5FOA super sensitivity (Figure 3.16A). Increasing cAMP concentration to 2.5 mM cAMP in the pre-growth medium did not result in a differential growth between positive and negative control conditions when different initial cell densities were tested (Figure 3.16B). Since *nmt* promoters can be transcriptionally repressed by thiamine, I used 2.5 μg/mL thiamine in the pre-growth medium along with 1 mM cAMP. From the 5FOA response, the expression level seem to

be decreased but differential growth was not achieved (Figure 3.17A). Finally, pre-growth conditions that previously have been shown to work with the highly active PDE4D bearing strain were tested. In this case, instead of using cAMP in the pre-growth medium, utilization of a PDE inhibitor or cGMP help to achieve differential growth conditions. I tested 0.5 mM cGMP or 50 μM BC69 in the pre-growth medium. As a result, cGMP pre-growth was found to produce differential growth for strain DDP42; however it did not respond to BC69 positive control (Figure 3.17B). On the other hand, BC69 pre-growth resulted in a very distinct differential growth for strain DDP40 between negative control and BC69 positive control (Figure 3.18). Although this strain under these conditions did not respond to high levels of cAMP, since a compound response was observed against BC69, the conditions were further refined by testing different concentrations of BC69 in the pre-growth medium. As a result, 20 μM BC69 was found to be the optimum condition that gives dramatic differential response between positive and negative control conditions for the PDE8A-catalytic domain expressing strain.

Figure 3.16 Optimization of a PDE8A-catalytic domain expressing strain for small molecule screening

(A) Average optical density values of strains expressing PDE8A-catalytic domain that were grown with 0.5 mM cAMP in the pre-growth medium and plated with $1x10^5$ cells/mL initial cell density are shown. **(B)** Effect of initial cell density is shown with 2.5 mM cAMP in the pre-growth medium. Their growth behaviors in the negative control condition (5FOA medium with DMSO) and in positive control conditions (20 μM BC69 or 5 mM cAMP) were monitored.

Figure 3.16 Optimization of a PDE8A-catalytic domain expressing strain for small molecule screening

A

	DMSO	cAMP	BC69
DDP46 (pNMT1, *gpa2Δ*)	0.48	0.38	0.44
DDP40 (pNMT1, *git*$^+$)	0.1	0.1	0.1
DDP42 (pNMT41, *gpa2Δ*)	0.09	0.08	0.08
DDP44 (pNMT41, *git*$^+$)	1.17	1.12	1.14

B

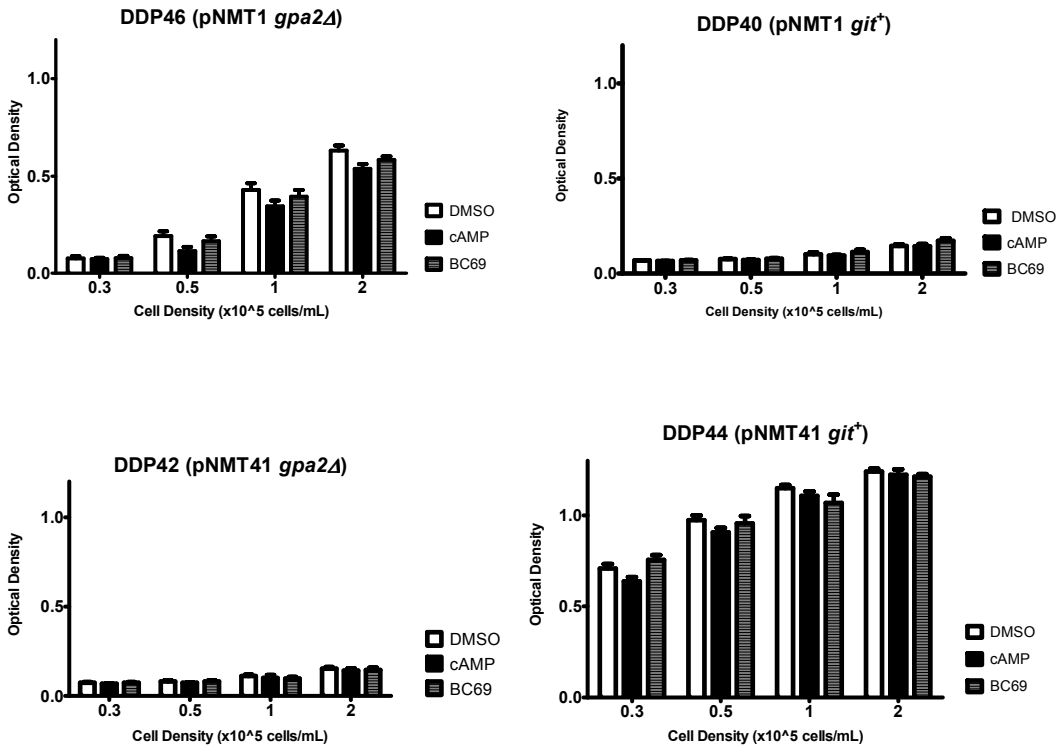

Figure 3.17 Effect of thiamine and cGMP in the pre-growth medium

The strains were grown in different pre-growth media: **(A)** 1 mM cAMP supplemented with 2.5 μg/mL thiamine, **(B)** 0.5 mM cGMP. Different strains were tested at 0.5 $x10^5$ or $1x10^5$ cells/mL initial cell density. Their growth behaviors in negative control condition (5FOA medium with DMSO) and in positive control conditions (20 μM BC69 or 5 mM cAMP) were monitored.

Figure 3.17 Effect of thiamine and cGMP in the pre-growth medium

A Effect of thiamine in pre-growth medium

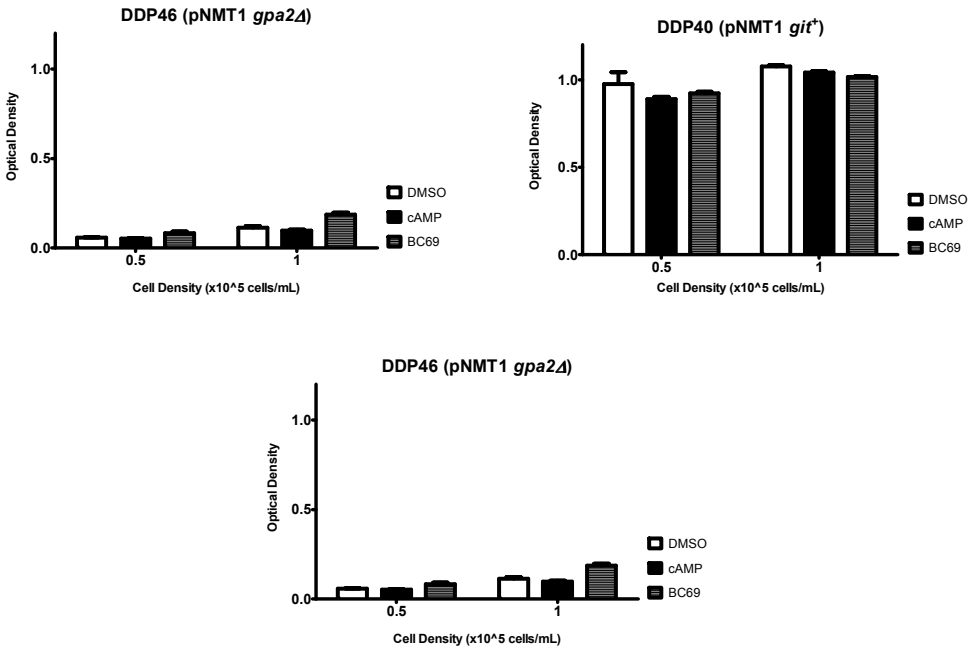

B Effect of cGMP in pre-growth medium

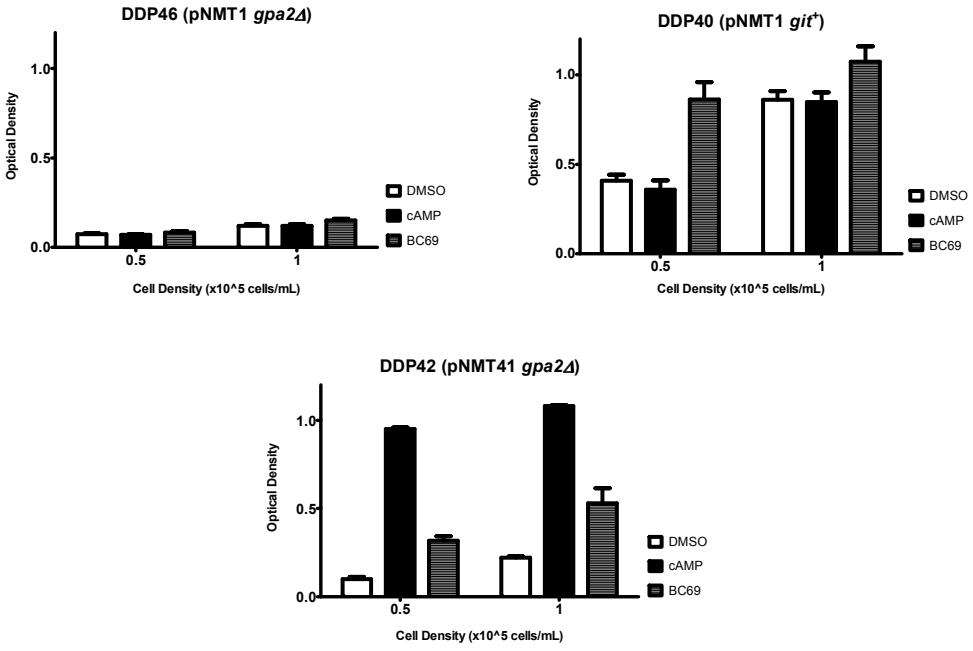

Figure 3.18 Effect of BC69 in the pre-growth medium

(A) The strains were grown in the presence of 50 μM BC69 in the pre-growth medium and tested at 0.5 $x10^5$ or $1x10^5$ cells/mL initial cell density. Their growth behaviors in negative control condition (5FOA medium with DMSO) and in positive control conditions (20 μM BC69 or 5 mM cAMP) were monitored. **(B)** The growth phenotype of DDP40 strain is shown when 20, 40 or 50 μM BC69 were supplemented in the pre-growth medium. Cells were plated at 0.5 $x10^5$ or $1x10^5$ cells/mL initial cell density.

Figure 3.18. Effect of BC69 in the pre-growth medium

A **Effect of BC69 in pre-growth**

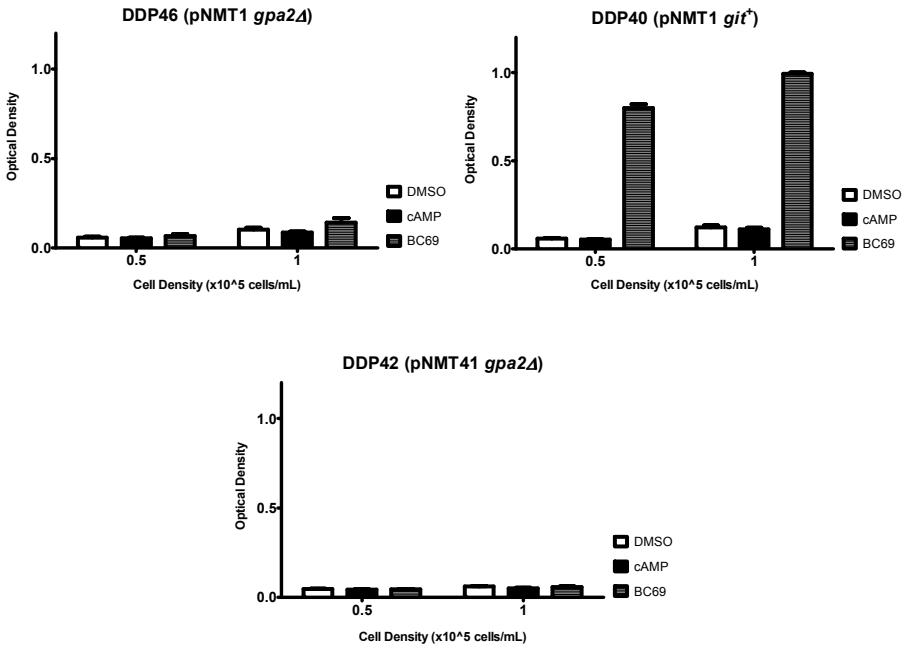

B

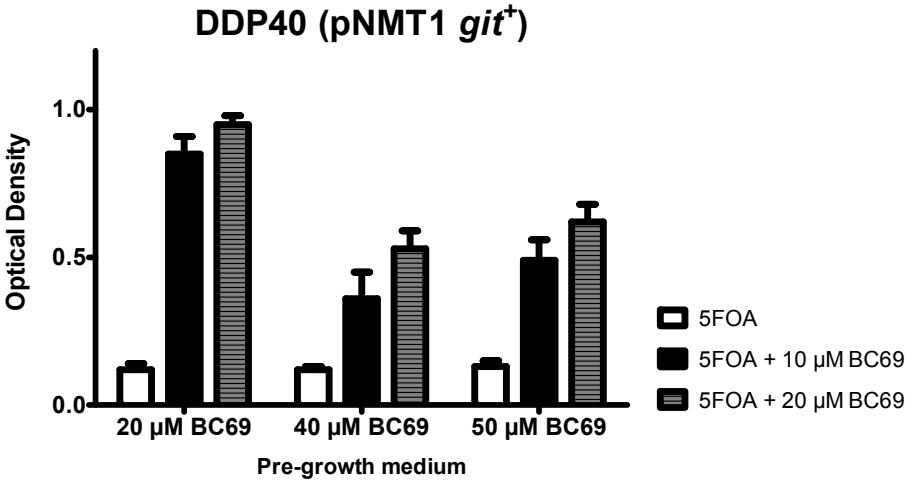

3.9 CONCLUSION

In this chapter, I demonstrated the utilization of the cAMP-dependent glucose sensing pathway of *S. pombe* for identification of inhibitors of PDE8A that has low activity when expressed in the yeast cells. The differential growth between the negative and positive control conditions was achieved by deleting the adenylyl cyclase gene. The ability of a compound to inhibit PDE8A was judged by the decrease in the amount of exogenous cAMP required to stimulate saturation growth in the 5FOA medium. This suggests that the adenylyl cyclase deletion strategy can be successfully adapted to other mammalian phosphodiesterases that have low activity in the fission yeast system. Among the fifty-six compounds that were identified from high-throughput screens against PDE4 and PDE7 families, I identified BC60, BC62, BC63 and BC69 as PDE8 inhibitors. Compound BC69 was shown to have the greatest inhibition potential on PDE8A, and was used for optimization of a strain that expresses the catalytic domain of PDE8A for small molecule screens. Furthermore, the PDE4/PDE8 dual specificity inhibitor BC69 can serve as a positive control for high-throughput screens of PDE8 inhibitors.

CHAPTER FOUR

4 DISCOVERY OF NOVEL PDE8 INHIBITORS THROUGH HIGH-THROUGHPUT SCREENING

4.1 OPTIMIZATION OF HIGH-THROUGHPUT SCREENING

In high-throughput screening, one of the prerequisites is to demonstrate that the negative and positive control conditions are drastically different from each other and they are consistent and reproducible within each group. One way of measuring this suitability is described by Zhang et al. (Zhang *et al*. 1999) as a concept called Z factor (see Material and Methods for the formula). The formula of Z factor takes the sum of the standard deviations of the negative and positive control conditions as well as the difference between the mean values of those conditions into account. If the Z factor is above 0.5, the screening conditions are considered to be suitable for HTS such that the positive hit values obtained are unlikely to be due to chance events. As the Z factor becomes higher, the quality of the HTS increases. For example, a screen with a Z factor of 0.9 is considered to have excellent conditions to allow for the detection of true positive hits. Thus, it is imperative to demonstrate that the selected conditions are optimized for HTS assays.

During the development of HTS conditions for the PDE8A-expressing strain CHP1204, several compounds (namely BC69, BC62 and BC63) that were obtained as PDE8A/PDE4

dual specific inhibitors in the low-throughput screening were tested in order to determine the best positive control compound that will result in the highest Z factor. Additionally, 5 mM cAMP was also included as a positive control. However in this case, the cAMP control is not as relevant as a positive control with an inhibitor compound since under screening conditions the ability of the strain to grow up to saturation is limited by the amount of exogenously provided cAMP in the assay.

During the HTS, compounds are transferred from the stock plates to the assay plates by the aid of 384-well steel pin arrays by a process referred to as pinning. Before starting compound pinning experiments, the initial tests with the indicated compounds were done by direct addition of the compounds into the 5FOA medium. The negative control conditions were set to 0.2 % DMSO, which is the concentration attained when 100 nL of compounds are pinned in each well. It was demonstrated that 10 μM BC69 is able to give the highest Z factor with a value of 0.77 as opposed to 0.69 and -5.6 obtained by BC62 and BC63, respectively. In this assay, the cyclic AMP control yields a Z factor value of 0.85 (Figure 4.1).

4.2 Z FACTOR TEST

Before starting actual screening of the compounds, a master plate with DMSO and 5 and 10 mM BC69, which gives 10 and 20 μM final compound concentration when 100 nL is pinned, was prepared (Figure 2.2A). The lower concentration was included as a reference

Figure 4.1 Z factor test identifies conditions with BC69 as excellent for HTS

Z factor test with DMSO as negative control conditions and 5 mM cAMP or 10 μM of BC69, BC62 or BC63 as positive control conditions indicates that BC69 is the best compound control. The plate pictures represent real growth data in a color scale that ranges from blue to red (blue-green-yellow-orange-red) with increasing OD values. Green indicates low OD, orange indicates high OD.

Figure 4.1 Z factor test identifies conditions with BC69 as excellent for HTS

(A)

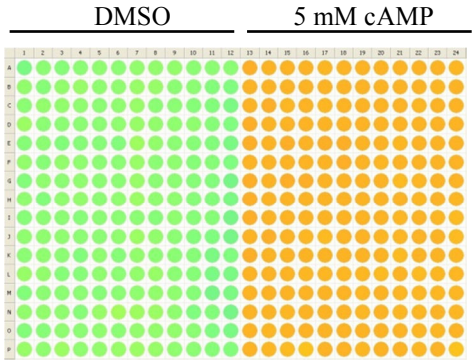

	Average OD_{600}	Standard Deviation	Z factor value
DMSO	0.12	0.012	
5 mM cAMP	0.816	0.023	0.85

(B)

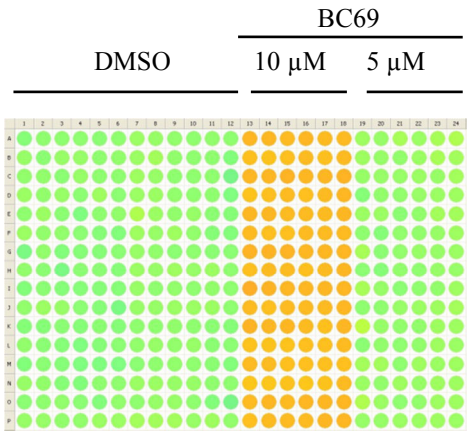

	Average OD_{600}	Standard Deviation	Z factor value
DMSO	0.129	0.012	
10 µM BC69	0.760	0.035	0.77
5 µM BC69	0.141	0.014	-5.6

(C)

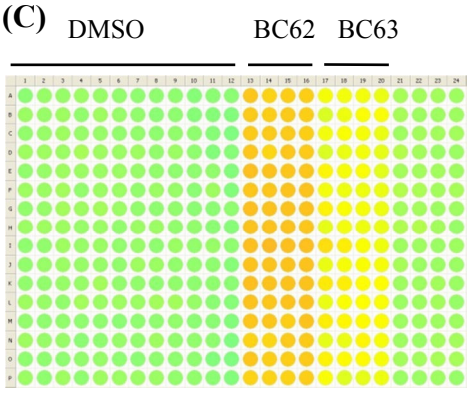

	Average OD_{600}	Standard Deviation	Z factor value
DMSO	0.136	0.013	
10 µM BC62	0.67	0.042	0.69
10 µM BC63	0.363	0.050	-5.6

point since some of the compounds in the available libraries are prepared in 5 mg/ml concentration. In addition, compounds with higher molecular weight this might result in lower initial concentrations.

Two independent Z factor tests were done under actual pinning conditions in order to ensure the reproducibility using both full length and catalytic domain PDE8A-expressing yeast strains CHP1204 and DDP40, respectively. The results of the control pinnings are summarized in Table 4.1. Both strains demonstrated screenable conditions with either 10 or 20 μM BC69 as the positive control.

4.3 SCREENING ASSAY WITH KNOWN BIOACTIVE COMPOUNDS

The first assay was performed against the known bioactives collection at the ICCB Screening facility, which includes BIOMOL ICCB Known Bioactives2- High Conc (number of compounds: 480), Prestwick1 Collection (number of compounds: 1,120) and NINDS Custom Collection 2 (number of compounds: 1,040). These compound libraries have 2,640 compounds from different classes of ion channel blockers, GPCR ligands, second messenger modulators, nuclear receptor ligands, actin and tubulin ligands, kinase inhibitors, protease inhibitors, gene regulation agents, lipid biosynthesis inhibitors, as well as other well-characterized compounds that perturb cell pathways and influence brain activity. 1,120 of these compounds are off-patent compounds with known safety and bioavailability in humans and 602 of them are FDA approved

Table 4.1 Independent control pinnings with BC69 against CHP1204 (full length PDE8A) and DDP40 (catalytic domain PDE8A)

(A)

Full-length PDE8A	Average OD_{600}	Standard Deviation	Z factor value
DMSO	0.12	0.01	
10 µM BC69	0.52	0.05	0.54
20 µM BC69	0.61	0.05	0.64

PDE8A-catalytic domain	Average OD_{600}	Standard Deviation	Z factor value
DMSO	0.24	0.03	
10 µM BC69	0.75	0.06	0.47
20 µM BC69	0.75	0.05	0.5

(B)

Full-length PDE8A	Average OD_{600}	Standard Deviation	Z factor value
DMSO	0.16	0.03	
10 µM BC69	0.80	0.06	0.6
20 µM BC69	0.83	0.06	0.61

PDE8A-catalytic domain	Average OD_{600}	Standard Deviation	Z factor value
DMSO	0.19	0.03	
10 µM BC69	0.78	0.07	0.49
20 µM BC69	0.78	0.04	0.65

(http://iccb.med.harvard.edu/screening/compound_libraries/#known; access date 12/29/2010).

The screening against known bioactive compounds was performed against full length (CHP1204) and catalytic domain PDE8A-expressing strains (DDP40) with the goal of prioritizing one strain to be used in the rest of the screening experiments. As shown in Table 4.2, Z factor values obtained from the master plate were excellent for full length PDE8A-expressing strain (CHP1204), while a very high background growth was observed for catalytic domain strain DDP40 that resulted in negative Z factor values for this particular experiment. Thus, CHP1204 was used in subsequent experiments for screening.

The overview of the results of this assay can be seen in Figure 4.2, where plate grids drawn with respect to optical density values are shown. In the known bioactives collection, only two compounds were found to promote growth of the PDE8A-expressing strain in 5FOA medium. The most effective compound from these collections is the steroid epiandrosterone, which is a natural metabolite of steroid hormone dehydroepiandrosterone (Plate/well no: 1569 G22). The average optical density values of some of the known phosphodiesterase inhibitors and cyclic nucleotide analogs that are present in the bioactives collection are shown in Table 4.3. None of these compounds promoted growth of the PDE8A-expressing strain. Obtaining a low number of hits in this collection is expected since there have been no previously developed inhibitors against PDE8A.

Table 4.2 Z factor values of the screen against known bioactives collection

Full-length PDE8A	Average OD_{600}	Standard Deviation	Z factor value
DMSO	0.094	0.015	
10 μM BC69	0.607	0.019	0.8
20 μM BC69	0.728	0.02	0.83

PDE8A-catalytic domain	Average OD_{600}	Standard Deviation	Z factor value
DMSO	0.637	0.029	
10 μM BC69	0.817	0.067	-0.637
20 μM BC69	0.801	0.035	-0.178

Figure 4.2 Plate grids with respect to optical density

Screening against known bioactives collection is illustrated as plate grids based on optical density values for CHP1204 **(A)** and DDP40 **(B)**. Color scale is from red (low OD) to blue (high OD). Plate CP-01 is the master plate that has controls DMSO in the left half and 5 or 10 mM BC69 in the second half. Plate CP-02 is the 5 mM cAMP control but the top half of the plate is empty due to cell delivery problems during the experiment. Gray color indicates empty wells. The compound that responds best is indicated with a circle (Plate 1569, well G22). A high background for DDP40 interferes with the interpretation of the results.

Figure 4.2 Plate grids with respect to optical density

(A) CHP1204 (Full-length PDE8A)

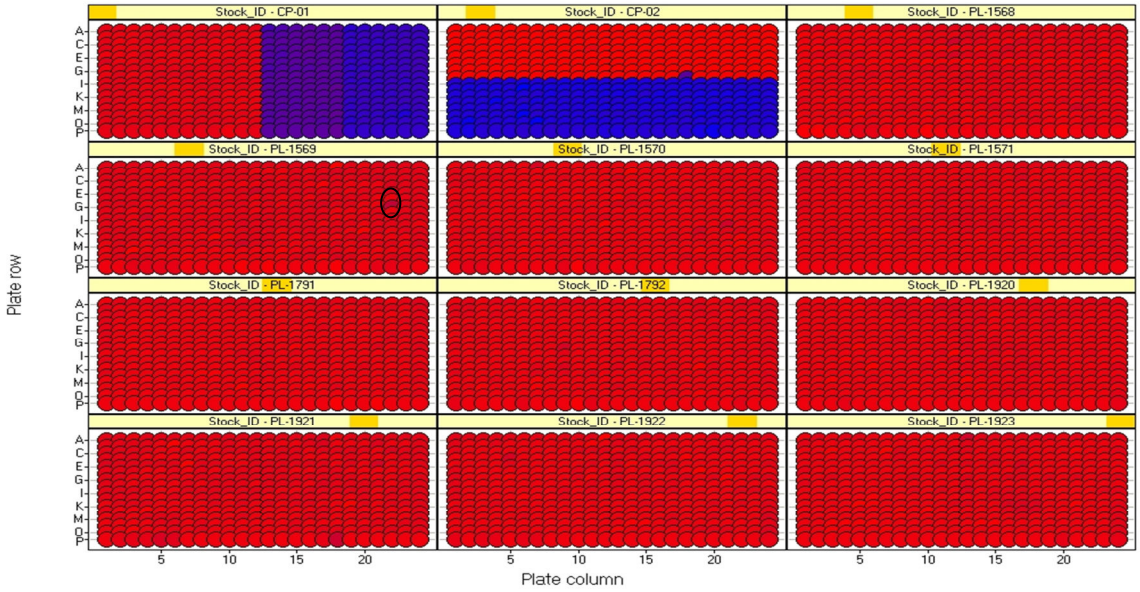

(B) DDP40 (Catalytic domain of PDE8A)

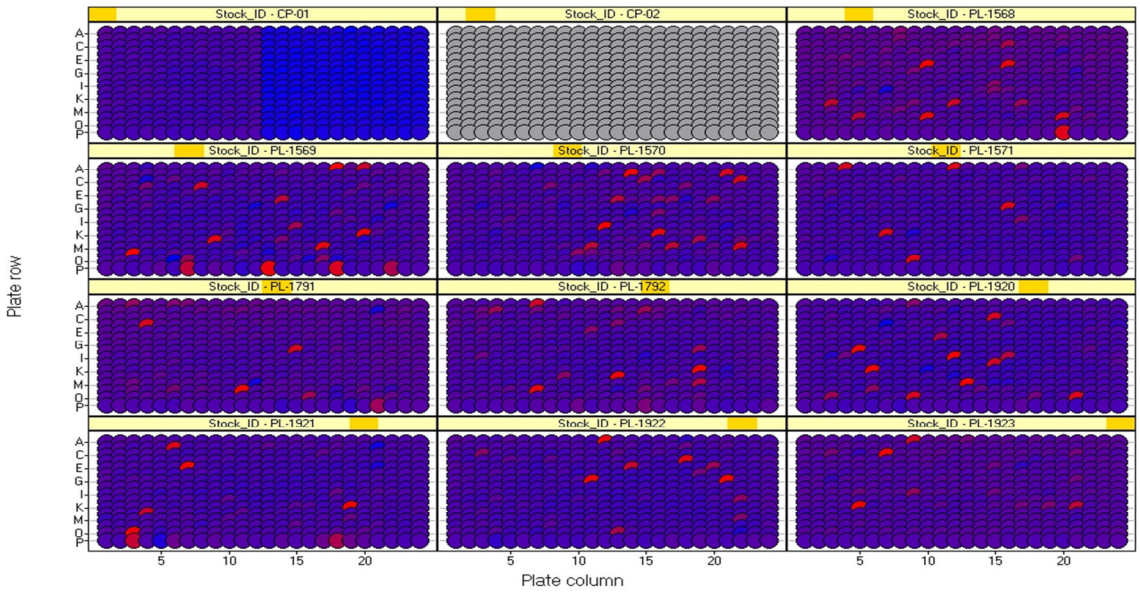

Low OD High OD

Table 4.3 Growth response of CHP1204 in the presence of known PDE inhibitors or cyclic nucleotide analogs

Plate/Well no		Compound name	Average Optical Density
1791	J04	8-methoxymethyl-IBMX	0.079
1791	L08	Bromo-cGMP [8-Bromo-cGMP]	0.068
1792	A19	dibutyrylcyclic AMP	0.0995
1792	A21	dibutyrylcyclic GMP	0.107
1568	M06	Dipyridamole	0.0635
1791	N16	Dipyridamole	0.066
1920	I10	Dipyridamole	0.076
1792	E03	EHNA	0.0815
1792	I15	IBMX	0.0955
1571	E12	Milrinone	0.0935
1791	H06	Milrinone	0.0735
1569	F08	Papaverine hydrochloride	0.0955
1920	F06	Papaverine hydrochloride	0.0805
1570	J10	Rolipram	0.0705
1791	D18	Rolipram	0.0835
1922	B19	Sildenafil	0.086
1791	D14	Trequinsin	0.085

All of the screening experiments were carried out in duplicate. This leads to the identification of hits in a more consistent way. Figure 4.3 shows scatter plots of absorbance values from two different replicates. For CHP1204 data, we can dissect the major characteristics of the screen by comparing the distribution of control and experimental wells in the chart. The clustering of negative control wells (dark blue circles) near the origin -located away from the positive control wells (yellow circles)- indicates the significant difference between those two conditions, which is also demonstrated by a high Z factor. Most data points are aligned diagonally. This shows the reproducibility of the assay.

4.4 DETERMINATION OF HITS

The screen for identification of PDE8A inhibitors was performed against 222,711 compounds from commercial libraries and known bioactives collections and 18,980 compounds from natural product libraries. In total, 241,691 small molecules from 700 different compound plates were screened at 23 separate pinning appointments. These compounds correspond to 40 different small molecule libraries (listed in Material and Methods).

For the interpretation of the screening data, besides the raw OD_{600} values, the Z scores for plate A (Zscore_A) and plate B (Zscore_B) were also calculated using the Standardize function of Microsoft Excel. The composite Z score values were calculated by scaling the vector [Zscore_A, Zscore_B] by the cosine correlation with a vector corresponding to

Figure 4.3 Screening against known bioactives collection typifies the quality of HTS

Scatter plot of absorbance values from plate A against plate B is shown. **(A)** Only control wells are demonstrated. Blue indicates negative control DMSO, yellow indicates 10 μM or 20 μM compound BC69. **(B)** Experimental wells are shown in red. The data set has a correlation value of 0.996.

Figure 4.3 Screening against known bioactives collection typifies the quality of HTS

(A)

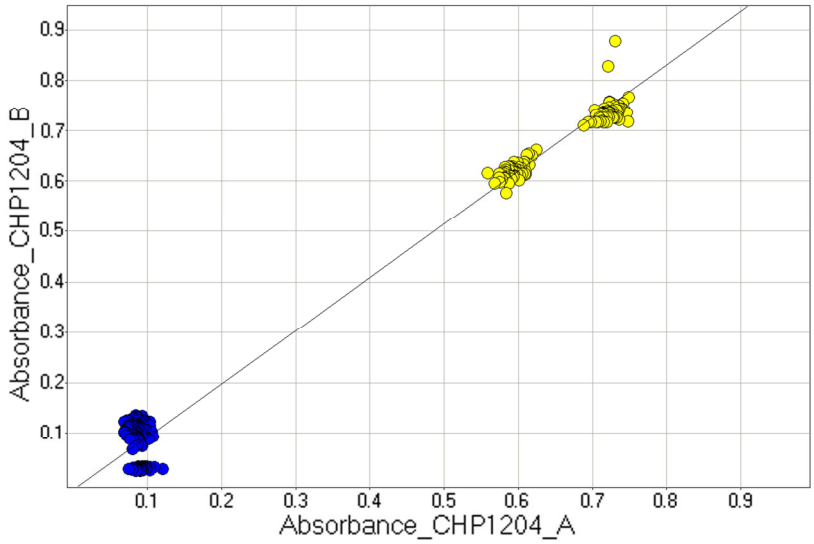

(B)

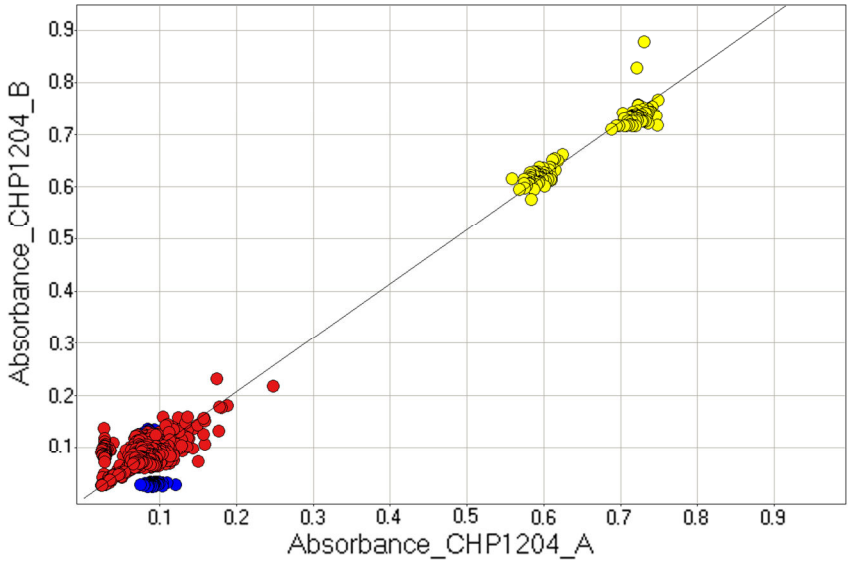

'perfect reproducibility' (i.e. equal Z-scores in both replicates). Compounds that produce composite Z scores above 8.53 are considered as hits. This cutoff value is determined according to previous work (Ivey *et al*. 2008; Seiler *et al*. 2007).

Once the compounds meet the composite Z score criterion, I categorized them according to their average absorbance values. We consider the compounds promoting growth with OD≥0.6 as strong hits. OD values between 0.2 and 0.4 are considered as weak hits and values between 0.4 and 0.6 are considered as moderate hits. For instance, the composite Z score value for epiandrosterone is 12.1, suggesting that this is a statistically significant hit but it is considered as a weak hit since the average optical density is 0.23. All screened compounds with their annotation as strong, moderate and weak positives are given in Figure 4.4.

According to these criteria, among **241,691** compounds **2,447 total hits (1.01%)** were identified. They were classified as follows:

- **Strong Positives :** 63 (0.03%)
- **Moderate Positives :** 390 (0.16%)
- **Weak Positives :** 1,994 (0.83%)

4.5 SCREENING AGAINST NATURAL PRODUCTS

PDE8A-expressing strain was tested against several natural product libraries (for list see Material and Methods). These libraries contain partially purified extracts from

Figure 4.4 Compounds that give positive response are categorized as strong, moderate or weak 'hits'

The data is annotated according to composite Z score and average absorbance values. The compounds that have composite Z score values below 8.53 are not considered as hits. The compounds that met this criterion are categorized according to their OD values as follows: OD $\geq$ 0.6 strong hit (indicated in red), 0.4$\leq$OD<0.6 moderate hit (indicated in dark blue), 0.2$\leq$OD<0.4 weak hit (indicated in light blue). The scatter plot shows all of the compounds screened from commercial libraries.

Figure 4.4 Compounds that give positive response are categorized as strong, moderate or weak 'hits'.

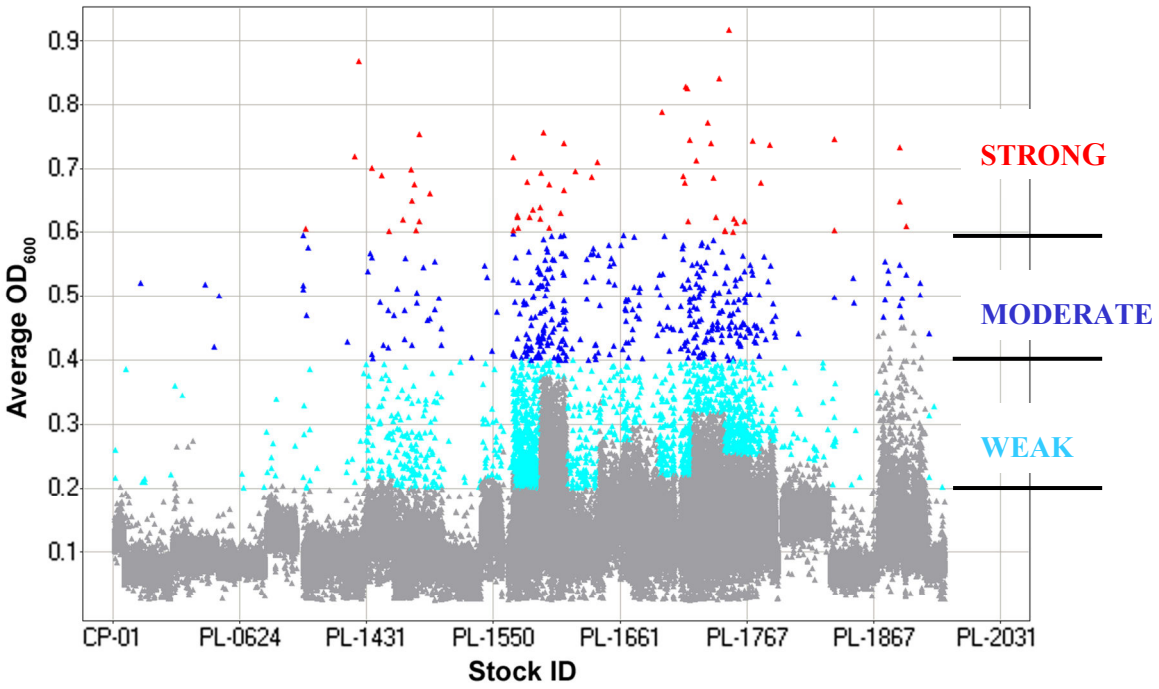

endophytic fungi (fungi that live in higher plants) or from diverse organisms that grow in Costa Rica, including lichens, cyanobacteria, and sponges. Crude extracts from the fungi were obtained and further fractionated to eliminate nuisance compounds, especially those of high molecular weight or high polarity (http://iccb.med.harvard.edu/screening/compound_libraries/ncddg1.htm; access date 2/19/2011). The Starr Foundation collection contains dried extracts from traditional Chinese medicinal plants. The dried extracts were all resuspended at ~15 mg/mL in DMSO (except for Organic fractions--NCI Plant and Fungal Extract library, which was prepared at 5 mg/mL). From these collections, no strong hits were detected (Table 4.4, Figure 4.5). Among the 18,980 compounds, 176 are annotated as weak hits and 2 are identified as moderate hits, which yielded average absorbance values of 0.49 (Plate/well no: 2031-F03; composite Z score: 27.8) and 0.41 (Plate/well no: 2028-D08; composite Z score: 23.5). The former compound was included in the secondary assays and resulted in a similar response (average OD: 0.45; Z score: 20).

4.6 SCREENING AGAINST COMMERCIAL LIBRARIES

I screened a total of 220,071 compounds from the commercial libraries (excluding known bioactives) against a full-length PDE8A-expressing strain (CHP1204). From these libraries 2,260 compounds were annotated as hits (63 strong hit, 388 moderate hit, 1815 weak hit; Figure 4.6). According to the result distribution from each library, the majority of hits are obtained from Asinex, Chembridge3, ChemDiv4, Enamine2, and Maybridge5 libraries. They all yielded at least 1% hit ratio (Table 4.5, Figure 4.7).

Table 4.4 Result distribution with respect to known bioactives and natural products

Known Bioactives	No. compounds	S hits	M hits	W hits	Total hits	Frequency of hits (%)
BIOMOL ICCB Known Bioactives 2	480				0	0
NINDS Custom Collection 2	1,040			1	1	0.1
Prestwick1 Collection	1,120			1	1	0.1

Natural Products	No. compounds	S hits	M hits	W hits	Total hits	Frequency of hits (%)
ICBG Fungal Extracts 12	2,816			48	48	1.7
ICBG Fungal Extracts 4	704				0	0.0
ICBG Fungal Extracts 5	2,112			10	10	0.5
Medicines for Malaria Venture	2,464			17	17	0.7
Medicines for Malaria Venture 2	2,464			16	16	0.6
Medicines for Malaria Venture 3	704		1	6	7	1.0
NCDDG1	380			14	14	3.7
NCDDG2	2,816			11	11	0.4
NCDDG3	1,056			5	5	0.5
NCDDG5	1,056		1	29	30	2.8
Organic NCI Plant and Fungal Extracts	1,408			1	1	0.1
Starr Foundation Extracts 2	1,000			20	20	2.0

Figure 4.5 No strong hits are identified from natural products collection

Scatter plots of average absorbance **(A)** or Z score **(B)** values of plate A against plate B are shown. In-plate controls are demonstrated; negative control DMSO wells are in blue, wells containing positive control BC69 are yellow. Experimental wells are shown in orange for average absorbance and in purple for Z score values. The data shows all natural compounds that were screened against CHP1204 except one set.

Figure 4.5 No strong hits are identified from natural products collection

A

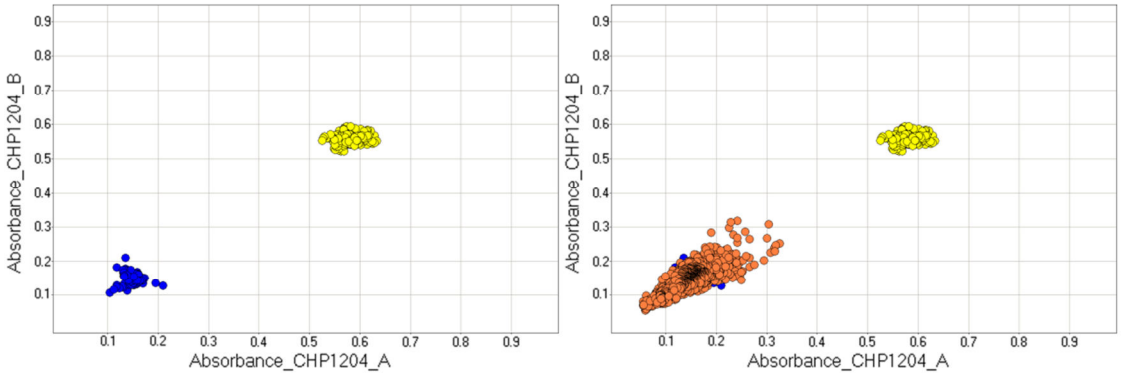

B

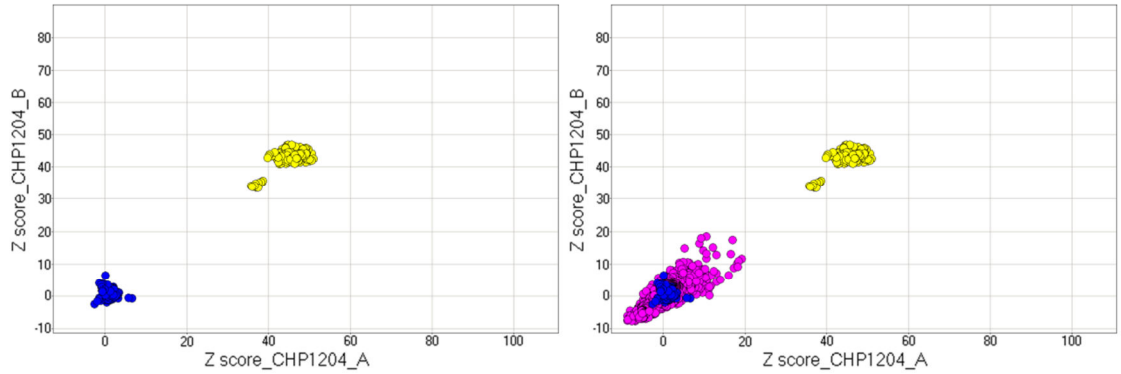

Figure 4.6 Strong hits are identified from commercial libraries

Scatter plots of average absorbance **(A)** or Z score **(B)** values of plate A against plate B are shown. In-plate controls are demonstrated; negative control DMSO wells are in blue, wells containing positive control BC69 are yellow. Experimental wells are shown in orange for average absorbance and in purple for Z score values. The data represents compounds from the entire commercial libraries that were screened against CHP1204.

Figure 4.6 Strong hits are identified from commercial libraries

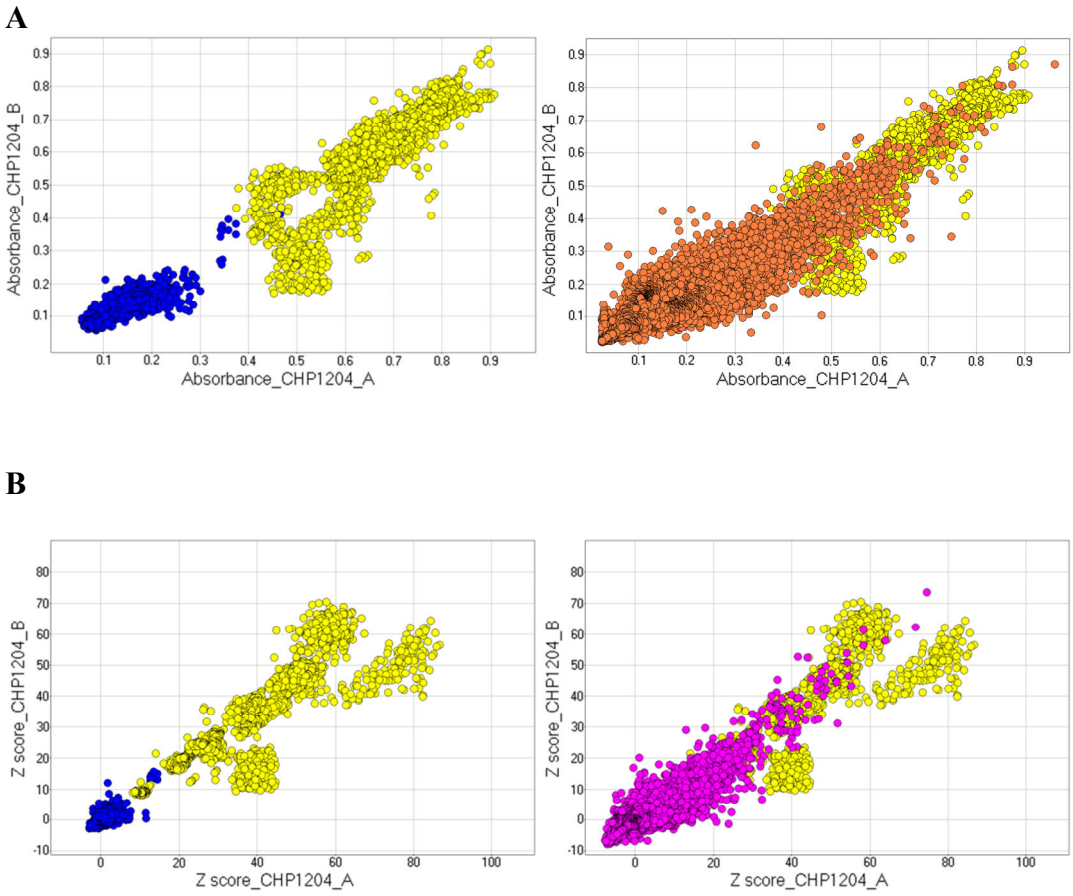

Table 4.5 Result distribution with respect to commercial compound libraries

Commercial	No. compounds	S hits	M hits	W hits	Total hits	Frequency of hits (%)
ActiMolTimTec1	8,517		4	37	41	0.5
Asinex 1	12,378	1	24	130	155	1.3
Bionet1	4,800			2	2	0.0
Bionet (Ryan Scientific) 2	1,700	1	2	6	9	0.5
CEREP	4,800		1	2	3	0.1
ChemBridge3	10,560	15	80	652	747	7.1
ChemDiv1 (Combilab and International)	28,863		3	11	14	0.0
Chemical Diversity 2	8,561			1	1	0.0
ChemDiv3	16,544	8	15	111	134	0.8
ChemDiv4	14,696	6	57	117	180	1.2
ChemDiv6	44,000	5	17	40	62	0.1
Enamine 1	6,004	2	1	7	10	0.2
Enamine 2	26,576	22	150	580	752	2.8
IFLab2	292		1		1	0.3
Life Chemicals 1	3,893		8	20	28	0.7
Maybridge1	7,744			3	3	0.0
Maybridge2	704		3	3	6	0.9
Maybridge3	7,639	3	9	54	66	0.9
Maybridge4	4,576		1	3	4	0.1
Maybridge5	3,212		12	33	45	1.4
Mixed Commercial Plate 1	352				0	0.0
Mixed Commercial Plate 2	320				0	0.0
Mixed Commercial Plate 3	255				0	0.0
Mixed Commercial Plate 5	268				0	0.0
Peakdale1	2,817			3	3	0.1

Figure 4.7 Some commercial libraries yielded higher frequency of hits

The data represent compounds from Asinex, Chembridge3, ChemDiv4, Enamine2, and Maybridge5 libraries. Scatter plots of average absorbance **(A)** or Z score **(B)** values of plate A against plate B are shown. In-plate controls are shown; negative control DMSO wells are in blue, wells containing positive control BC69 are in yellow. Experimental wells are shown in light blue for average absorbance and in red for Z score values.

Figure 4.7 Some commercial libraries yielded higher number of hits

A

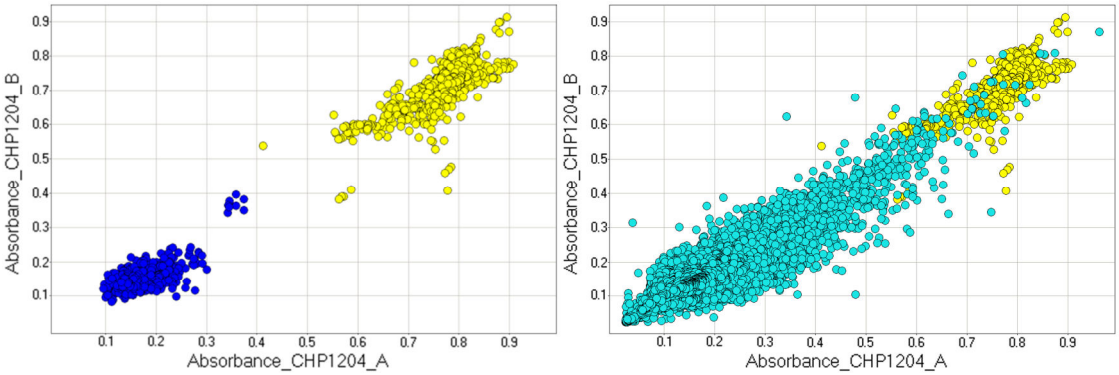

B

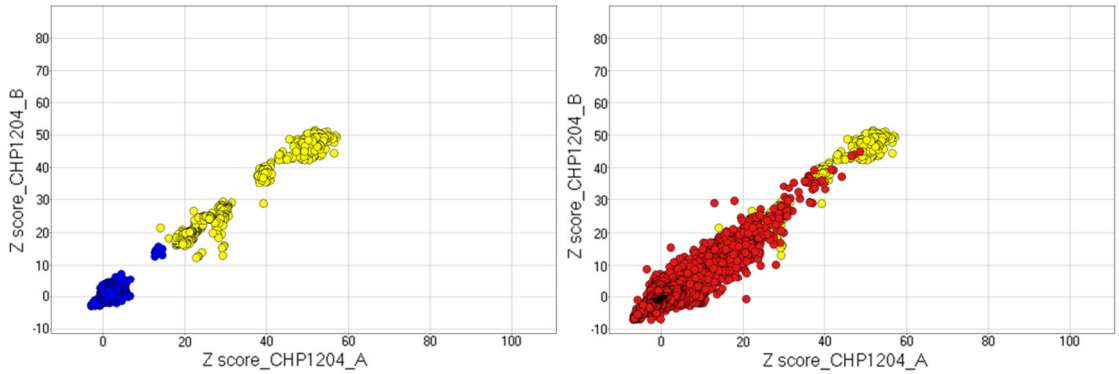

4.7 OVERALL EVALUATION OF THE SCREEN

The result distribution histograms with respect to average absorbance and composite Z score values are plotted in Figure 4.8. Two peaks can be observed for the results distribution of average absorbance data, which indicates that the average of the basal growth was different in certain experiments. When this distribution is plotted with respect to composite Z score, the data is normalized with respect to the basal growth for that assay and produces a single peak. One interesting feature of both of these distribution curves is the presence of a right-hand tail. The range of the tails reaches up to composite Z score of 129 and average absorbance of 0.89. When the distribution chart is drawn to show the standard deviations, we see that 2684 wells displayed positive values greater than 3 standard deviations away from the mean. The positive hits are selected from this group.

In order to monitor the response plate by plate in the experiments following known bioactives screening, in-plate positive and negative controls of 4 wells were also included into each plate. This helped to control plate based problems and was useful in determining if prolonged experimentation time (i.e. the time from the start to the finish of the cell delivery process) adversely affected the plates processed at a later time than previous ones so that preventive measures for obtaining reproducibility and consistency for each plate could be implemented.

Figure 4.8 Result distribution histograms have a right-hand tail

Result distribution histograms display a right-hand tail where the positive hits are located. **(A)** Result distribution with respect to average absorbance values is shown (left panel). Distribution by standard deviation shows that 2633 compounds have OD values greater than 3 standard deviations apart from the mean (right panel). **(B)** Result distribution with respect to composite Z score values is shown (left panel). The right-tail is shown in enlarged scale in the right panel.

Figure 4.8 Result distribution histograms have a right-hand tail

A

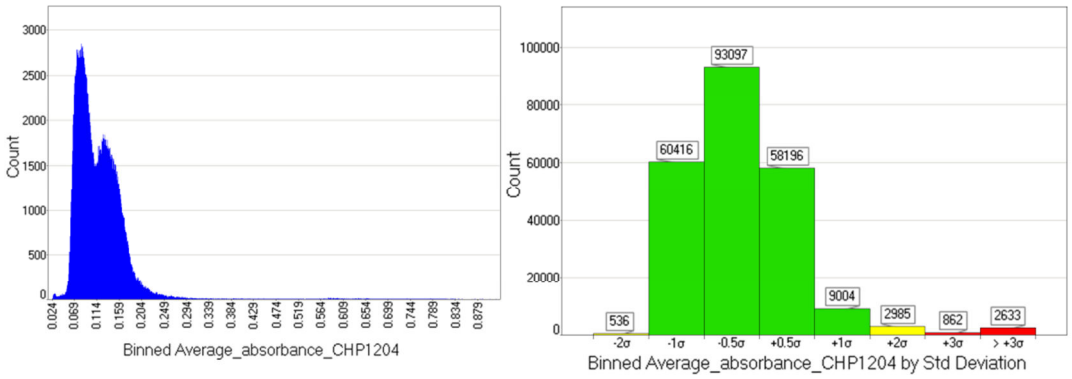

B

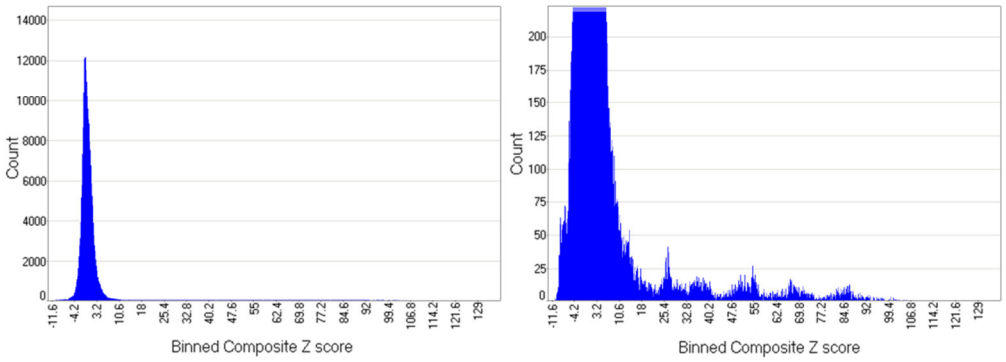

For instance, in the early experiments, I was delivering the cells that were resuspended in 5FOA medium into the wells that contains 2x cAMP and the compounds. After observing that the optical density values for the positive control plates are decreasing in the plates that received the cells toward the end of the experiment (i.e. experienced a longer wait time in the 5FOA medium), I changed the delivery medium to 5FOA with 2x cAMP (this time the plate contains the compounds in 5FOA lacking cAMP) in order to give more chance for the cells to stay in the '5FOA resistant' state. During the experiments, where approximately 40 compound plates were pinned, the indicated problem was still observed such that the optical density values in duplicate plates differ from each other, hence affecting the reproducibility. In order to circumvent that, I started to resuspend the cells separately for the second duplicates so that the time that cells spend in the 5FOA medium prior to delivery and incubation is minimized. This helped to prevent seeing sharp OD changes between duplicate plates as monitored by the positive control wells.

Throughout the screen, although each set of experiments resulted in high Z factors for each plate, the basal growth and highest optical density that the cells can reach showed some variation from experiment to experiment. For instance, high OD values in negative control wells were observed in one experiment such that the data points are located further from other data points with negative control wells in the scatter plot (Figure 4.6). Depending on these variation, a given optical density value might correspond to different composite Z scores. Figure 4.9 shows this variation among different experiments.

Figure 4.9 Experimental variations are observed between average absorbance values and their corresponding composite Z scores

Scatter plot of average absorbance values against composite Z scores is shown. Positive control wells are shown in yellow, negative control wells are in blue, experimental wells are in gray.

Figure 4.9 Experimental variations are observed between average absorbance values and their corresponding composite Z scores

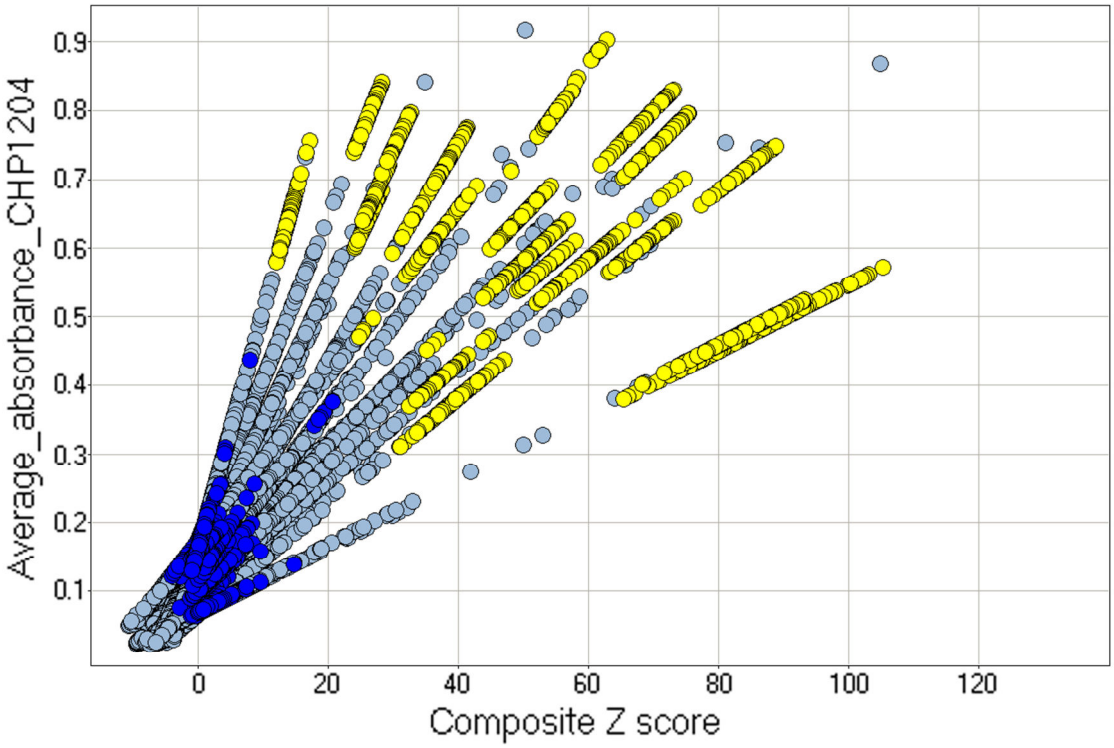

For example, an optical density of 0.5 corresponds to a composite Z score value less than 20 for some assays, while in other assays it can represent composite Z scores up to 60 – even more than 80 in one instance. The data from individual pinnings form single lines some of which overlap with each other. Regardless of this, each group had a good separation between the negative and positive controls and was informative in terms of the identification of the hit compounds.

4.8 SECONDARY SCREENING: CHERRYPICKING

Secondary screening of the selected compounds was done in two sets. The compounds were picked by careful examination of the primary screening data. Strong and moderate hits were picked but most weak hits with low OD values were omitted. During the first round of cherrypicking 280 compounds were selected, while 87 compounds were included in the second set. The volume of compounds that was provided for cherrypicking assays was slightly greater than 1 µL. Firstly, I wanted to repeat the primary screening conditions and screened CHP1204 (full-length PDE8A-expressing strain) against the selected compounds at the same concentration as the primary screen, which is achieved by transferring 100 nL of compounds into each well by the aid of pocket tips. According to the OD values after 48 h of growth, 56 % of the compounds retested as promoting growth if we consider compounds that increased the OD above 0.2 for the first set. For the second set, I set the cutoff as 0.3 since the average OD of the negative values were higher and 73 % of the compounds were confirmed. When the Z score values that are above 5.0 were considered, 65 % of the compounds were confirmed

to promote growth in the 5FOA medium for both sets (Figure 4.10). One of the reasons for failure of some of the compounds to promote growth in 5FOA medium as seen in the primary screen could be the inefficiency of the compound transfer by the pocket tips compared to the pinning process.

In addition to testing against full-length PDE8A-expressing strain, I wanted to test these compounds against the strain that expresses the catalytic domain of PDE8A (DDP40). In this way, we are able to obtain additional data to suggest the ability of the test compounds to inhibit PDE8A. At the same time, if a response is not seen this could lead to detection of compounds that inhibit PDE8A through interactions with the regulatory domain. The compounds were tested against DDP40 at the same concentration as the primary screen (Figure 4.11). Unfortunately, only 71 of these compounds promoted growth in 5FOA to yield Z score values above 8.0.

As a way of determining the selectivity of these compounds toward PDE8A, the cherrypick plates were also screened against strains expressing PDE4A or PDE7 enzymes (Figure 4.12). These families were chosen since they are the other two phosphodiesterases that specifically hydrolyze cAMP. For the first set of experiments, CHP1262 (PDE4A) and CHP1189 (PDE7A) strains were tested by the transfer of 50 nL of the compounds into assay wells. This corresponds to the half of the concentration used during the primary screen. For the second set, instead of CHP1189, PDE7B-expressing strain CHP1209 was used since more overlap in 5FOA growth was being observed for PDE7B relative to PDE7A.

Figure 4.10 Comparison of primary and secondary screens

(A) Scatter plot of absorbance values from cherrypick assay against average absorbance values from the primary screen is shown. **(B)** Scatter plot of Z score values from cherrypick assay against Z score value of plate A from primary screen is shown. Compounds tested in the first set of cherrypick experiments are shown in red, second set are shown in blue.

Figure 4.10 Comparison of primary and secondary screens

A

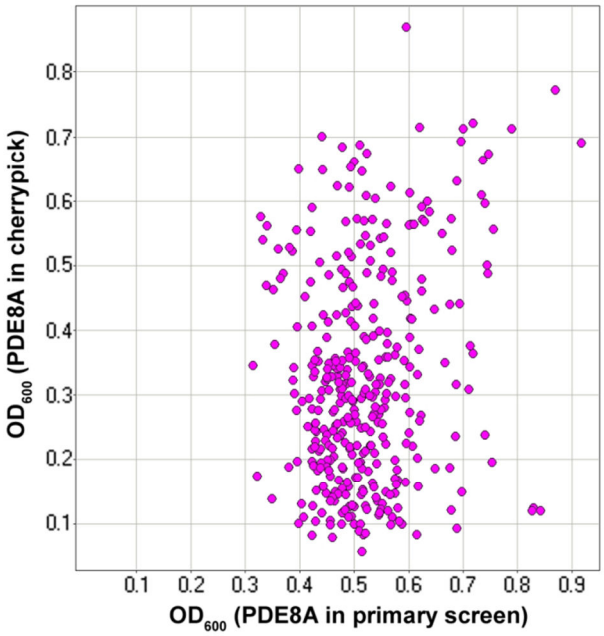

B

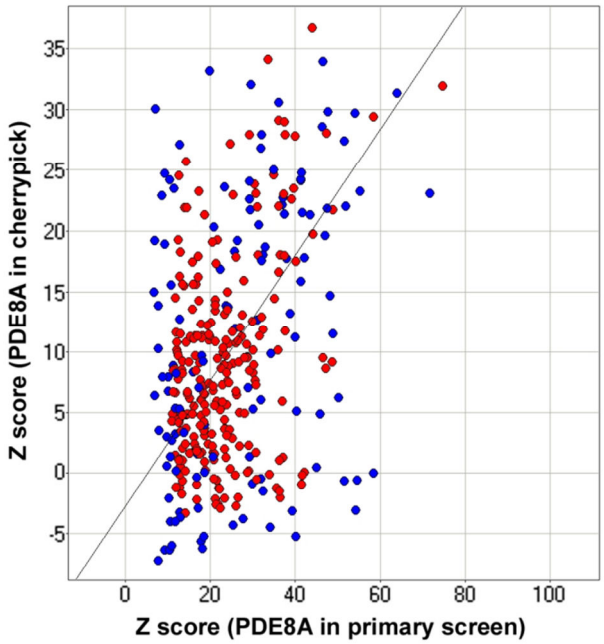

Figure 4.11 Comparison of response by strains that express full-length or catalytic domain PDE8A in the cherrypick assay

Scatter plot of absorbance values of CHP1204 strain (full-length) against DDP40 (catalytic domain) are shown. Thirty eight compounds out of 366 yielded absorbance values above 0.5 for CHP1204 and above 0.4 for DDP40.

Figure 4.11. Comparison of response by strains that express full-length or catalytic domain PDE8A in the cherrypick assay

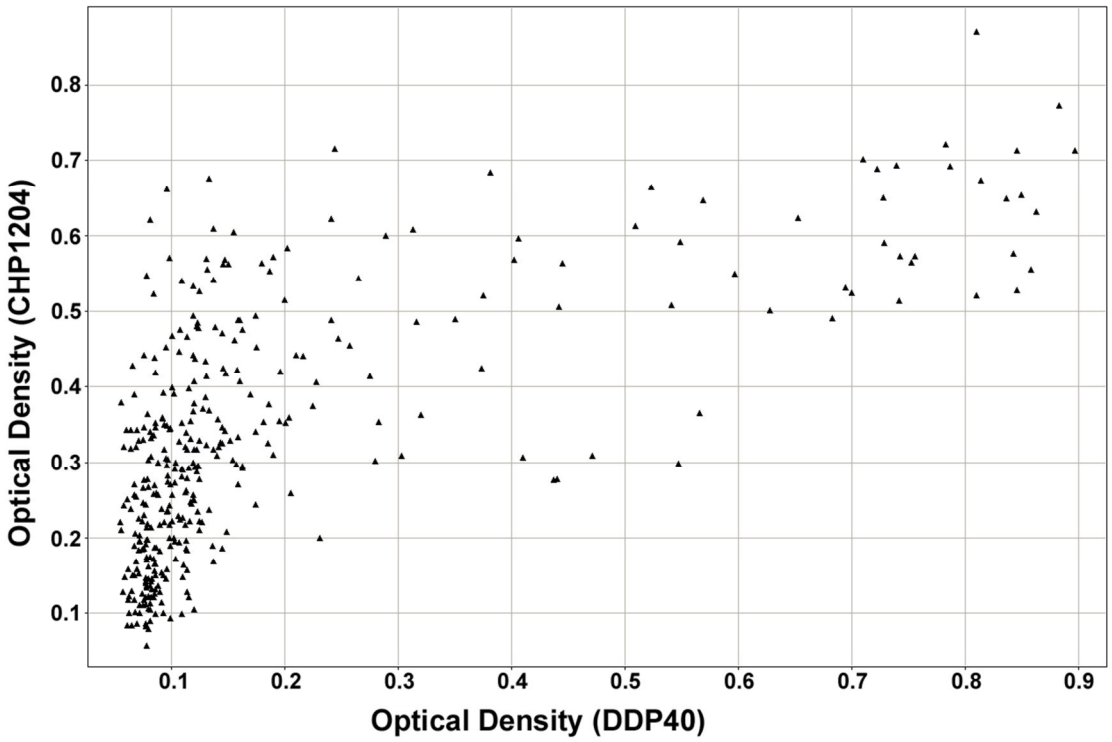

Figure 4.12 Cherrypick results

Cherrypick results from the second set are shown. The plate pictures represent real growth data in a color scale that ranges from blue to red (blue-green-yellow-orange-red) with increasing OD values. Green indicates low OD, red indicates high OD. For CHP1204 (PDE8A) and DDP40 (PDE8A-catalytic domain) 100 nL of compounds are transferred, for CHP1262 (PDE4A) and CHP1209 (PDE7A) half of this concentration was tested. Two rows from each side of the plate are kept empty, the plates contain 87 test compounds.

Figure 4.12 Cherrypick results

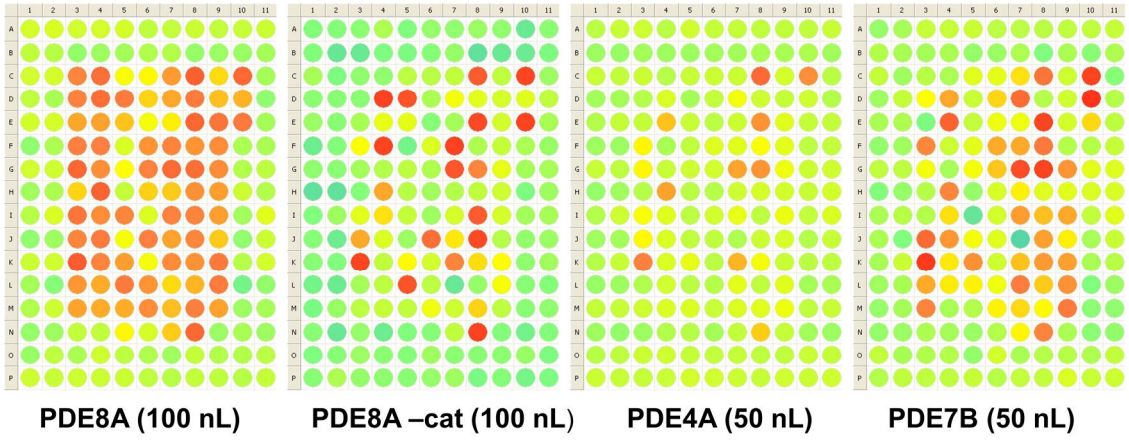

Figure 4.13 Comparison of response by the PDE8A-expressing strain against strains that express PDE4A or PDE7A/B in the cherrypick assay

(A) Scatter plot of Z score values from PDE4A–expressing strain (CHP1262) is shown against CHP1204. **(B)** Scatter plot of Z score values from PDE7A (CHP1189) or PDE7B (1209) expressing strains is shown against CHP1204. PDE7A is tested in the first set of cherrypicking assay (shown in red), while PDE7B is used in the second one (shown in blue).

Figure 4.13 Comparison of response by the PDE8A-expressing strain against strains that express PDE4A or PDE7A/B in the cherrypick assay

A

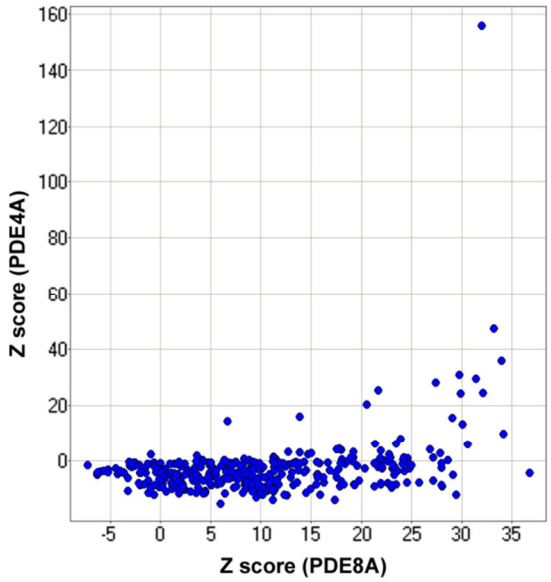

B

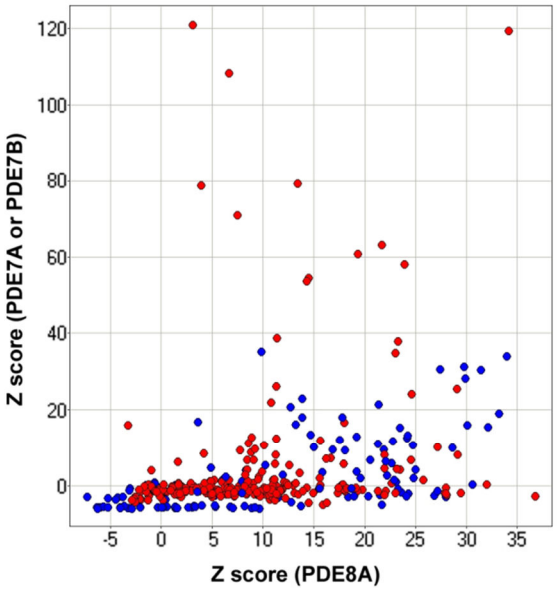

The compound that resulted in the best growth response for CHP1262 strain (PDE4A) is BC69 that resulted in Z score value of 155. There are 20 compounds that yielded Z score values above 5.0 (Figure 4.13A). On the other hand, CHP1189 (PDE7A) also yielded Z score values above 100 for three compounds (Plate/well no: 1665 A07, 1785 B07, 1728 H22). There are 20 compounds that have absorbance values above 0.100 (this corresponds to Z score value of approximately 16). Testing against CHP1209 (PDE7B) helped to eliminate 33 compounds out of 87 (Figure 4.13B).

Upon examination of the cherrypick data along with the primary screen results, 30 compounds, 28 of which are structurally-distinct, were purchased to be pursued in further analyses.

4.9 CONCLUSION

I optimized high-throughput screening conditions for adenylyl cyclase deletion strain CHP1204 that expresses full-length PDE8A using BC69 as a positive control. The assay conditions yield Z factor values between 0.6 and 0.9 in different experiments, which indicates a robust high-throughput screen. A total of 241,691 compounds from known bioactives, natural products, and commercial libraries were screened; 2447 total hits were identified. The positive hits are mostly from commercial libraries. Secondary assays with the selected compounds confirmed the effect of approximately 70% of these compounds on the 5FOA growth of strain CHP1204. Some of the non-specific compounds were eliminated by determining their effect on PDE4A, PDE7A or PDE7B-expressing strains.

Based on our assessment of the potency and selectivity of the cherry-picked candidates, thirty compounds were purchased to be further analyzed.

CHAPTER FIVE

5 EVALUATION OF THE COMPOUNDS IDENTIFIED IN HTS

Thirty compounds (Table 5.1) selected from the cherrypick collection are confirmed by their dose response profile on PDE8A-expressing strains. They are further evaluated in terms of their dose dependent effect on the growth of yeast strains that express other mammalian PDEs. The inhibitory effect of these compounds on PDE8A is verified by *in vitro* enzyme assays.

5.1 DOSE REPSONSE PROFILING AGAINST PDE8A

Thirty compounds that were found to promote growth of the PDE8A-expressing strain CHP1204 were tested against the same strain under concentrations increasing from 0.1 μM to 100 μM. The dose response profiles of the compounds are given in Figure 5.1. as separate graphs. Compound BC8-8 and BC8-20 increase the growth of PDE8A-expressing strain to higher OD values at lower concentrations compared to other compounds (Figure 5.1.A). Compound BC8-17 and BC8-1H show a bell-shaped dose response profile suggesting growth inhibition at high concentrations. Among the tested compounds only BC8-3, BC8-7, BC8-25 and BC8-27 fail to promote growth of PDE8A-expressing strain (Figure 5.1.E-F). Although BC8-3 was able to increase OD value of CHP1204 in the primary and secondary screens, BC8-7, BC8-25 and BC8-27 did not confirm in the cherrypick assays either. Inability of the purchased form of the compounds

to stimulate growth in the 'in house' tests might be due to the presence of different forms of active molecules in the compound stocks. Although no significant compound degradation has been observed by freeze/thaw cycles during HTS practices (Kozikowski *et al*. 2003), some degradation can be seen over time due to the exposure of the compounds to DMSO. In this case, the storage conditions might have led to the active form or simply the purchased compound might be impure.

I also tested these compounds against strain DDP40 that expresses the catalytic domain of PDE8A. Only twelve compounds (BC8-1, BC8-1F, BC8-1H, BC8-2, BC8-5, BC8-6, BC8-8, BC8-9, BC8-14, BC8-15, BC8-16, and BC69) promote the growth of this strain (Figure 5.2). When compared to cherrypick data, all of these compounds -except BC8-23- showed the same inhibition profile. On the other hand, BC8-23 worked in the cherrypick assays against strain DDP40, while it did not promote growth during 'in house' dose response tests.

5.2 DOSE RESPONSE PROFILING AGAINST OTHER STRAINS

After verifying their effect against PDE8A-expressing strains, I tested the compounds against other strains that express different phosphodiesterases to determine the PDE inhibition profile of these compounds and to identify the ones that are selective to PDE8A.

Table 5.1 Primary and secondary screening data for selected compounds

	Primary Screen		Cherrypick assays (Absorbance)			
Hoffman Lab ID	Average Absorbance	Composite Z Score	PDE8A	PDE8Acat	PDE4A	PDE7A or PDE7B (in bold)
BC69	0.8685	104.8	0.772	0.883	0.592	0.051
BC8-1	0.679	57.6	0.524	0.7	0.104	0.046
BC8-2	0.7395	24.0	0.596	0.406	0.11	0.185
BC8-3	0.693	22.0	0.441	0.21	0.111	0.092
BC8-4	0.7555	24.7	0.556	0.132	0.098	0.045
BC8-5	0.7885	54.3	0.713	0.897	0.172	0.141
BC8-6	0.8295	57.6	0.125	0.085	0.115	0.047
BC8-7	0.8265	57.4	0.12	0.077	0.097	0.044
BC8-8	0.595	68.2	0.869	0.81	0.112	0.04
BC8-9	0.5145	19.2	0.646	0.569	0.102	0.055
BC8-10	0.629	19.3	0.568	0.402	0.101	0.041
BC8-11	0.6255	52.1	0.571	0.098	0.117	0.045
BC8-12	0.62	51.5	0.715	0.244	0.11	0.079
BC8-13	0.567	16.7	0.622	0.241	0.102	0.074
BC8-14	0.634	52.9	0.6	0.289	0.1	0.065
BC8-15	0.423	35.0	0.59	0.729	0.099	0.043
BC8-16	0.9165	50.3	0.691	0.787	0.099	0.048
BC8-17	0.4905	39.6	0.621	0.081	0.118	**0.106**
BC8-18	0.5385	45.1	0.604	0.155	0.189	**0.112**
BC8-19	0.4200	31.6	0.475	0.108	0.131	**0.104**
BC8-20	0.5005	54.7	0.661	0.096	0.208	**0.18**
BC8-21	0.34	34.7	0.562	0.146	0.131	**0.109**
BC8-22	0.7330	16.5	0.609	0.137	0.157	**0.141**
BC8-23	0.6610	69.6	0.55	0.597	0.123	**0.151**
BC8-24	0.3610	32.4	0.526	0.125	0.121	**0.06**
BC8-25	0.4325	41.3	0.117	0.062	0.109	**0.098**
BC8-26	0.6470	14.0	0.433	0.13	0.139	**0.154**
BC8-27	0.4775	46.9	0.183	0.114	0.133	**0.153**
BC8-28	0.4235	40.2	0.128	0.114	0.116	**0.088**
BC8-1F	0.7185	84.7	0.721	0.783	0.089	0.043
BC8-1H	0.559	57.0	0.565	0.753	0.105	**0.126**

Figure 5.1 Dose response profiling of identified compounds against CHP1204

The 5FOA growth phenotype of full-length PDE8A-expressing strain CHP1204 was tested in the presence of compounds that were identified from HTS. **(A-F)** The compounds are grouped according to their ED_{50} values, which is the effective dose to exert the half-maximal response. Panel F also includes dose response profile of PDE4/8 dual specificity inhibitor BC69.

Figure 5.1 Dose response profiling of identified compounds against CHP1204

A

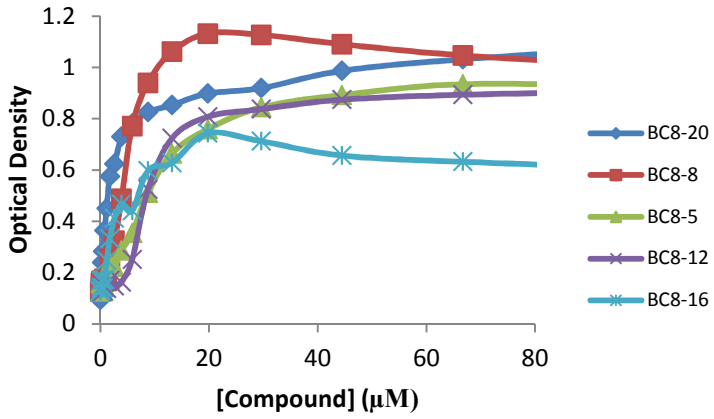

B

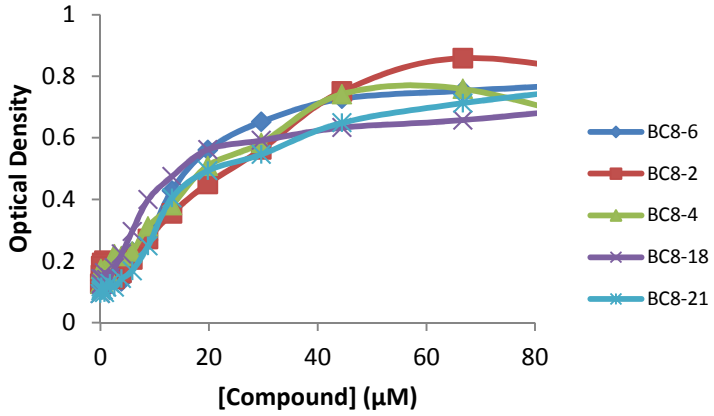

C

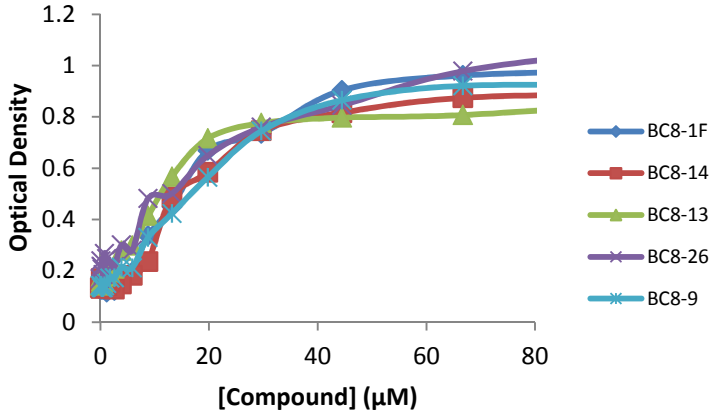

D

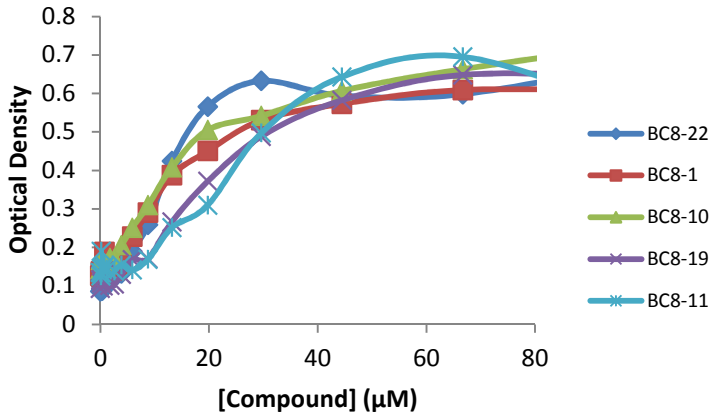
Optical Density
0.8
0.7
0.6
0.5
0.4
0.3
0.2
0.1
0
0
20
40
60
80
[Compound] (µM)
BC8-22
BC8-1
BC8-10
BC8-19
BC8-11

E

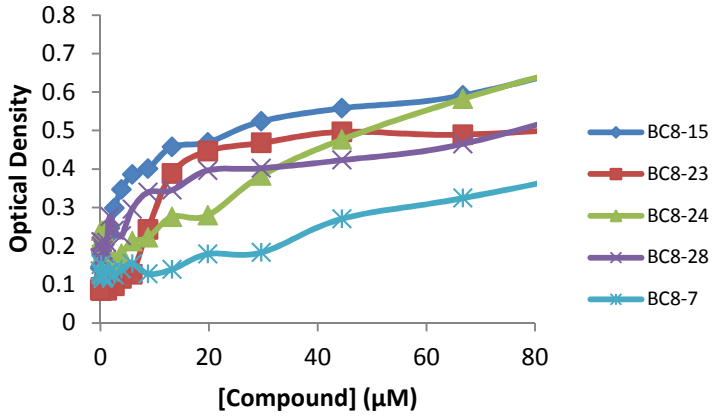
Optical Density
0.8
0.7
0.6
0.5
0.4
0.3
0.2
0.1
0
0
20
40
60
80
[Compound] (µM)
BC8-15
BC8-23
BC8-24
BC8-28
BC8-7

F

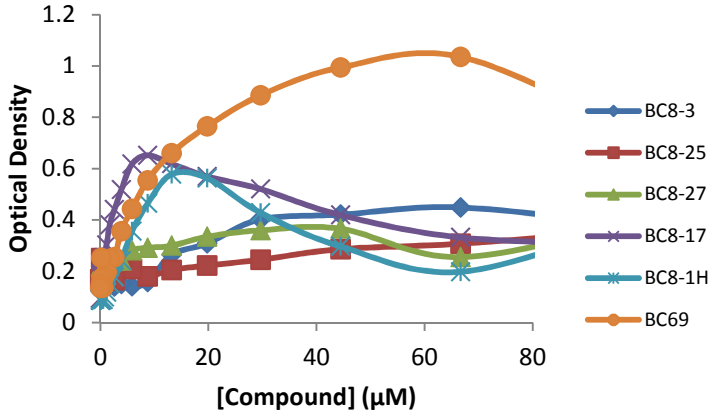
Optical Density
1.2
1
0.8
0.6
0.4
0.2
0
0
20
40
60
80
[Compound] (µM)
BC8-3
BC8-25
BC8-27
BC8-17
BC8-1H
BC69

Figure 5.2 Dose response profiling of identified compounds against DDP40

The 5FOA growth phenotype of DDP40 strain that expresses the catalytic domain of PDE8A is assessed in the presence of compounds that were identified from HTS. **(A)** Compounds that promote growth are shown. **(B)** Compounds that fail to promote growth are shown.

Figure 5.2 Dose response profiling of identified compounds against DDP40

A

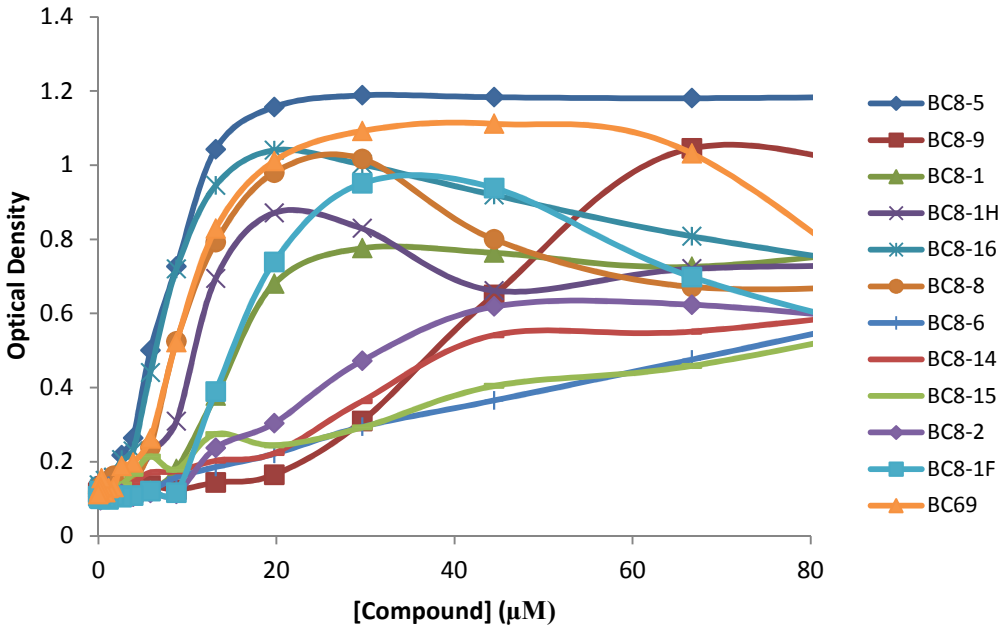

B

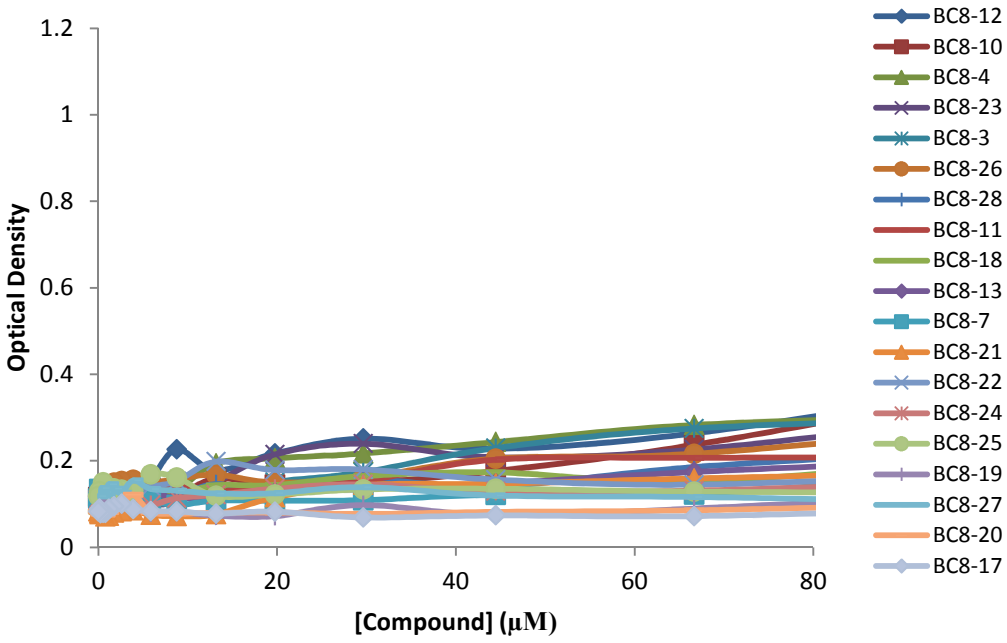

The Hoffman lab strain collection contains 15 different strains that express different PDE enzymes representing each PDE family except PDE6. The 5FOA growth phenotype of different strains identified compounds with different inhibition profiles. When PDE4 inhibitor rolipram is profiled, consistent with its well-established pharmacological characteristics, it promoted the 5FOA growth of only PDE4A, PDE4B and PDE4D-expressing strains (Figure 5.3).

5.2.1 Compounds That Promote the 5FOA Growth of Most PDE-Expressing Strains

Compounds BC8-2, BC8-6, BC8-12, BC8-13, BC8-14, BC8-18, BC8-19, BC8-20, BC8-21, and BC8-26 elevated the 5FOA growth of many strains that express different PDEs (Figure 5.4). The observation of a similar effect against different strains may suggest that these compounds act via a non-PDE target to promote growth in the 5FOA medium. However, the presence of some strains that do not respond to any of these compounds was also observed. For instance, the PDE inhibition profile of these compounds is similar in their failure to promote the growth of PDE4D-expressing strain (CHP1186). A similar phenomenon was observed for PDE4B-expressing strain (CHP1268); it did not respond to any of these compounds but only had a slight increase in OD in the presence of BC8-12. PDE4A-expressing strain (CHP1262) did not respond to any of the compounds from this group except BC8-19, BC8-20 and BC8-21. Similarly, a strain that expresses PDE3A (CHP1249) did not respond to other compounds except BC8-19 and slightly responded to BC8-20 and BC8-21. On the other hand, DDP40 that expresses the PDE8A-catalytic

domain did not respond to most of the compounds with the exception of BC8-2, BC8-6, and BC8-14. Except for a slight elevation in OD in the presence of BC8-21 or BC8-26; PDE5A-expressing strain CHP1223 did not respond to these compounds. Finally, strains CHP1189 and CHP1209, which express PDE7A and PDE7B respectively, showed some elevation in their OD values in the presence of these compounds except for BC8-18, BC8-19 and BC8-21.

5.2.2 Compounds That Promote the 5FOA Growth of Several Strains

Compounds BC8-3, BC8-4, and BC8-28 promote the growth of several strains that express different phosphodiesterases, but not all of them. As stated previously, BC8-3 did not work well on the PDE8A-expressing strain (CHP1204); likewise it slightly promoted growth for PDE7A strain (CHP1189). However, a profound effect in growth was observed for strains expressing PDE7B (CHP1209), PDE11A (CHP1224), PDE10A (CHP1455) and PDE9A (CHP1218). On the other hand, BC8-4 mainly promoted the growth of PDE8A (CHP1204), PDE10A (CHP1455), PDE2A (CHP1403), PDE3B (CHP1194), PDE1B (CHP1222), PDE1C (CHP1220) and PDE9A-expressing (CHP1218) strains. Similarly, a slight effect was observed on PDE8A-expressing strain by compound BC8-28 but it promoted growth of PDE1B, PDE1C, PDE10, and PDE11-expressing strains (Figure 5.5).

Figure 5.3 Rolipram promotes the growth of PDE4A, PDE4B and PDE4D-expressing strains

Dose response profiling with rolipram against yeast strains that express different PDEs promotes only the growth of PDE4A (CHP1262), PDE4B (CHP1268), and PDE4D (CHP1186) expressing strains. The strains shown are CHP1222 (PDE1B), CHP1220 (PDE1C), CHP1403 (PDE2A), CHP1249 (PDE3A), CHP1194 (PDE3B), CHP1262 (PDE4A), CHP1268 (PDE4B), CHP1186 (PDE4D), CHP1223 (PDE5A), CHP1189 (PDE7A), CHP1209 (PDE7B), CHP1204 (PDE8A), DDP40 (PDE8Acat), CHP1218 (PDE9A), CHP1224 (PDE11A), CHP1445 (PDE10A), and CHP1224 (PDE11A).

Figure 5.3 Rolipram promotes the growth of PDE4A, PDE4B and PDE4D-expressing strains

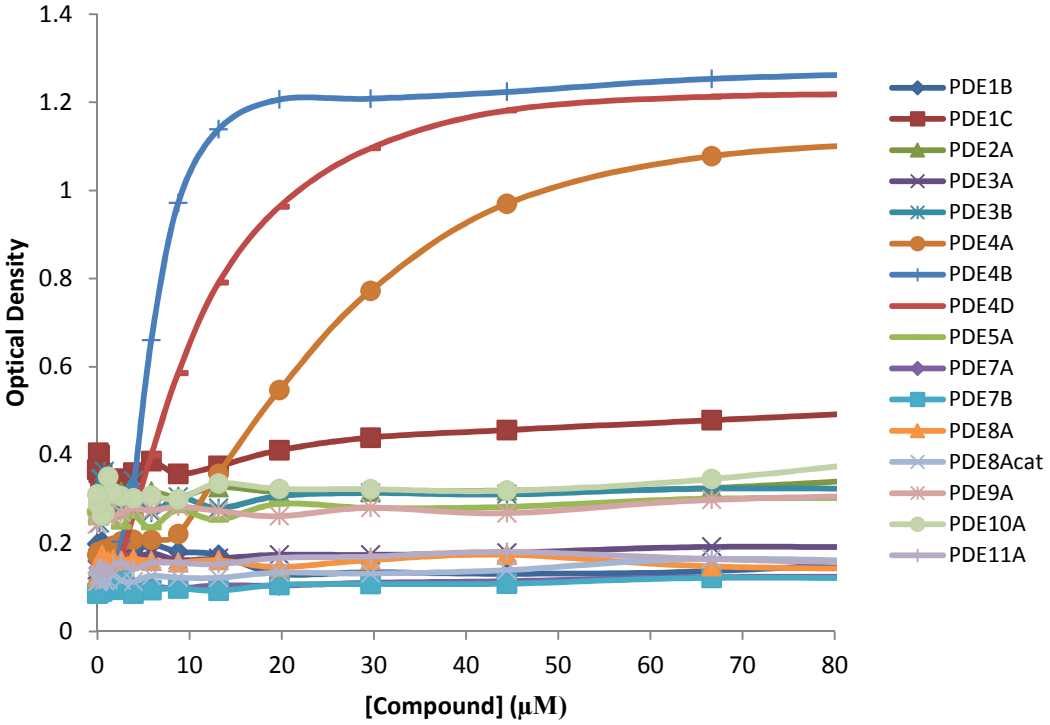

Figure 5.4 Compounds that promote the 5FOA growth of most PDE-expressing strains

The 5FOA growth responses of yeast strains that express different phosphodiesterases are shown in the presence of individual compounds in separate graphs. The strains shown are CHP1222 (PDE1B), CHP1220 (PDE1C), CHP1403 (PDE2A), CHP1249 (PDE3A), CHP1194 (PDE3B), CHP1262 (PDE4A), CHP1268 (PDE4B), CHP1186 (PDE4D), CHP1223 (PDE5A), CHP1189 (PDE7A), CHP1209 (PDE7B), CHP1204 (PDE8A), DDP40 (PDE8Acat), CHP1218 (PDE9A), CHP1224 (PDE11A), CHP1445 (PDE10A), and CHP1224 (PDE11A). **(A-J)** Compounds BC8-2, BC8-6, BC8-12, BC8-13, BC8-14, BC8-18, BC8-19, BC8-20, BC8-21, BC8-26.

Figure 5.4 Compounds that promote the 5FOA growth of most PDE-expressing strains

A

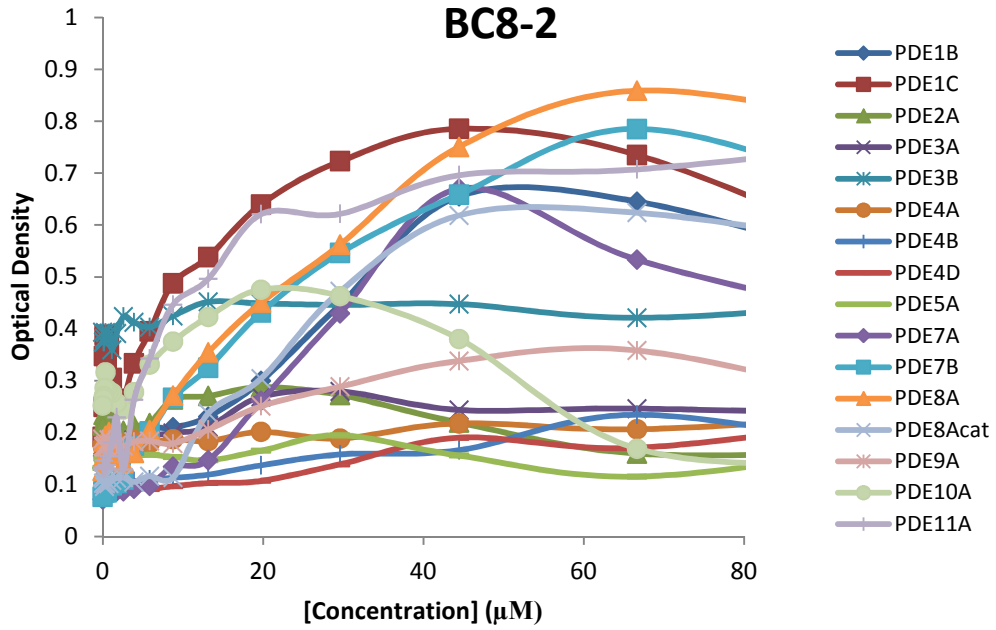

B

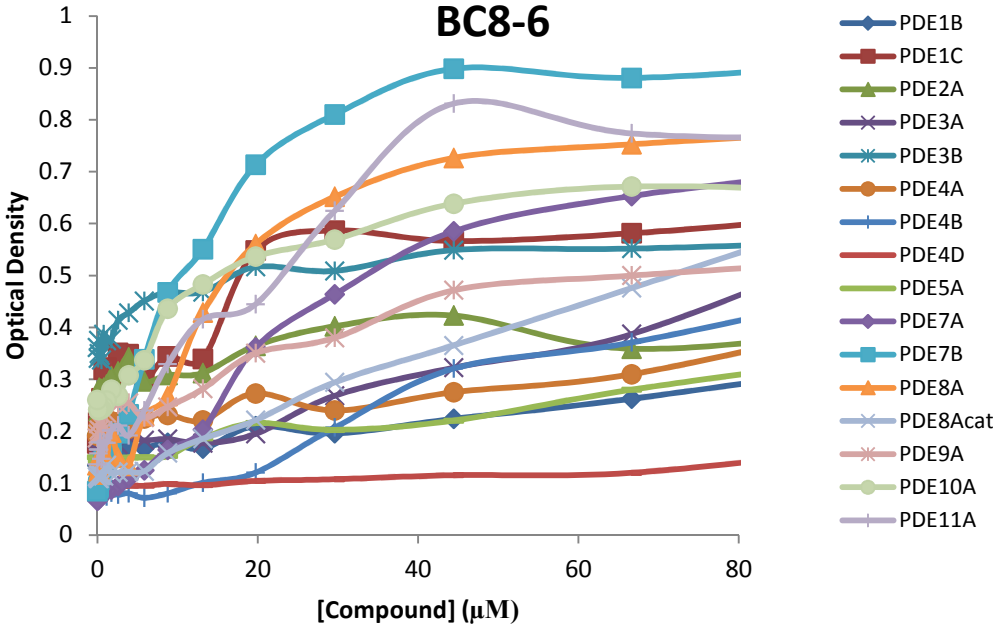

C

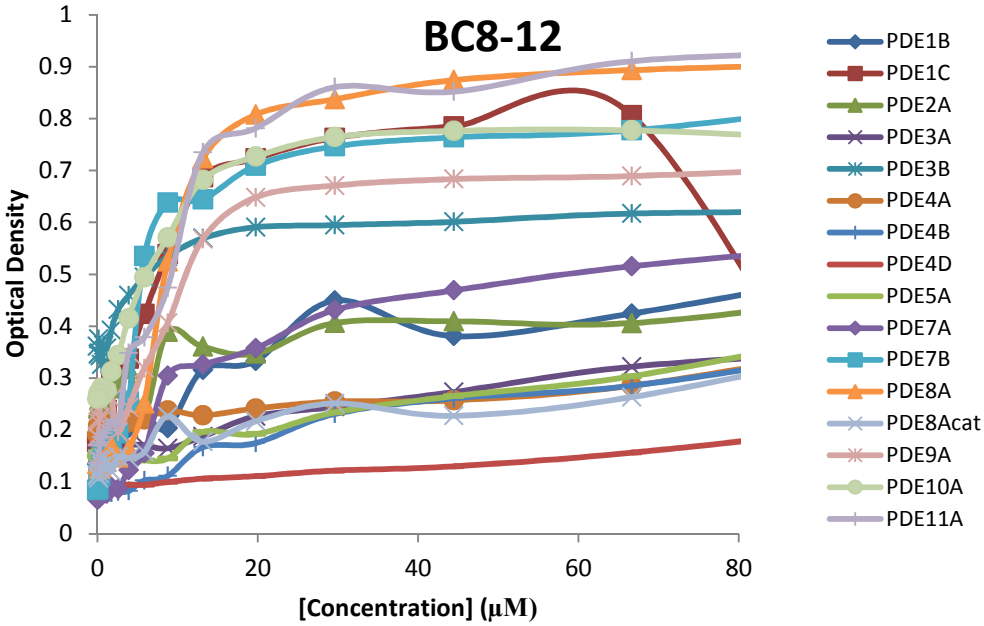
BC8-12
Optical Density
[Concentration] (µM)
0
0.1
0.2
0.3
0.4
0.5
0.6
0.7
0.8
0.9
1
0
20
40
60
80
PDE1B
PDE1C
PDE2A
PDE3A
PDE3B
PDE4A
PDE4B
PDE4D
PDE5A
PDE7A
PDE7B
PDE8A
PDE8Acat
PDE9A
PDE10A
PDE11A

D

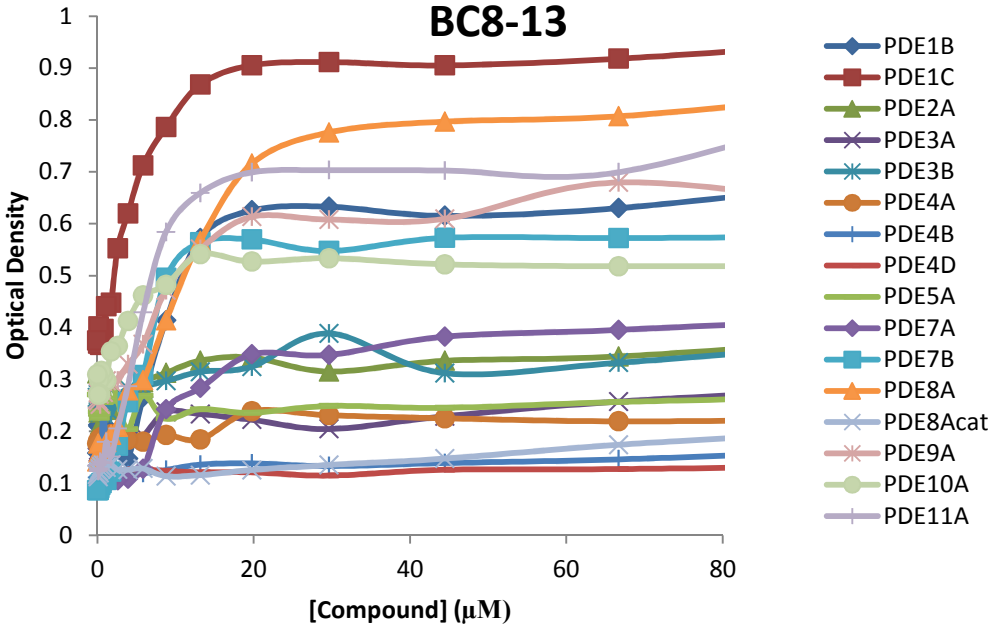
BC8-13
Optical Density
[Compound] (µM)
0
0.1
0.2
0.3
0.4
0.5
0.6
0.7
0.8
0.9
1
0
20
40
60
80
PDE1B
PDE1C
PDE2A
PDE3A
PDE3B
PDE4A
PDE4B
PDE4D
PDE5A
PDE7A
PDE7B
PDE8A
PDE8Acat
PDE9A
PDE10A
PDE11A

E

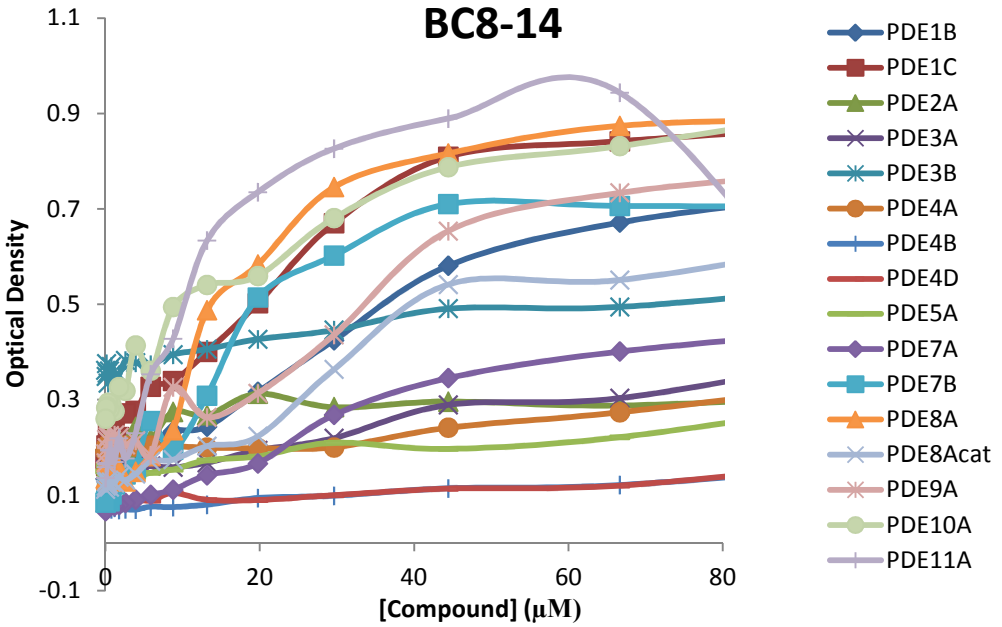
BC8-14
Optical Density
1.1
0.9
0.7
0.5
0.3
0.1
-0.1
0
20
40
60
80
[Compound] (µM)
PDE1B
PDE1C
PDE2A
PDE3A
PDE3B
PDE4A
PDE4B
PDE4D
PDE5A
PDE7A
PDE7B
PDE8A
PDE8Acat
PDE9A
PDE10A
PDE11A

F

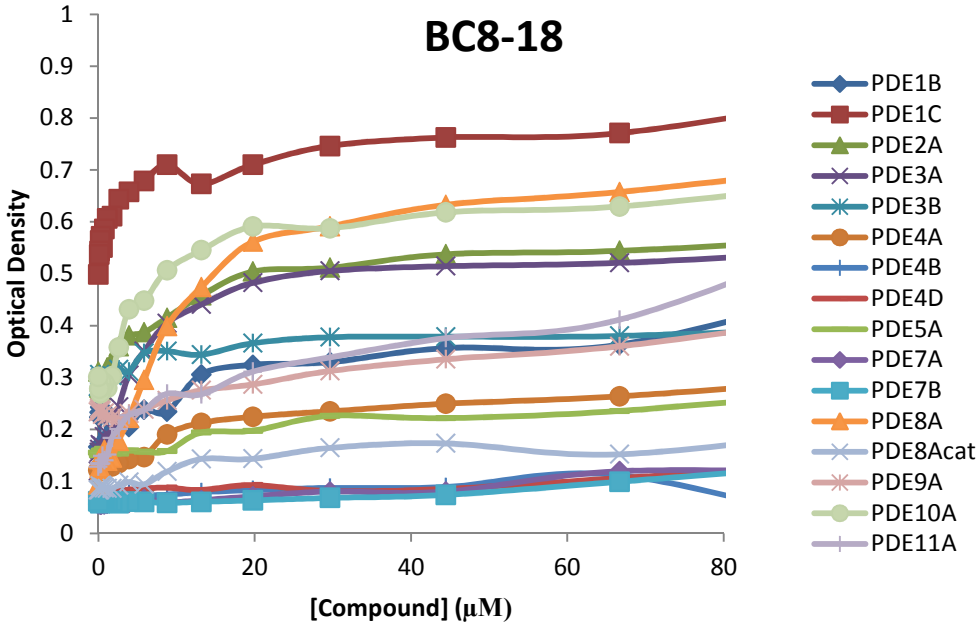
BC8-18
Optical Density
1
0.9
0.8
0.7
0.6
0.5
0.4
0.3
0.2
0.1
0
0
20
40
60
80
[Compound] (µM)
PDE1B
PDE1C
PDE2A
PDE3A
PDE3B
PDE4A
PDE4B
PDE4D
PDE5A
PDE7A
PDE7B
PDE8A
PDE8Acat
PDE9A
PDE10A
PDE11A

G

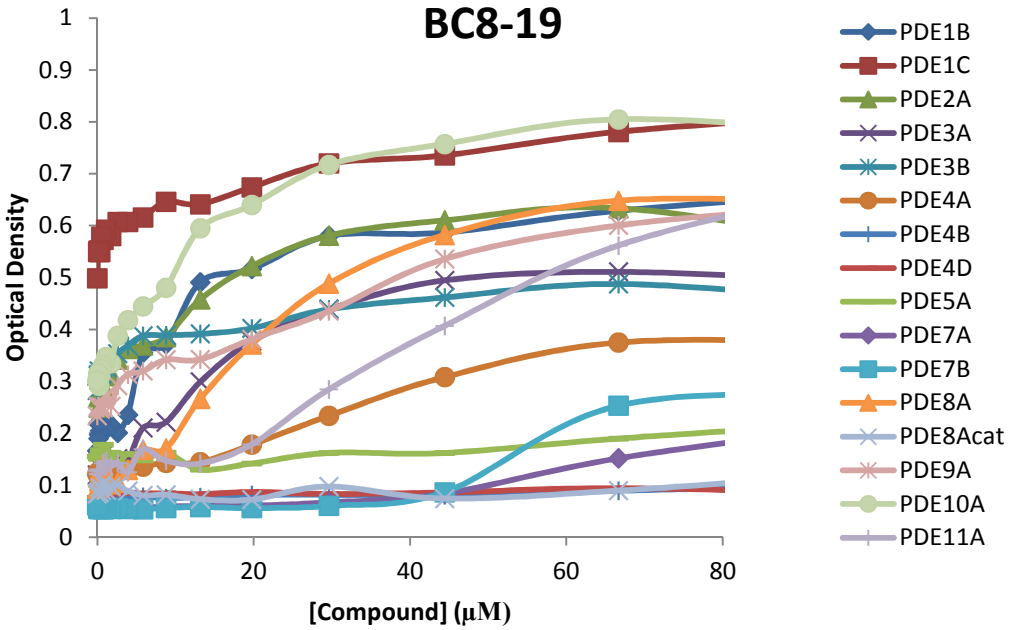
BC8-19
Optical Density
[Compound] (µM)
0
0.1
0.2
0.3
0.4
0.5
0.6
0.7
0.8
0.9
1
0
20
40
60
80
PDE1B
PDE1C
PDE2A
PDE3A
PDE3B
PDE4A
PDE4B
PDE4D
PDE5A
PDE7A
PDE7B
PDE8A
PDE8Acat
PDE9A
PDE10A
PDE11A

H

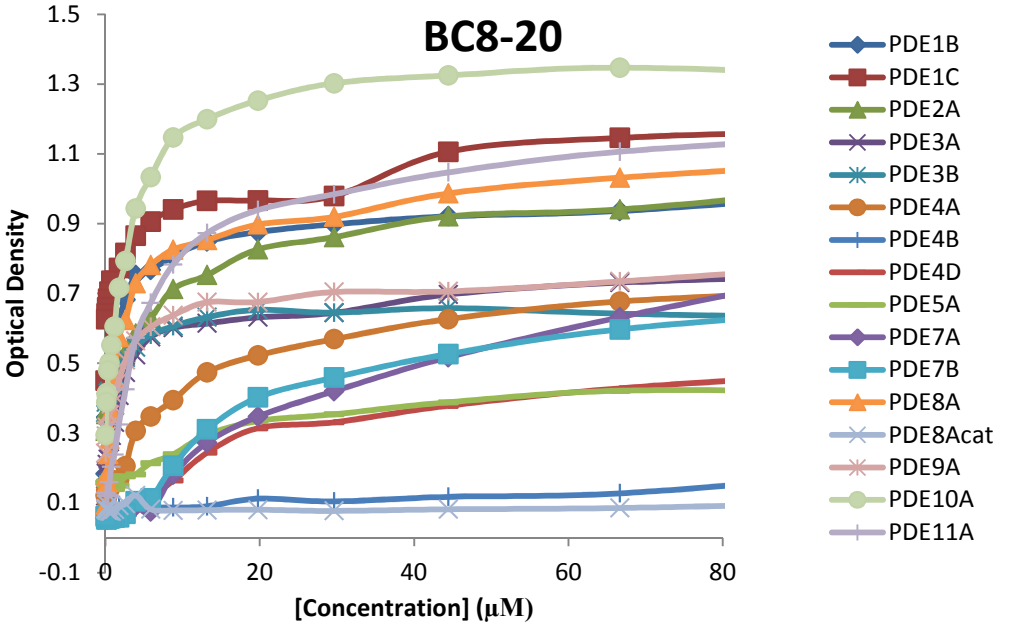
BC8-20
Optical Density
[Concentration] (µM)
-0.1
0.1
0.3
0.5
0.7
0.9
1.1
1.3
1.5
0
20
40
60
80
PDE1B
PDE1C
PDE2A
PDE3A
PDE3B
PDE4A
PDE4B
PDE4D
PDE5A
PDE7A
PDE7B
PDE8A
PDE8Acat
PDE9A
PDE10A
PDE11A

I

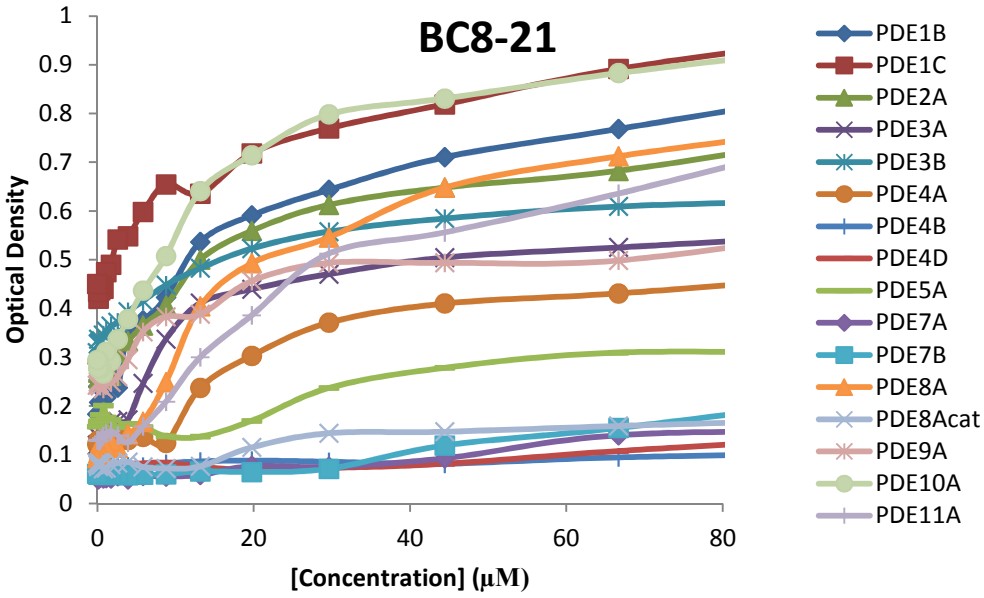
BC8-21
Optical Density
[Concentration] (µM)
0
0.1
0.2
0.3
0.4
0.5
0.6
0.7
0.8
0.9
1
0
20
40
60
80
PDE1B
PDE1C
PDE2A
PDE3A
PDE3B
PDE4A
PDE4B
PDE4D
PDE5A
PDE7A
PDE7B
PDE8A
PDE8Acat
PDE9A
PDE10A
PDE11A

J

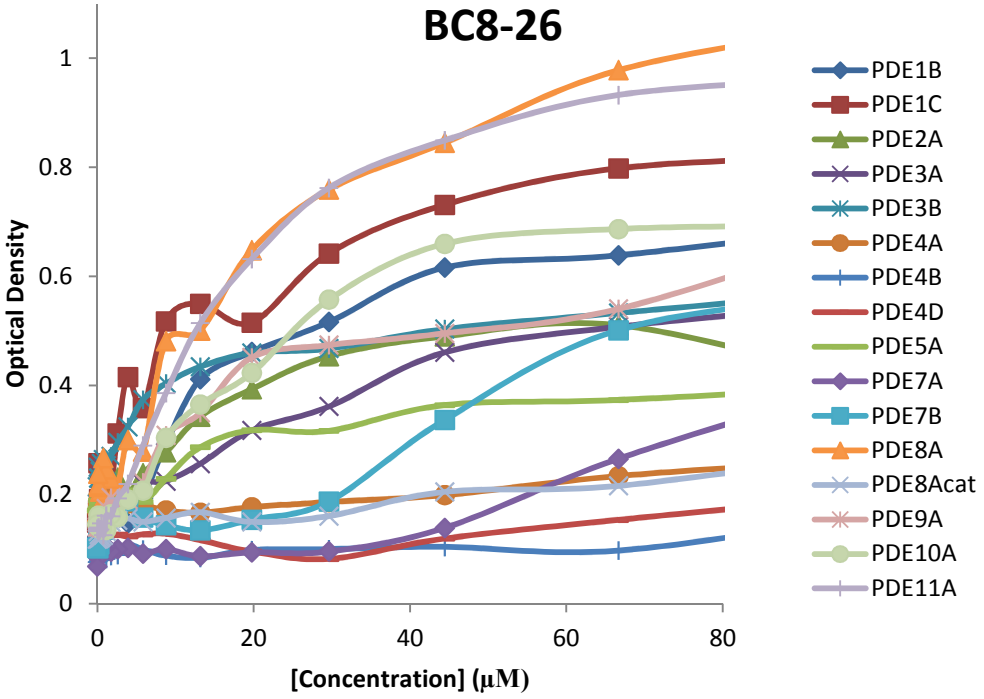
BC8-26
Optical Density
[Concentration] (µM)
0
0.2
0.4
0.6
0.8
1
0
20
40
60
80
PDE1B
PDE1C
PDE2A
PDE3A
PDE3B
PDE4A
PDE4B
PDE4D
PDE5A
PDE7A
PDE7B
PDE8A
PDE8Acat
PDE9A
PDE10A
PDE11A

Figure 5.5 Compounds that promote the 5FOA growth of several strains

The 5FOA growth responses of yeast strains that express different phosphodiesterases are shown in the presence of individual compounds in separate graphs. The strains shown are CHP1222 (PDE1B), CHP1220 (PDE1C), CHP1403 (PDE2A), CHP1249 (PDE3A), CHP1194 (PDE3B), CHP1262 (PDE4A), CHP1268 (PDE4B), CHP1186 (PDE4D), CHP1223 (PDE5A), CHP1189 (PDE7A), CHP1209 (PDE7B), CHP1204 (PDE8A), DDP40 (PDE8Acat), CHP1218 (PDE9A), CHP1224 (PDE11A), CHP1445 (PDE10A), and CHP1224 (PDE11A). **(A-C)** Compounds BC8-3, BC8-4, BC8-28.

Figure 5.5 Compounds that promote the 5FOA growth of several strains

A

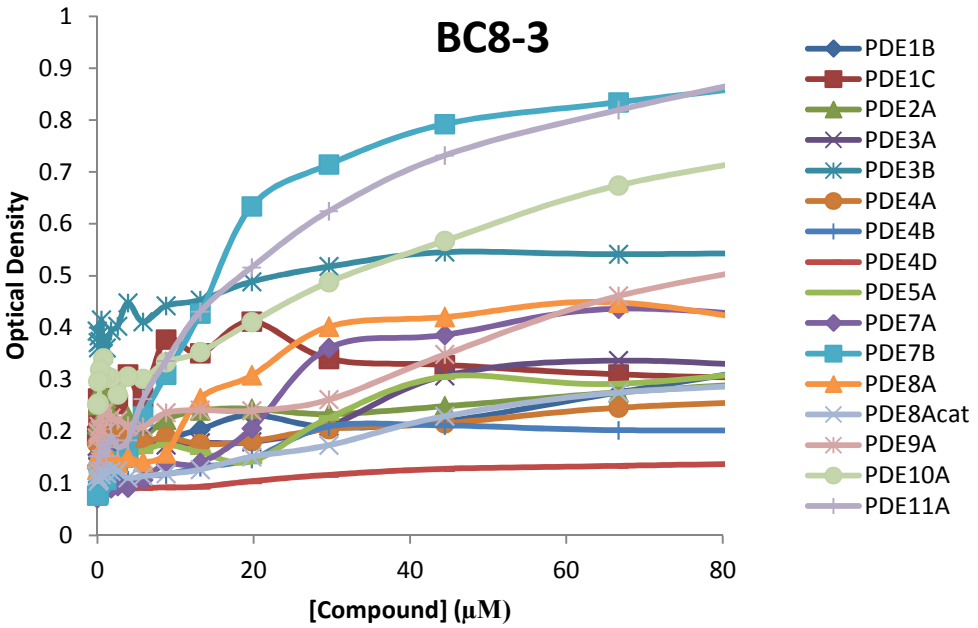

B

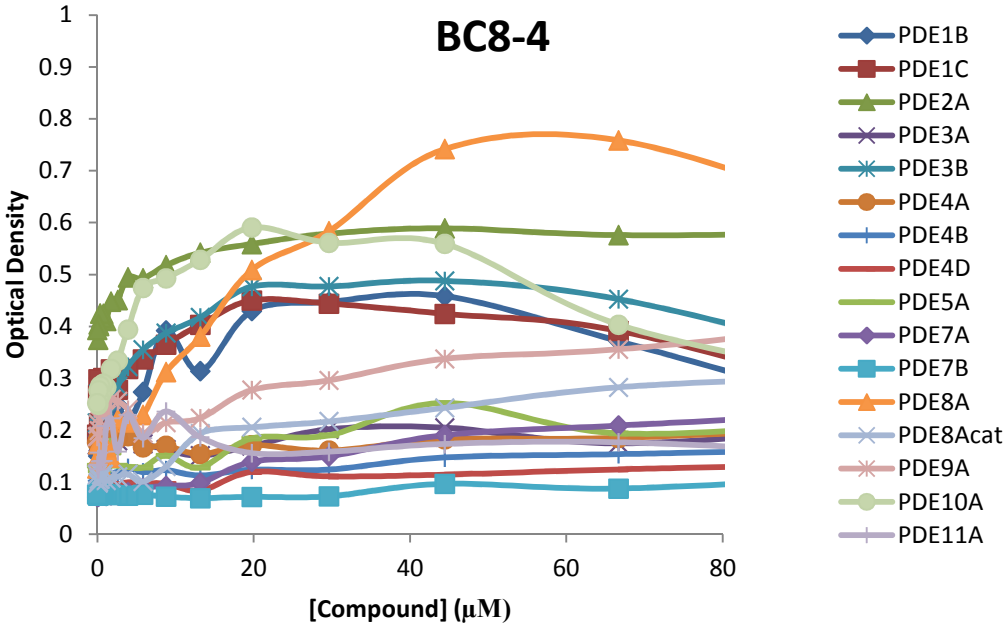

C

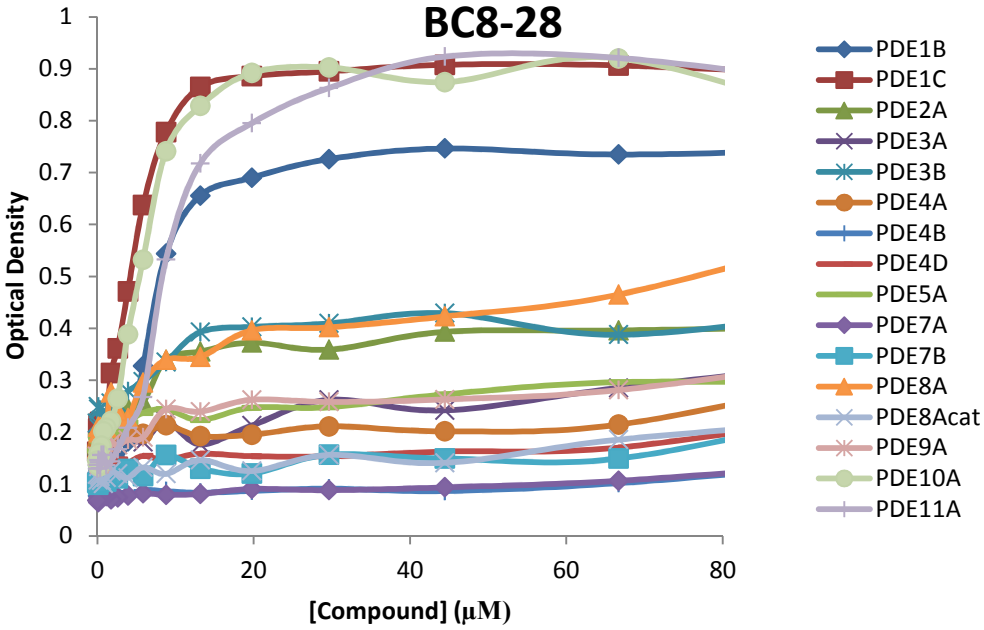
BC8-28
Optical Density
[Compound] (µM)
0
0.1
0.2
0.3
0.4
0.5
0.6
0.7
0.8
0.9
1
0
20
40
60
80
PDE1B
PDE1C
PDE2A
PDE3A
PDE3B
PDE4A
PDE4B
PDE4D
PDE5A
PDE7A
PDE7B
PDE8A
PDE8Acat
PDE9A
PDE10A
PDE11A

5.2.3 BC8-5 Promotes the 5FOA Growth of Strains Expressing cAMP-Specific PDEs

Dose response curves against different PDE-expressing strains identified an interesting profile by compound BC8-5, which only promoted the growth of PDE8A (CHP1204), PDE8Acat (DDP40), PDE7A (CHP1189), PDE7B (CHP1209), PDE4A (CHP1262) and PDE4B-expressing (CHP1268) strains. These are the members of the PDE superfamily that specifically hydrolyze cAMP (Figure 5.6). This compound also failed to promote the growth of PDE4D-expressing strain (CHP1186).

5.2.4 Compounds That Promote the 5FOA Growth of Strains That Express Enzymes from PDE8 and PDE7 Families

Two compounds, BC8-9 and BC8-16, mainly promoted the growth of PDE8A, PDE8Acat, PDE7A, and PDE7B-expressing strains. In addition, BC8-9 slightly affected PDE4A, PDE4B, and PDE10A-expressing strains. BC8-16 also promoted the growth of PDE10A-expressing strain and it affected PDE11A-expressing strain at high concentrations (Figure 5.7).

5.2.5 Compounds That Promote the 5FOA Growth of Strains That Express Enzymes from PDE8 and PDE4 Families

Compound BC8-15 increased the growth of strains that express PDE8A, PDE8Acat, PDE4A and PDE4B-expressing strains. At the highest test concentration, it seems to affect PDE1C, PDE10A and PDE11A-expressing strains slightly.

Figure 5.6 BC8-5 promotes the 5FOA growth of strains expressing cAMP-specific PDEs

Compound BC8-5 promoted the 5FOA growth of strains CHP1262, CHP1268, CHP1189, CHP1209, CHP1204, and DDP40; expressing PDE4A, PDE4B, PDE7A, PDE7B, PDE8A, PDE8Acat, respectively.

Figure 5.6 BC8-5 promotes the 5FOA growth of strains expressing cAMP-specific PDEs

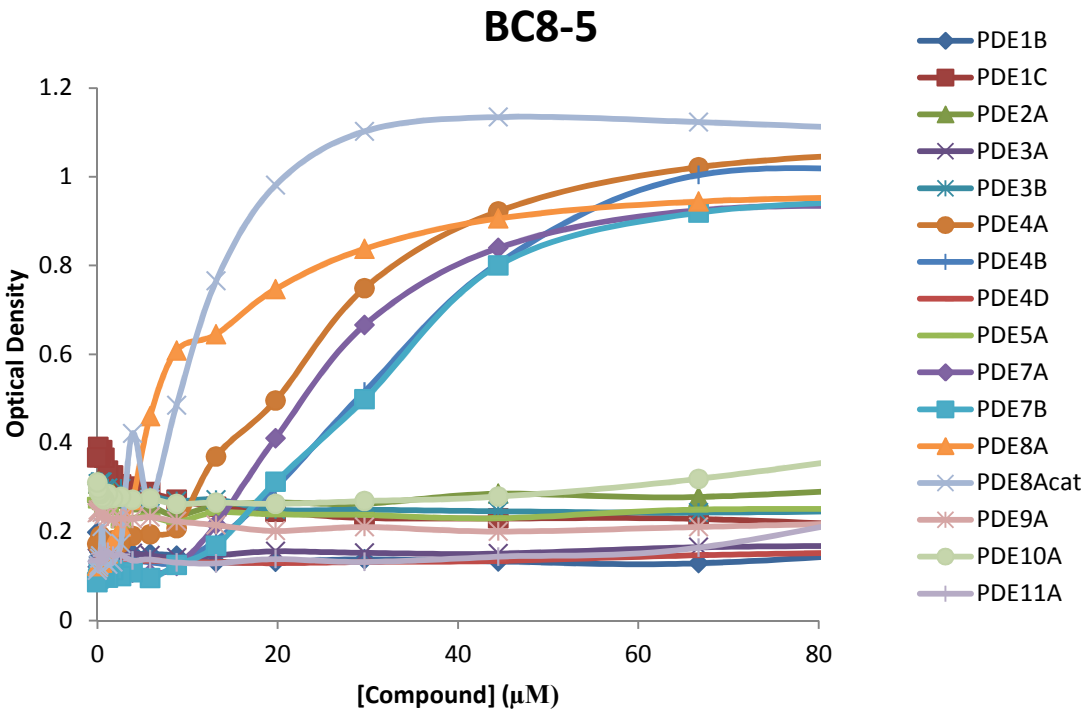

Figure 5.7 Compounds that promote the 5FOA growth of strains that express enzymes from PDE8 and PDE7 families

The 5FOA growth responses of yeast strains that express different phosphodiesterases are shown in the presence of individual compounds in separate graphs. The strains shown are CHP1222 (PDE1B), CHP1220 (PDE1C), CHP1403 (PDE2A), CHP1249 (PDE3A), CHP1194 (PDE3B), CHP1262 (PDE4A), CHP1268 (PDE4B), CHP1186 (PDE4D), CHP1223 (PDE5A), CHP1189 (PDE7A), CHP1209 (PDE7B), CHP1204 (PDE8A), DDP40 (PDE8Acat), CHP1218 (PDE9A), CHP1224 (PDE11A), CHP1445 (PDE10A), and CHP1224 (PDE11A). **(A)** Compound BC8-9 **(B)** Compound BC8-16.

Figure 5.7 Compounds that promote the 5FOA growth of strains that express enzymes from PDE8 and PDE7 families

A

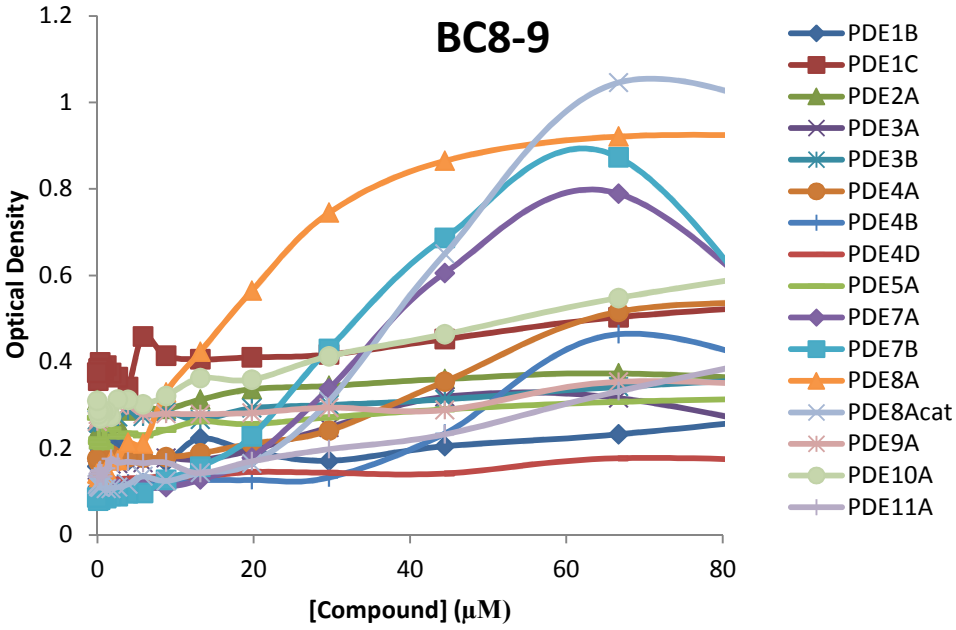

B

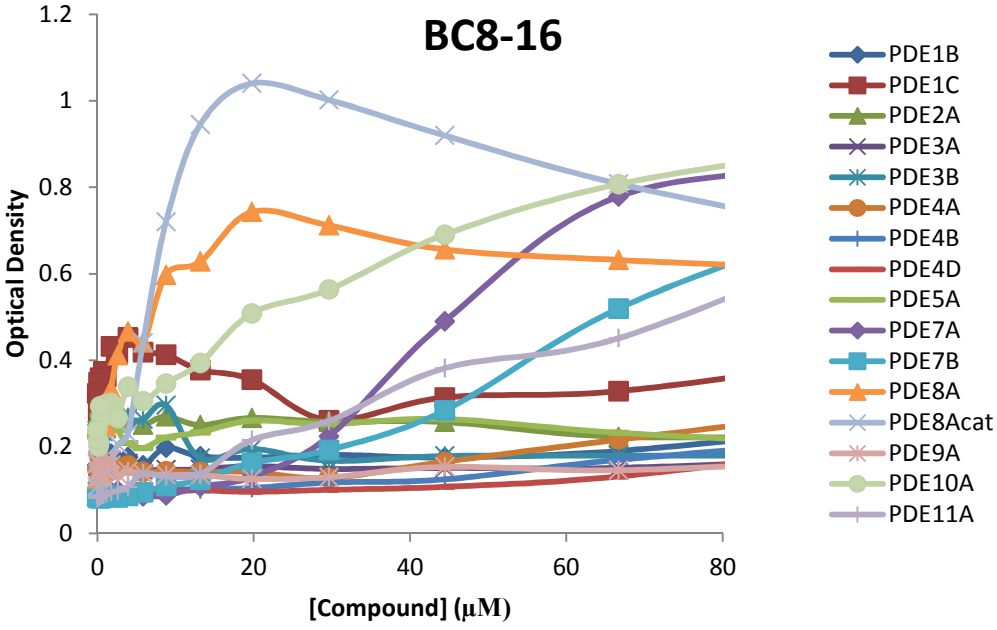

Figure 5.8 Compounds that promote the 5FOA growth of strains that express enzymes from PDE8 and PDE4 families

The 5FOA growth responses of yeast strains that express different phosphodiesterases are shown in the presence of individual compounds in separate graphs. The strains shown are CHP1222 (PDE1B), CHP1220 (PDE1C), CHP1403 (PDE2A), CHP1249 (PDE3A), CHP1194 (PDE3B), CHP1262 (PDE4A), CHP1268 (PDE4B), CHP1186 (PDE4D), CHP1223 (PDE5A), CHP1189 (PDE7A), CHP1209 (PDE7B), CHP1204 (PDE8A), DDP40 (PDE8Acat), CHP1218 (PDE9A), CHP1224 (PDE11A), CHP1445 (PDE10A), and CHP1224 (PDE11A). **(A)** Compound BC8-15 **(B)** Compound BC69.

Figure 5.8 Compounds that promote the 5FOA growth of strains that express enzymes from PDE8 and PDE4 families

A

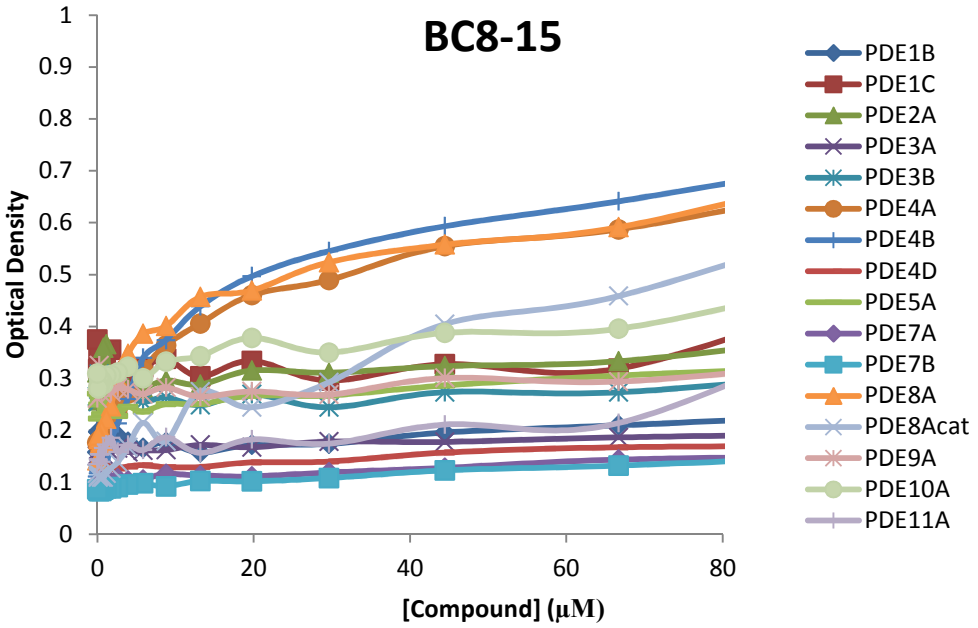

B

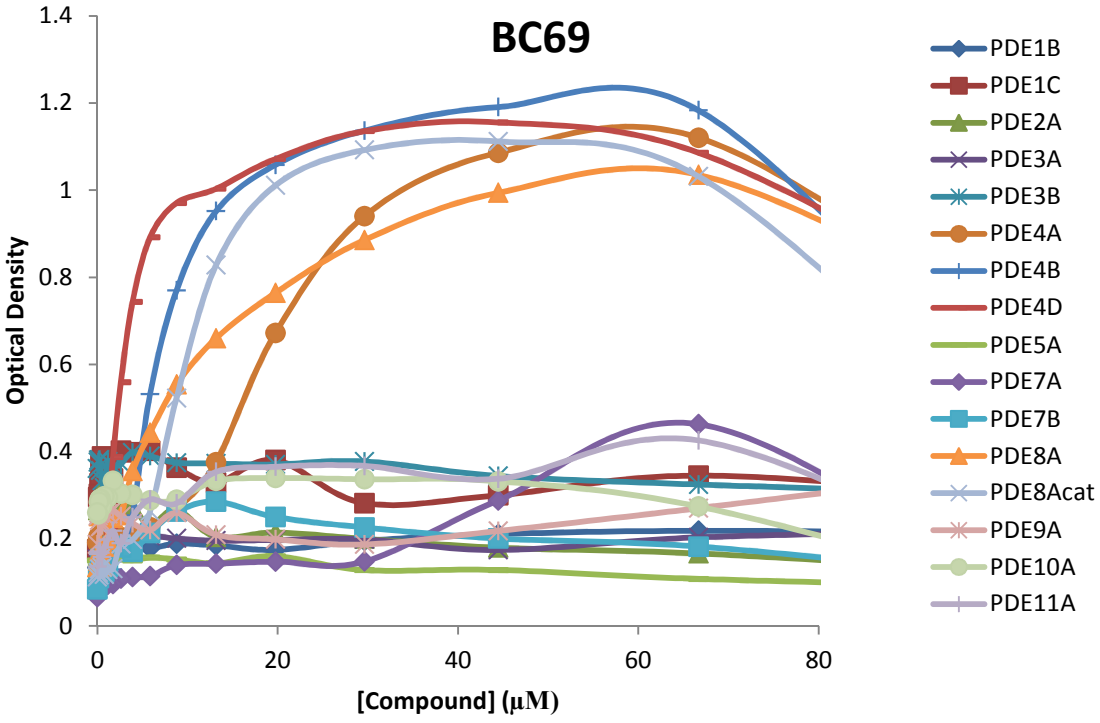

A similar profile was observed with the compound BC69 such that it only affects the strains that express enzymes from PDE4 and PDE8 families. Unlike BC8-15, BC69 also promoted the growth of PDE4D-expressing strain CHP1186 (Figure 5.8).

5.2.6 Compounds That Promote the Growth of Only Strains That Express the Full-Length or Catalytic Domain of PDE8A

Two compounds, BC8-1 and BC8-8 mainly promote the growth of strains CHP1204 and DDP40 that express full length and catalytic domain of PDE8A, respectively (Figure 5.9).

5.2.7 Compounds That Promote the Growth of Only Full-Length PDE8A-Expressing Strain

Dose response profiling assays against strains expressing different PDEs identified several compounds that promote the 5FOA growth of only full-length PDE8A-expressing strain CHP1204. These compounds are BC8-10, BC8-11, BC8-17, BC8-22, BC8-23, and BC8-24 (Figure 5.10). It should be noted that none of these compounds elevated the growth of DDP40 strain that expresses the catalytic domain of PDE8A. Also, although an effect was seen with BC8-24 against CHP1204, it did not promote growth in an earlier assay, indicating possible solubility problems.

Figure 5.9 Compounds that promote the growth of only strains that express the full length or catalytic domain of PDE8A

The 5FOA growth responses of yeast strains that express different phosphodiesterases are shown in the presence of individual compounds in separate graphs. The strains shown are CHP1222 (PDE1B), CHP1220 (PDE1C), CHP1403 (PDE2A), CHP1249 (PDE3A), CHP1194 (PDE3B), CHP1262 (PDE4A), CHP1268 (PDE4B), CHP1186 (PDE4D), CHP1223 (PDE5A), CHP1189 (PDE7A), CHP1209 (PDE7B), CHP1204 (PDE8A), DDP40 (PDE8Acat), CHP1218 (PDE9A), CHP1224 (PDE11A), CHP1445 (PDE10A), and CHP1224 (PDE11A). **(A)** BC8-1**, (B)** BC8-8.

Figure 5.9 Compounds that promote the growth of only strains that express the full length or catalytic domain of PDE8A

A

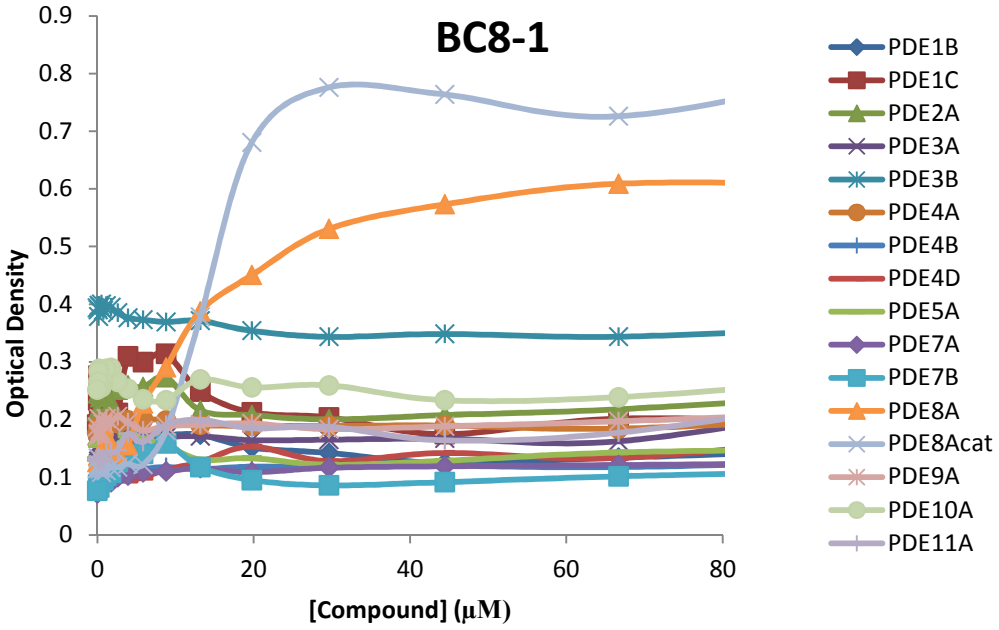

B

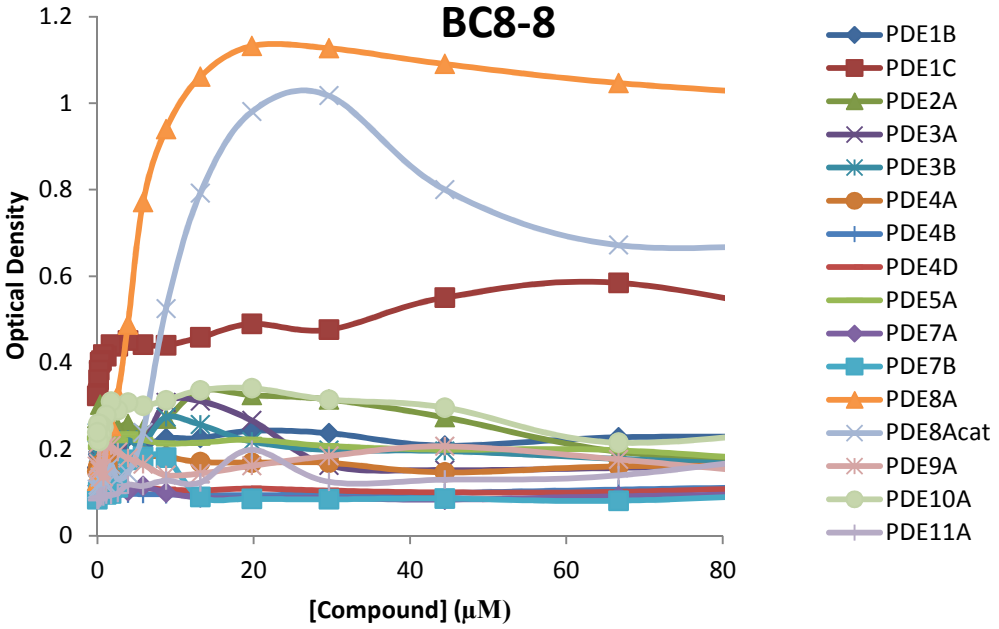

Figure 5.10 Compounds that promote the growth of only full-length PDE8A-expressing strain

The 5FOA growth responses of yeast strains that express different phosphodiesterases are shown in the presence of individual compounds in separate graphs. The strains shown are CHP1222 (PDE1B), CHP1220 (PDE1C), CHP1403 (PDE2A), CHP1249 (PDE3A), CHP1194 (PDE3B), CHP1262 (PDE4A), CHP1268 (PDE4B), CHP1186 (PDE4D), CHP1223 (PDE5A), CHP1189 (PDE7A), CHP1209 (PDE7B), CHP1204 (PDE8A), DDP40 (PDE8Acat), CHP1218 (PDE9A), CHP1224 (PDE11A), CHP1445 (PDE10A), and CHP1224 (PDE11A). **(A-F)** Compounds BC8-10, BC8-11, BC8-17, BC8-22, BC8-23, BC8-24.

Figure 5.10 Compounds that promote the growth of only full-length PDE8A-expressing strain

A

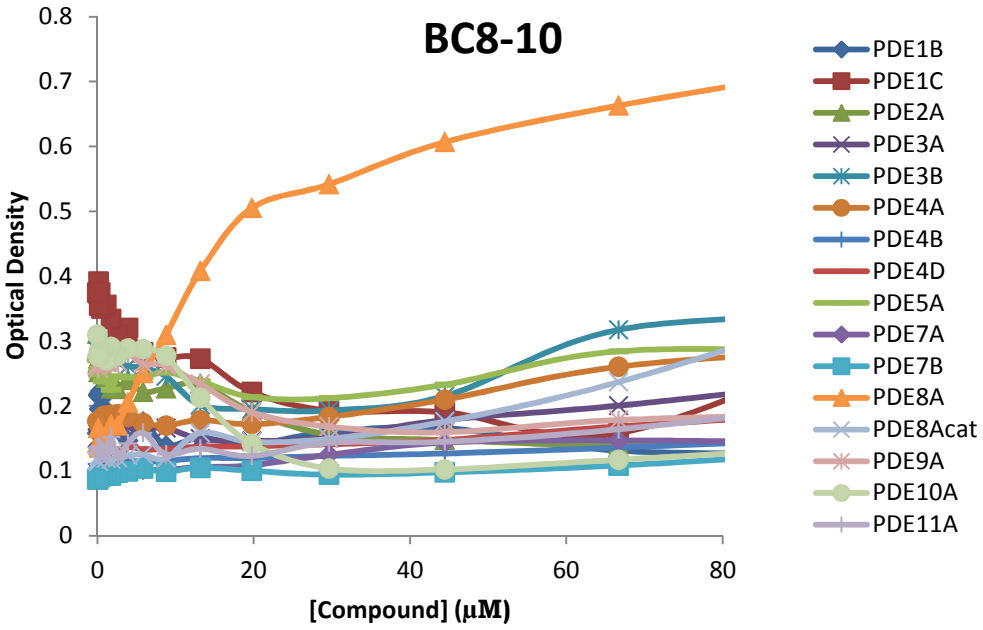

B

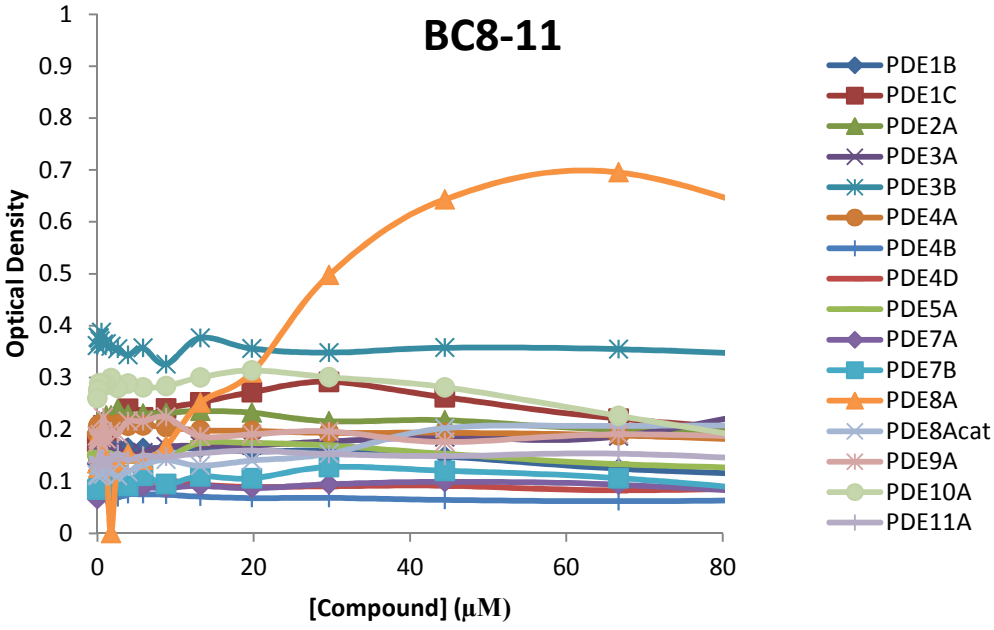

C

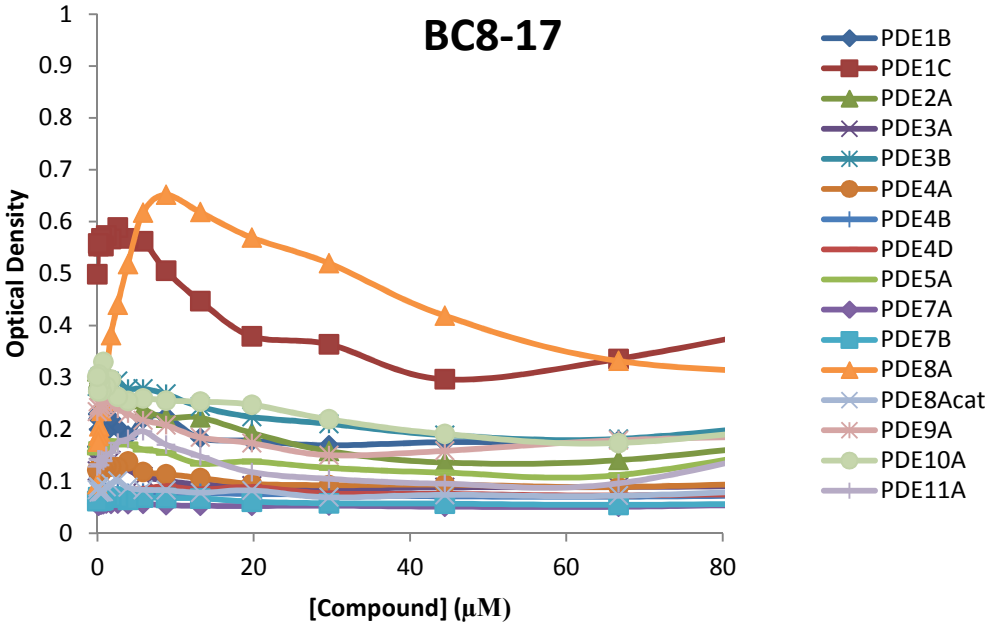
BC8-17
Optical Density
[Compound] (µM)
PDE1B
PDE1C
PDE2A
PDE3A
PDE3B
PDE4A
PDE4B
PDE4D
PDE5A
PDE7A
PDE7B
PDE8A
PDE8Acat
PDE9A
PDE10A
PDE11A

D

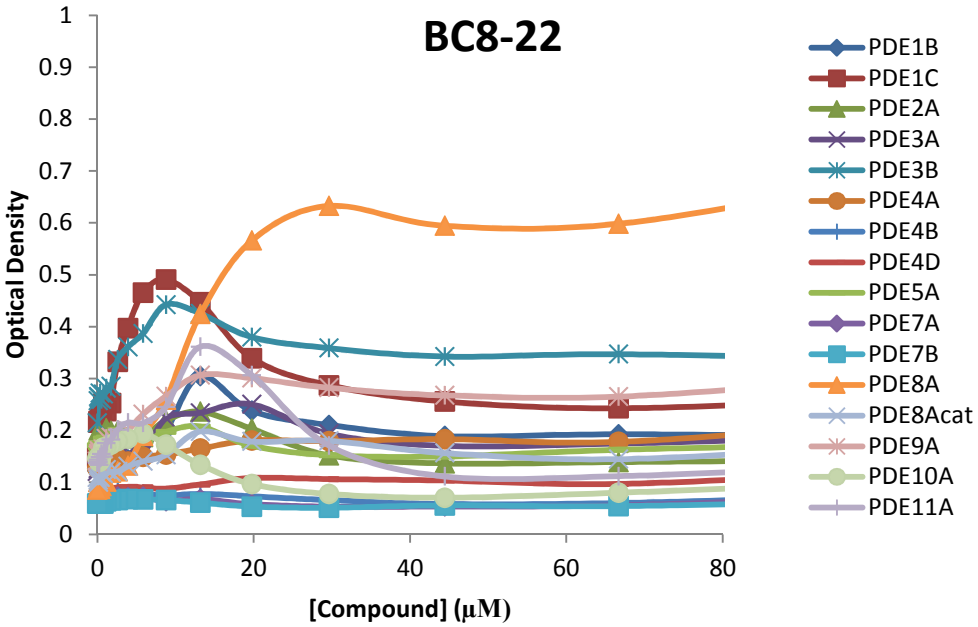
BC8-22
Optical Density
[Compound] (µM)
PDE1B
PDE1C
PDE2A
PDE3A
PDE3B
PDE4A
PDE4B
PDE4D
PDE5A
PDE7A
PDE7B
PDE8A
PDE8Acat
PDE9A
PDE10A
PDE11A

E

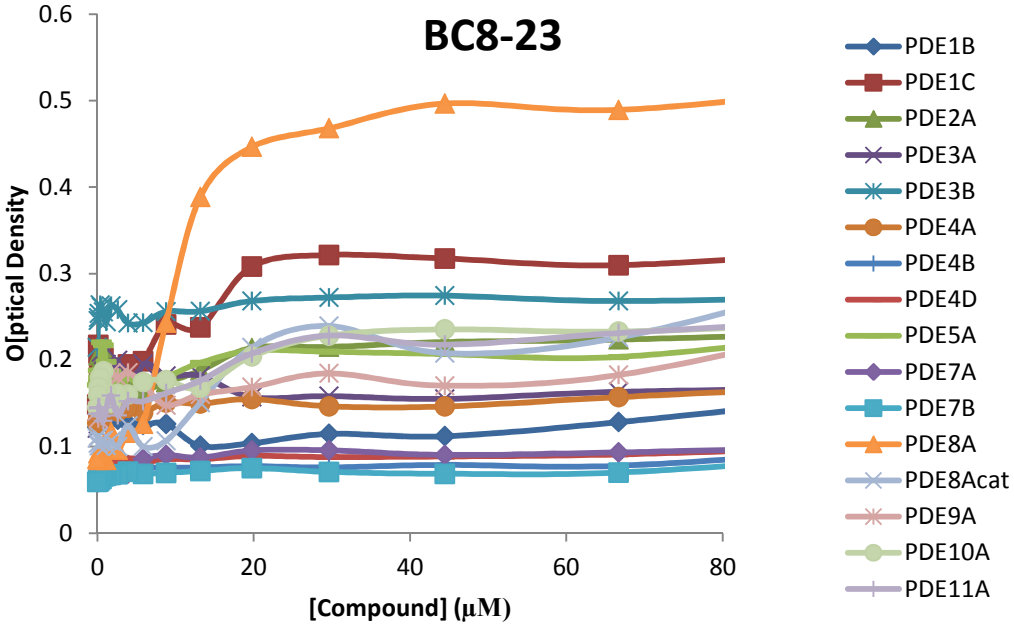
BC8-23
O[ptical Density
0.6
0.5
0.4
0.3
0.2
0.1
0
0
20
40
60
80
[Compound] (µM)
PDE1B
PDE1C
PDE2A
PDE3A
PDE3B
PDE4A
PDE4B
PDE4D
PDE5A
PDE7A
PDE7B
PDE8A
PDE8Acat
PDE9A
PDE10A
PDE11A

F

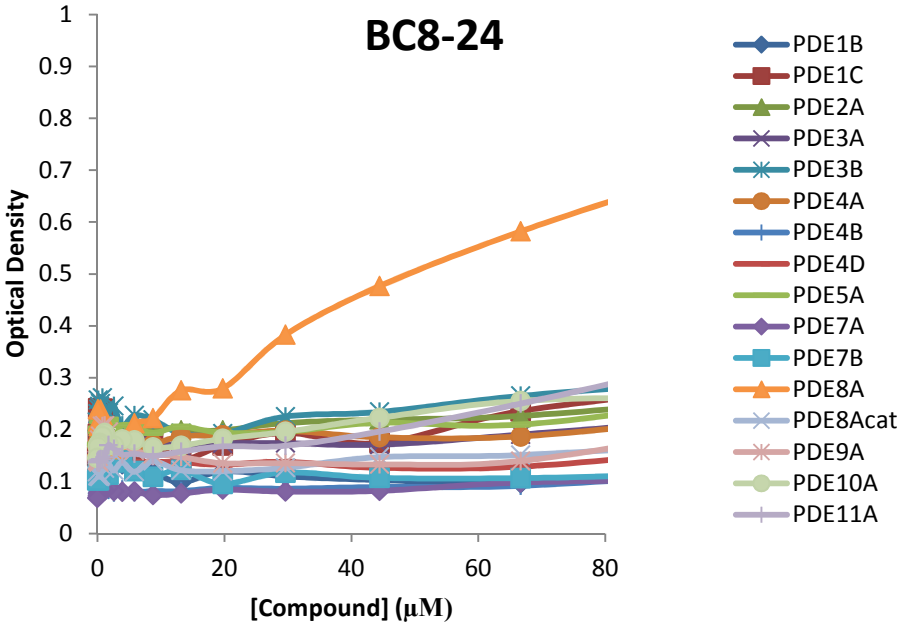
BC8-24
Optical Density
1
0.9
0.8
0.7
0.6
0.5
0.4
0.3
0.2
0.1
0
0
20
40
60
80
[Compound] (µM)
PDE1B
PDE1C
PDE2A
PDE3A
PDE3B
PDE4A
PDE4B
PDE4D
PDE5A
PDE7A
PDE7B
PDE8A
PDE8Acat
PDE9A
PDE10A
PDE11A

5.2.8 Compounds That Do Not Stimulate 5FOA Growth in Yeast Strains

In contrast to the class of compounds that were described above, some compounds did not show any effect in the 5FOA growth of yeast strains that express different PDEs. Compounds BC8-7, BC8-25 and BC8-27 fail to promote growth of all of the yeast strains similar to its failure to reproduce the stimulatory effect on the PDE8A-expressing strain described in the previous section (Figure 5.11).

5.3 *IN VITRO* ENZYME ASSAYS

The compounds shown in Table 5.2 were tested against recombinant human full length PDE8A enzyme by means of *in vitro* enzyme assays. The changes in the cyclic AMP hydrolytic activity of the PDE8A enzyme were evaluated in the presence of 10 μM of test compounds. Compounds BC8-1, BC8-2, BC8-5, BC8-7, BC8-8, BC8-9, BC8-15, BC8-16, BC8-21, BC8-22, BC8-23, BC8-28, BC8-1F, and BC8-1H were confirmed to have inhibitory activity on PDE8A enzyme. This corresponds to approximately a 50 % confirmation rate. The results of a set of representative *in vitro* assays are given as percent inhibition by the compounds was calculated in comparison to the no-compound control along with the ED_{50} values of the compounds for the 5FOA growth of the PDE8A-expressing strain (Table 5.2). ED_{50} values are calculated by normalizing the data using the OD values of negative control and positive control conditions and estimating the concentration that leads to half-maximal optical density through non-linear regression analysis. The structures of the compounds that inhibit or fail to inhibit PDE8A in the *in vitro* assays are given in Tables 5.3 and 5.4, respectively.

Figure 5.11 Compounds that do not stimulate 5FOA growth in yeast strains

Compounds BC8-7, BC8-25 and BC8-27 failed to promote growth of yeast strains that express different PDEs. The 5FOA growth responses are shown in the presence of individual compounds in separate graphs. The strains shown are CHP1222 (PDE1B), CHP1220 (PDE1C), CHP1403 (PDE2A), CHP1249 (PDE3A), CHP1194 (PDE3B), CHP1262 (PDE4A), CHP1268 (PDE4B), CHP1186 (PDE4D), CHP1223 (PDE5A), CHP1189 (PDE7A), CHP1209 (PDE7B), CHP1204 (PDE8A), DDP40 (PDE8Acat), CHP1218 (PDE9A), CHP1224 (PDE11A), CHP1445 (PDE10A), and CHP1224 (PDE11A). **(A-C)** Compounds BC8-7, BC8-25, BC8-27.

Figure 5.11 Compounds that do not stimulate 5FOA growth in yeast strains

A

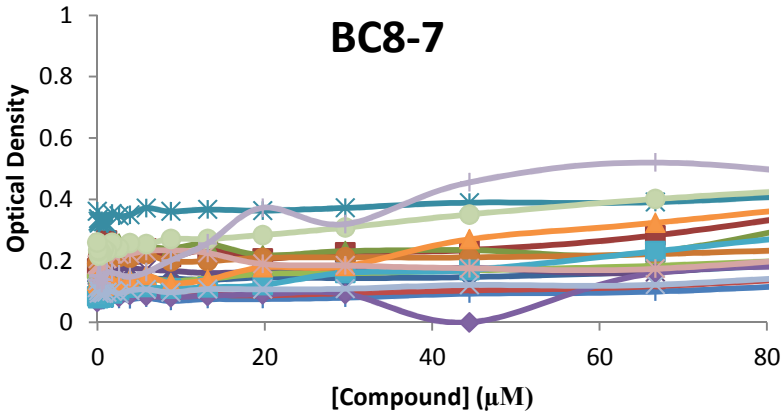

B

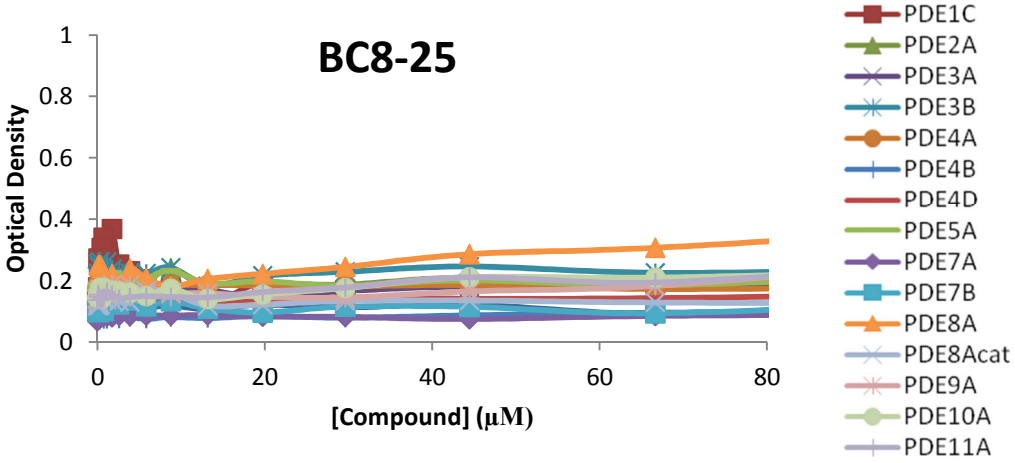

C

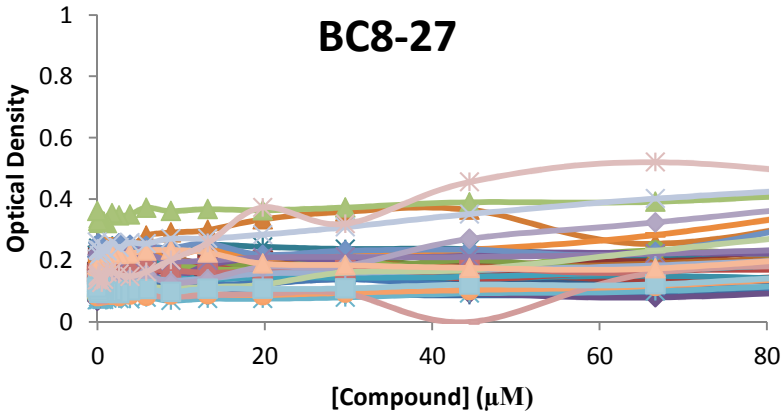

Table 5.2 Percent inhibition of PDE8A enzyme in comparison to yeast growth assay

(Compounds that inhibited the PDE8A enzyme more than 10% are shown in red; BC8-1 and BC8-8 had higher inhibition levels in other repetitions of the assay)

Compound name	ED_{50} value for 5FOA growth in yeast	Percent inhibition of PDE8A at 10 µM compound concentration
BC8-1	50	46
BC8-2	28	12
BC8-3	>100	-10
BC8-4	31	-9
BC8-5	11	72
BC8-6	27	-3
BC8-7	>100	51
BC8-8	4	46
BC8-9	24	87
BC8-10	51	-7
BC8-11	55	-9
BC8-12	12	-12
BC8-13	21	-6
BC8-14	21	-5
BC8-15	66	86
BC8-16	12	60
BC8-17	6	8
BC8-18	32	-2
BC8-19	53	2
BC8-20	2	3
BC8-21	35	12
BC8-22	35	40
BC8-23	74	54
BC8-24	83	-5
BC8-25	>100	-2
BC8-26	22	-3
BC8-27	>100	-7
BC8-28	>100	18
BC8-1F	16	67
BC8-1H	12	50
BC69	9	37

Table 5.3 Structures of compounds that inhibit PDE8A *in vitro*

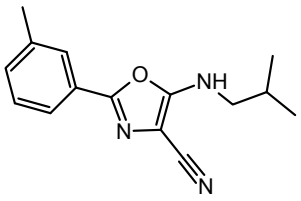

BC8-1

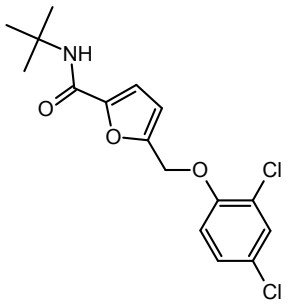

BC8-2

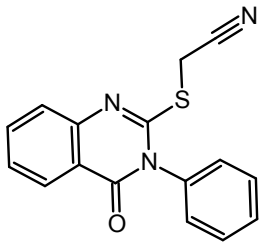

BC8-5

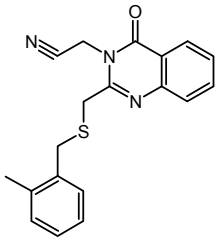

BC8-7

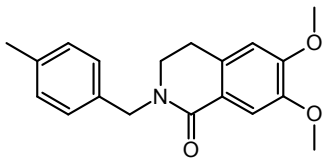

BC8-8

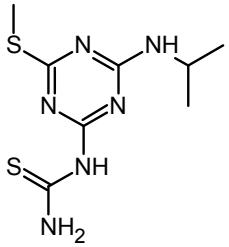

BC8-9

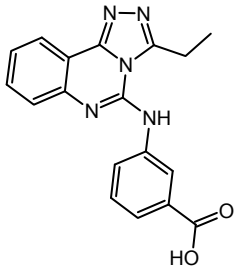

BC8-15

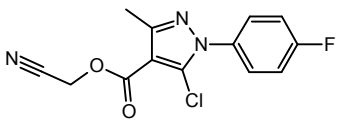

BC8-16

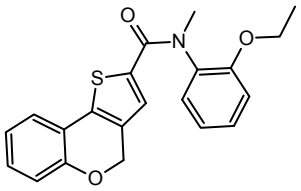

BC8-21

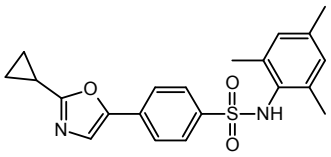

BC8-21

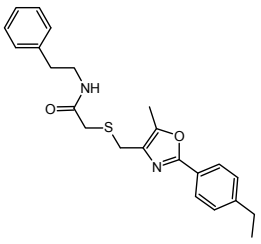

BC8-23

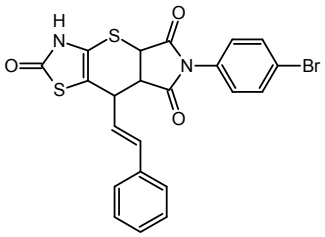

BC8-28

Table 5.4 Structure of compounds that fail to inhibit PDE8A *in vitro*

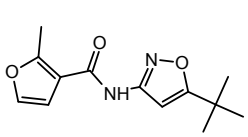

BC8-3

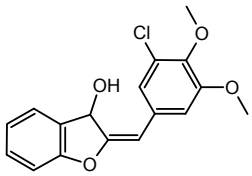

BC8-4

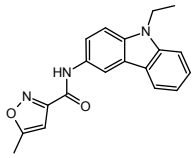

BC8-6

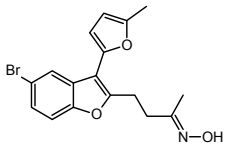

BC8-10

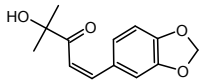

BC8-11

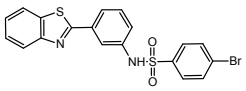

BC8-12

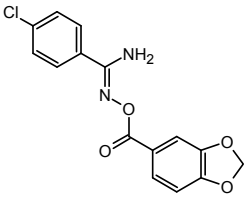

BC8-13

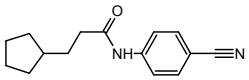

BC8-14

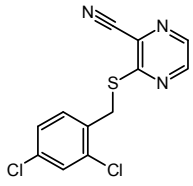

BC8-17

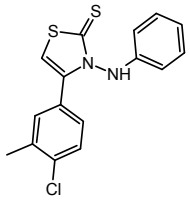

BC8-18

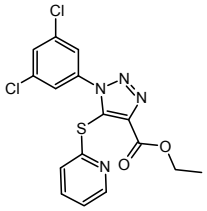

BC8-19

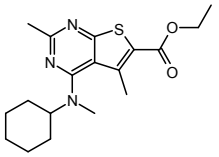

BC8-20

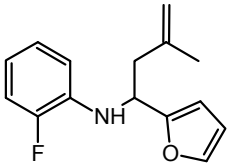

BC8-24

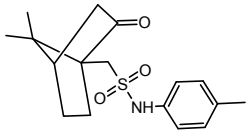

BC8-25

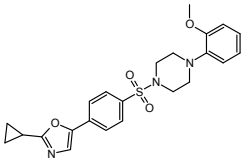

BC8-26

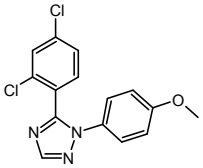

BC8-27

When these results are compared to the yeast growth profiles, it can be seen that the compounds that made most yeast strains grow do not inhibit PDE8A *in vitro*. Among this group of compounds only BC8-2 and BC8-21 inhibit PDE8A *in vitro*. This reinforces the notion that most compounds in this group are acting through a non-PDE target. PDE-independent 5FOA resistant growth can be achieved in several ways. Activating a component in the pathway that is downstream of cAMP generation such as activation of PKA will promote growth in 5FOA. Alternatively, a compound that inhibits orotidine-5'-phosphate (OMP) decarboxylase or orotate phosphoribosyltransferase would prevent the conversion of 5FOA into the toxic product leading to 5FOA resistant growth. Although these compounds lead to the growth of many strains that express different PDEs in the 5FOA medium, not all strains were affected the same way.

Secondly, among the group of compounds that did not promote growth of any of the yeast strains (i.e. BC8-7, BC8-25, and B8-27), only BC8-7 inhibited the PDE8A enzyme *in vitro*. The other group of compounds that fails to inhibit PDE8 *in vitro* consists of compounds that promote the growth of only the full-length PDE8A expressing strain CHP1204. It should be noted that the enzyme used in the *in vitro* assays is human recombinant enzyme while the one expressed in the yeast is murine PDE8A. Species-dependent differences might be one of the causes of this discrepancy since mouse and human PDE8A share only 85% sequence identity within the catalytic domain (Soderling *et al*. 1998b).

Also, a lack of inhibition *in vitro* while observing growth only for the full-length PDE8A-expressing strain might suggest an effect of the compound through the regulatory domains of the enzyme. It should also be kept in mind that the *in vitro* enzyme assay measures the remaining substrate concentration after the reaction. Since the counts are very large numbers, the assay is not extremely sensitive to detect small effects on the enzyme activity.

The cyclic AMP hydrolysis rate of the human PDE8A enzyme was analyzed as shown in Figure 5.12. The data fit to Michaelis-Menten curve yields a V_{max} value of 34.6 + 2.9 picomols/min.µg and a K_m of 111.8+20.6 nM (n=5). The enzyme activities were also measured in the presence of changing concentrations of PDE8 inhibitors at a given condition in order to determine the half maximal inhibitory concentration (IC_{50}). The IC_{50} values of several compounds against PDE8A, PDE4A or PDE7A enzymes are given in Table 5.5. Compound BC8-15 with the K_i value of 275 nM (determined by nonlinear regression of the Michaelis-Menten curve in the absence and presence of the compound) is the most potent PDE8 inhibitor *in vitro*.

Finally, the compounds were also tested against human PDE8B enzyme using *in vitro* enzyme assays. The compounds that showed inhibition on recombinant PDE8A enzyme also inhibited PDE8B (Figure 5.13).

Figure 5.12 Michaelis-Menten kinetics of PDE8A

The cAMP hydrolysis rate of human PDE8A enzyme under changing substrate concentrations is shown (n= 5).

Figure 5.12 Michaelis-Menten Kinetics of PDE8A

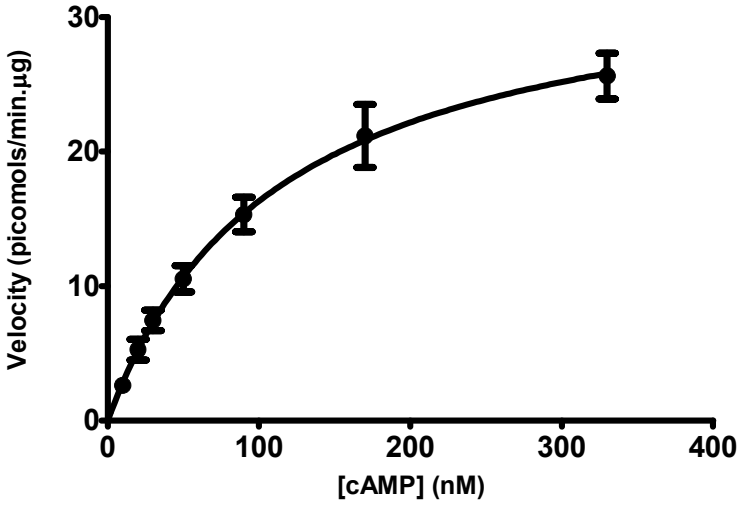

Table 5.5 IC_{50} values of selected PDE inhibitors

IC_{50} values of the indicated compounds were tested against PDE8A, PDE4A10 or PDE7A enzymes. The substrate concentrations for PDE8A enzyme are either 50 nM (for BC8-1, BC8-5 and BC8-1H) or 10 nM (for BC8-8, BC8-15, BC8-22 and BC8-23). IC_{50} values for PDE4A are tested either at 2 µM (for BC8-5, BC8-8, BC8-15) or at 50 nM (for BC8-1 and BC8-23) substrate concentration. PDE7A was tested at either 35 nM (for BC8-5, BC8-8, BC8-15) or at 10 nM (BC8-1, BC8-23). The values are given in µM.

IC_{50}	PDE8A	PDE4A	PDE7A
BC8-1	4.7	51.9	8.4
BC8-5	2.9	2.0	1.1
BC8-8	9.4	75.4	72.0
BC8-15	0.6	0.3	16.2
BC8-22	13.2	N/A	N/A
BC8-23	4.3	274.6	18.8
BC8-1H	9.7	N/A	N/A

Figure 5.13 PDE8A inhibitors also inhibit PDE8B

The percent inhibition values of compounds BC8-1, BC8-5, BC8-8, BC8-9, BC8-15, BC8-16, BC8-22, BC8-23, BC69 and dipyridamole are shown in the graph. Compounds were tested at 1 or 10 μM against PDE8A and PDE8B enzymes. The substrate concentration is 50 nM for PDE8A and 1 μM for PDE8B.

Figure 5.13 PDE8A inhibitors also inhibit PDE8B

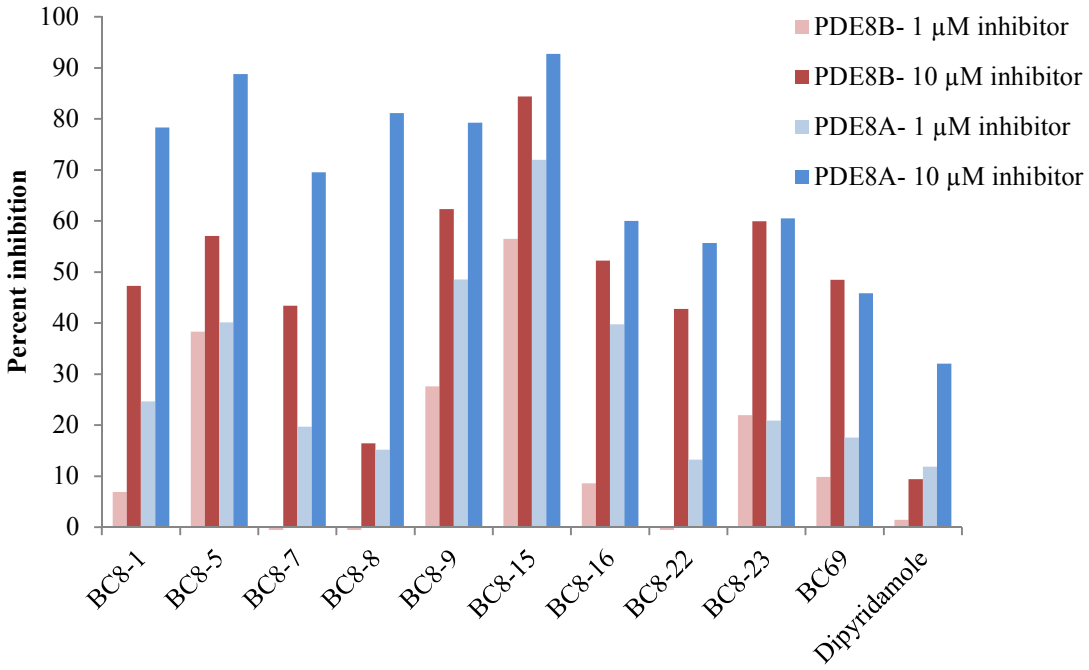

5.4 ANALYSIS OF STRUCTURALLY RELATED COMPOUNDS

Compounds structurally related to BC69, BC8-1, BC8-5, BC8-8, BC8-15 and BC8-23 are evaluated via yeast growth assays or *in vitro* enzyme assays in an attempt to understand the pharmacophore of each molecule and to determine important parts of the molecule that influence the selectivity or potency of the test compounds.

5.4.1 BC69 Series

Six compounds that are structurally related to BC69 were tested for their ability to promote growth of yeast strains expressing different phosphodiesterases (Table 5.6, Figure 5.14). As mentioned earlier, BC69 inhibits PDE8A and promotes the growth of yeast strains that express PDE4 and PDE8 enzymes including PDE4D. Compound BC69-1 has a carbonitrile group the acetonitrile group found in the parent molecule. This change abolished the ability of the compound to promote growth of the yeast strains, indicating that the acetonitrile group could be important in terms of inhibitory activity. On the other hand, changing the acetonitrile group to carbaldehyde oxime in compound BC69-2 and BC69-3 changes the yeast inhibition profile such that these compounds promote growth of only the PDE4D-expressing strain. These compounds differ only in one of the phenyl groups, which was changed to a thiophene in BC69-3. Both of these compounds show a slight effect on the PDE4A-expressing strain. When tested with *in vitro* assays, BC69, BC69-2 and BC69-3 have IC_{50} values between 10-13 μM for PDE4A (at 500 nM substrate concentration) and 210-460 nM for PDE4D (at 200 nM substrate concentration).

Table 5.6 Structures of BC69 derivatives

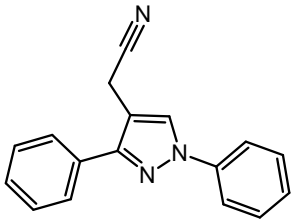

BC69

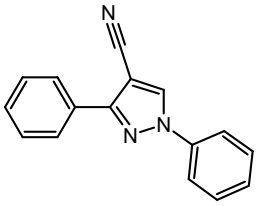

BC69-1

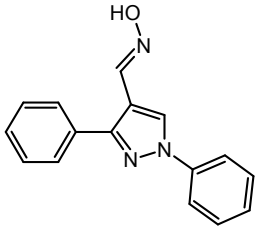

BC69-2

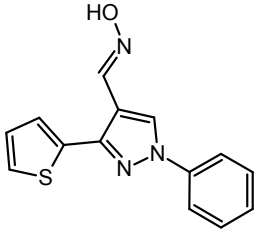

BC69-3

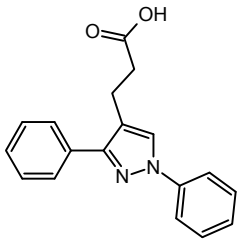

BC69-4

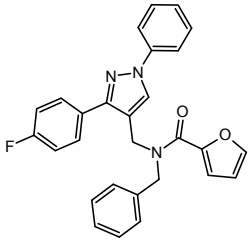

BC69-5

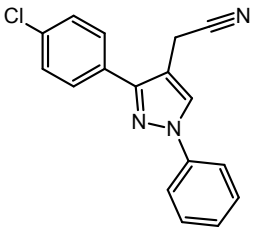

BC69-6

Figure 5.14 5FOA growth response of compounds structurally related to BC69

The 5FOA growth responses of yeast strains that express different phosphodiesterases are shown in the presence of individual compounds in separate graphs. The strains shown are CHP1222 (PDE1B), CHP1220 (PDE1C), CHP1403 (PDE2A), CHP1249 (PDE3A), CHP1194 (PDE3B), CHP1262 (PDE4A), CHP1268 (PDE4B), CHP1186 (PDE4D), CHP1223 (PDE5A), CHP1189 (PDE7A), CHP1209 (PDE7B), CHP1204 (PDE8A), DDP40 (PDE8Acat), CHP1218 (PDE9A), CHP1224 (PDE11A), CHP1445 (PDE10A), and CHP1224 (PDE11A). **(A-F)** Compounds BC69-1, BC69-2, BC69-3, BC69-4, BC69-5, BC69-6. BC69-6 was tested against only PDE3A, PDE4A-B-D, PDE7A-B, PDE8A-8Acat expressing strains.

Figure 5.14 5FOA growth response of compounds structurally related to BC69

A

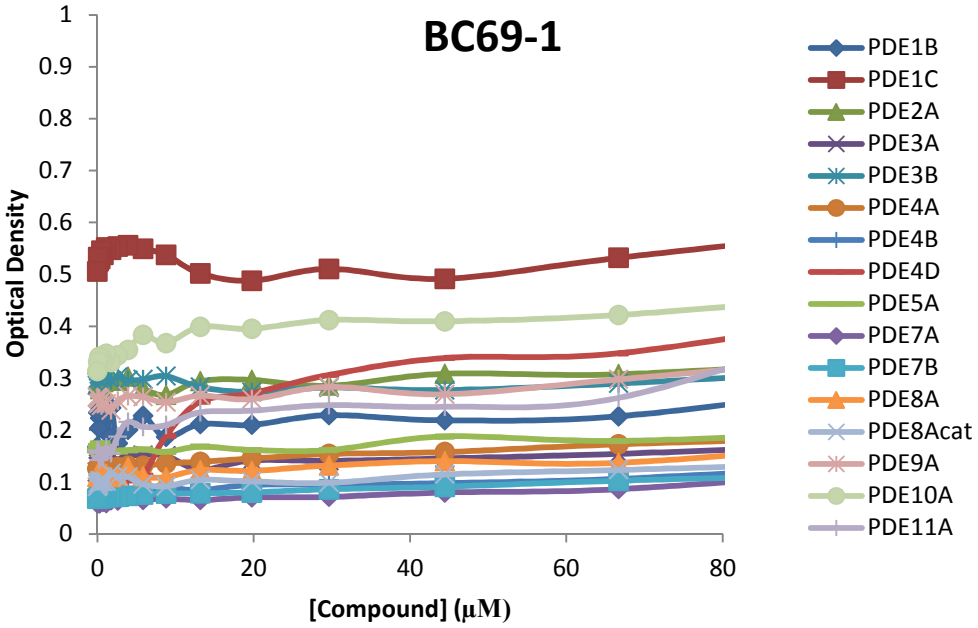

B

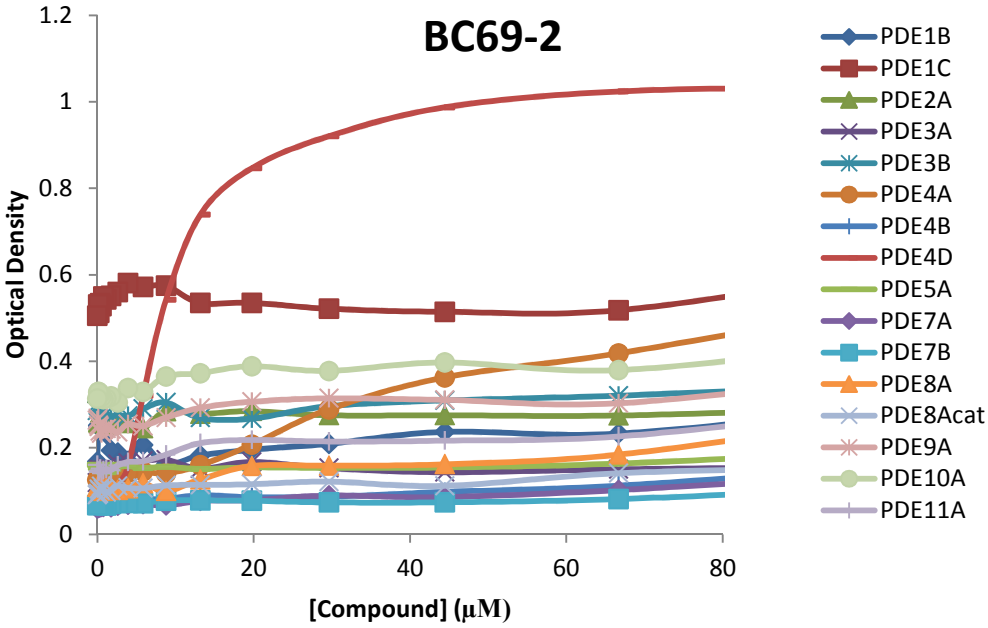

C

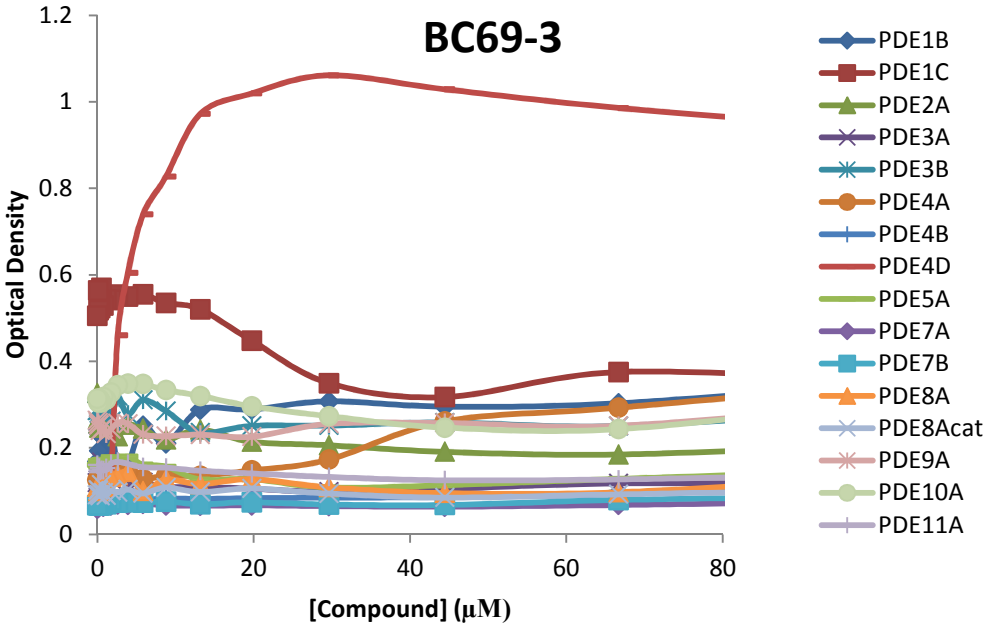
BC69-3
Optical Density
1.2
1
0.8
0.6
0.4
0.2
0
0
20
40
60
80
[Compound] (µM)
PDE1B
PDE1C
PDE2A
PDE3A
PDE3B
PDE4A
PDE4B
PDE4D
PDE5A
PDE7A
PDE7B
PDE8A
PDE8Acat
PDE9A
PDE10A
PDE11A

D

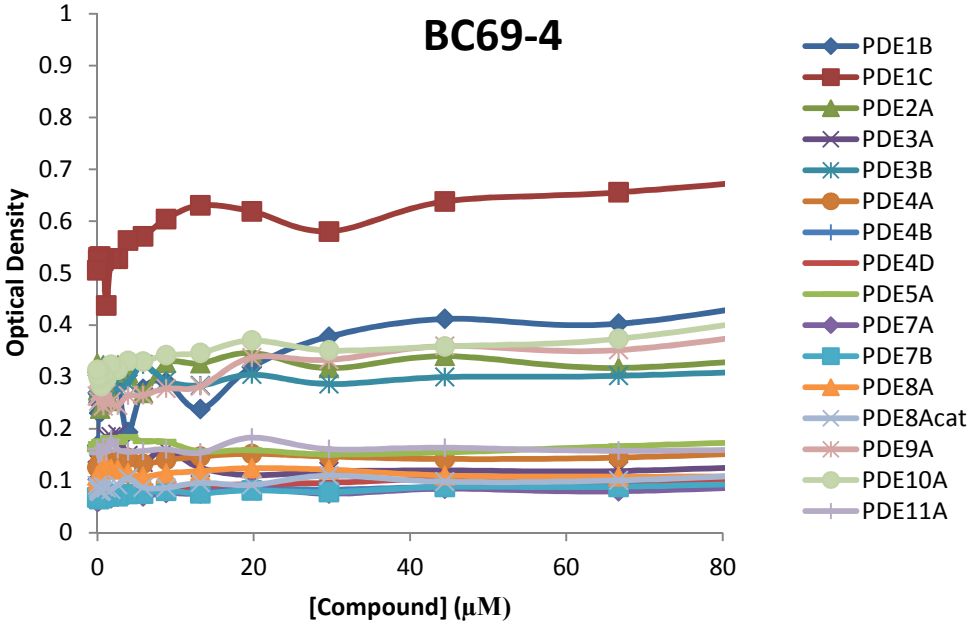
BC69-4
Optical Density
1
0.9
0.8
0.7
0.6
0.5
0.4
0.3
0.2
0.1
0
0
20
40
60
80
[Compound] (µM)
PDE1B
PDE1C
PDE2A
PDE3A
PDE3B
PDE4A
PDE4B
PDE4D
PDE5A
PDE7A
PDE7B
PDE8A
PDE8Acat
PDE9A
PDE10A
PDE11A

E

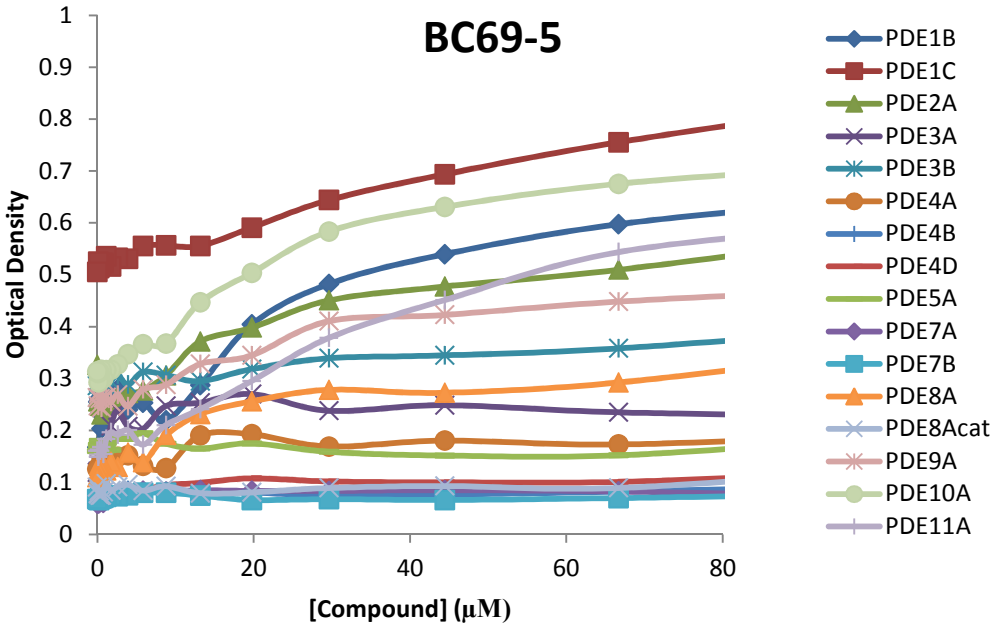
BC69-5
Optical Density
[Compound] (µM)
0
0.1
0.2
0.3
0.4
0.5
0.6
0.7
0.8
0.9
1
0
20
40
60
80
PDE1B
PDE1C
PDE2A
PDE3A
PDE3B
PDE4A
PDE4B
PDE4D
PDE5A
PDE7A
PDE7B
PDE8A
PDE8Acat
PDE9A
PDE10A
PDE11A

F

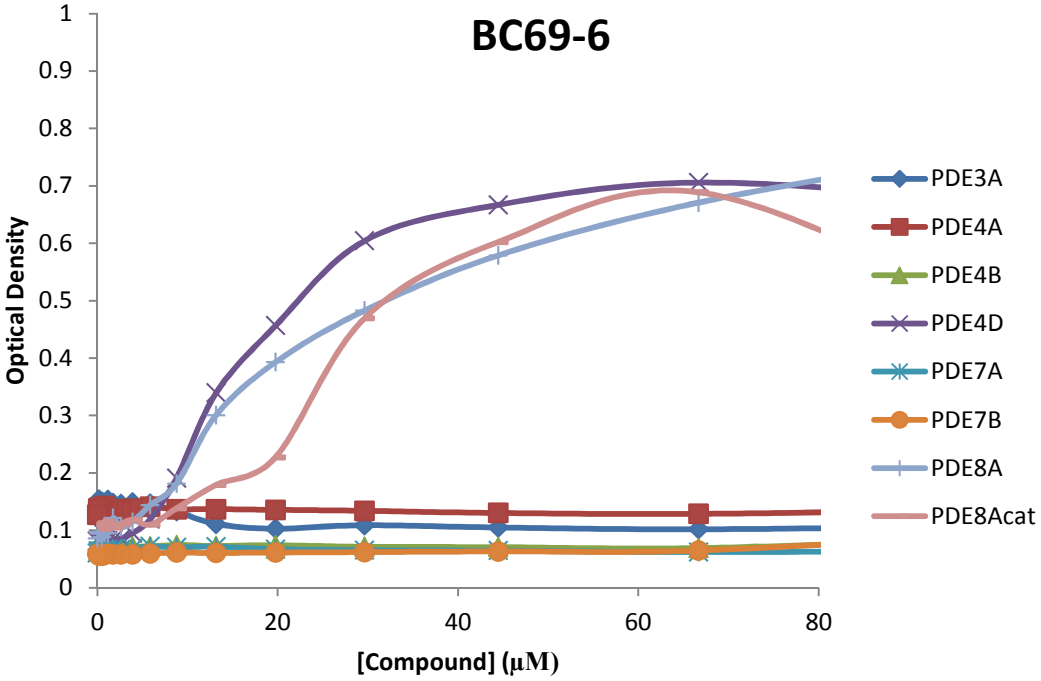
BC69-6
Optical Density
[Compound] (µM)
0
0.1
0.2
0.3
0.4
0.5
0.6
0.7
0.8
0.9
1
0
20
40
60
80
PDE3A
PDE4A
PDE4B
PDE4D
PDE7A
PDE7B
PDE8A
PDE8Acat

For BC69-4, when the acetonitrile group is changed to propionic acid, all PDE-inhibitory activity appears to be lost. On the other hand, when this group is replaced with a bulky moiety the compound starts to promote the growth of PDE4A, PDE4D, PDE7A, PDE7B and PDE8Acat-expressing strains and show a slight effect on PDE1C, PDE1B, PDE2A, PDE9A, PDE10A, PDE11A-expressing strains. This effect of BC69-5, along with those of BC69-1 and BC69-4, suggests that the acetonitrile group is important for the inhibitory potential of this compound. Finally, as seen with BC69-6, when one of the phenyl groups is changed with chlorophenyl, the compound promotes the growth of PDE4D, PDE8A and PDE8Acat-expressing strains, which shows that the effect on PDE4A and PDE4B-expressing strains is abolished.

5.4.2 BC8-1 Series

Eight compounds that are structurally related to BC8-1 (Table 5.7) were tested against different strains in a dose response 5FOA yeast growth assay (Figure 5.15). Two of these compounds are BC8-1F and BC8-1H, which were identified from the primary screen and confirmed with *in vitro* assays. As described previously, BC8-1 promotes the growth of only PDE8A and PDE8Acat expressing strains in the 5FOA growth assay. Compound BC8-1A differs from BC8-1 only in the location of the methyl group on the phenyl ring. This causes the compound to lose its ability to promote growth of PDE8-expressing strains. Similarly, BC8-1D, which has a chlorine group in the phenyl ring instead of a methyl group at the same position where methyl group is located in BC8-1A, lacks activity in the yeast growth.

Table 5.7 Structures of BC8-1 derivatives

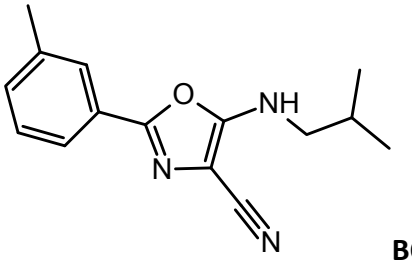

BC8-1

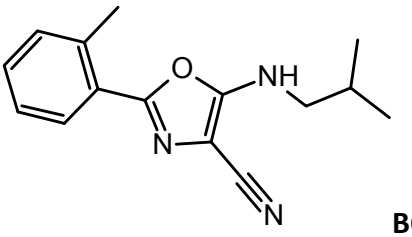

BC8-1A

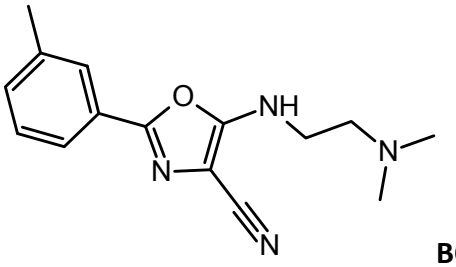

BC8-1B

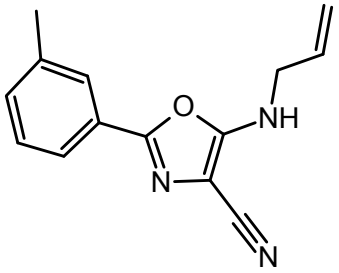

BC8-1C

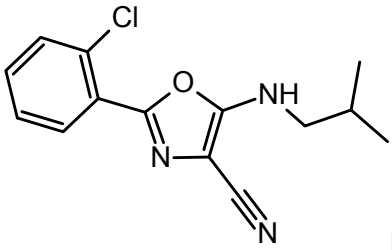

BC8-1D

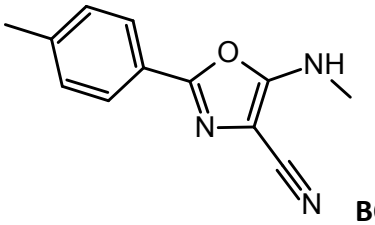

BC8-1E

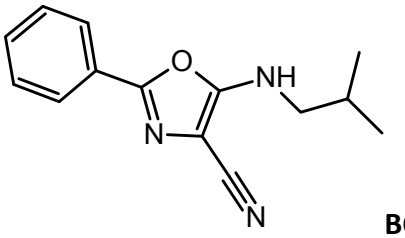

BC8-1F

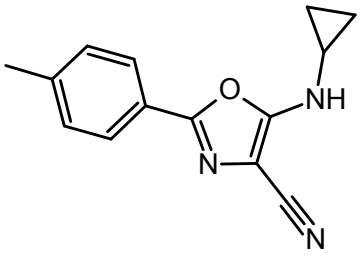

BC8-1G

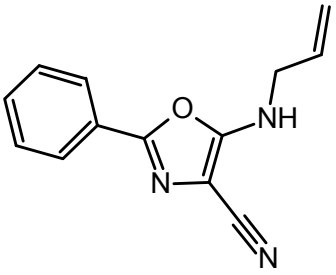

BC8-1H

Figure 5.15 5FOA growth response of compounds structurally related to BC8-1

The 5FOA growth responses of yeast strains that express different phosphodiesterases are shown in the presence of individual compounds in separate graphs. The strains shown are CHP1222 (PDE1B), CHP1220 (PDE1C), CHP1403 (PDE2A), CHP1249 (PDE3A), CHP1194 (PDE3B), CHP1262 (PDE4A), CHP1268 (PDE4B), CHP1186 (PDE4D), CHP1223 (PDE5A), CHP1189 (PDE7A), CHP1209 (PDE7B), CHP1204 (PDE8A), DDP40 (PDE8Acat), CHP1218 (PDE9A), CHP1224 (PDE11A), CHP1445 (PDE10A), and CHP1224 (PDE11A). **(A-H)** Compounds BC8-1A – BC8-1H.

Figure 5.15 5FOA growth response of compounds structurally related to BC8-1

A

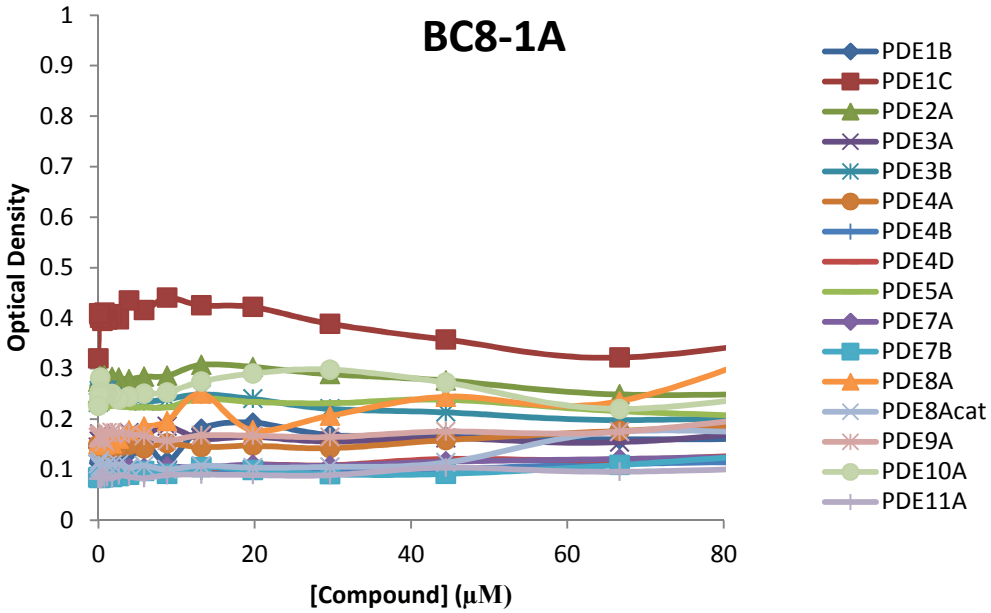

B

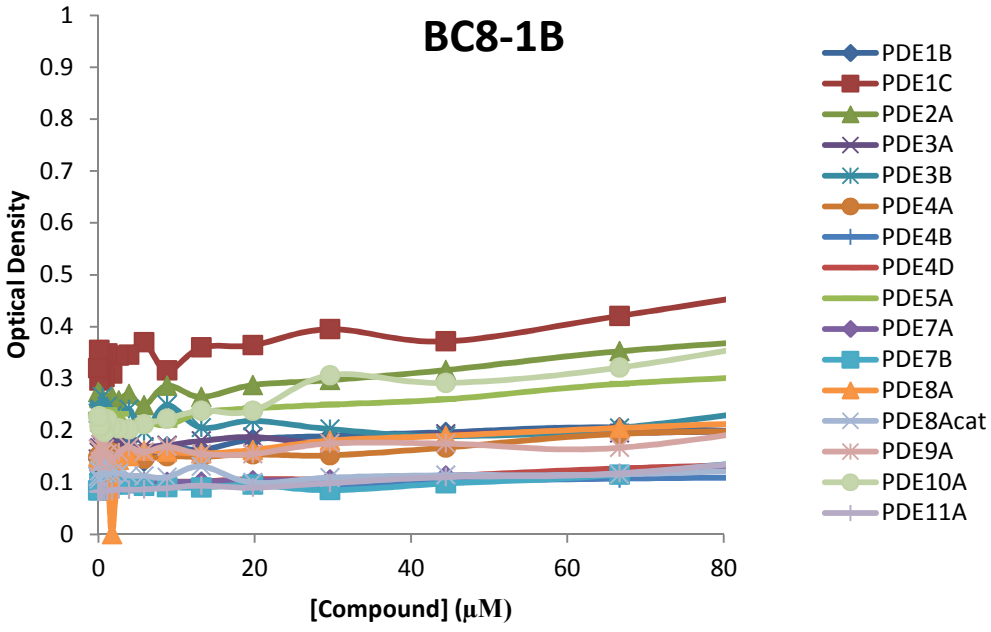

C

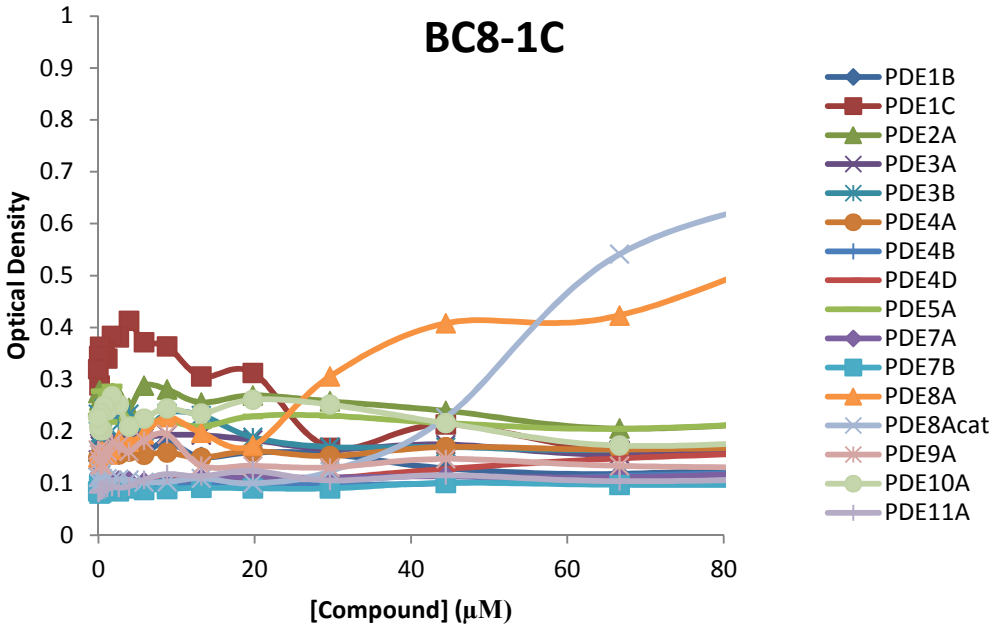
BC8-1C
Optical Density
[Compound] (µM)
PDE1B
PDE1C
PDE2A
PDE3A
PDE3B
PDE4A
PDE4B
PDE4D
PDE5A
PDE7A
PDE7B
PDE8A
PDE8Acat
PDE9A
PDE10A
PDE11A

D

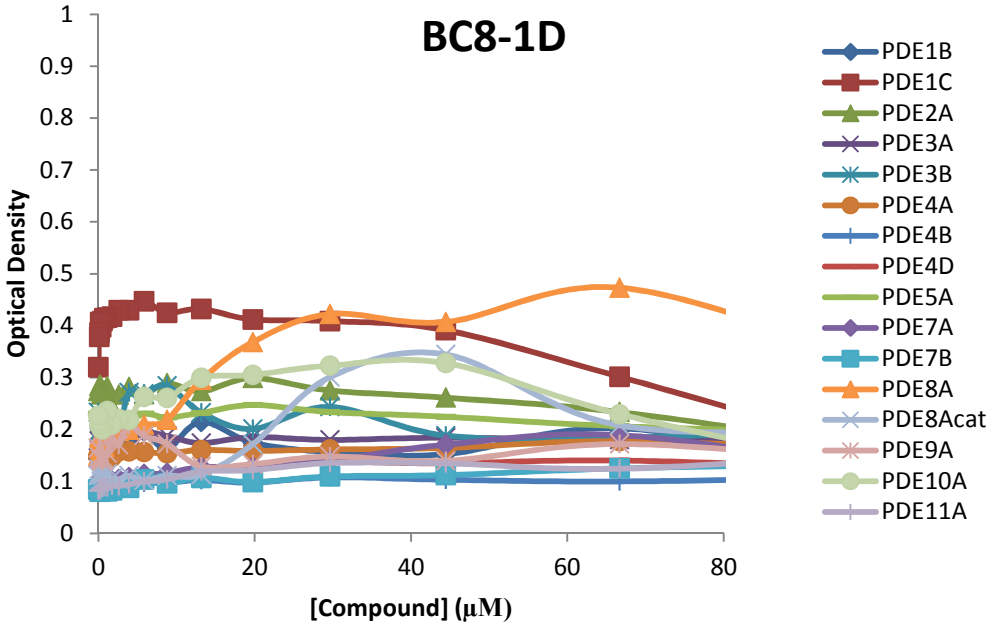
BC8-1D
Optical Density
[Compound] (µM)
PDE1B
PDE1C
PDE2A
PDE3A
PDE3B
PDE4A
PDE4B
PDE4D
PDE5A
PDE7A
PDE7B
PDE8A
PDE8Acat
PDE9A
PDE10A
PDE11A

E

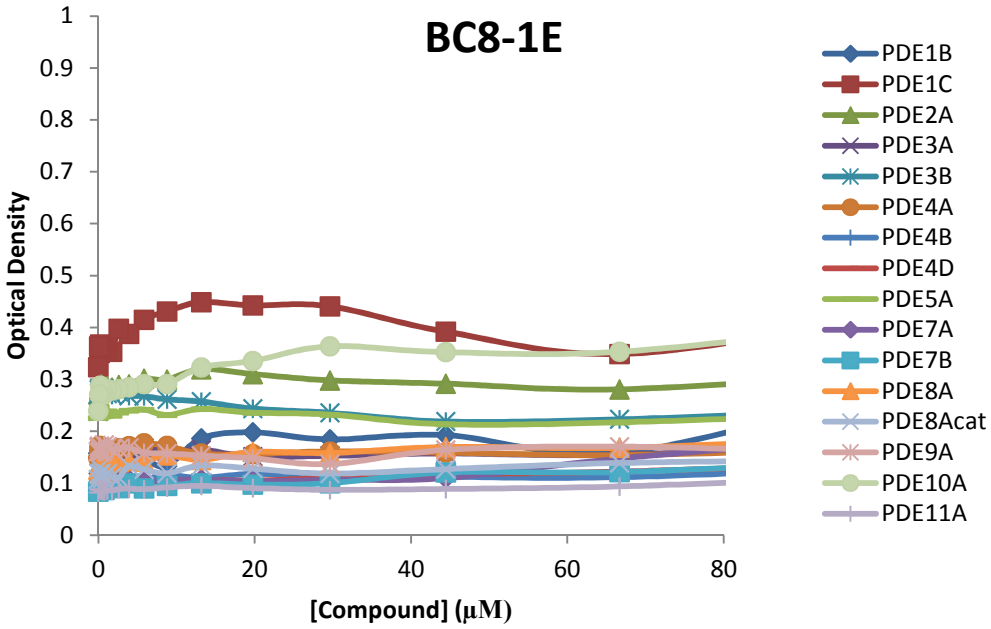
BC8-1E
Optical Density
[Compound] (µM)
PDE1B
PDE1C
PDE2A
PDE3A
PDE3B
PDE4A
PDE4B
PDE4D
PDE5A
PDE7A
PDE7B
PDE8A
PDE8Acat
PDE9A
PDE10A
PDE11A

F

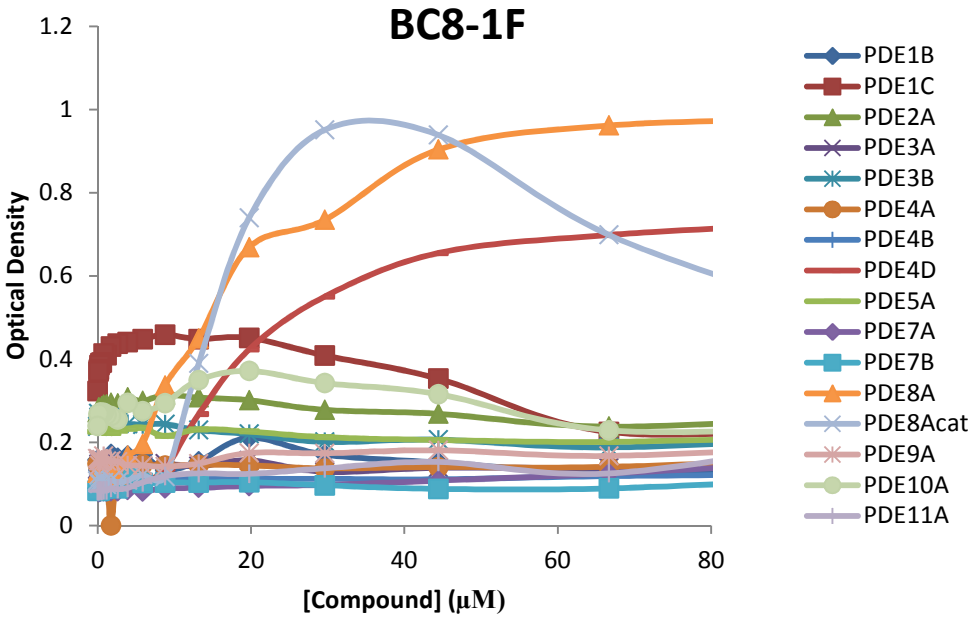
BC8-1F
Optical Density
[Compound] (µM)
PDE1B
PDE1C
PDE2A
PDE3A
PDE3B
PDE4A
PDE4B
PDE4D
PDE5A
PDE7A
PDE7B
PDE8A
PDE8Acat
PDE9A
PDE10A
PDE11A

G

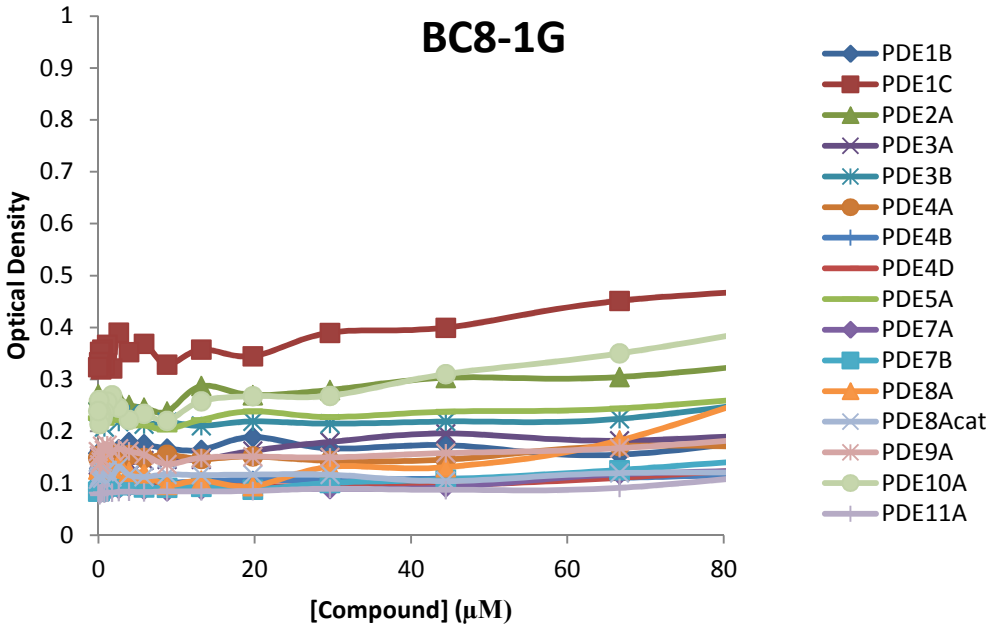
BC8-1G
Optical Density
[Compound] (µM)
0
0.1
0.2
0.3
0.4
0.5
0.6
0.7
0.8
0.9
1
0
20
40
60
80
PDE1B
PDE1C
PDE2A
PDE3A
PDE3B
PDE4A
PDE4B
PDE4D
PDE5A
PDE7A
PDE7B
PDE8A
PDE8Acat
PDE9A
PDE10A
PDE11A

H

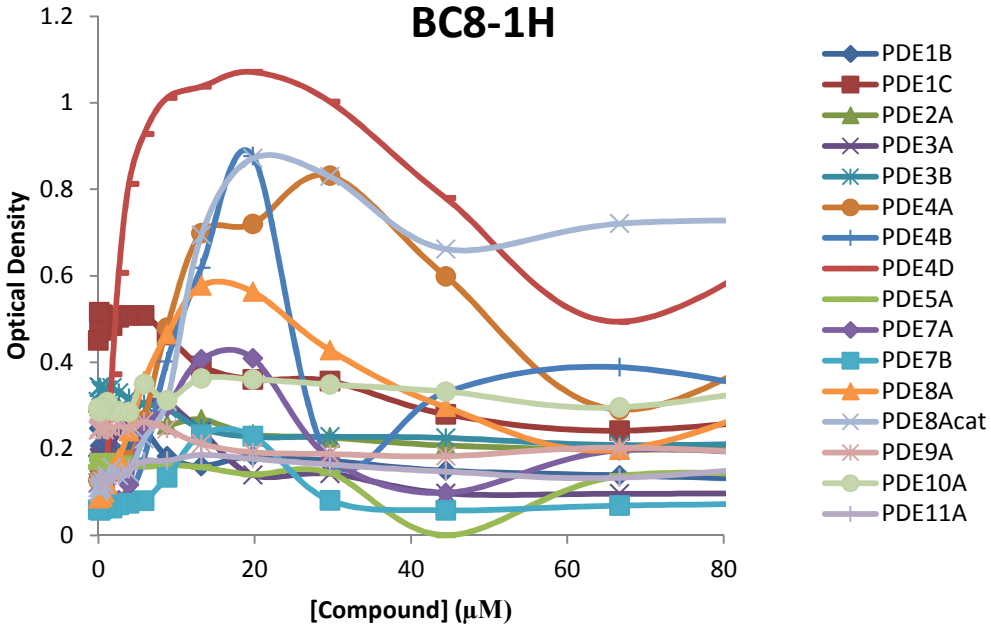
BC8-1H
Optical Density
[Compound] (µM)
0
0.2
0.4
0.6
0.8
1
1.2
0
20
40
60
80
PDE1B
PDE1C
PDE2A
PDE3A
PDE3B
PDE4A
PDE4B
PDE4D
PDE5A
PDE7A
PDE7B
PDE8A
PDE8Acat
PDE9A
PDE10A
PDE11A

In addition, the modifications that are made on the methylpropylamino group also cause the compounds to become ineffective in the yeast growth assays as seen with BC8-1B, BC8-1E, and BC8-1G. These inefficacies could be due to loss of the inhibitory activity of the compounds on the PDE8 enzyme or due to changes in compounds' solubility, stability or entrance into the cells. One compound that retained its ability to promote the growth of the PDE8A strains despite having a change in the methylpropylamino group is BC8-1C. Although it has lower efficacy (i.e. lower OD values at a given compound concentration compared to BC8-1) in the yeast growth assays, it has a similar selectivity profile as BC8-1. On the other hand, compounds BC8-1F and BC8-1H have different selectivity profiles than BC8-1 according to the yeast growth assays. In addition to their effect on PDE8A-expressing strains, BC8-1F also stimulates the growth of the PDE4D-expressing strain and BC8-1H promotes the growth of PDE4A, PDE4B and PDE4D-expressing strains. Structurally, BC8-1F and BC8-1H differ from BC8-1 and BC8-1C -respectively- by the lack of the methyl group from the phenyl ring. This suggests that the removal of the methyl group from the phenyl ring decreases the selectivity. Both BC8-1F and BC8-1H inhibit PDE8A enzyme in the *in vitro* assays.

5.4.3 BC8-5 Series

Three compounds that are structurally related to BC8-5 (Table 5.8) were tested for their ability to promote the 5FOA growth of yeast strains that express different PDEs (Figure 5.16). As shown previously, BC8-5 promotes the 5FOA growth of strains that express cAMP PDEs PDE8A, PDE8Acat, PDE4A, PDE4B, PDE7A, and PDE7B. When a methyl

group is introduced to the phenyl ring as in BC8-5A, the compound promotes the growth of only PDE7A and PDE7B-expressing strains. If the methyl group is located at another position (i.e. 4 methylphenyl instead of 2 methylphenyl; BC8-5B), the compound can no longer promote the growth of PDE7 strains but slightly increases the growth of full-length PDE8A-expressing strain. On the contrary, introduction of a methoxy group instead of a methyl group in the same position blocks the PDE inhibition as judged by both the yeast-based and *in vitro* assays. The yeast growth phenotypes are consistent with *in vitro* assays with the exception of PDE4 data (Figure 5.16, Table 5.9) in that the compounds BC8-5A and BC8-5B retain significant activity against PDE4A, yet lose activity in the yeast based assay.

5.4.4 BC8-8 Series

Two compounds that are structurally related to BC8-8 were tested by *in vitro* enzyme assays against PDE4A and PDE8A enzymes. The terminal methylbenzene group is changed to fluorobenzene for BC8-8A and to cholorobenzene for BC8-8B. Both of these compounds can still inhibit PDE8A (BC8-8A has lower efficacy) but they also become better PDE4A inhibitors (Table 5.10).

Table 5.8 Structures of BC8-5 derivatives

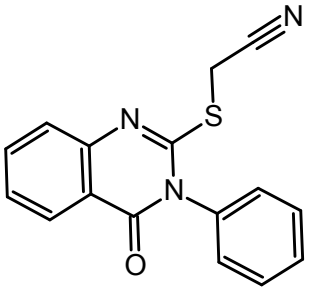

BC8-5

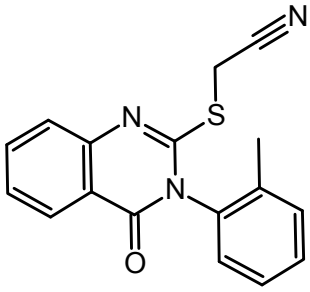

BC8-5A

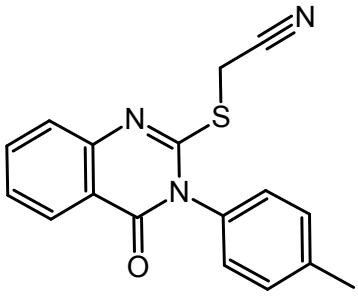

BC8-5B

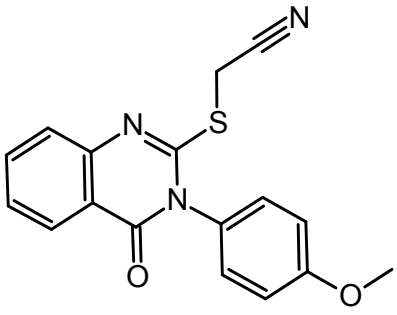

BC8-5C

Figure 5.16 5FOA growth response of compounds structurally related to BC8-5

The 5FOA growth responses of yeast strains that express different phosphodiesterases are shown in the presence of individual compounds in separate graphs. The strains shown are CHP1222 (PDE1B), CHP1220 (PDE1C), CHP1403 (PDE2A), CHP1249 (PDE3A), CHP1194 (PDE3B), CHP1262 (PDE4A), CHP1268 (PDE4B), CHP1186 (PDE4D), CHP1223 (PDE5A), CHP1189 (PDE7A), CHP1209 (PDE7B), CHP1204 (PDE8A), DDP40 (PDE8Acat), CHP1218 (PDE9A), CHP1224 (PDE11A), CHP1445 (PDE10A), and CHP1224 (PDE11A). **(A-C)** Compounds BC8-5A – BC8-5C.

Figure 5.16 5FOA growth response of compounds structurally related to BC8-5

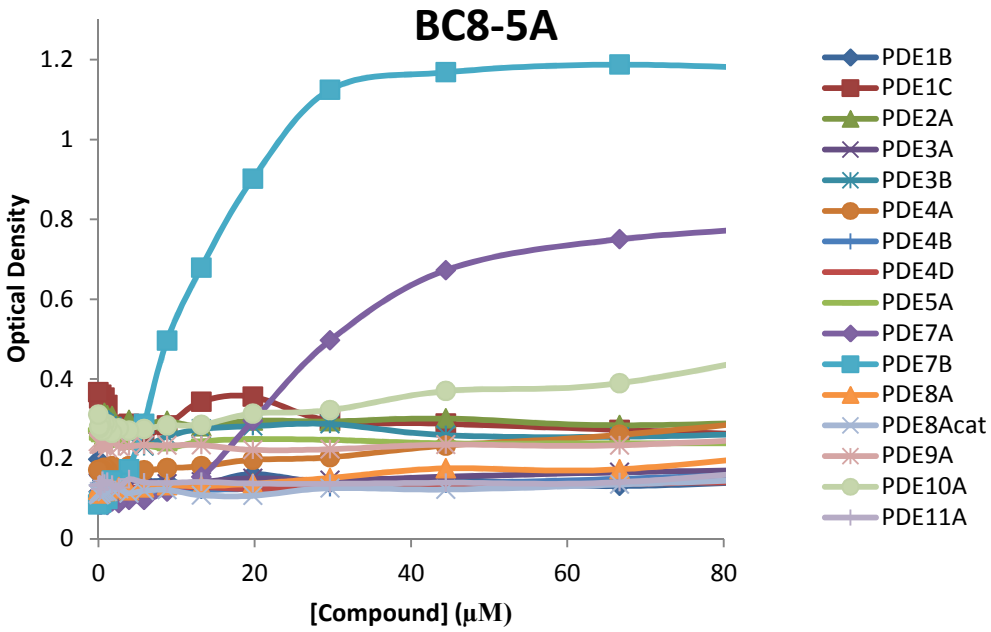

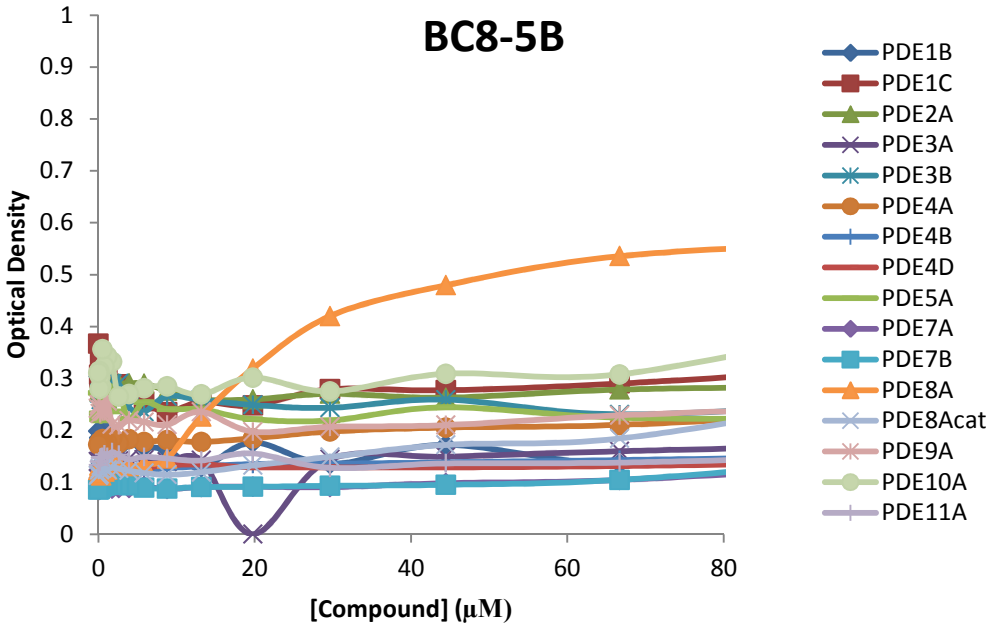

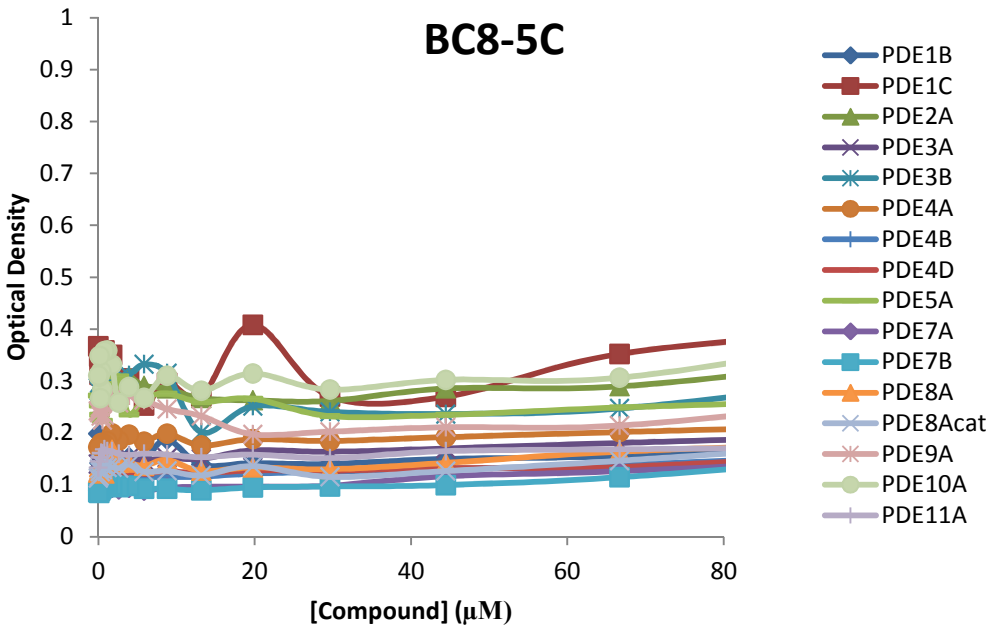

Table 5.9 *In vitro* enzyme assays with BC8-5 derivatives

IC_{50} values (given in µM) are determined at following substrate concentrations: 10 nM for PDE8A, 35 nM for PDE7A, 1 µM for PDE4A.

	PDE8A	PDE4A	PDE7A
BC8-5	1.9	2.5	1.6
BC8-5A	5.5	0.7	0.2
BC8-5B	3.8	4.9	15.9
BC8-5C	100.2	25.7	3213.7

Table 5.10 Structures of BC8-8 derivatives and their effect on PDE4A/PDE8A

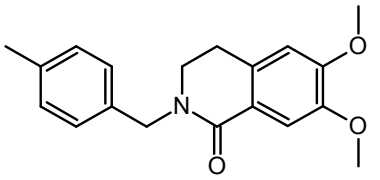

BC8-8

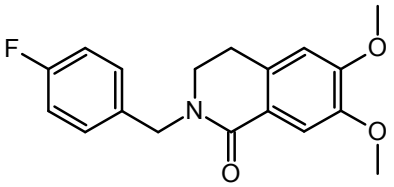

BC8-8A

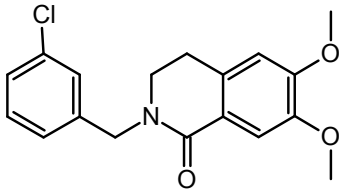

BC8-8B

	Percent inhibition at 10 μM		Percent inhibition at 1 μM	
	PDE8A	PDE4A	PDE8A	PDE4A
BC8-8	61	12	17	0
BC8-8A	27	46	3	10
BC8-8B	57	72	8	17

5.4.5 BC8-15 Series

Sixteen compounds that are structurally related to BC8-15 were tested by *in vitro* enzyme assays against PDE4A -catalytic domain of PDE4A10- and PDE8A –full-length PDE8A1 (Table.5.11, 5.12). BC8-15 inhibits PDE4A and PDE8A with an IC_{50} of 260 and 610 nM, respectively. As it can be seen with compounds BC8-15A and BC8-15B, the presence of a methyl group instead of an ethyl group on the triazole ring or changing the position of carboxyl group on the phenyl ring slightly decreases the inhibitory activity. Furthermore, the presence of the carboxyl group on the phenyl ring (i.e. a benzoic acid) seems very important in terms of the ability of the compound to inhibit PDE8A. When the carboxyl group is removed (i.e. benzoic acid is changed to a phenyl ring) as in BC8-15D or changed to a hydroxyl group as in BC8-15E or the benzoic acid group is change to a ethylbenzoate as in BC8-15F; the inhibition on PDE8A diminishes almost by half compared to BC8-15 while all of these compounds are still able to inhibit PDE4A effectively. Changing the original benzoic acid group to dimethoxyphenyl also diminishes inhibition on PDE8A and slightly decreases the effect on PDE4A. Also, changing the benzoic acid group to chlorobenzene almost totally abolishes the inhibition on PDE8A but the compound can still inhibit PDE4A. The addition of a six-membered aromatic ring to the phenyl ring instead of a carboxyl group as shown for BC8-15L decreases the inhibition potential of the compound for both PDE4 and PDE8. On the other hand, addition of a five-membered aromatic ring instead of the carboxyl group (BC8-15J) abolishes inhibition on PDE8 while the compound can still inhibit PDE4A. Additional modifications on the benzoic acid group as seen in compound BC8-15I, BC8-

15K, BC8-15M, BC8-15N, BC8-15O, and BC8-15P make the compounds lose the inhibitory potential for both enzymes.

5.4.6 BC8-23 Series

Five compounds that are structurally related to BC8-23 were tested by *in vitro* enzyme assays against PDE8A and PDE4A (Table 5.13, 5.14). BC8-23 inhibits PDE8A but not PDE4A. Compound BC8-23A has a methyl group in the terminal phenyl group instead of an ethyl group and BC8-23B has lacks one carbon in the backbone compared to BC8-23. Both of these compounds still do not inhibit PDE4A and can inhibit PDE8A with slightly lower efficacy than BC8-23. On the other hand, the modifications in the terminal benzene (changing to chlorobenzene as in BC8-23D or dimethoxybenzene as in BC8-23E) decrease the efficacy toward PDE8A approximately by half. Finally having oxygen bound to the sulfur atom totally abolishes the inhibition.

Table 5.11 Structures of BC8-15 derivatives

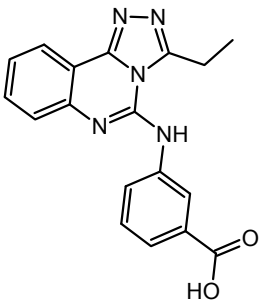

BC8-15

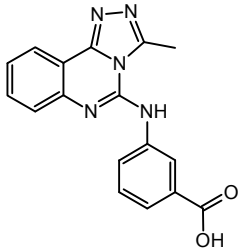

BC8-15A

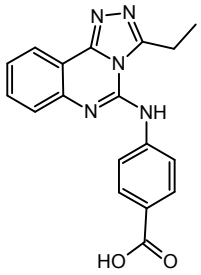

BC8-15B

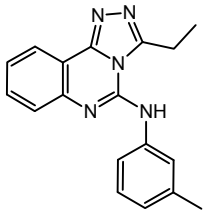

BC8-15C

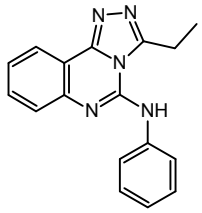

BC8-15D

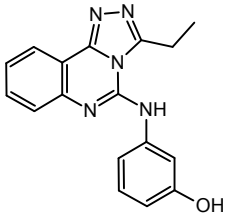

BC8-15E

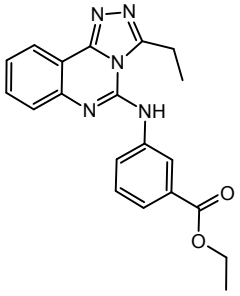

BC8-15F

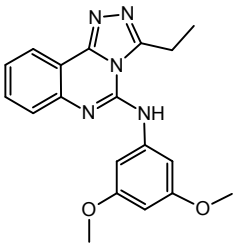

BC8-15G

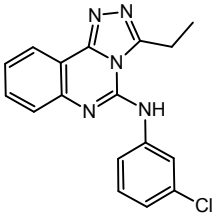

BC8-15H

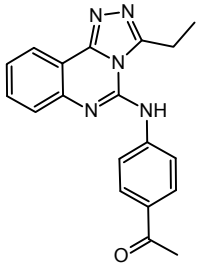

BC8-15I

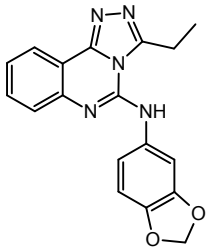

BC8-15J

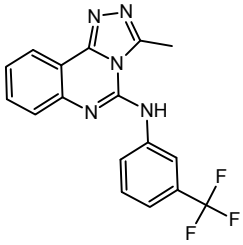

BC8-15K

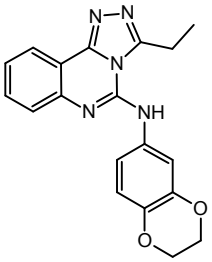

BC8-15L

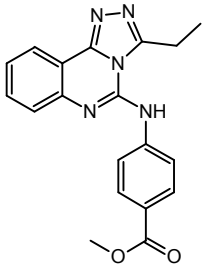

BC8-15M

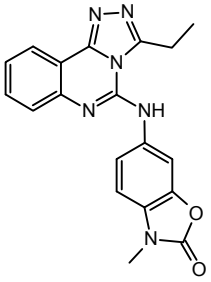

BC8-15N

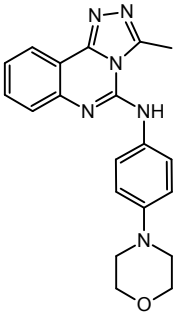

BC8-15O

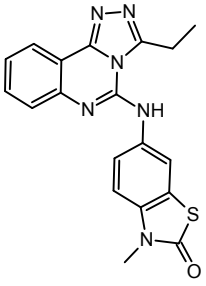

BC8-15P

Table 5.12 The effect of BC8-15 derivatives on PDE4A and PDE8A

Enzyme assays are performed at 1μM cAMP for PDE4A and 10 nM cAMP for PDE8A.

	Percent inhibition at 10 μM		Percent inhibition at 1 μM	
	PDE8A	PDE4A	PDE8A	PDE4A
BC8-15	84	92	70	92
BC8-15A	85	77	49	35
BC8-15B	79	86	41	45
BC8-15C	40	93	4	78
BC8-15D	44	100	7	93
BC8-15E	60	94	12	80
BC8-15F	44	94	7	62
BC8-15G	45	79	9	31
BC8-15H	13	94	5	83

	Percent inhibition at 10 μM	
	PDE8A	PDE4A
BC8-15	95	100
BC8-15I	20	14
BC8-15J	10	78
BC8-15K	13	38
BC8-15L	65	67
BC8-15M	29	18
BC8-15N	28	5
BC8-15O	38	22
BC8-15P	34	34

Table 5.13 Structures of BC8-23 derivatives

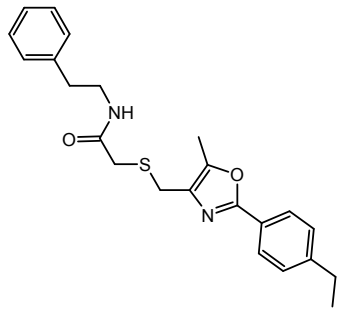

BC8-23

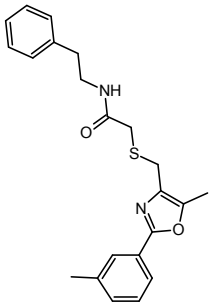

BC8-23A

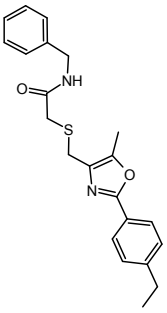

BC8-23B

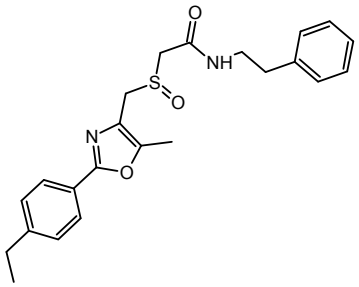

BC8-23C

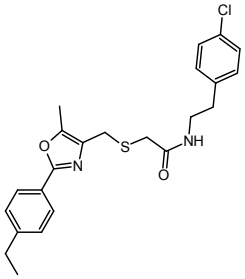

BC8-23D

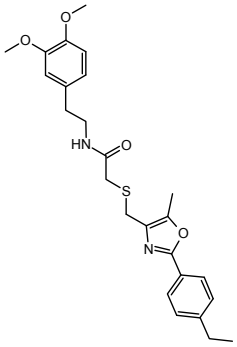

BC8-23E

Table 5.14 The effect of BC8-23 derivatives on PDE4A and PDE4B

Percent inhibition at 10 μM		
	PDE8A	PDE4A
BC8-23	69	7
BC8-23A	47	7
BC8-23B	52	8
BC8-23C	4	0
BC8-23D	35	5
BC8-23E	32	15

5.5 EFFECT OF PDE8 INHIBITORS ON MAMMALIAN SYSTEMS

One of the demonstrated functions of PDE8A is its regulatory role in steroidogenesis in the Leydig cells, which are the interstitial cells located adjacent to the seminiferous tubules in the testes. Lutenizing hormone (LH) stimulates testosterone synthesis in the Leydig cells through binding the receptor on the cell membrane and inducing cAMP synthesis (Haider. 2007). Activation of PKA is needed for the transport of cholesterol from the cytoplasmic pool to mitochondria. This is the rate limiting step of steroidogenesis and it is initiated by steroidogenic acute regulatory protein (StAR) (Hauet *et al*. 2002). It has been previously shown by the Beavo lab that the Leydig cells from PDE8A knock-out mice are more sensitive to LH for testosterone production. The sensitivity to LH seen by the ablation of PDE8A function is much more pronounced than the slight effect that was observed by PDE inhibitor IBMX (which does not inhibit PDE8). Furthermore, additional sensitivity to LH response is potentiated when Leydig cells from PDE8A knock-out mice are treated with IBMX, suggesting the role of another phosphodiesterase in this process (Vasta *et al*. 2006).

I tested the effect of our candidate PDE8 inhibitors in the steroidogenesis response from Leydig cells. Leydig tumor cell line MA-10 was used to monitor the changes in the progesterone production upon compound treatment. These cells express very low or undetectable amounts of P450c17, which is the enzyme with 17 alpha-hydroxylase and 17,20 lyase activities in the synthesis of steroid hormones. Thus, progesterone is considered as the major steroid output in this cell line. Upon treatment for 4 hours,

compounds BC8-1, BC8-5, BC8-8 and BC8-15 elevated in the progesterone production. BC8-15 had a more pronounced effect than other compounds. Also, the compounds were more effective at 40 μM. During the same assay, some wells were treated with LH for two hours following two hours of compound treatment. Increased progesterone release was also observed for compounds BC8-5, BC8-8 and BC8-15 after LH stimulation (Figure 5.17). The highest amount of steroid production was attained by compound BC8-15 and followed by BC8-5. The effect that was seen with compound BC8-15 was dose dependent and reproducible. Figure 5.18 shows the dose dependent increase in progesterone release as BC8-15 concentration increases. It should be noted that BC8-15 is a PDE4/PDE7 dual specificity inhibitor and BC8-5 inhibits PDE4/7/8. This is consistent with the observations where IBMX (i.e. inhibition of other PDEs) in a PDE8 null background has synergistic effect in steroid production. Also, according to *in vitro* enzyme assays BC8-15 has the lowest IC_{50} value against PDE8A among the compounds that are identified from HTS. This may be relevant to the increased potency of this compound compared to other test compounds in the mammalian assays.

We also tested the effect of these compounds on primary Leydig cells that were isolated from testes of wild type and PDE8A/8B knock-out adult mice. Following isolation and incubation to allow cell attachment, cells were treated with compounds at two concentrations (10 and 40 μM) for three hours.

Figure 5.17 Effect of PDE8 inhibitors on progesterone levels from MA-10 cells

The effect of compounds BC8-1, BC8-5, BC8-8, BC8-15, BC8-22 and BC8-23 alone and in the presence of IBMX are shown. **(A)** Progesterone release from MA-10 cells after 4 hours of compound treatment **(B)** Progesterone release after 2 hours of LH stimulation. Cells were treated with the compounds 2 hours prior to hormone stimulation.

Figure 5.17 Effect of PDE8 inhibitors on progesterone levels from MA-10 cells

A

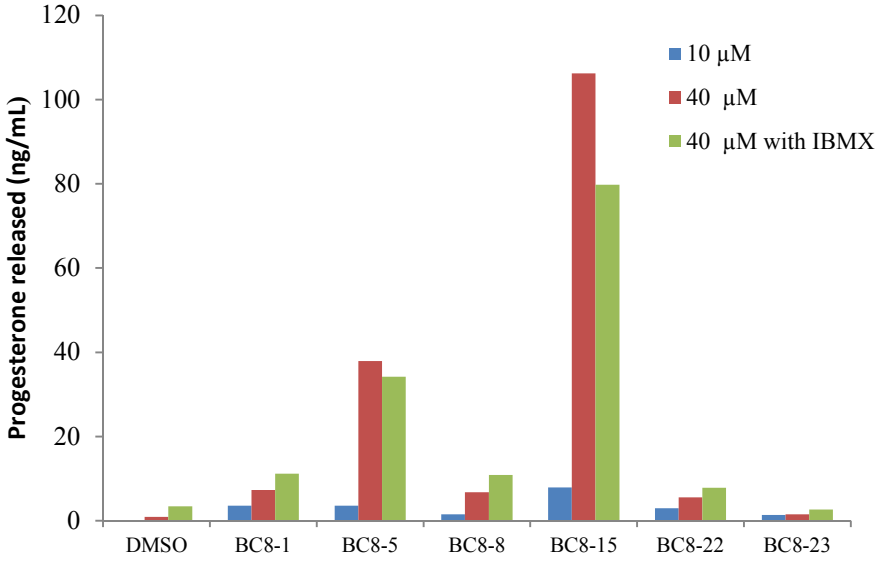

B

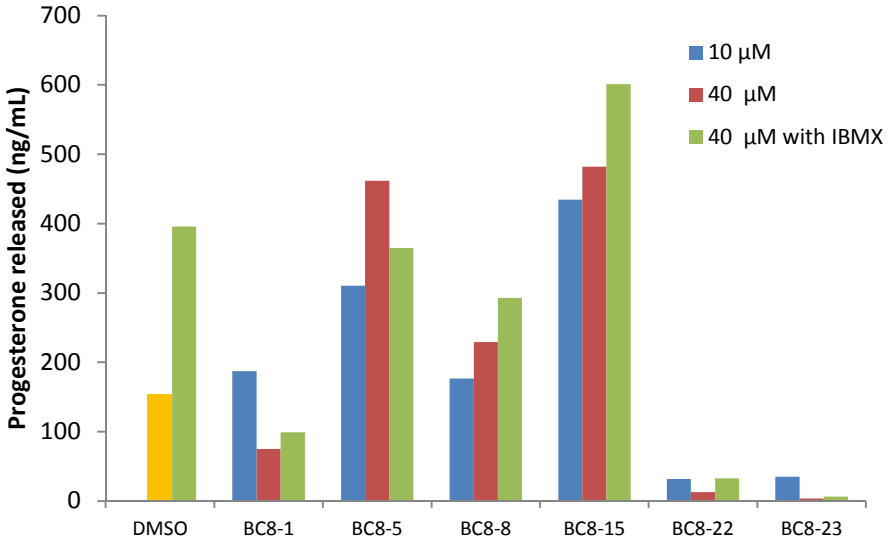

Figure 5.18 BC8-15 elevates progesterone levels in a dose dependent way

The increase in the progesterone release in response to different concentrations of BC8-15 treatment is shown.

Figure 5.18 BC8-15 elevates progesterone levels in a dose dependent way

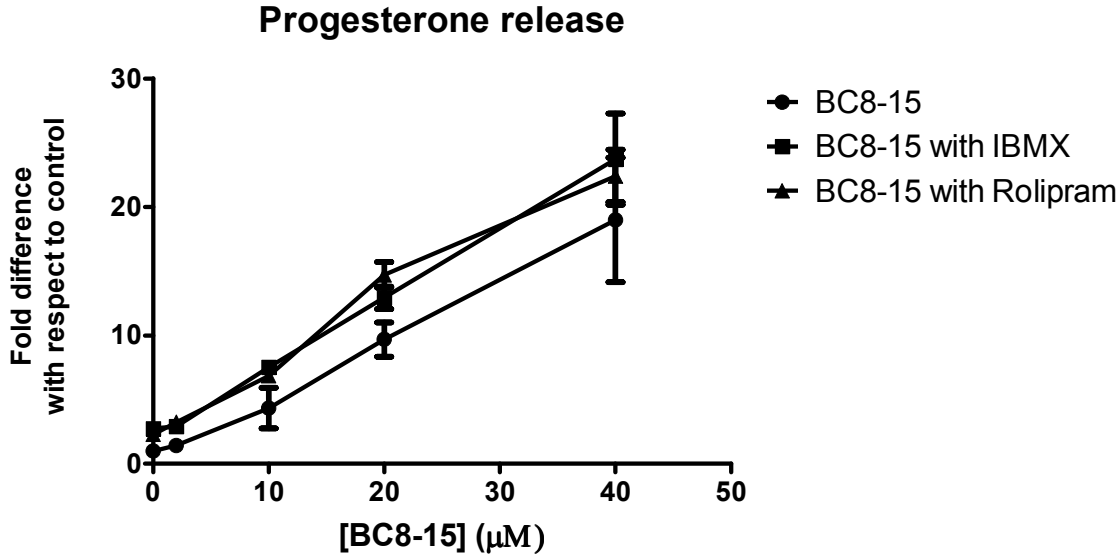

As expected, compared to the wild type Leydig cells, cells from the knock-out animal showed a higher basal level of testosterone production. Cell preparations had similar 3β-hydroxysteroid dehydrogenase activities, which is a marker enzyme of Leydig cells. Its activity is monitored by reduction of nitroblue tetrazolium (cell suspensions displayed OD_{570} values of 0.17 and 0.18) to ensure the number of isolated Leydig cells are comparable. Consistent with the notion that the cAMP pool in the Leydig cells is governed by mainly PDE8 but secondarily by other PDE(s), IBMX or rolipram did not cause any change in testosterone production in the wild type background while they elevate testosterone levels for cells from the PDE8 knock-out animal. No change was detected with compounds BC8-1 or BC8-8. A slight increase with BC8-5 is observed. The response stimulated by BC8-15 is consistent with its PDE inhibition profile. It elevates the testosterone production of the wild type cells at 10 μM and the effect at 40 μM is much greater. On the other hand, PDE8 knock-out cells did not display great levels of elevation in testosterone levels. The amount of testosterone released in the presence of BC8-15 is similar to the amount released when cells are treated with the PDE4 inhibitor rolipram. The lack of a further increase in testosterone levels suggests that the effect observed by BC8-15 in wild type cells is due to inhibition of PDE4 and PDE8 enzymes and the compound seems to not have an immediate target to affect testosterone levels at short incubation periods (Figure 5.19).

Figure 5.19 Effect of BC8-15 on primary Leydig cells is consistent with its PDE inhibition profile

The effect of compounds on the testosterone release from primary Leydig cells from wild type and PDE8A /PDE8B knock-out mice is shown.

Figure 5.19 Effect of BC8-15 on primary Leydig cells is consistent with its PDE inhibition profile

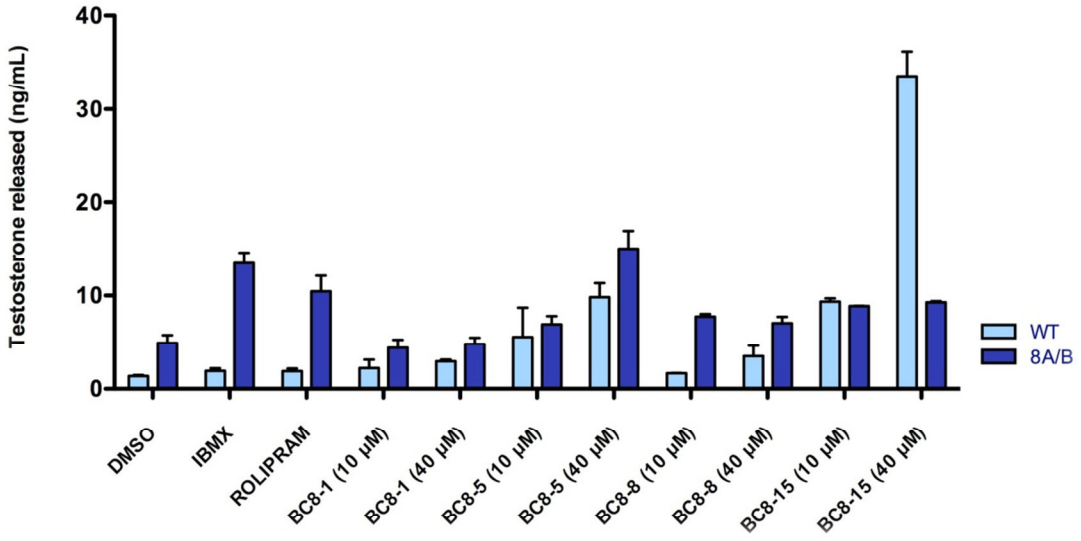

Figure 5.20 Correlation between progesterone response and PDE8 inhibitory activity in BC8-15 derivatives

The effect of BC8-15 derivatives on progesterone release is shown. BC8-15H and BC8-15J do not have PDE8 inhibitory activity and they behave as a PDE4 inhibitor.

Figure 5.20 Correlation between progesterone response and PDE8 inhibitory activity in BC8-15 derivatives

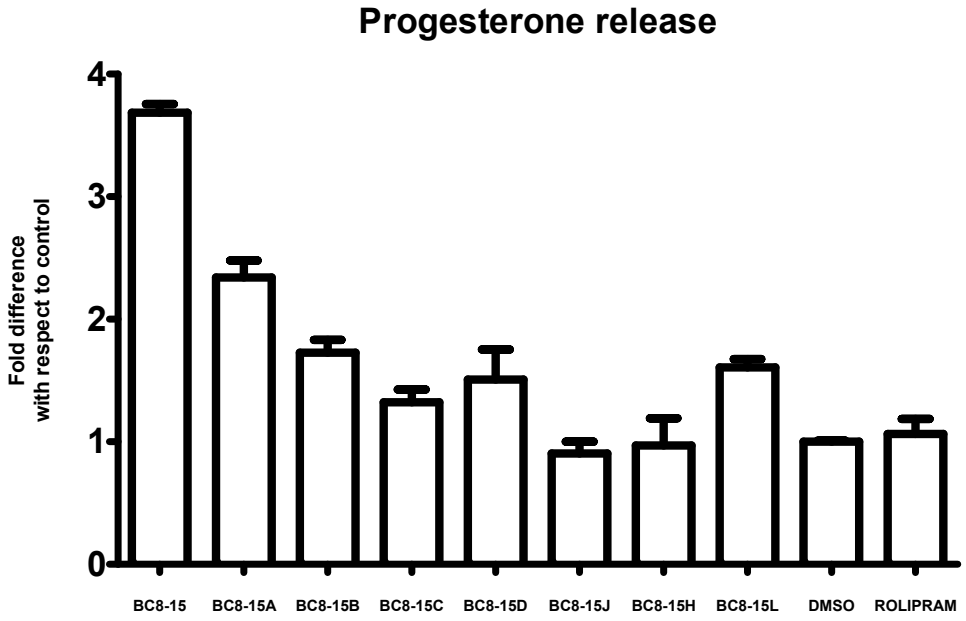

Finally, the effect of BC8-15 on the progesterone release from MA-10 cells was retested using structural derivatives of BC8-15. As described in the previous section, BC8-15A, and BC8-15B are PDE4/8 inhibitors with slightly lower efficacy than BC8-according to the *in vitro* enzyme assays. BC8-15L also has a similar profile but much lower efficacy. Compared to BC8-15, BC8-15C and BC8-15D has lower efficacy toward PDE8A but retain their ability to inhibit PDE4A. Finally, BC8-15J and BC8-15H almost completely lose their inhibition on PDE8A while they can inhibit PDE4A. When the progesterone release was measured in response to these compounds, a correlation was seen with regard to PDE8A, but not PDE4A inhibition as measured by *in vitro* enzyme assays (Figure 5.20).

5.6 CONCLUSION

Thirty compounds identified from HTS were characterized by their ability to affect the 5FOA growth of yeast strains that express different phosphodiesterases and by their behavior in *in vitro* enzyme assays. Dose response profiling of compounds against 16 different strains expressing various PDEs identified compounds of different patterns of inhibition. Most of the compounds that do not promote growth of all of the yeast strains confirmed to inhibit human PDE8A *in vitro*. Similarly, these compounds also inhibit human PDE8B enzyme. In conclusion, eleven structurally distinct PDE8 inhibitors were identified. The most potent compound identified by the *in vitro* enzyme assays is the PDE4/8 dual specificity inhibitor BC8-15. Progesterone release assays from MA-10 cells indicate that BC8-15 elevates steroid production in these cells as a function of its PDE8

inhibition. Furthermore, BC8-15 causes elevated testosterone production from wild type primary Leydig cells but -consistently with its PDE inhibition profile- its effect does not exceed the effect of PDE4 inhibitor rolipram in PDE8A/B knock out mouse. Thus, I have successfully identified PDE8 inhibitors that are biologically active even prior to efforts to enhance pharmacokinetic properties via medicinal chemistry.

CHAPTER SIX

6 SUMMARY AND FUTURE DIRECTIONS

From unicellular organisms to humans, cyclic AMP dependent signal transduction pathways mediate a diverse range of cellular responses. One of the important components of the cyclic nucleotide signaling pathways is phosphodiesterases. Through hydrolysis of cyclic AMP/GMP, they serve as the major enzymes to control the amplitude and duration of the signal. Twenty one genes in the PDE superfamily along with various splice variants have distinct roles controlling specific physiological conditions and disease states. Recently, the PDE8 family has been found to be important in steroid production from the adrenal gland and testis. The unavailability of PDE8 inhibitors has limited the functional studies of PDE8 enzymes that may also be important therapeutic targets. The aim of this thesis is to develop a screenable platform for inhibitors of PDE8 and to find and characterize novel PDE8 inhibitors.

6.1 DEVELOPMENT OF A SCREENING PLATFORM FOR PDE8 INHIBITORS

The mouse PDE8A gene was successfully cloned into the yeast chromosome. Initial attempts to optimize the full-length PDE8A expressing strain were not successful due to the absence of a clean 5FOA sensitivity phenotype when tested in a 384-well microtiter dish format leading to high background values. I successfully employed an adenylyl

cyclase deletion strategy to create a strain that expresses full-length PDE8A (CHP1204). Adenylyl cyclase deleted strains require exogenous addition of cAMP to repress *fbp1* transcription and their PDE activity is judged by the increased levels of exogenous cAMP needed to confer 5FOA resistant growth. I optimized the pre-growth conditions and cAMP concentration in the 5FOA medium that produces a distinct growth response when comparing a PDE-lacking strain to a PDE8A-expressing strain. This allowed me to test the effects of candidate PDE inhibitors on the 5FOA growth of the PDE8A strain.

6.2 LOW-THROUGHPUT SCREENING

I tested fifty-six compounds identified from high-throughput screens against PDE4 and PDE7 families for their ability to promote growth of the PDE8A-expressing strain CHP1204. Several compounds promoted growth of CHP1204 in 5FOA. When I tested these compounds against a strain that lacks PDE activity, some of them (BC21, BC42, BC51, BC55) shifted the cAMP titration curve to the left, suggesting that these compounds promote growth via a PDE-independent route. In contrast, several compounds such as BC24, BC60, BC63, BC69 and BC76 not only shifted the cAMP titration curve of only the PDE8A-expressing strain (in comparison to the strain that lacks PDE activity) but also inhibited PDE8A in *in vitro* enzyme assays. I demonstrated that the PDE4 inhibitor compound BC69 was the most effective compound in promoting the growth of PDE8A-expressing strain, and identified it as an effective PDE8 inhibitor both in yeast growth and *in vitro* enzyme assays.

These findings successfully demonstrate that it is possible to use the glucose sensing pathway of the fission yeast to study mammalian phosphodiesteases for strains in which the PDE activity is insufficient to confer 5FOA sensitivity even in strains carrying mutations to reduce adenylyl cyclase activation. In addition, since strains lacking the adenylyl cyclase gene respond to either exogenous cAMP or cGMP to activate PKA, the use of adenylyl cyclase deletion strains extended our ability for utilization of this fission yeast based screening platform to detect the inhibitors of phosphodiesterases that hydrolyze cGMP or are dual specific. As a proof of this concept, I identified BC76 as an inhibitor of the cGMP specific phosphodiesterase PDE5A with an IC_{50} of 232 nM (Demirbas *et al*. 2010).

Finally, I also cloned the catalytic domain of PDE8A under *nmt* promoters (*nmt*1 and *nmt*41) and identified the strain with the most suitable genetic background that confers 5FOA sensitivity. Since the catalytic domain of PDE8A shows high phosphodiesterase activity when expressed under *nmt1* promoter, the strain with an intact *git* pathway (DDP40) showed 5FOA sensitivity and was optimized to respond to compound BC69.

6.3 HIGH-THROUGHPUT SCREENING AGAINST PDE8A

I optimized the full-length PDE8A expressing strain CHP1204 for high-throughput screening using compound BC69 as the positive control. Z factor tests for optimized screening conditions yield values between 0.6-0.9 in different experiments. This indicates the robustness of the screening conditions. I screened 241,691 compounds from known bioactives, natural products, and commercial libraries; and identified 2447 total hits. The

positive hits are mostly from commercial libraries and no strong hits were obtained form the natural product libraries. Secondary cherrypick assays with 367 selected compounds confirmed the effect of approximately 70% of these compounds on the 5FOA growth of strain CHP1204. We believe that some of these compounds fail to promote the growth in 5FOA medium due to inefficient compound transfer from stock plate to assay plates by the pocket tips. Although the provided amount of cherrypick compounds is only 1 μL, the remaining compounds from the unconfirmed wells can be diluted and retested using micropipets to transfer compounds into wells. This could increase the confirmation ratio of the compounds in the secondary assays.

One aspect of the cherrypick assays was to test the compounds against strains that express other phosphodiesterases to identify non-selective compounds. I used PDE4A and PDE7A or PDE7B-expressing strains CHP1262, CHP1189, CHP1209, respectively. These enzymes are also cAMP specific phosphodiesterases, so some compounds that inhibit PDE8A may also be able to inhibit PDE4 or PDE7 enzymes. Although PDE4A and PDE7-expressing strains helped eliminate some of the compounds as non-selective inhibitors, several compounds that were not very effective at promoting the growth of these strains in the cherrypick assays stimulated growth in the follow-up assays.

6.4 CHARACTERIZATION OF IDENTIFIED COMPOUNDS

Thirty compounds were selected by their effect on primary screening and on cherrypick assays, including the compounds that seem to have hightest potency and/or selectivity. After confirming their ability to promote growth of PDE8A-expressing strain CHP1204, I

tested these compounds against other strains that express various PDEs. Ten compounds out of thirty (BC8-2, BC8-6, BC8-12, BC8-13, BC8-14, BC8-18, BC8-19, BC8-20, BC8-21, and BC8-26) promoted the growth of most of the yeast strains that express different PDEs. Furthermore, eight of them (all except BC8-2 and BC8-21) failed to inhibit PDE8A in *in vitro* enzyme assays. This suggests that these compounds act through a non-PDE target to promote growth of yeast strains. These targets could act downstream of cAMP generation by activating PKA or inhibiting enzymes that convert 5FOA into the toxic product. Since this group constitutes the major source of false positive results, it should be addressed in the future HTS practices. As seen from the dose response profiles, PDE4 and PDE7 strains do not always grow in 5FOA in the presence of these compounds that act through non-PDE targets. These strains have a very clean 5FOA sensitivity phenotype without being adenylyl cyclase deficient. Due to the differences in the genetic background, they may not be as sensitive to non-selective compounds that promote growth of many yeast strains as the adenylyl cyclase deletion strains. This suggests that utilization of an adenylyl cyclase deletion strain during the cherrypick assays could have been helpful in eliminating these false positives.

At the time of this project, no prior data related to 5FOA growth of yeast strains was available. Although the data from the high throughput screens against PDE4 and PDE7 enzymes performed at the Broad Institute had some overlapping compound libraries, they constituted the small fraction of the screened compounds. Recently, Hoffman Lab member Ozge Ceyhan completed an HTS using a PDE11 strain. The comparison of hits

from that screen shows that ten of the identified compounds (BC8-3, BC8-6, BC8-12, BC8-13, BC8-14, BC8-16, BC8-20, BC8-22, BC8-25, and BC8-27) were also annotated as hits in the PDE11 screen (Ozge Ceyhan, unpublished data). Eight of these compounds did not confirm PDE8 inhibition in the *in vitro* assays, while BC8-16 and BC8-22 inhibits PDE8.

6.5 RE-EVALUATION OF THE SCREENING DATA

I examined the compounds that were selected for cherrypicking from PDE8A screen with respect to their response in the PDE11 screen (Ozge Ceyhan, unpublished data). 362 of the cherrypicked compounds were screened against PDE11. 263 of these compounds were not annotated as hits for PDE11. Seventy of these compounds had composite Z scores above 35 for PDE8A screen, twelve of which are already in the 'in house' collection (BC69, BC8-1, BC8-11, BC8-15, BC8-17, BC8-18, BC8-1F, BC8-1H, BC8-23, BC8-28, BC8-5, BC8-7) that were characterized during this thesis project. Among the remaining 58 compounds, 35 were confirmed in cherrypick assays for promoting growth of PDE8A. I eliminated eleven compounds from this group due to their high Z score values against PDE7-expressing strains. The primary and secondary assay responses of the remaining 24 compounds are given in Table 6.1 and the structural description of these compounds as SMILES (simplified molecular input line entry specification) are given in Table 6.2. Five of these compounds (1589 K14, 1598 O16, 1490 B16, 1722 D08, and 1598 I16) are structurally similar to BC8-1. Similarly, two compounds (1626 O16 and

Table 6.1 PDE8 hits

	Primary Screen		Cherrypick assays (Absorbance)			
Plate/well ID	Average Absorbance	Composite Z Score	PDE8A	PDE8Acat	PDE4A	PDE7A or PDE7B
1722 D08[a]	0.75	50.8	0.488	0.16	0.10	0.05
1772 M19	0.74	39.4	0.501	0.63	0.10	0.06
1643 K05	0.71	66.2	0.309	0.14	0.11	0.04
1626 O10[b]	0.70	64.6	0.693	0.74	0.10	0.04
1778 I10	0.68	35.3	0.573	0.76	0.11	0.04
1598 I16[a]	0.64	53.4	0.583	0.20	0.10	0.05
1581 G07	0.61	50.1	0.417	0.15	0.12	0.03
1577 E20	0.60	38.3	0.446	0.11	0.09	0.03
1696 L14	0.59	38.6	0.317	0.11	0.09	0.04
1640 B10	0.58	51.5	0.362	0.32	0.10	0.05
1589 K14[a]	0.57	46.3	0.49	0.68	0.10	0.05
1504 N14	0.55	56.3	0.494	0.17	0.13	0.22
1591 I14	0.52	41.5	0.386	0.13	0.11	0.05
1598 O16[a]	0.52	41.0	0.569	0.13	0.10	0.07
1490 B16[a]	0.51	50.3	0.573	0.74	0.12	0.22
1507 B17	0.50	49.2	0.437	0.12	0.14	0.25
1504 M14	0.48	47.1	0.466	0.11	0.11	0.18
1598 O11	0.47	36.5	0.309	0.47	0.09	0.05
1582 F07	0.47	36.3	0.34	0.08	0.10	0.04
1630 B11	0.43	36.0	0.368	0.13	0.11	0.05
1642 G02	0.43	35.3	0.329	0.13	0.10	0.05
527 J07	0.39	66.6	0.523	0.08	0.14	0.12
1837 E05	0.36	37.8	0.48	0.12	0.14	0.16
1915 D02[b]	0.33	53.0	0.576	0.84	0.13	0.27

[a] Compounds structurally related to BC8-1, [b] compounds structurally related to BC8-23.

Table 6.2 SMILES table

Plate	Well	Compound SMILES
1722	D08	N#Cc1nc(oc1NCC1CCCO1)c1ccccc1
1772	M19	N#CCOC(=O)c1c(C)nn(Cc2ccccc2)c1Cl
1643	K05	CCOC(=O)c1noc2ncnc(N3CCc4cc(OC)c(OC)cc4C3C)c12
1626	O10	CCc1ccc(cc1)c1oc(C)c(CSCC(=O)NCc2ccco2)n1
1778	I10	N#CCn1c(CSc2ccc3OCCOc3c2)nc2ccccc2c1=O
1598	I16	N#Cc1nc(Cc2ccccc2)oc1NCCc1ccccc1
1581	G07	NC(=O)N/N=C(/C=C\c1ccccc1)\C(C)(C)O
1577	E20	CC(=O)OC(C)(C)C(=O)/C=C\c1ccccc1
1696	L14	CCn1c(=O)c2ccccc2n(Cc2cccc(Cl)c2)c1=O
1640	B10	CCOC(=O)c1c(C)oc2ncnc(N(C)Cc3ccccc3)c12
1589	K14	C=CCNc1oc(nc1C#N)c1cccs1
1504	N14	c1ccc2nc(NC3CC3)c3nnnn3c2c1
1591	I14	Cc1ccc(o1)c1nn(cc1CN(Cc1ccccc1)C(=O)c1ccco1)c1ccccc1
1598	O16	CCOc1ccc(cc1)Nc1oc(Cc2ccccc2)nc1C#N
1490	B16	CCOc1ccc(cc1)c1oc(NCC(C)C)c(C#N)n1
1507	B17	CCCN(c1ccc(Cl)c(Cl)c1)C(=O)c1ccc2c(c1)nc1CCCCn1c2=O
1504	M14	CCc1n[nH]c(=O)c2cc3oc(C)cc3n12
1598	O11	CCC(C)Oc1c(Cl)cc(C#N)cc1OC
1582	F07	O/N=C\C(=N\O)/C12CC3CC(CC(C3)C2)C1
1630	B11	Cc1ccc(C)c(c1)N1CCN(CC1)C(=O)c1ccc2nc(sc2c1)N1CCOCC1
1642	G02	O=C(N1CCCC1)c1ccc(s1)N1CCCc2ccccc12
527	J07	C(CCN(S(c1ccc(CCC)cc1)(=O)=O)[H])CCC
1837	E05	S(=O)(=O)(c1ccc(cc1)C)c2cnc(c3c2Nc(cc4)ccc4OCC)ccc(OC)c3
1915	D02	n1c(CSCC(NCCc2ccccc2)=O)c(oc1c3ccc(cc3)OCC)C

1915 D02) are structurally related to BC8-23. In future studies, other hits from this collection can also be characterized.

6.6 EVALUATION OF STRUCTURALLY RELATED COMPOUNDS

The compounds that are structurally related to BC69, BC8-1, BC8-5, BC8-8, BC8-15 and BC8-23 were tested either in yeast growth assays or through *in vitro* enzyme assays. As described in Chapter 5, minor changes in the parent molecule can alter the selectivity or potency of the compounds. For example, the removal of the carboxylic acid moiety from the phenyl ring of BC8-15 decreases the efficacy of the compound for PDE8A while it can still inhibit PDE4A. The preliminary docking analysis of BC8-15 into PDE4A and PDE8A enzyme structures demonstrates the possible binding orientation of the compound. This shows that carboxylic acid group interacts with PDE8A through the unique tyrosine 748 residue while this interaction is not involved in its binding to PDE4A (Figure 6.1).

The preliminary data on the structurally related compounds can help to guide medicinal chemistry efforts to increase the potency and selectivity of the identified PDE8 inhibitors. Also, improvements in the pharmacokinetic properties such as solubility, bioavailability etc. can also be implemented via medicinal chemistry approaches. These steps would greatly enhance the utility of these compounds in both cell culture and whole animal studies.

6.7 EFFECTS OF IDENTIFIED COMPOUNDS IN MAMMALIAN ASSAYS

The selected compounds were tested in mammalian systems to evaluate their effect in steroid production. Compound BC8-15 increased the progesterone release from MA-10 cells in a dose dependent manner. Also, a correlation between progesterone response and PDE8 inhibitory activity was observed with BC8-15 derivatives. These promising results on the effect of BC8-15 on steroid production from MA-10 cells and primary Leydig cells suggest that these compounds can be further developed and could be used in physiological conditions and diseases related to testosterone deficiency or adrenal steroid production. For example, low testosterone levels are observed in hypogonadism and aging (Harman *et al*. 2001; Matsumoto. 2002). It is associated with andropause, idiopathic male infertility, metabolic syndrome and cardiovascular disease (Makhsida *et al*. 2005; Ochsenkuhn and de Kretser. 2003); (Traish *et al*. 2009). Also, low serum testosterone levels and abnormalities in adrenal function are common in HIV patients (Dube *et al*. 2007; Lo and Grinspoon. 2010). Thus, effective PDE8 inhibitors can be therapeutically used in aging, hypogonadism and andropause; they can also be used for reducing the loss of muscle and bone mass in AIDS patients.

Figure 6.1 Docking simulation of BC8-15 on PDE8A and PDE4A structures

The docking simulation of a BC8-15 for PDE8A and PDE4A enzymes was carried out using the AutoDock4 software through the AutoDockTools GUI.

Figure 6.1. Docking simulation of BC8-15 on PDE8A and PDE4A structures

PDE8A

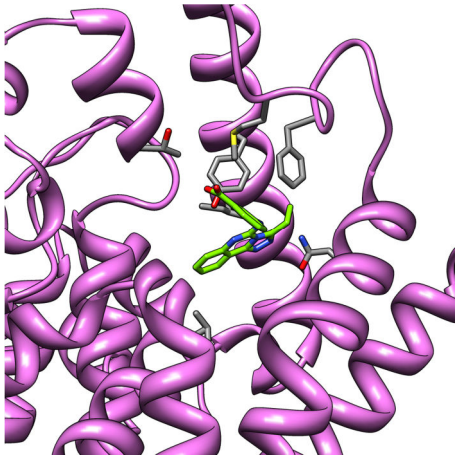

PDE4A

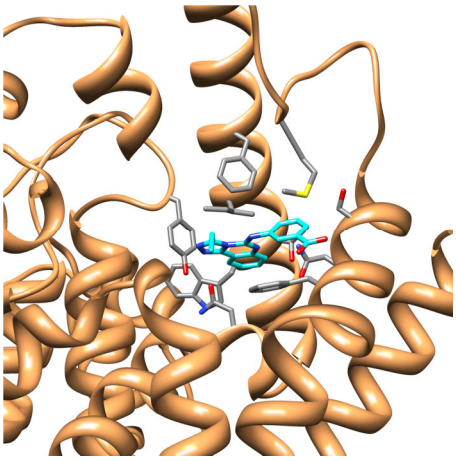

APPENDIX

PART I: DEVELOPMENT OF A CHEMICAL SCREEN FOR ACTIVATORS OF PDE8A

A1.1 INTRODUCTION

PDE8A is a high affinity, cAMP-specific phosphodiesterase which is mostly expressed in the testis, eye, liver, skeletal muscle, heart, kidney, ovary and brain (Soderling *et al*. 1998). PDE8 is unique among PDE families in containing a PAS (Per-Arnt-Sim) domain along with a putative REC domain (signal receiver domain) in its N terminus. PDE8A is important for the regulation of steroidogenesis in Leydig cells and in adrenal gland (Tsai *et al*. 2010; Vasta *et al*. 2006). A PDE8A activator would -in theory- decrease local production of testosterone in the Leydig cells and can be used as a male contraceptive drug. The possibility of reducing testosterone pharmacologically might also provide advantages for the treatment of prostate cancer (Vasta *et al*. 2006).

A1.2 BASIS OF SCREENING

A screen for an activator is based on the ability of yeast strains to grow in a medium lacking uracil when *fbp1-ura4* expression is derepressed in a cAMP dependent manner. The starting strain for an activator strain should have high enough cAMP levels to repress the *fbp1* promoter and thus should not be able to grow in the absence of uracil. In the

presence of an activator of the PDE in question, PDE8A in this case, cAMP levels would be lower than that of the starting strain and *fbp1-ura4* would be expressed and cells would be able to grow in a medium lacking uracil in the presence of an activator (Figure A1).

A1.3 DETERMINATION OF THE SUITABLE STRAIN FOR THE SCREENING

In order to select the right strain to be utilized in the activator screen, PDE8A strains containing different levels of defects in the cAMP producing pathway were grown in SC-Ura, EMM-Ura and 5FOA media. Figure A2 shows the growth pattern of those strains in EMM-Ura, SC-Ura and 5FOA with various initial cell densities. It was suggested by these data that CHP1149 strain, which has a wild type *git* pathway, is more suitable for screening since it showed very low optical density after 48h in EMM-Ura and SC-Ura. The data also suggest that SC-Ura is a more restrictive medium than EMM-Ura. Thus, EMM-Ura medium was selected to be used in screening experiments in that it might permit growth more readily in the presence of an activator.

As a control for the screening, a strain which has *S. pombe* phosphodiesterase instead of mammalian PDEs was planned to be used in order to monitor and eliminate potential hits that might arise by affecting a component of the cAMP pathway other than PDE.

Figure A1: Basis of activator screen

In PDE8A-expressing strains, cAMP levels are high and *fbp1-ura4* expression is repressed. The cells cannot grow in medium lacking uracil. In the presence of a PDE8A activator, cAMP levels will be lower to allow *fbp1-ura4* expression, which makes cells able to grow in a medium lacking uracil.

Figure A1: Basis of activator screen

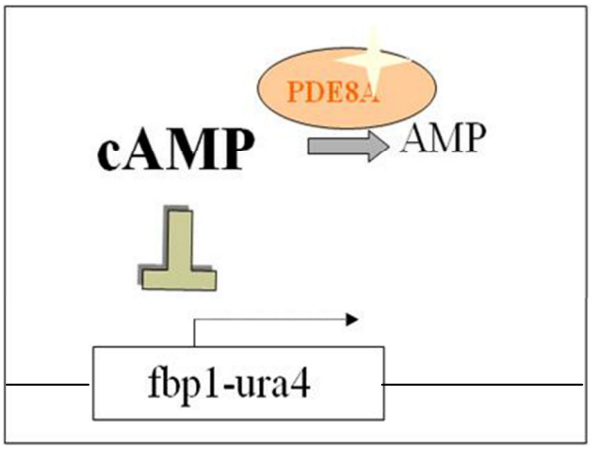

Cells are not able to grow in medium lacking uracil

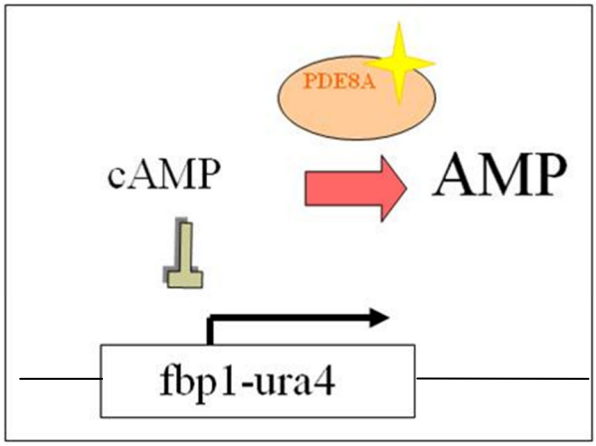

Cells can grow in medium lacking uracil

Figure A2: Growth of PDE8A-expressing candidate strains in different media

Optical density values of strains CHP1139, CHP1140, CHP1148 and CHP1149 in 5FOA, EMM-Ura and SC-Ura media after 48 h are shown.

Figure A2: Growth of PDE8A-expressing candidate strains in different media

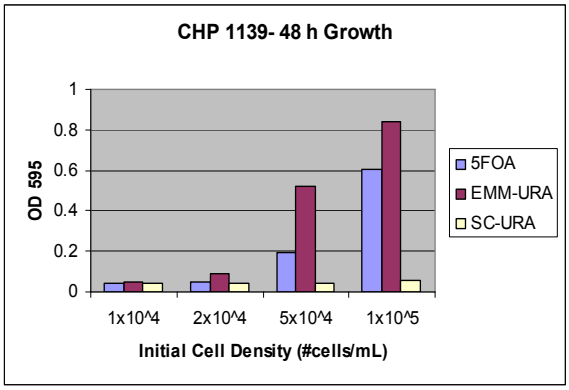

pap1Δ::ura4⁻ cgs2::PDE8A git3::kan

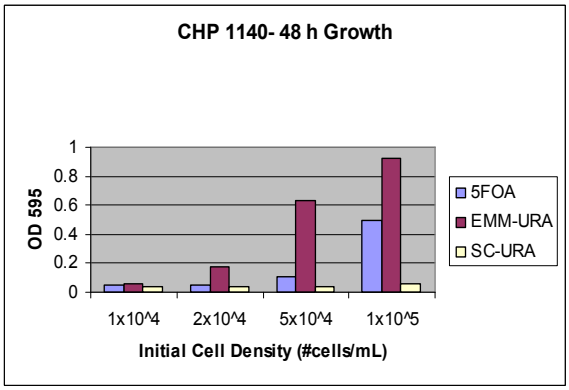

pap1Δ::ura4⁻ cgs2::PDE8A gpa2::his3⁺

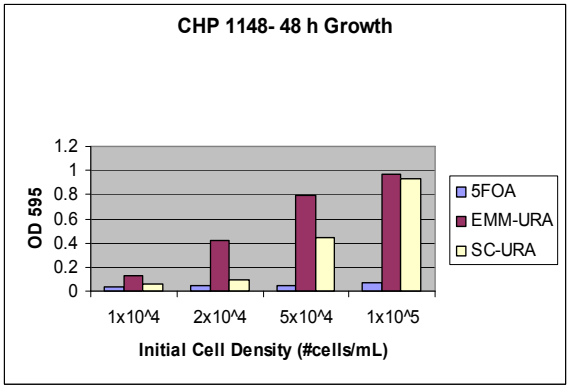

pap1Δ::ura4⁻ cgs2::PDE8A gpa2::his3⁺

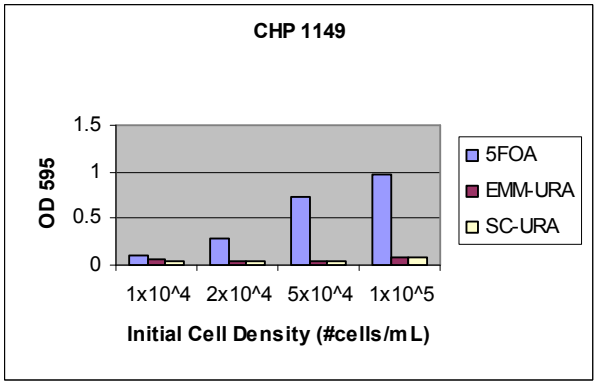

pap1Δ::ura4⁻ cgs2::PDE8A

For optimization purposes two strains, one with a wild type *git* pathway and one with a *git11* deletion were used. Both strains showed an inability to grow in the absence of uracil (Figure A3).

A1.4 EVALUATION OF SCREENING STRAINS WITH DMSO PINNING

Prior to DMSO pinning, CHP1149 (*pap1Δ cgs2::PDE8A*) and CHP1187 (*pap1Δ cgs2-s1*) were tested and their coefficient of variation were calculated (Table A1). Accordingly, CHP1149 at $5x10^4$ cells/mL initial cell density seems to be suitable for screening, however since there is no positive control for this experiment; it is not known if the culture will pass the threshold and reach a visible amount of growth after 48 h incubation. Thus, I tested $0.75x10^5$ and $1x10^5$ cells/mL initial cell densities for DMSO pinning experiments. The experiments were done in a 384 well plate as 2 sets from two independent cultures and performed on two separate days. The CV values for Day 1 and Day 2 was shown in Table A2. Although the obtained CV values are higher than 15 % threshold employed by the Broad Institute, CHP1149 (PDE8A) strain was approved by the high throughput assay supervisor due to the small OD values. However, CHP1187 (*cgs2* strain) did not pass the test due to its high mean value.

Figure A3: Growth of Cgs2-expressing candidate strains in different media

Optical density values of strains CHP1187 and CHP1188 in 5FOA, EMM-Ura and SC-Ura media after 48 h are shown.

Figure A3: Growth of Cgs2-expressing candidate strains in different media

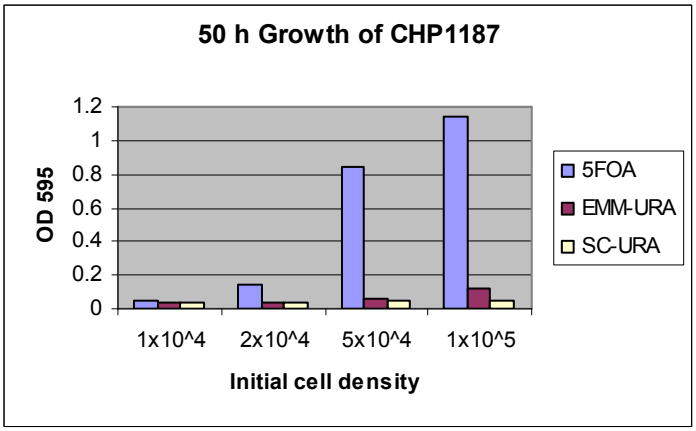

pap1Δ::ura4⁻ cgs2-s1

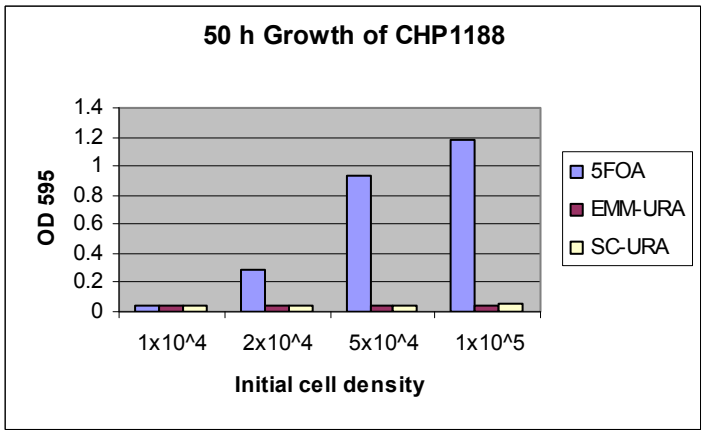

pap1Δ::ura4⁻ cgs2-s1 git11::kan

Table A1: Coefficient of variation values for CHP1149 and CHP1187

Strain	Cell density	Average	StDev	CV	CV (%)
CHP1149	$5x10^4$	0.041	0.007	0.16	16
CHP1149	$1x10^5$	0.051	0.014	0.28	28
CHP1149	$2x10^5$	0.073	0.015	0.21	21
CHP1187	$5x10^4$	0.060	0.012	0.20	20
CHP1187	$1x10^5$	0.134	0.012	0.09	9
CHP1187	$2x10^5$	0.438	0.040	0.09	9

Table A2: Coefficient of variation values of CHP1149 and CHP1187 after DMSO pinning

DMSO PINNING- DAY1

Strain	Experiment	Cell density	Mean	StDev	CV %
CHP1149	Set1	$0.75x10^5$	0.047	0.011	23
CHP1149	Set2	$0.75x10^5$	0.042	0.009	21
CHP1149	Set1	$1x10^5$	0.052	0.010	20
CHP1149	Set2	$1x10^5$	0.049	0.010	21
CHP1187	Set1	$0.75x10^5$	0.121	0.022	18
CHP1187	Set2	$0.75x10^5$	0.126	0.032	25
CHP1187	Set1	$1x10^5$	0.200	0.040	20
CHP1187	Set2	$1x10^5$	0.194	0.047	24

DMSO PINNING- DAY2

Strain	Experiment	Cell density	Mean	StDev	CV %
CHP1149	Set1	$0.75x10^5$	0.047	0.012	26
CHP1149	Set2	$0.75x10^5$	0.049	0.017	35
CHP1149	Set1	$1x10^5$	0.049	0.008	16
CHP1149	Set2	$1x10^5$	0.052	0.016	30
CHP1187	Set1	$0.75x10^5$	0.261	0.027	10
CHP1187	Set2	$0.75x10^5$	0.130	0.014	11
CHP1187	Set1	$1x10^5$	0.410	0.026	6
CHP1187	Set2	$1x10^5$	0.213	0.019	9

A1.5 SCREENING RESULTS

High throughput screening was performed at the Broad Institute using CHP1149 (*pap1Δ cgs2::PDE8A*) as the screening strain with $0.75x10^5$ cells/mL as the initial cell density in EMM-Ura medium in 384-well plates. The optical density at 600 nm was measured at the end of 48 h. 18 compound plates from the Bioactives library, 26 compound plates from the PKO4 library, 8 compound plates from Analyticon, 7 compound plates from Forma, 5 compound plates from natural extracts and 46 compound plates from commercial chemical libraries were screened. For each compound plate, the assay was performed in duplicate. After the readings were completed, the data were analyzed by the Data Analysis department of the Broad Institute and expressed as Z scores which express the divergence of the experimental result from the mean result as a number of standard deviations. In high throughput analyses, compounds with composite Z scores higher than 8.53 is generally considered as a 'hit'.

The Bioactive compound library was screened and among 5802 compounds, four had a composite Z score higher than 8.53. When the data were examined carefully, only two of these compounds had reproducible raw data in the duplicate plates (Figure A4). At the end of high throughput screening, a total 38,327 compounds were screened from 5 different compound libraries. Results are given in Figure A5.

Figure A4: Screen with known bioactives collection

The scatter plot of Z score of plate A is plotted against Z score of plate B. Two positive hits are indicated as Compound A and Compound B.

Figure A4: Screen with known bioactives collection

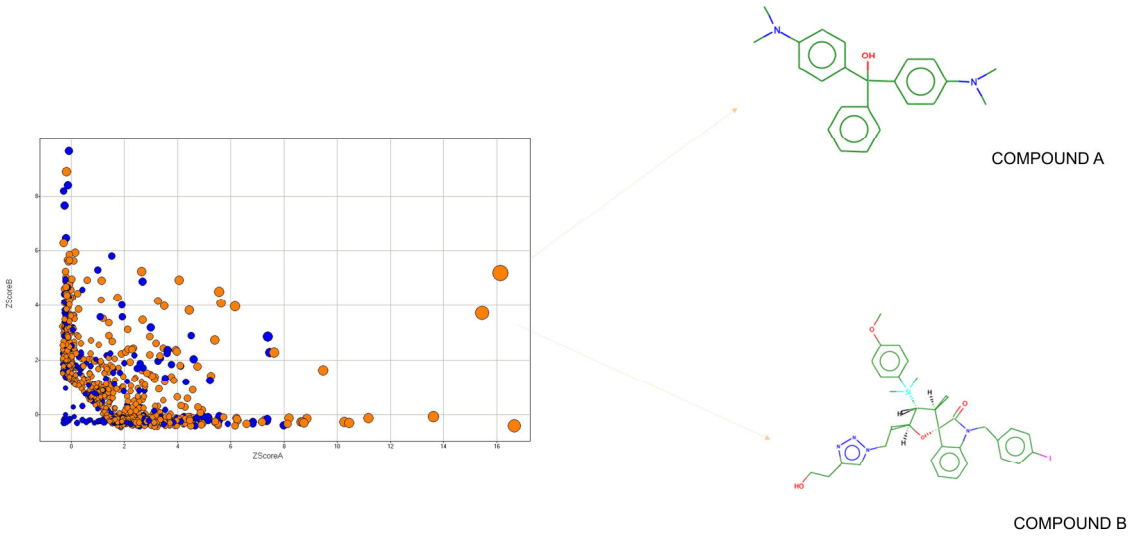

Plate	Well	RawValueA	ZScoreA	RawValueB	ZScoreB	CompositeZ	Reproducibility
2099	C20	0.446	16.14	0.203	5.19	15.1	0.890
XW-DalcDM1	I14	0.426	15.44	0.161	3.71	13.5	0.853
XW-DalcDM1	P20	0.456	16.66	0.04	-0.39	11.5	0.690
2105	B07	0.383	13.61	0.045	-0.06	9.6	0.704

Figure A5: Screening Results

Screening results are shown. (A) Scatter plot of Z score A against Z score B for 38,327 compounds is shown. (B) Compounds with composite Z score above 8.5 are shown. (C) Compounds with composite Z score aboce 8.5 and reproducibility above 0.9 are demonstrated, DMSO well is shown with arrow. (D) Top six compounds are shown. (E) The structure of BC18 is given.

Figure A5: Screening Results

A. 38,327 compounds

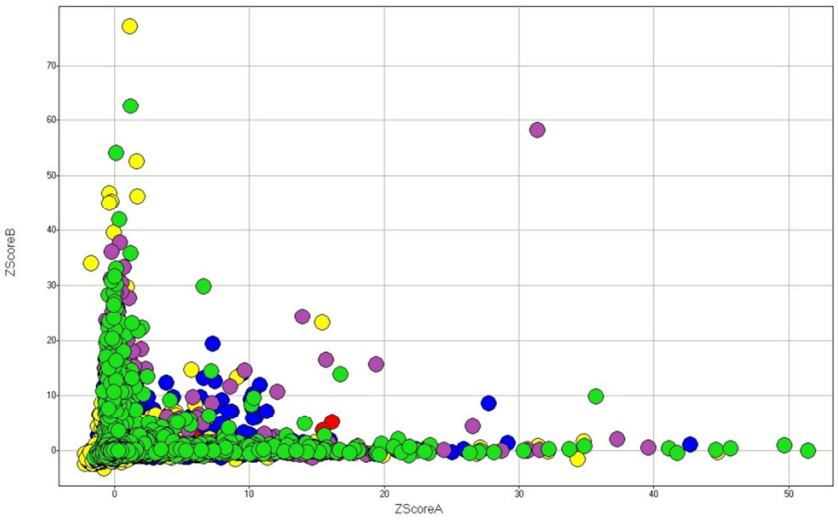

BioactivesPKO4

Forma+Analyticon

Natural comps +

Commercials -1

Commercials -2

B. Compounds with composite Z score above 8.5

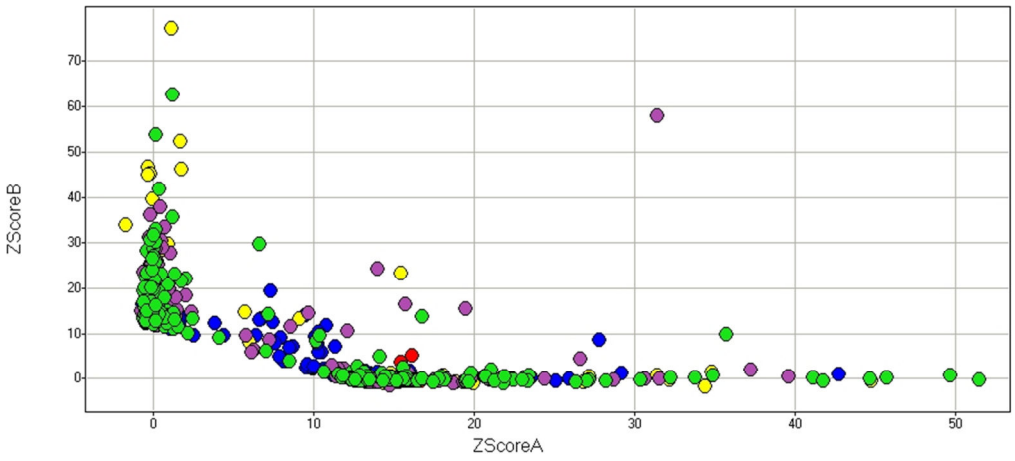

C. Compounds with compozite Z above 8.5 and reproducibility above 0.9 : 43 compounds, 1 DMSO

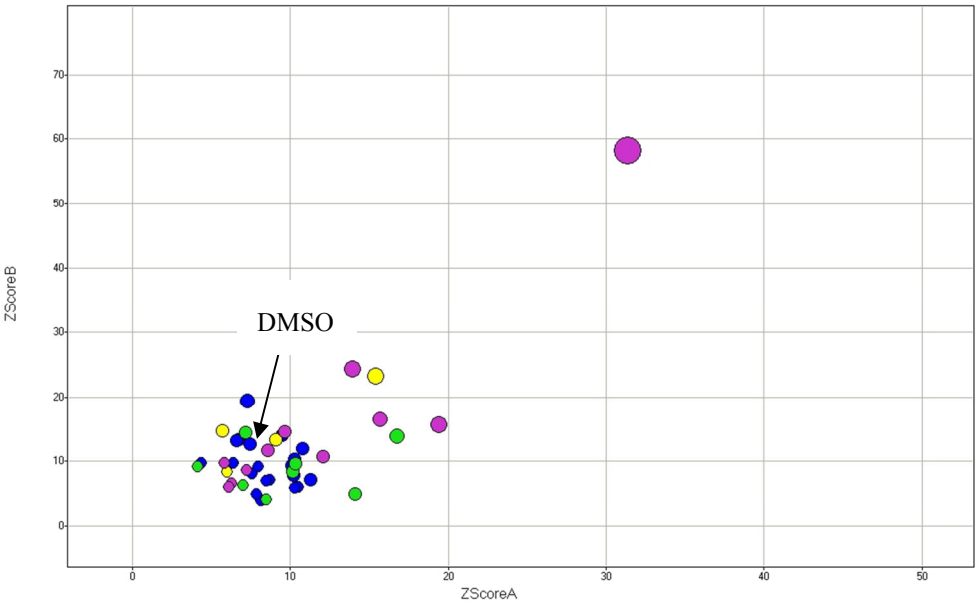

D.

Plate	Well	RawValueA	RawValueB	CompositeZ
2019	E17	0.349	0.57	63.3
2002	D08	0.142	0.161	27.4
2023	P18	0.184	0.262	27.1
2018	H11	0.231	0.189	24.8
2024	H06	0.197	0.193	22.8
2050	F06	0.134	0.116	21.7

E. 2019 E17 is Compound BC18

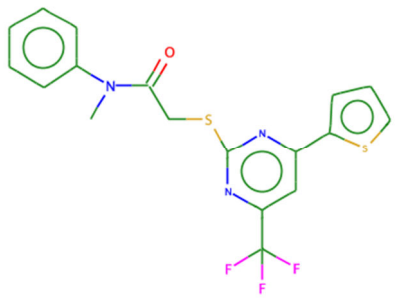

A1.6 EVALUATION OF THE SCREEN

The activator screen data contained many false positives revealed as data points with high Z score along only one axis when Z score A vs Z score B plot is examined. For an authentic hit, a plot of the Z score A vs the Z score B plot should give a data point located along the diagonal, which is a sign of reproducibility. One should also expect that plots of DMSO wells, which are the negative controls, should gather around the origin. This type of trend has not been observed in the current activator screen data.

When the data is filtered by composite Z score higher than 8.5 and reproducibility 0.9; 43 compounds were detected. Among them, 1 was found to be arising from a DMSO well which indicates that those hits might have arisen as chance events. The top 6 compounds are shown in Figure A5. The most promising compound (BC18) did not increase the activity of PDE8A enzyme in the follow-up experiments (data not shown); suggesting that all compounds identified might be false positives.

The general problem with the activator screen was that some data points were not reproducible in plate A and plate B. For example, for the same compound plate the OD_{600} was found to be 0.316 for plate A and 0.045 for plate B. This problem raises the possibility that plate A represents a false positive or plate B represents a false negative. If the problem is the presence of a false positive then it might have arisen due to mutations, contamination or cell delivery problems such as clumping. Some possible reasons for the presence of false negatives would be problems due to vortexing or clumping in the well, which might prevent the homogenous optical density reading of the well in question.

Since no such problem had been observed in a similar screen for PDE inhibitors where 5FOA medium was used instead of EMM-Ura, the possibility of presence of mutations was investigated. Cells were struck from potential false positive compound wells and their growth in solid medium lacking uracil was checked. It was found that cells arising from a potential false positive well were able to grow on medium lacking uracil while the starting screening strain CHP1149 could not (Figure A6). This suggests that the presence of the false positive data points is due to random mutations.

Figure A6: Growth of CHP1149 and false positive hits on EMM-Ura

Cells taken from the false positive wells (candidates #1-6) are struck on EMM-Ura medium. Their growth is compared to the growth phenotype of CHP1149.

Figure A6: Growth of CHP1149 and false positive hits on EMM-Ura

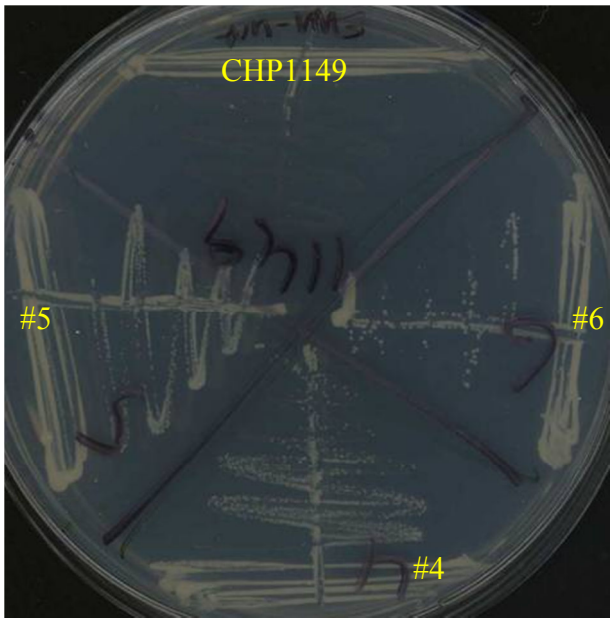

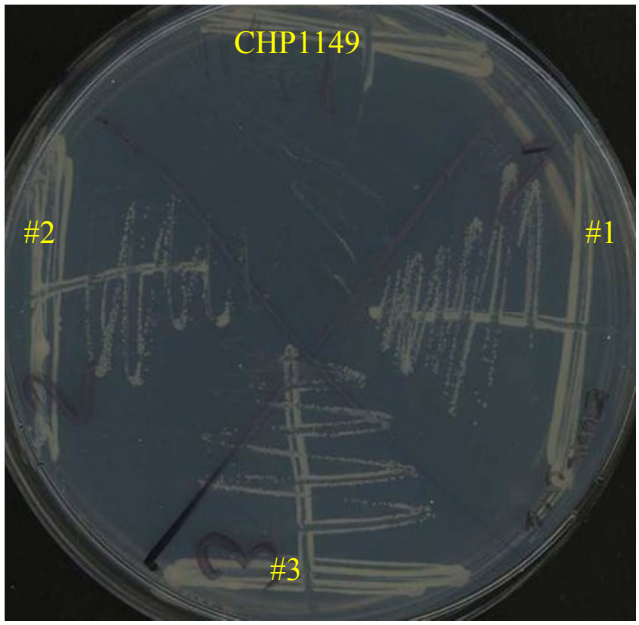

PART II: STRATEGIES TO UNCOVER PDE8 ACTIVATORS BY DATA MINING

PDE8 activators were sought by using the inhibitor screen data. As mentioned before, in the inhibitor screen cells are grown in 5FOA medium. The initial screening conditions do not allow cells to grow and the ability of the test compounds to promote the growth of PDE8A-expressing cells was evaluated to identify PDE8 inhibitors. The compounds that lower the optical density in 5FOA medium below the background levels are usually toxic compounds. We wanted to test the hypothesis that potential activators might also lower the optical density in 5FOA medium. Since there is no available PDE activator to be used as a positive control, the degree of change in the growth phenotype in the presence of PDE activators is unknown.

We did data mining in the inhibitor data set by comparing the PDE8A inhibitor screen data with data from PDE11A inhibitor screen (Ceyhan, O; unpublished data). Compounds that lower the optical density in both data sets were considered as toxic whereas the compounds that decrease the growth in PDE8A-expressing strain while still allowing growth of PDE11A-expressing strain were considered as potential PDE8 activators. Figure A9 shows the scatter plot of PDE8A vs PDE11A data. Nine of the selected compounds were tested by yeast growth assays and *in vitro* enzyme assays. Figure A8 shows the effect of these compounds in cyclic nucleotide titration curves.

Figure A7: Comparison of data from PDE8 and PDE11 screens

(A) Scatter plot of average absorbance values of PDE8A-expressing strain against PDE11A-expressing strain. **(B)** Compounds that have lower OD values for PDE8A-expressing strain, while did not decrease the OD values of PDE11A-expressing strain are filtered.

Figure A7: Comparison of data from PDE8 and PDE11 screens

A.

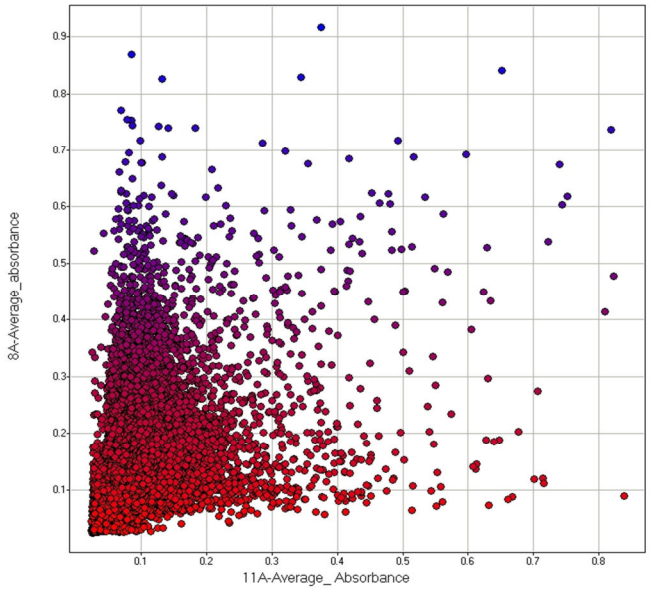

B.

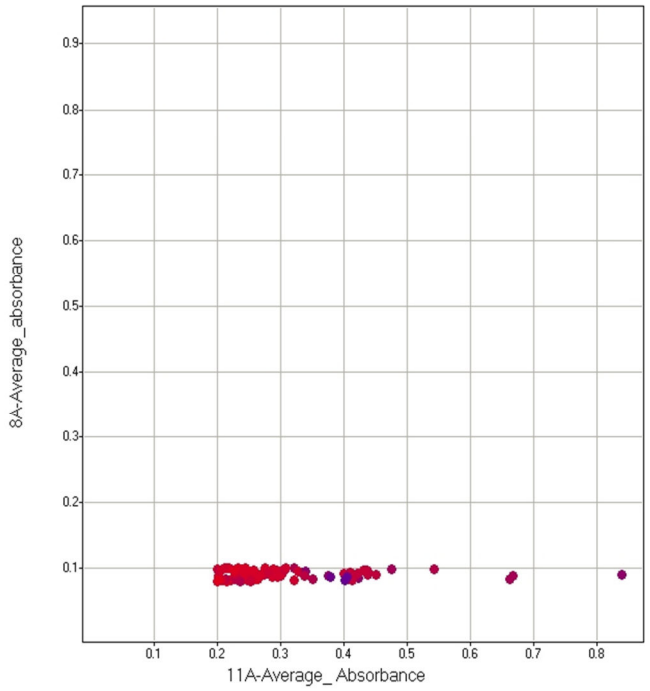

Table A3: Primary screen data of selected PDE8A activator candidates

PDE8A	Absorbance 1	Absorbance 2	Average Abs	Z score 1	Z score 2	Composite Z
BC8-A1	0.032	0.029	0.031	-6.18	-6.40	-8.89
BC8-A2	0.061	0.058	0.060	-4.08	-4.30	-5.92
BC8-A3	0.06	0.075	0.068	-4.15	-3.06	-5.10
BC8-A4	0.066	0.064	0.065	-3.72	-3.86	-5.36
BC8-A5	0.035	0.036	0.036	-5.96	-5.89	-8.38
BC8-A6	0.072	0.067	0.070	-3.28	-3.64	-4.90
BC8-A7	0.026	0.026	0.026	-6.30	-6.30	-8.91
BC8-A8	0.032	0.028	0.030	-5.43	-6.01	-8.09
BC8-A9	0.072	0.075	0.074	-5.79	-5.62	-8.07

PDE11A	Absorbance 1	Absorbance 2	Average Abs	Z score 1	Z score 2	Composite Z
BC8-A1	0.114	0.084	0.099	8.48	2.07	7.46
BC8-A2	0.095	0.126	0.111	4.42	11.05	10.94
BC8-A3	0.156	0.205	0.181	17.46	27.93	32.10
BC8-A4	0.101	0.102	0.102	5.70	5.92	8.22
BC8-A5	0.107	0.103	0.105	6.99	6.13	9.28
BC8-A6	0.33	0.325	0.328	54.64	53.58	76.52
BC8-A7	0.067	0.066	0.067	0.21	0.01	0.16
BC8-A8	0.086	0.09	0.088	4.03	4.83	6.27
BC8-A9	0.075	0.086	0.081	1.82	4.03	4.13

Since PDE8A is a cAMP specific enzyme, the presence of a PDE8 activator will decrease the internal cAMP levels and more cAMP will be required to promote growth in 5FOA medium, leading to a right-ward shift compared to the no compound conditions. On the other hand, a candidate PDE8 activator should not affect the cGMP levels and thus the cGMP titration curve. Figure A8 shows both cyclic nucleotide titration curves in the presence of candidate PDE8 activators. Compound BC8-A2 seems to shift the curve of strain CHP1204 to the right in the presence of cAMP while no shift is observed with cGMP. However, the data was not reproducible and no significant increase was observed in the activity of PDE8 enzyme in the *in vitro* enzyme assays.

CONCLUSION

Although, the data mining approach did not yield any activators of PDE8A, it clearly shows that the compounds that are not activators (i.e. decrease OD values in 5FOA medium possibly by exerting toxic effects) lower the OD values in both cAMP and cGMP containing 5FOA media. This suggests that the use of increased levels of cyclic nucleotides to promote a higher level of growth in 5FOA medium could be used in HTSs to detect PDE activators.

Figure A8: Growth curve of CHP1204 in the presence of candidate PDE8A activator compounds in 5FOA medium in response to varying cyclic nucleotide concentrations

The cyclic nucleotide titration growth curve of CHP1204 in the presence of candidate activator compounds is shown. The growth curve is expected to shift to the right compared to the no compound curve in the presence of an activator molecule. **(A)** cAMP titration **(B)** cGMP titration.

Figure A8: Growth curve of CHP1204 in the presence of candidate PDE8A activator compounds in 5FOA medium in response to varying cyclic nucleotide concentrations

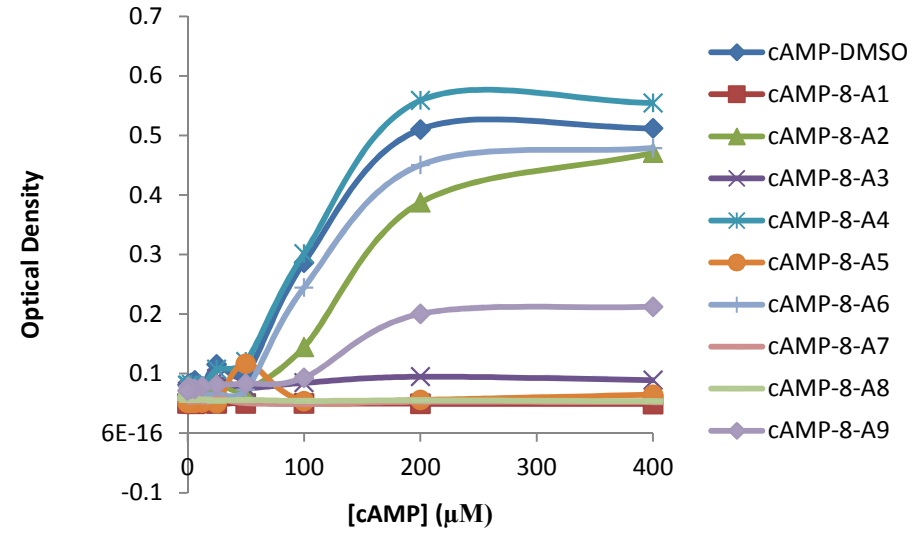

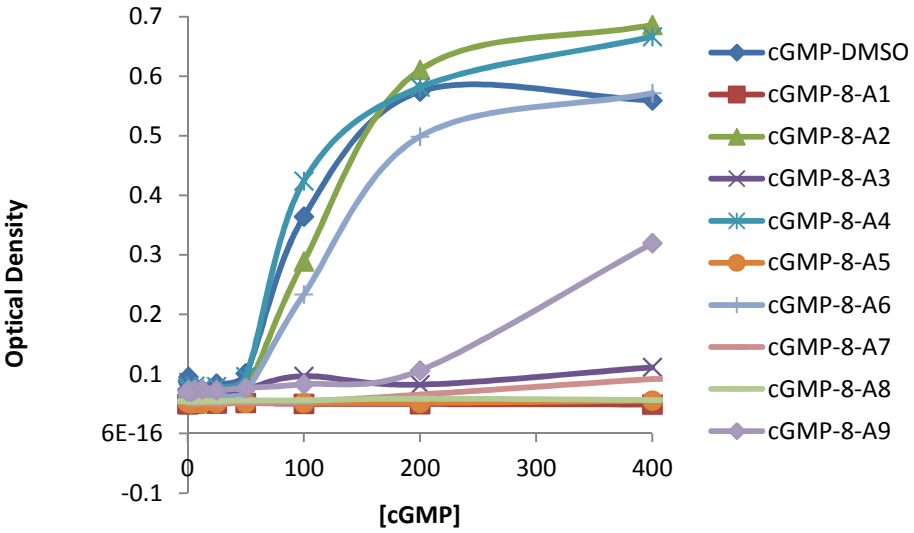

LITERATURE CITED

Adamo, C. M., D. F. Dai, J. M. Percival, E. Minami, M. S. Willis *et al*, 2010 Sildenafil reverses cardiac dysfunction in the mdx mouse model of Duchenne muscular dystrophy. Proc. Natl. Acad. Sci. U. S. A. **107:** 19079-19083.

Alaamery, M. A., and C. S. Hoffman, 2008 *Schizosaccharomyces pombe* Hsp90/Git10 is required for glucose/cAMP signaling. Genetics **178:** 1927-36.

Alaamery, M. A., A. R. Wyman, F. D. Ivey, C. Allain, D. Demirbas *et al*, 2010 New classes of PDE7 inhibitors identified by a fission yeast-based HTS. Journal of Biomolecular Screening **15:** 359-367.

Arnaud-Lopez, L., G. Usala, G. Ceresini, B. D. Mitchell, M. G. Pilia *et al*, 2008 Phosphodiesterase 8B gene variants are associated with serum TSH levels and thyroid function. Am. J. Hum. Genet. **82:** 1270-1280.

Beavo, J. A., and L. L. Brunton, 2002 Cyclic nucleotide research - still expanding after half a century. Nature Reviews Molecular Cell Biology **3:** 710-718.

Beavo, J. A., and D. H. Reifsnyder, 1990 Primary sequence of cyclic-nucleotide phosphodiesterase isozymes and the design of selective inhibitors. Trends Pharmacol. Sci. **11:** 150-155.

Bender, A. T., and J. A. Beavo, 2006 Cyclic nucleotide phosphodiesterases: Molecular regulation to clinical use. Pharmacol Rev **58:** 488-520.

Berthet, J., E. W. Sutherland and T. W. Rall, 1957 The assay of glucagon and epinephrine with use of liver homogenates. J. Biol. Chem. **229:** 351-361.

Bischoff, J. R., D. Casso and D. Beach, 1992 Human p53 inhibits growth in *Schizosaccharomyces pombe*. Mol Cell Biol **12:** 1405-11.

Bloom, T. J., and J. A. Beavo, 1996 Identification and tissue-specific expression of PDE7 phosphodiesterase splice variants. Proc Natl Acad Sci U S A **93:** 14188-92.

Boswell-Smith, V., D. Spina and C. P. Page, 2006 Phosphodiesterase inhibitors. Br. J. Pharmacol. **147:** S252-S257.

Butcher, R. W., and E. W. Sutherland, 1962 Adenosine 3',5'-phosphate in biological materials .1. purification and properties of cyclic 3',5'-nucleotide phosphodiesterase and use sf this enzyme to characterize adenosine 3',5'-phosphate in human urine. J. Biol. Chem. **237:** 1244-&.

Calverley, P. M. A., K. F. Rabe, U. M. Goehring, S. Kristiansen, L. M. Fabbri *et al*, 2009 Roflumilast in symptomatic chronic obstructive pulmonary disease: Two randomised clinical trials. Lancet **374:** 685-694.

Card, G. L., L. Blasdel, B. P. England, C. Zhang, Y. Suzuki *et al*, 2005 A family of phosphodiesterase inhibitors discovered by cocrystallography and scaffold-based drug design. Nat Biotechnol **23:** 201-7.

Carr, R. A. E., M. Congreve, C. W. Murray and D. C. Rees, 2005 Fragment-based lead discovery: Leads by design. Drug Discov. Today **10:** 987-992.

Colicelli, J., C. Nicolette, C. Birchmeier, L. Rodgers, M. Riggs *et al*, 1991 Expression of three mammalian cDNAs that interfere with RAS function in *Saccharomyces cerevisiae*. Proc Natl Acad Sci U S A **88:** 2913-7.

Colicelli, J., C. Birchmeier, T. Michaeli, K. O'Neill, M. Riggs *et al*, 1989 Isolation and characterization of a mammalian gene encoding a high-affinity cAMP phosphodiesterase. Proc Natl Acad Sci U S A **86:** 3599-603.

Conti, M., and J. Beavo, 2007 Biochemistry and physiology of cyclic nucleotide phosphodiesterases: Essential components in cyclic nucleotide signaling. Annu Rev Biochem **76:** 481-511.

Coudray, C., C. Charon, N. Komas, G. Mory, F. Diot-Dupuy *et al*, 1999 Evidence for the presence of several phosphodiesterase isoforms in brown adipose tissue of zucker rats: Modulation of PDE2 by the fa gene expression. FEBS Lett. **456:** 207-210.

Daniel, P. B., W. H. Walker and J. F. Habener, 1998 Cyclic AMP signaling and gene regulation. Annu. Rev. Nutr. **18:** 353-383.

Demirbas, D., O. Ceyhan, A. R. Wyman, F. D. Ivey, C. Allain *et al*, 2011 Use of a *Schizosaccharomyces pombe* PKA-repressible reporter to study cGMP metabolising phosphodiesterases. Cell Signal. **23**:594-601.

Dong, H., V. Osmanova, P. M. Epstein and S. Brocke, 2006 Phosphodiesterase 8 (PDE8) regulates chemotaxis of activated lymphocytes. Biochem Biophys Res Commun **345:** 713-9.

Dov, A., E. Abramovitch, N. Warwar and R. Nesher, 2008 Diminished phosphodiesterase-8B potentiates biphasic insulin response to glucose. Endocrinology **149:** 741-748.

D'Souza, C. A., and J. Heitman, 2001 Conserved cAMP signaling cascades regulate fungal development and virulence. FEMS Microbiol Rev **25:** 349-64.

D'Souza, C. A., J. A. Alspaugh, C. Yue, T. Harashima, G. M. Cox *et al*, 2001 Cyclic AMP-dependent protein kinase controls virulence of the fungal pathogen cryptococcus neoformans. Mol Cell Biol **21:** 3179-91.

Dube, M. P., R. A. Parker, K. Mulligan, P. Tebas, G. K. Robbins *et al*, 2007 Effects of potent antiretroviral therapy on free testosterone levels and fat-free mass in men in a prospective, randomized trial: A5005s, a substudy of AIDS clinical trials group study 384. Clinical Infectious Diseases **45:** 120-126.

Fabbri, L. M., B. Beghe, U. Yasothan and P. Kirkpatrick, 2010 Roflumilast. Nature Reviews Drug Discovery **9:** 761-762.

Fawcett, L., R. Baxendale, P. Stacey, C. McGrouther, I. Harrow *et al*, 2000 Molecular cloning and characterization of a distinct human phosphodiesterase gene family: PDE11A. Proc. Natl. Acad. Sci. U. S. A. **97:** 3702-3707.

Fisher, D. A., J. F. Smith, J. S. Pillar, S. H. St Denis and J. B. Cheng, 1998a Isolation and characterization of PDE8A, a novel human cAMP-specific phosphodiesterase. Biochem. Biophys. Res. Commun. **246:** 570-577.

Fisher, D. A., J. F. Smith, J. S. Pillar, S. H. St Denis and J. B. Cheng, 1998b Isolation and characterization of PDE9A, a novel human cGMP-specific phosphodiesterase. J. Biol. Chem. **273:** 15559-15564.

Francis, S. H., K. R. Sekhar, H. Ke and J. D. Corbin, 2011 Inhibition of cyclic nucleotide phosphodiesterases by methylxanthines and related compounds. Handb. Exp. Pharmacol. 93-133.

Friedmann, Y., A. Shriki, E. R. Bennett, S. Golos, R. Diskin *et al*, 2006 JX401, A p38 alpha inhibitor containing a 4-benzylpiperidine motif, identified via a novel screening system in yeast. Mol. Pharmacol. **70:** 1395-1405.

Gamanuma, M., K. Yuasa, T. Sasaki, N. Sakurai, J. Kotera *et al*, 2003 Comparison of enzymatic characterization and gene organization of cyclic nucleotide phosphodiesterase 8 family in humans. Cell. Signal. **15:** 565-574.

George, M., and M. Jeffrey, 2006 Medicinal chemistry of PDE4 inhibitors in *Cyclic Nucleotide Phosphodiesterases in Health and Disease*. CRC Press.

Giordano, D., M. E. De Stefano, G. Citro, A. Modica and M. Giorgi, 2001 Expression of cGMP-binding cGMP-specific phosphodiesterase (PDE5) in mouse tissues and cell lines using an antibody against the enzyme amino-terminal domain. Biochim. Biophys. Acta-Mol. Cell Res. **1539:** 16-27.

Glavas, N. A., C. Ostenson, J. B. Schaefer, V. Vasta and J. A. Beavo, 2001 T cell activation up-regulates cyclic nucleotide phosphodiesterases 8A1 and 7A3. Proc. Natl. Acad. Sci. U. S. A. **98:** 6319-6324.

Gloerich, M., and J. L. Bos, 2010 Epac: Defining a new mechanism for cAMP action. Annu. Rev. Pharmacol. Toxicol. **50:** 355-375.

Grandoch, M., S. S. Roscioni and M. Schmidt, 2010 The role of Epac proteins, novel cAMP mediators, in the regulation of immune, lung and neuronal function. Br. J. Pharmacol. **159:** 265-284.

Grozinger, C. M., E. D. Chao, H. E. Blackwell, D. Moazed and S. L. Schreiber, 2001 Identification of a class of small molecule inhibitors of the sirtuin family of NAD-dependent deacetylases by phenotypic screening. J. Biol. Chem. **276:** 38837-38843.

Gutz, H., H. Heslot, U. Leupold and N. Loprieno, 1974 *Schizosaccharomyces pombe*, pp. 395-446 in *Handbook of Genetics*, edited by R. C. King. Plenum Press, New York, NY.

Haider, S. G., 2007 Leydig cell steroidogenesis: Unmasking the functional importance of mitochondria. Endocrinology **148:** 2581-2582.

Harman, S. M., E. J. Metter, J. D. Tobin, J. Pearson and M. R. Blackman, 2001 Longitudinal effects of aging on serum total and free testosterone levels in healthy men. Journal of Clinical Endocrinology & Metabolism **86:** 724-731.

Harndahl, L., N. Wierup, S. Enerback, H. Mulder, V. C. Manganiello *et al*, 2004 Beta-cell-targeted overexpression of phosphodiesterase 3B in mice causes impaired insulin secretion, glucose intolerance, and deranged islet morphology. J. Biol. Chem. **279:** 15214-15222.

Hauet, T., J. Liu, H. Li, M. Gazouli, M. Culty *et al*, 2002 PBR, StAR, and PKA: Partners in cholesterol transport in steroidogenic cells. Endocr. Res. **28:** 395-401.

Hayashi, M., Y. Shimada, Y. Nishimura, T. Hama and T. Tanaka, 2002 Genomic organization, chromosomal localization, and alternative splicing of the human phosphodiesterase 8B gene. Biochem. Biophys. Res. Commun. **297:** 1253-1258.

Hayashi, M., K. Matsushima, H. Ohashi, H. Tsunoda, S. Murase *et al*, 1998a Molecular cloning and characterization of human PDE8B, a novel thyroid-specific isozyme of 3',5'-cyclic nucleotide phosphodiesterase. Biochem. Biophys. Res. Commun. **250:** 751-756.

Hayashi, M., K. Matsushima, H. Ohashi, H. Tsunoda, S. Murase *et al*, 1998b Molecular cloning and characterization of human PDE8B, a novel thyroid-specific isozyme of 3',5'-cyclic nucleotide phosphodiesterase. Biochem Biophys Res Commun **250:** 751-6.

Hebb, A. L. O., H. A. Robertson and E. M. Denovan-Wright, 2004 Striatal phosphodiesterase mRNA and protein levels are reduced in huntington's disease transgenic mice prior to the onset of motor symptoms. Neuroscience **123:** 967-981.

Hoffman, C. S., 2005a Glucose sensing via the protein kinase A pathway in *Schizosaccharomyces pombe*. Biochem Soc Trans **33:** 257-60.

Hoffman, C. S., 2005b Except in every detail: Comparing and contrasting G protein signaling in *Saccharomyces cerevisiae* and *Schizosaccharomyces pombe*. Eukaryotic Cell **4:** 495-503.

Hoffman, C. S., and F. Winston, 1991 Glucose repression of transcription of the *Schizosaccharomyces pombe fbp1* gene occurs by a cAMP signaling pathway. Genes Dev **5:** 561-71.

Hoffman, C. S., and F. Winston, 1990 Isolation and characterization of mutants constitutive for expression of the *fbp1* gene of *Schizosaccharomyces pombe*. Genetics **124:** 807-16.

Hoffman, C. S., and F. Winston, 1987 A ten-minute DNA preparation from yeast efficiently releases autonomous plasmids for transformation of *Escherichia coli*. Gene **57:** 267-72.

Horvath, A., and C. A. Stratakis, 2008 Unraveling the molecular basis of micronodular adrenal hyperplasia. Curr. Opin. Endocrinol. Diabetes Obes. **15:** 227-233.

Horvath, A., V. Mericq and C. A. Stratakis, 2008a Mutation in PDE8B, a cyclic AMP-specific phosphodiesterase in adrenal hyperplasia. N. Engl. J. Med. **358:** 750-752.

Horvath, A., C. Giatzakis, K. Tsang, E. Greene, P. Osorio *et al*, 2008b A cAMP-specific phosphodiesterase (PDE8B) that is mutated in adrenal hyperplasia is expressed widely in human and mouse tissues: A novel PDE8B isoform in human adrenal cortex. Eur. J. Hum. Genet. **16:** 1245-1253.

Houslay, M. D., and D. R. Adams, 2003 PDE4 cAMP phosphodiesterases: Modular enzymes that orchestrate signalling cross-talk, desensitization and compartmentalization. Biochem. J. **370:** 1-18.

Houslay, M. D., and G. Milligan, 1997 Tailoring cAMP-signalling responses through isoform multiplicity. Trends Biochem. Sci. **22:** 217-224.

Ivey, F. D., L. Wang, D. Demirbas, C. Allain and C. S. Hoffman, 2008 Development of a fission yeast-based high-throughput screen to identify chemical regulators of cAMP phosphodiesterases. J. Biomol. Screen. **13:** 62-71.

Jin, M., M. Fujita, B. M. Culley, E. Apolinario, M. Yamamoto *et al*, 1995 *sck1*, a high copy number suppressor of defects in the cAMP-dependent protein kinase pathway in fission yeast, encodes a protein homologous to the *Saccharomyces cerevisiae* SCH9 kinase. Genetics **140:** 457-67.

Jin, S. L. C., and M. Conti, 2002 Induction of the cyclic nucleotide phosphodiesterase PDE4B is essential for LPS-activated TNF-alpha responses. Proc. Natl. Acad. Sci. U. S. A. **99:** 7628-7633.

Jin, S. L. C., F. J. Richard, W. P. Kuo, A. J. D'Ercole and M. Conti, 1999 Impaired growth and fertility of cAMP-specific phosphodiesterase PDE4D-deficient mice. Proc. Natl. Acad. Sci. U. S. A. **96:** 11998-12003.

Kakkar, R., R. V. S. Raju and R. K. Sharma, 1999 Calmodulin-dependent cyclic nucleotide phosphodiesterase (PDE1). Cell Mol. Life Sci. **55:** 1164-1186.

Kao, R. S., E. Morreale, L. Wang, F. D. Ivey and C. S. Hoffman, 2006 *Schizosaccharomyces pombe* Git1 is a C2-domain protein required for glucose activation of adenylate cyclase. Genetics **173:** 49-61.

Kaupp, U. B., and R. Seifert, 2002 Cyclic nucleotide-gated ion channels. Physiol. Rev. **82:** 769-824.

Kobayashi, T., M. Gamanuma, T. Sasaki, Y. Yamashita, K. Yuasa *et al*, 2003 Molecular comparison of rat cyclic nucleotide phosphodiesterase 8 family: Unique expression of PDE8B in rat brain. Gene **319:** 21-31.

Kozikowski, B. A., T. M. Burt, D. A. Tirey, L. E. Williams, B. R. Kuzmak *et al*, 2003 The effect of freeze/thaw cycles on the stability of compounds in DMSO. Journal of Biomolecular Screening **8:** 210-215.

Landry, S., and C. S. Hoffman, 2001 The git5 Gβ and git11 Gγ form an atypical Gβγ dimer acting in the fission yeast glucose/cAMP pathway. Genetics **157:** 1159-68.

Landry, S., M. T. Pettit, E. Apolinario and C. S. Hoffman, 2000 The fission yeast *git5* gene encodes a Gβ subunit required for glucose-triggered adenylate cyclase activation. Genetics **154:** 1463-1471.

Lee, M. G., and P. Nurse, 1987 Complementation used to clone a human homologue of the fission yeast cell cycle control gene *cdc2*. Nature **327:** 31-5.

Lengeler, K. B., R. C. Davidson, C. D'Souza, T. Harashima, W. C. Shen *et al*, 2000 Signal transduction cascades regulating fungal development and virulence. Microbiol Mol Biol Rev **64:** 746-85.

Lerner, A., and P. M. Epstein, 2006 Cyclic nucleotide phosphodiesterases as targets for treatment of haematological malignancies. Biochem J **393:** 21-41.

Lo, J., and S. K. Grinspoon, 2010 Adrenal function in HIV infection Curr. Opin. Endocrinol. Diabetes Obes. **17:** 205-209.

Logue, J. S., and J. D. Scott, 2010 Organizing signal transduction through A-kinase anchoring proteins (AKAPs). Febs Journal **277:** 4370-4375.

Loughney, K., T. J. Martins, E. A. S. Harris, K. Sadhu, J. B. Hicks *et al*, 1996 Isolation and characterization of cDNAs corresponding to two human calcium, calmodulin-regulated, 3',5'-cyclic nucleotide phosphodiesterases. J. Biol. Chem. **271:** 796-806.

Lugnier, C., 2006 Cyclic nucleotide phosphodiesterase (PDE) superfamily: A new target for the development of specific therapeutic agents. Pharmacol Ther **109:** 366-98.

Ma, P., S. Wera, P. Van Dijck and J. M. Thevelein, 1999 The PDE1-encoded low-affinity phosphodiesterase in the yeast *Saccharomyces cerevisiae* has a specific function in controlling agonist-induced cAMP signaling. Mol Biol Cell **10:** 91-104.

Makhsida, N., J. Shah, G. Yan, H. Fisch and R. Shabsigh, 2005 Hypogonadism and metabolic syndrome: Implications for testosterone therapy. J. Urol. **174:** 827-834.

Manallack, D. T., R. A. Hughes and P. E. Thompson, 2005 The next generation of phosphodiesterase inhibitors: Structural clues to ligand and substrate selectivity of phosphodiesterases. J. Med. Chem. **48:** 3449-3462.

Martinez, S. E., A. Y. Wu, N. A. Glavas, X. B. Tang, S. Turley *et al*, 2002 The two GAF domains in phosphodiesterase 2A have distinct roles in dimerization and in cGMP binding. Proc. Natl. Acad. Sci. U. S. A. **99:** 13260-13265.

Martins, T. J., M. C. Mumby and J. A. Beavo, 1982 Purification and characterization of a cyclic GMP-stimulated cyclic-nucleotide phosphodiesterase from bovine-tissues. J. Biol. Chem. **257:** 1973-1979.

Masciarelli, S., K. Horner, C. Y. Liu, S. H. Park, M. Hinckley *et al*, 2004 Cyclic nucleotide phosphodiesterase 3A-deficient mice as a model of female infertility. J. Clin. Invest. **114:** 196-205.

Matsumoto, A. M., 2002 Andropause: Clinical implications of the decline in serum testosterone levels with aging in men. Journals of Gerontology Series A-Biological Sciences and Medical Sciences **57:** M76-M99.

McHale, M. M., L. B. Cieslinski, W. K. Eng, R. K. Johnson, T. J. Torphy *et al*, 1991 Expression of human recombinant cAMP phosphodiesterase isozyme IV reverses growth arrest phenotypes in phosphodiesterase-deficient yeast. Mol Pharmacol **39:** 109-13.

Michaeli, T., T. J. Bloom, T. Martins, K. Loughney, K. Ferguson *et al*, 1993 Isolation and characterization of a previously undetected human cAMP phosphodiesterase by complementation of cAMP phosphodiesterase-deficient *Saccharomyces cerevisiae*. J Biol Chem **268:** 12925-32.

Miro, X., J. M. Casacuberta, M. D. Gutierrez-Lopez, M. O. de Landazuri and P. Puigdomenech, 2000 Phosphodiesterases 4D and 7A splice variants in the response of HUVEC cells to TNF-alpha. Biochem. Biophys. Res. Commun. **274:** 415-421.

Mori, F., S. Perez-Torres, R. De Caro, A. Porzionato, V. Macchi *et al*, 2010 The human area postrema and other nuclei related to the emetic reflex express cAMP phosphodiesterases 4B and 4D. J. Chem. Neuroanat. **40:** 36-42.

Naganuma, K., A. Omura, N. Maekawara, M. Saitoh, N. Ohkawa *et al*, 2009 Discovery of selective PDE4B inhibitors. Bioorg. Med. Chem. Lett. **19:** 3174-3176.

Nikawa, J., P. Sass and M. Wigler, 1987a Cloning and characterization of the low-affinity cyclic AMP phosphodiesterase gene of *Saccharomyces cerevisiae*. Mol Cell Biol **7:** 3629-36.

Nikawa, J., S. Cameron, T. Toda, K. M. Ferguson and M. Wigler, 1987b Rigorous feedback control of cAMP levels in *Saccharomyces cerevisiae*. Genes Dev **1:** 931-7.

Nocero, M., T. Isshiki, M. Yamamoto and C. S. Hoffman, 1994 Glucose repression of *fbp1* transcription of *Schizosaccharomyces pombe* is partially regulated by adenylate cyclase activation by a G protein α subunit encoded by *gpa2* (*git8*). Genetics **138:** 39-45.

Ochsenkuhn, R., and D. M. de Kretser, 2003 The contributions of deficient androgen action in spermatogenic disorders. Int. J. Androl. **26:** 195-201.

Patrucco, E., M. S. Albergine, L. F. Santana and J. A. Beavo, 2010 Phosphodiesterase 8A (PDE8A) regulates excitation-contraction coupling in ventricular myocytes. J. Mol. Cell. Cardiol. **49:** 330-333.

Pauvert, O., D. Salvail, E. Rousseau, C. Lugnier, R. Marthan *et al*, 2002 Characterisation of cyclic nucleotide phosphodiesterase isoforms in the media layer of the main pulmonary artery. Biochem. Pharmacol. **63:** 1763-1772.

Perez-Torres, S., R. Cortes, M. Tolnay, A. Probst, J. M. Palacios *et al*, 2003 Alterations on phosphodiesterase type 7 and 8 isozyme mRNA expression in Alzheimer's disease brains examined by in situ hybridization. Exp. Neurol. **182:** 322-334.

Pillai, R., S. F. Staub and J. Colicelli, 1994 Mutational mapping of kinetic and pharmacological properties of a human cardiac cAMP phosphodiesterase. J Biol Chem **269:** 30676-81.

Pillai, R., K. Kytle, A. Reyes and J. Colicelli, 1993 Use of a yeast expression system for the isolation and analysis of drug-resistant mutants of a mammalian phosphodiesterase. Proc Natl Acad Sci U S A **90:** 11970-4.

Podzuweit, T., P. Nennstiel and A. Muller, 1995 Isozyme-selective inhibition of cgmp-stimulated cyclic-nucleotide phosphodiesterases by erythro-9-(2-hydroxy-3-nonyl) adenine. Cell. Signal. **7:** 733-738.

Rall, T. W., and E. W. Sutherland, 1958 Formation of a cyclic adenine ribonucleotide by tissue particles. J Biol Chem **232:** 1065-76.

Rentero, C., A. Monfort and P. Puigdomenech, 2003 Identification and distribution of different mRNA variants produced by differential splicing in the human phosphodiesterase 9A gene. Biochem. Biophys. Res. Commun. **301:** 686-692.

Robichaud, A., P. B. Stamatiou, S. L. Jin, N. Lachance, D. MacDonald *et al*, 2002 Deletion of phosphodiesterase 4D in mice shortens alpha(2)-adrenoceptor-mediated anesthesia, a behavioral correlate of emesis. J Clin Invest **110:** 1045-52.

Sass, P., J. Field, J. Nikawa, T. Toda and M. Wigler, 1986 Cloning and characterization of the high-affinity cAMP phosphodiesterase of *Saccharomyces cerevisiae*. Proc Natl Acad Sci U S A **83:** 9303-7.

Schadick, K., H. M. Fourcade, P. Boumenot, J. J. Seitz, J. L. Morrell *et al*, 2002 Schizosaccharomyces pombe Git7p, a member of the *Saccharomyces cerevisiae* Sgtlp family, is required for glucose and cyclic AMP signaling, cell wall integrity, and septation. Eukaryot Cell **1:** 558-67.

Schneider, H. H., R. Schmiechen, M. Brezinski and J. Seidler, 1986 Stereospecific binding of the antidepressant rolipram to brain protein structures. Eur J Pharmacol **127:** 105-15.

Schoeffter, P., C. Lugnier, F. Demesywaeldele and J. C. Stoclet, 1987 Role of cyclic AMP-phosphodiesterases and cyclic GMP-phosphodiesterases in the control of cyclic-nucleotide levels and smooth-muscle tone in rat isolated aorta - a study with selective inhibitors. Biochem. Pharmacol. **36:** 3965-3972.

Seiler, K. P., G. A. George, M. P. Happ, N. E. Bodycombe, H. A. Carrinski *et al*, 2007 ChemBank: A small-molecule screening and cheminformatics resource database. Nucleic Acids Res .

Senzaki, H., C. H. Chen, S. Masutani, M. Taketazu, J. Kobayashi *et al*, 2001 Assessment of cardiovascular dynamics by pressure-area relations in pediatric patients with congenital heart disease. J. Thorac. Cardiovasc. Surg. **122:** 535-547.

Shimizu-Albergine, M., E. Patrucco, L. Tsai, J. S. Campbell and J. A. Beavo, 2008 *Role of Phosphodiesterase 8A in Lipid Metabolism in Liver*.

Smith, S. J., S. Brookes-Fazakerley, L. E. Donnelly, P. J. Barnes, M. S. Barnette *et al*, 2003 Ubiquitous expression of phosphodiesterase 7A in human proinflammatory and immune cells. Am. J. Physiol. -Lung Cell. Mol. Physiol. **284:** L279-L289.

Soderling, S. H., and J. A. Beavo, 2000 Regulation of cAMP and cGMP signaling: New phosphodiesterases and new functions. Curr. Opin. Cell Biol. **12:** 174-179.

Soderling, S. H., S. J. Bayuga and J. A. Beavo, 1998a Cloning and characterization of a cAMP-specific cyclic nucleotide phosphodiesterase. Proc. Natl. Acad. Sci. U. S. A. **95:** 8991-8996.

Soderling, S. H., S. J. Bayuga and J. A. Beavo, 1998b Cloning and characterization of a cAMP-specific cyclic nucleotide phosphodiesterase. Proc Natl Acad Sci U S A **95:** 8991-6.

Soderling, S. H., S. J. Bayuga and J. A. Beavo, 1998c Identification and characterization of a novel family of cyclic nucleotide phosphodiesterases. J. Biol. Chem. **273:** 15553-15558.

Stiefel, J., L. Wang, D. A. Kelly, R. T. K. Janoo, J. Seitz *et al*, 2004 Suppressors of an adenylate cyclase deletion in the fission yeast *Schizosaccharomyces pombe*. Eukaryotic Cell **3:** 610-619.

Stratakis, C. A., 2009 New genes and/or molecular pathways associated with adrenal hyperplasias and related adrenocortical tumors. Mol Cell Endocrinol **300:** 152-157.

Terrett, N. K., A. S. Bell, D. Brown and P. Ellis, 1996 Sildenafil (VIAGRA(TM)), a potent and selective inhibitor of type 5 cGMP phosphodiesterase with utility for the treatment of male erectile dysfunction. Bioorg. Med. Chem. Lett. **6:** 1819-1824.

Thevelein, J. M., and J. H. de Winde, 1999 Novel sensing mechanisms and targets for the cAMP-protein kinase A pathway in the yeast *Saccharomyces cerevisiae*. Mol Microbiol **33:** 904-18.

Thevelein, J. M., L. Cauwenberg, S. Colombo, J. H. De Winde, M. Donation *et al*, 2000 Nutrient-induced signal transduction through the protein kinase A pathway and its role in the control of metabolism, stress resistance, and growth in yeast. Enzyme Microb Technol **26:** 819-825.

Tommasino, M., and K. Maundrell, 1991 Uptake of thiamine by *Schizosaccharomyces pombe* and its effect as a transcriptional regulator of thiamine-sensitive genes. Curr. Genet. **20:** 63-66.

Torphy, T. J., J. M. Stadel, M. Burman, L. B. Cieslinski, M. M. McLaughlin *et al*, 1992 Coexpression of human cAMP-specific phosphodiesterase activity and high affinity rolipram binding in yeast. J Biol Chem **267:** 1798-804.

Traish, A. M., F. Saad, R. J. Feeley and A. Guay, 2009 The dark side of testosterone deficiency: III. cardiovascular disease. J. Androl. **30:** 477-494.

Tsai, L. C., M. Shimizu-Albergine and J. A. Beavo, 2010 The high affinity cAMP-specific phosphodiesterase 8B (PDE8B) controls steroidogenesis in the mouse adrenal gland. Mol. Pharmacol. doi:10.1124/mol.110.069104.

Vang, A. G., S. Z. Ben-Sasson, H. Dong, B. Kream, M. P. DeNinno *et al*, 2010 PDE8 regulates rapid teff cell adhesion and proliferation independent of ICER. PLoS One **5:** e12011.

Vasta, V., 2006 cAMP-phosphodiesterase 8 family in *Cyclic Nucleotide Phosphodiesterases in Health and Disease*, edited by J. A. Beavo, S. H. Francis and M. D. Houslay.

Vasta, V., M. Shimizu-Albergine and J. A. Beavo, 2006 Modulation of Leydig cell function by cyclic nucleotide phosphodiesterase 8A. Proc. Natl. Acad. Sci. U. S. A. **103:** 19925-19930.

Verhoest, P. R., D. S. Chapin, M. Corman, K. Fonseca, J. F. Harms *et al*, 2009a Discovery of a novel class of phosphodiesterase 10A inhibitors and identification of clinical candidate 2-[4-(1-methyl-4-pyridin-4-yl-1H-pyrazol-3-yl)-phenoxymethyl]-quinoline (PF-2545920) for the treatment of schizophrenia. J. Med. Chem. **52:** 5188-5196.

Verhoest, P. R., C. Proulx-Lafrance, M. Corman, L. Chenard, C. J. Helal *et al*, 2009b Identification of a brain penetrant PDE9A inhibitor utilizing prospective design and chemical enablement as a rapid lead optimization strategy. J. Med. Chem. **52:** 7946-7949.

Wang, H., Y. Liu, Y. Chen, H. Robinson and H. Ke, 2005 Multiple elements jointly determine inhibitor selectivity of cyclic nucleotide phosphodiesterases 4 and 7. J Biol Chem **280:** 30949-55.

Wang, H., Z. Yan, S. Yang, J. Cai, H. Robinson *et al*, 2008 Kinetic and structural studies of phosphodiesterase-8A and implication on the inhibitor selectivity. Biochemistry **47:** 12760-8.

Wang, L., K. Griffiths, Y. H. Zhang, F. D. Ivey and C. S. Hoffman, 2005 *Schizosaccharomyces pombe* adenylate cyclase suppressor mutations suggest a role for cAMP phosphodiesterase regulation in feedback control of glucose/cAMP signaling. Genetics **171:** 1523-33.

Wang, P., P. Wu, R. W. Egan and M. M. Billah, 2001a Human phosphodiesterase 8A splice variants: Cloning, gene organization, and tissue distribution. Gene **280:** 183-94.

Wang, P., P. Wu, R. W. Egan and M. M. Billah, 2001b Human phosphodiesterase 8A splice variants: Cloning, gene organization, and tissue distribution. Gene **280:** 183-194.

Wayman, C., S. Phillips, C. Lunny, T. Webb, L. Fawcett *et al*, 2005 Phosphodiesterase 11 (PDE11) regulation of spermatozoa physiology. Int. J. Impotence Res. **17:** 216-223.

Wells, J. N., and J. R. Miller, 1988 Methylxanthine inhibitors of phosphodiesterases. Meth. Enzymol. **159:** 489-496.

Welton, R. M., and C. S. Hoffman, 2000 Glucose monitoring in fission yeast via the Gpa2 Gα, the Git5 Gβ, and the Git3 putative glucose receptor. Genetics **156:** 513-21.

Wilkins, M. R., J. Wharton, F. Grimminger and H. A. Ghofrani, 2008 Phosphodiesterase inhibitors for the treatment of pulmonary hypertension. European Respiratory Journal **32:** 198-209.

Wu, P., and P. Wang, 2004 Per-Arnt-Sim domain-dependent association of cAMP-phosphodiesterase 8A1 with IkappaB proteins. Proc. Natl. Acad. Sci. U. S. A. **101:** 17634-17639.

Yan, C., A. Z. Zhao, J. K. Bentley and J. A. Beavo, 1996 The calmodulin-dependent phosphodiesterase gene PDE1C encodes several functionally different splice variants in a tissue-specific manner. J. Biol. Chem. **271:** 25699-25706.

Yan, C., A. Z. Zhao, J. K. Bentley, K. Loughney, K. Ferguson *et al*, 1995 Molecular-cloning and characterization of a calmodulin-dependent phosphodiesterase enriched in olfactory sensory neurons. Proc. Natl. Acad. Sci. U. S. A. **92:** 9677-9681.

Yanaka, N., Y. Kurosawa, K. Minami, E. Kawai and K. Omori, 2003 cGMP-phosphodiesterase activity is up-regulated in response to pressure overload of rat ventricles. Biosci. Biotechnol. Biochem. **67:** 973-979.

Yu, J., S. L. Wolda, A. L. B. Frazier, V. A. Florio, T. J. Martins *et al*, 1997 Identification and characterisation of a human calmodulin-stimulated phosphodiesterase PDE1B1. Cell. Signal. **9:** 519-529.

Yuasa, K., J. Kotera, K. Fujishige, H. Michibata, T. Sasaki *et al*, 2000 Isolation and characterization of two novel phosphodiesterase PDE11A variants showing unique structure and tissue-specific expression. J. Biol. Chem. **275:** 31469-31479.

Zaks-Makhina, E., Y. Kim, E. Aizenman and E. S. Levitan, 2004 Novel neuroprotective K^+ channel inhibitor identified by high-throughput screening in yeast. Mol. Pharmacol. **65:** 214-219.

Zhang, H. T., Y. Huang, S. L. C. Jin, S. A. Frith, N. Suvarna *et al*, 2002 Antidepressant-like profile and reduced sensitivity to rolipram in mice deficient in the PDE4D phosphodiesterase enzyme. Neuropsychopharmacology **27:** 587-595.

Zhang, J. H., T. D. Chung and K. R. Oldenburg, 1999 A simple statistical parameter for use in evaluation and validation of high throughput screening assays. J Biomol Screen **4:** 67-73.